

# Chapter 2

## Successes in Application of Pulse-Amplitude Modulated Fluorescence

### Contents

2.1	Fluorescence Spectroscopy in Amino Acid Analysis .....	48
2.2	Theory of the Energetic Basis of the Resistance of Green Cells to Abiotic Environmental Factors .....	54
2.2.1	Influence of Negative Temperatures on the Kinetics of Pulse-Amplitude Modulated Fluorescence Parameters ( $F_0$ , $F_m$ , $F_v$ ) .....	61
2.2.2	Association of High Temperature Stress to the Signal Harmonics Change in Pulse-Amplitude Modulated Fluorescence ( $F_0$ , $F_m$ , $F_v$ ) .....	67
2.2.3	The Coupling of Mechanisms of Green Cell Resistance to Changes in the Pulse-Amplitude Modulated Fluorescence Parameters Under the Influence of Atmospheric Drought .....	74
2.2.4	The Influence of $\text{Na}^+$ , $\text{Cl}^-$ , and $\text{SO}_4^{2-}$ Ions on the Change in Pulse-Amplitude Modulated Fluorescence Kinetics. Resistance Features of the Phototrophic Function of Photosystem 2 at Salification .....	91
2.2.5	The Concept of the Energetic Basis of Green Cell Resistance to the Influence of Extreme Environmental Factors .....	99
2.2.6	Additional Material for Substantiation of the Energetic Basis of the Theory of <i>Procarvota</i> and <i>Eucaryota</i> Phototrophic Cell Tolerance to the Influence of Abiotic Environmental Factors .....	109
2.2.7	Features of the Fluorescence Change in $F_0$ and $F_m$ in Response to Dithiothreitol Inhibition of Zeaxanthin Formation .....	114
2.2.8	Specifics of $\gamma$ -Radiation Influence on the Stability of Energetics and the Pigment System of the Photosynthetic Device .....	120
2.2.9	Features of the Structural Stability of the Light-Harvesting Complex of Photosystem 2 Under the Influence of $\gamma$ -Radiation .....	125
2.2.10	New Data on the Development of the Hypothesis on the Localization of Damaging EFE Influences in a Green Leaf; After-effect of $\gamma$ -Radiation on the Energetics of Chloroplasts .....	132
2.2.11	Specifics of Change in the Coefficients of Pulse-Amplitude Modulated Fluorescence Quenching ( $q_q$ and $q_E$ ) During the after-effect of $\gamma$ -Irradiation .....	140
2.2.12	The Specifics of the Fine Structural Changes in the Photosynthetic Device Under the Influence of $\gamma$ -Radiation .....	148
	References .....	168

## 2.1 Fluorescence Spectroscopy in Amino Acid Analysis

Fluorescence is used not only in studying the *functions* of molecules, as demonstrated by the example of photosynthetic reactions (see Chap. 1), but also for an assessment of changes in molecular *structure* as a consequence of protein interactions with other molecules (e.g., with other proteins or DNA) or caused by the influence of damaging agents such as temperature, light, chemical agents, and radiation (see Chap. 4).

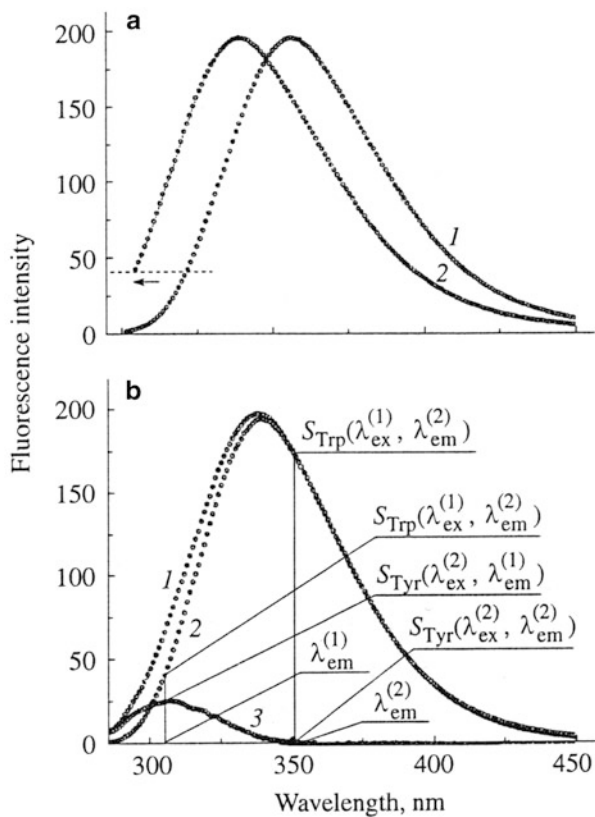
We remind the reader that the amino acid residues tryptophan, tyrosine, and phenylalanine fluoresce, although the phenylalanine quantum yield is very low and usually its fluorescence is not detectable (Cantor and Schimmel 1984). Also, the fluorescence of tyrosine residues included in proteins is much weaker than that of tryptophan ones, not only because of the lower yield of pure tyrosine compared with tryptophan but also because the incorporation of a tyrosine residue in a peptide bond reduces the tyrosine fluorescence by approximately 32 % (Chen and Edelhock 1976). Tyrosine residues, hydroxyl groups of which are involved in the formation of the hydrogen bond (TyrOH), cannot fluoresce at all (Chen and Edelhock 1976), and, at last, under favorable conditions, excited tyrosine residues (“donor residues”) transfer energy to acceptor residues of tryptophan and TyrOH through non-radiative dipole–dipole coupling. This phenomenon takes place when, simultaneously, the donor *emission* spectrum overlaps with the acceptor *absorption* spectrum, chromophores are located not farther than a certain distance from each other, and their dipole moments are in proper relative orientation. The phenomenon is called Förster resonance energy transfer (FRET), after the German physicist T. Förster (in the case of tyrosine and tryptophan, it is singlet–singlet transfer) (Cantor and Schimmel 1980).

Therefore, although the spectra of tyrosine and tryptophan fluorescence have maxima at different wavelengths, the tyrosine fluorescence spectrum cannot be separately registered because of the tryptophan residues in the protein. Thus, at an excitation wavelength of 275 nm, the total spectrum of tryptophan and tyrosine emission is recorded. Nevertheless, the spectrum of tyrosine fluorescence can be obtained from the total spectrum of tyrosine and tryptophan fluorescence with the help of the method described by Isaev-Ivanov et al. (2000).

The principle of the method consists of subtracting two spectra from the total spectrum recorded in the range of 285–450 nm at an excitation wavelength of 275 nm: (1) the tryptophan emission spectrum in the range 305–450 nm at the excitation wavelength 295 nm and (2) the emission spectrum of *N*-acetyl-L-tryptophan amide (NATrpA) in the range of 300–320 nm at an excitation wavelength of 275 nm, shifted to the maximum of the total spectrum (see Fig. 2.1).

The use of data from X-ray crystallographic analysis, nuclear magnetic resonance, or electron microscopy, which can be found, for example, in the database of the RCSB Protein Data Bank (PDB), containing more than 72,000 structures (<http://www.pdb.org/>) (Berman et al. 2000), considerably helps in the analysis of results

**Fig. 2.1** (a) Line shapes of emission spectra of *N*-acetyl-L-tryptophanamide (1) and tryptophan (2) at  $\lambda_{\text{ex}} = 275$  nm. (b) Examples of the recorded total emission spectrum of DNase I (1), the reconstructed tryptophan emission spectrum (2), and the separated tyrosine emission spectrum (3)



from fluorescence spectroscopy. The programs for viewing molecular structures (e.g., *Swiss-PdbViewer*, <http://www.expasy.org/spdbv/>; Guex and Peitsch 1997) allow, in particular, TyrOH residues to be found. Also, using the coordinates of atoms from PDB files, it is possible to calculate the parameters and efficiency of resonance energy transfer using known formulae (Cantor and Schimmel 1980):

$$E = \frac{R_0^6}{R_0^6 + r^6} \quad R_0 = 9.7 \times 10^3 (k^2 n^{-4} \Phi_D J)^{1/6}$$

$$k^2 = (\cos \theta_T - 3 \cos \theta_D \cos \theta_A)^2 \quad J = \int S_F^D(\lambda) \varepsilon_A(\lambda) \lambda^4 d\lambda$$

where  $E$  is the FRET efficiency;  $R_0$ , the Förster radius;  $r$ , the distance between the donor and the acceptor;  $k^2$ , the geometric orientation factor characterizing the mutual orientation of the donor and acceptor dipoles;  $n$ , the refractive index of the medium;  $\Phi_D$ , the fluorescence quantum yield of the donor in the absence of the acceptor;  $J$ , the overlap integral for the donor emission spectrum and the acceptor absorption spectrum;  $\theta_T$ , the angle between the emitting dipole of the donor and the

absorbing dipole of the acceptor;  $\theta_D$  and  $\theta_A$ , angles between these dipoles and the vector directed from the donor to the acceptor;  $S_F^D$ , the donor emission spectrum normalized to the area under this spectrum; and  $\varepsilon_A(\lambda)$ , the extinction coefficient of the acceptor, which depends on the wavelength  $\lambda$ .

It should be noted that in protein, for one tyrosine donor residue, there can exist several ( $n$ ) acceptor residues, each of which ( $i$ th) is characterized by the FRET efficiency  $E_i$  and the energy transfer rate constant  $k_T^i$  ( $i = 1 \dots n$ ).

The transfer rate constants  $k_T^i$  are calculated according to the formula (Cantor and Schimmel 1980)

$$k_T^i = \frac{1}{\tau_D} \left( \frac{R_{0i}}{R_i} \right)^6 = \frac{E_i}{\tau_D(1 - E_i)},$$

where  $\tau_D$  is the excited-state lifetime of the donor in the absence of acceptors.

So the total energy transfer constant  $K$  is calculated as the sum:

$$K = \sum_{i=1}^n k_T^i = \sum_{i=1}^n \frac{E_i}{\tau_D(1 - E_i)}.$$

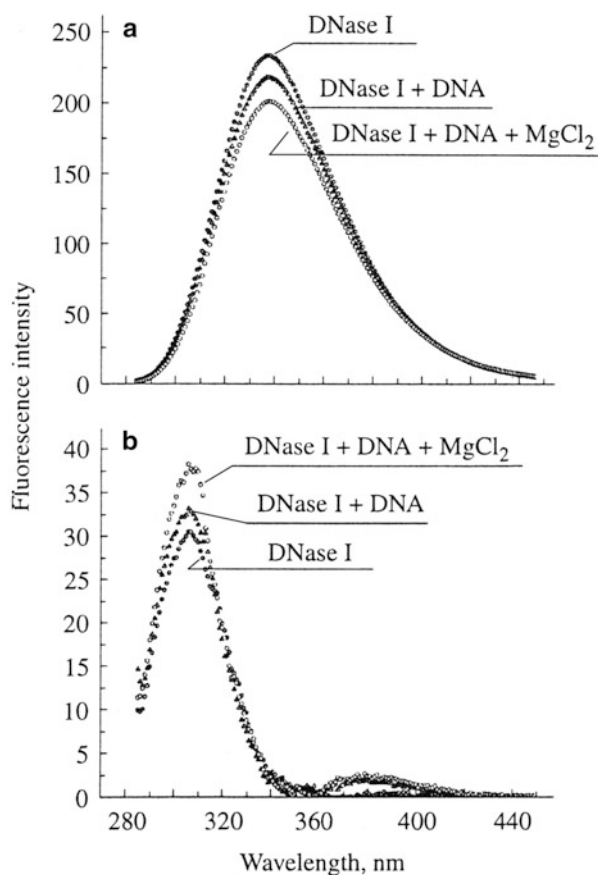
The total efficiency  $E$  of the transfer from one tyrosine residue to several acceptor residues can be calculated using the formula (Danilova et al. 2005)

$$E = \frac{\sum_{i=1}^n \frac{E_i}{1 - E_i}}{1 + \sum_{i=1}^n \frac{E_i}{1 - E_i}}.$$

As an illustration, we consider the protein bovine pancreatic deoxyribonuclease I (DNase I), the enzymatic activity of which, as well as of many other endonucleases, is activated by divalent cations ( $Mg^{2+}$ ,  $Ca^{2+}$ ,  $Mn^{2+}$ ) and inhibited by physiological concentrations of monovalent cations ( $K^+$ ,  $Na^+$ ,  $Cs^+$ ,  $Cd^+$ ,  $Li^+$ ) (Junowicz and Spencer 1973; Oshima and Price 1974). As shown by the results of dynamic light scattering, in the absence of any salts, this protein binds to DNA, and in the presence of monovalent cations, the dissociation of the protein–DNA complex takes place (Danilova et al. 2005).

From the primary structure of DNase I, it follows that the fluorescence of this protein molecule is defined by three tryptophan and 15 tyrosine residues. Analysis of the tridimensional DNase I structure (its identification number in the protein database RCSB PDB is 3DNJ) (Oefner and Suck 1986) and of DNase I complexes with model turns of DNA (1DNK and 2DNJ) (Weston et al. 1992; Lahm and Suck 1991) showed that, with high probability, five of the 15 tyrosine residues cannot fluoresce because they are TyrOH residues. The fluorescence of two other tyrosine

**Fig. 2.2** Examples of (a) tryptophan and (b) tyrosine fluorescence emission spectra obtained by separation of the protein emission spectra recorded after sequential addition of phage M13 single-stranded DNA and  $\text{MgCl}_2$  to the protein solution



residues is significantly quenched because of the high FRET efficiency (93–95 %) to tryptophan residues. Furthermore, four tyrosine residues are not quenched at all (efficiency, 0 %), but they are located not only far from acceptors but also far from the enzyme active center (AC) and from the enzyme DNA-binding site (DBS). So 11 tyrosine residues cannot contribute to the fluorescence changes caused by protein binding to DNA and by enzymatic activity.

Residues Tyr175 and Tyr253 are closest to the AC and DBS. Also, the DBS includes the tyrosine residue Tyr211 and one of the TyrOH residues, Tyr76. Positioned 20 residues from Tyr76 is Tyr97, which manifests some mobility in crystals with model DNA turns. No tryptophan residues are present in the AC and DBS (Danilova et al. 2005).

Figure 2.2 shows examples of emission spectra of the tyrosine and tryptophan fluorescence of DNase I, obtained by separation from the protein emission spectra recorded after consecutive addition of 12  $\mu\text{M}$  circular single-stranded DNA of phage M13 and 5 mM  $\text{MgCl}_2$  to a solution of 1.6  $\mu\text{M}$  DNase I in Tris buffer. In Table 2.1, the numerical values of fluorescence changes are presented for cases when DNA and

**Table 2.1** Changes in tryptophan and tyrosine fluorescence of DNase I after addition of salts and/or DNA to the protein solution

Sample	Changes in fluorescence with respect to FI of protein solution	
	Quenching of tryptophan FI (%)	Change in tyrosine FI (%)
Protein + MgCl <sub>2</sub>	6.6 ± 1.3	Not changed
Protein + NaCl	4.9 ± 1.5	Not changed
Protein + MgCl <sub>2</sub> +NaCl	8.5 ± 1.2	Not changed
Protein + DNA	5.0 ± 1.6	Increase by 9.4 ± 1.8
Protein + DNA + MgCl <sub>2</sub>	11.1 ± 1.7	Increase by 17.8 ± 1.3
Protein + DNA + NaCl	11.3 ± 1.1	Increase by 16.9 ± 2.1
Protein + DNA + MgCl <sub>2</sub> + NaCl	15.2 ± 1.5	Increase by 22.3 ± 1.6
Protein + DNA + NaCl + MgCl <sub>2</sub>	14.6 ± 1.2	Increase by 13.5 ± 1.4

monovalent and/or bivalent cations and their mixes were added to the protein solution. Fluorescence changes were calculated as the difference between the areas under spectra, expressed as a percentage of the protein solution fluorescence.

The simultaneous quenching of tryptophan fluorescence and the increase in intensity of tyrosine fluorescence means that the change in FRET efficiency is caused by conformational modifications (1) in DBS, when DNA was added to protein or when NaCl was added to the protein–DNA mixture and caused the dissociation of protein–DNA complexes; (2) in AC, after addition of MgCl<sub>2</sub> to the protein–DNA mixture that promoted the enzymatic activity; and (3) in AC, after addition of NaCl to protein–DNA or protein–DNA–MgCl<sub>2</sub> mixtures, because addition of MgCl<sub>2</sub> to the protein–DNA–NaCl mixture did not cause an increase in tyrosine fluorescence (in contrast to the situation when the protein–DNA mixture was without NaCl). Consequently, Na<sup>+</sup> ions influenced the AC conformation and not only the conformation of DBS. Thus, Mg<sup>2+</sup> affects the AC conformation, and Na<sup>+</sup> affects DBS and AC.

Nevertheless, because protein complex structures containing amino acid residues are collisional quenchers of tyrosine and tryptophan fluorescence (Lakowicz 1983; Chen and Edelhock 1976), and because of the probability of breaking TyrOH hydrogen bonds as a result of conformational changes, it is impossible to determine conformational changes unequivocally and exactly and to conclude what part of the fluorescence change is caused by variations in FRET efficiency without using additional special fluorescent probes and mutagenesis.

For example, the addition of salts to the protein solution results in only the reliable change in tryptophan fluorescence; therefore, a change in FRET efficiency does not occur. So, because salts influence tryptophan fluorescence, the observed effects in mixtures of protein, DNA, and salt cannot be explained only by changes in FRET efficiency. The effects of salt in protein–salt mixtures are very probably caused by an increase in the influence of collisional quenchers of tryptophan fluorescence, namely, in pairs Trp158–Asp93 and Trp181–Asp198. In crystals

grown at the same concentration of NaCl as used in experiments on fluorescence (150 mM), the distance between these residues in pairs is as little as approximately 5 Å.

The other case is protein binding to DNA, that is, in the protein–DNA mixture. One of the DBS residues, asparagine (Asn) 170, is a collisional quencher of two tyrosine residues, Tyr175 and Tyr211. After formation of the protein–DNA complex, the level of collisional quenching probably decreases, which additionally contributes to the increase in tyrosine fluorescence. Also, the TyrOH residue Tyr76 is included in DBS. However, breaking the hydrogen bond for Tyr76 seems improbable because then the increase in the intensity of tyrosine fluorescence would be more considerable (approximately 16 %) because of its zero FRET efficiency (Danilova et al. 2005).

Because the fluorescence of tyrosine and sometimes of tryptophan residues in protein is quite difficult to analyze, some special synthetic aromatic and polyaromatic, polyunsaturated, condensed compounds that are able to fluoresce are often used in research and are being applied as probes for research in molecular dynamics (Nytek Instruments 2004). Probes can be introduced even if the direct fluorescence of the studied substance is not registered. The fluorescent probe specifically binds or is covalently attached to a molecule of this substance. As a rule, when choosing a probe, the wavelength of its maximum absorption  $\lambda_{\text{max}}$  should differ from  $\lambda_{\text{max}}$  of the studied molecule, so all received information belongs to the probe (Cantor and Schimmel 1980).

Widely applied probes are (1) dansyl chloride and 1,5-I-AEDANS, which covalently bind to Lys and Cys residues of proteins; (2) fluorescein isothiocyanate (FITC), which covalently attaches to Lys; (3) 8-anilino-1-naphthalene sulfonate (ANS), which non-covalently binds to proteins; (4) ethenoadenosine and its derivatives, which are analogues of nucleotides and bind to both proteins and nucleic acids; (5) ethidium bromide, which non-covalently binds to nucleic acids; (6) proflavine mono-semicarbazide, which covalently joins to the 3' end of RNA; and (7) pyrene and its derivatives, which are used in polarization measurements in large systems (Cantor and Schimmel 1980).

Some probes, for example, ANS, fluoresce only after binding with proteins, which is convenient for studying protein–protein interactions. For example, the fluorescence of ANS bound to apomyoglobin is easily noticeable. After adding heme, the fluorescence decreases because ANS is competitively replaced from the protein (Dobretsov 1987).

Also, probes are used for research into cellular membranes, namely, the determination of lipid affinity to a membrane, calculation of ligand penetration speed through a membrane, registration of ligand accumulation in cell organelles, and estimation of surface and transmembrane fields. Changes in probe fluorescence allow conclusions to be made about changes in the probe–membrane binding. The competition between a probe and a ligand for membrane-binding centers depends on the charge similarity of these molecules. After adding the ligand, the quantity of

membrane-bound probes, which have the same charge as the added ligand, decreases and the number of oppositely charged probes increases (Dobretsov 1987).

To determine protein location in a membrane, probes serving as acceptors of tryptophan fluorescence are used. The higher the extent of protein fluorescence quenching, the closer the protein is to a membrane surface. Another method is the application of donor probes quenched by studied proteins. A universal probe is terphenyl, with an emission spectrum in the region above 300 nm. Registering the quenching speed of terphenyl fluorescence after adding the studied substance to model liposomes containing a terphenyl probe allows conclusions to be made about the speed of substance penetration through a membrane (Dobretsov 1987).

The use of membrane probes in medical research is of great value. With the help of ANS and pyrene, it was possible to demonstrate considerable structural damage to cellular membranes and changes in membrane potential at hypertensive disease, experimental hyperthyrosis and myocarditis, and chemical carcinogenesis, as well as structural damage to liver microsomes in cases of vitamin A deficiency (see review by Ivanova and Kirpichenok 2008, and the literature cited within it). In other experiments, the application of tetracycline as a probe demonstrated abnormalities of calcium transport through membranes of lymphocytes in patients with bronchial asthma and other pulmonary diseases.

The possibility of using a fluorescent probe to study Alzheimer's disease and malignant neoplasms was also shown, and fluorescence tests were developed for diagnosis of myocardial infarction, unstable stenocardia, hypertensive cardiomyopathy, chronic alcoholism, and liver disease; an early prognosis of peritonitis development; an assessment of the severity and prognosis of acute pancreatitis; and identification of allergens (Ivanova and Kirpichenok 2008).

Fluorescent probes have been intensively developed in the Laboratory of Biophysical Methods of Diagnostics of the Department of Biophysics, the Scientific Research Institute of Physical and Chemical Medicine (PSBI SRI PhChM FMBA of Russia, Moscow). The main achievements of this laboratory are presented on the website <http://niifhm.ru/nauchnye-issledovaniya/otdel-biofiziki/laboratorija-biofizicheskikh-metodov-dagnostiki/>.

Thus, in this section we have described the possibility of a wider range of fluorescence analysis applications than was presented in the introduction to this book (Chap. 1).

## 2.2 Theory of the Energetic Basis of the Resistance of Green Cells to Abiotic Environmental Factors

Another type of analytical approach is applied when using a new variant of fluorescence analysis, namely, pulse-amplitude modulated fluorescence (PAMF). The method gained especially wide application in ecological and physiological research in cases of intravital studies (including *in situ*) of plant tissues of *Procaryota* and *Eucaryota*.



The research into plant resistance to the influence of environmental stress factors of anthropogenous and natural origin is of paramount importance for Russia because the combination of the most diverse set of climatic zones, features of soil covering, and the complex ecological factors of negative targeting have created a danger to the harvest of cultivated plants and to the capability of forests, water pools, and the ocean to renew oxygen stocks in the atmosphere.

To understand the adaptation or failure mechanisms, there is a need to consider the set of in-depth mechanisms forming the basis of green cell adaptive reactions to the action of extreme factors of the environment (EFEs). Speaking of tolerance stability, it is necessary to remember and to accurately differentiate between enzymatic–biochemical reactions and energetic reactions in chloroplasts, protoplasm and their organelles, separate organs of plants, and plant productivity in toto. Only by performing such investigations based on modern techniques and theoretical constructions is it possible to create a general picture of the resistance of a plant organism to the influence of EFEs (Chen and Edelhock 1976; Bilger et al. 2001).

Development of modern molecular spectroscopy methods was interconnected with successes in improving the hardware base of electrooptical instrumentation and, by the end of the twentieth century, allowed plant research in vivo, often with contactless techniques, without interruption of the physiological processes inherent in plant cells. The possibility of this type of research is substantially caused by the existence of chlorophyll *a*, the presence of which unites autotrophic organisms such as *Cyanophyceae* in *Procaryota* with the *Eucaryota* kingdom.

Research on a number of barley mutants lacking chlorophyll *b*, investigations of the large variety of *Chlamydomonas* and *Scenedesmus* mutants with different light sensitivities, and studies of the cultivar variety collection in the N.I. Vavilov Institute of Plant Industry have laid the foundation for ideas on the localization of the damaging effect of environmental factors in the electron transport chain (ETC) of the photosynthetic apparatus. The independence of quantitative variability of a pigment spectrum on the plant manifestation of destruction reactions was shown. As a result, it was hypothesized that there exist centers in eukaryotic chloroplast thylakoids in which the influence of EFEs is localized and the activity of which determines the degree of leaf stability against the action of EFEs. These centers coincide with the reaction centers (RCs) of photosystems and with centers of pigment biosynthesis (Saakov 1971a, b; Baranov et al. 1974–1976; Saakov et al. 1975). Change in *F* shows to functional damage to the state of reaction centers of PSII (Saakov 1971a, b).

Imbalance of the sequence of ETC reactions leads to the impossibility of capturing light energy from the antenna chlorophyll in RCs; oxidized  $P_{680}^{+}$  does not catch energy and the RCs are closed and characterized by the maximum yield of fluorescence. Research carried out in subsequent years promoted an accumulation of facts in favor of the suggested hypothesis (Saakov 1987, 1990; Saakov and Leontjev 1988; Saakov et al. 1993).

Ideas developed by us found support and were expanded by works that studied fluorescence changes in response to a broad set of damaging effects of

environmental factors. Success in this direction was connected with introduction of the method of PAM fluorescence registration (Saakov et al. 1993; Saakov 1993a–d, 1998a, b; Lichtenthaler and Rinderle 1988; Rubin 2000a) and was published in a number of works in specialized monographic and journal editions. Experimental data from the past 15–25 years (Saakov 1987, 1990; Saakov and Leontjev 1988; Saakov and Barashkova 1999; Saakov and Shiryaev 2000) have supported and developed our concepts. The conclusions of Russian and European researchers on the response of the photosynthetic ETC to various influences gave confidence in the correctness of the chosen direction (Lichtenthaler and Rinderle 1988; Saakov and Barashkova 1999; Saakov and Shiryaev 2000; Saakov 2000a–e). It should be noted that studying the action of an EFE is closely connected with the manifestation of its aftereffect because assessment of the aftereffect is conveniently related to a prognosis of the development of adaptive or lethal situations when a green leaf performs the phototrophic function.

The midday depression of intensity of carbon dioxide fixation by green cells under conditions of increased temperature reduces plant productivity not only in arid zones but also under conditions of moderate climate areas in a hot season. Along with structural changes in the photosynthetic apparatus, significant damage to chloroplast functional activity is registered.

The range of temperatures at which photosynthesis breaks down was identified by us (Semikhatova and Saakov 1962) and later confirmed in European research (Armond et al. 1978; Weis 1981a, b; Havaux 1988; Heber and Santarius 1973; Fork et al. 1985; Gounaris et al. 1983; Monson et al. 1982; Snel and van Kooten 1990). The boundary temperature,  $T^0$ , was +35 °C, at which significant suppression of CO<sub>2</sub> assimilation was observed. The effect of temperatures of 39–41 °C was a 60–80 % decrease in photosynthesis from control values. After exposure to +41 °C, the reparation of photosynthesis intensity in 17–19 h back to 70 % of the initial level (Semikhatova and Saakov 1962) was possible. Higher temperatures (42 °C) resulted in irreversible failure of photosynthesis.

Years later, in 1999, the work of Bungard et al. (1999) was published. These authors found the range of temperatures for which the reversible recovery of the photosynthesis process can take place. Their range exactly corresponds to those temperatures about which we wrote in 1962, 37 years before. This fact serves as example that sometimes scientific information can't be easily found or accessed. It's regrettable, because, more precisely, in 1958, these data were reported at a master's thesis defense (Saakov 1959) at the Leningrad State University, and the usual delay with publications in Russia allowed us to print our material only in 1962 (Semikhatova and Saakov 1962).

Acclimatization or adaptation to the influence of temperature means an increase in the reliability of the interaction system between light-harvesting complexes of pigments and the RCs of photosystems (Armond et al. 1978) because the dissociation of complexes induced by elevated temperatures manifests as a decrease in electron

transport and change in energy distribution between photosystems PS-1 and PS-2 (Weis 1981a, b). The registered decrease in electron transport in PS-2 is noted at +35 °C. Photophosphorylation becomes unstable and is progressively inhibited from +35 °C (Monson et al. 1982). Thus, functional damage to CO<sub>2</sub> assimilation and the simultaneous decrease in the electron transfer speed in PS-2 at incubatory temperatures above +35 °C are not in doubt, but Bungard et al. (1999) do not mention it.

In the process of creating theoretical constructions, we carried out a comparative study of the character of signal harmonic kinetics (PAMF) under the influence of  $\gamma$ -radiation, various temperatures, drought, fumigation, and herbicides, hoping to find answers about the specificity or non-specificity of the response of the ETC photosynthetic apparatus to the chosen EFE and to limit questions regarding the possible localization of these influences.

Since the end of the 1980s, researchers have been registering stationary ( $F_0$ ), variable ( $F_V$ ), and maximum ( $F_m$ ) fluorescence with the help of the pulse fluorometer Walz 101-103 (Effeltrich, Germany). The developments by Prof. Schreiber and the device manufactured by Walz brought about a methodological revolution in scientific research. The convenience of the method consisted in the speed of obtaining results about the changes in the main measured parameters directly from an intact leaf and the possibility of working not in darkness but in light. The properties of this method were tested in details and checked in many laboratories in the USA and Europe. The calculation of photochemical ( $q_q$ ), non-photochemical ( $q_E$ ), and other coefficients of fluorescence quenching and the interpretation of their changes were carried out using the accepted technique (see Schreiber and Neubauer 1990 and the special issue of *Photosynthesis Research* edited by van Kooten and Snel 1990a).

An example of experimental results on research into PAMF kinetics is presented in Fig. 2.3, and calculations of fluorescence coefficients are shown in Table 2.2. The level of  $F_0$  arising after the dark period of leaf adaption, which is preceding and necessary for the experiment, when photosynthetic membranes are in the non-energized state and all RCs of PS-2 are “open,” is caused by the radiation of excited chlorophyll *a* molecules. This takes place before the energy migration into RCs and when the first stable acceptor of PS-2,  $Q_A^+$ , is completely oxidized; at that point, the coefficients  $q_q = 1$  and  $q_E = 0$ .  $F_0$  is determined when the measured light flux of approximately 0.1  $\mu\text{E}/(\text{m}^2 \text{ s})$  is switched on. From the data in Fig. 2.3, it follows that the  $F_0$  value ( $F_0^t$  is the stationary fluorescence in any interval of time) increases with action of EFEs, which causes a change in the state of PS-2 pigments and leads to photoinhibition (PhIn). The data obtained over many years show that the influence of ionizing radiation, temperature, dehydration, and herbicides significantly changes the  $F_0$  level after light induction.

In the experiment, after switching on the light impulse (3,000–3,500  $\mu\text{E}/(\text{m}^2 \text{ s})$ ) or the actinic light flow, the maximum fluorescence,  $F_m$ , increases, and its first increase (the variable fluorescence  $F_V$ ) corresponds to the reduction  $Q_A^+ \rightarrow Q_A^-$  and results in closing of RCs in PS-2. The  $F_V$  level shows that all non-photochemical extinguishing processes are minimal and that both  $q_q$  and  $q_E$  are equal to zero. The  $F_V$  value (including values of variable fluorescence  $F_V^t$  at any

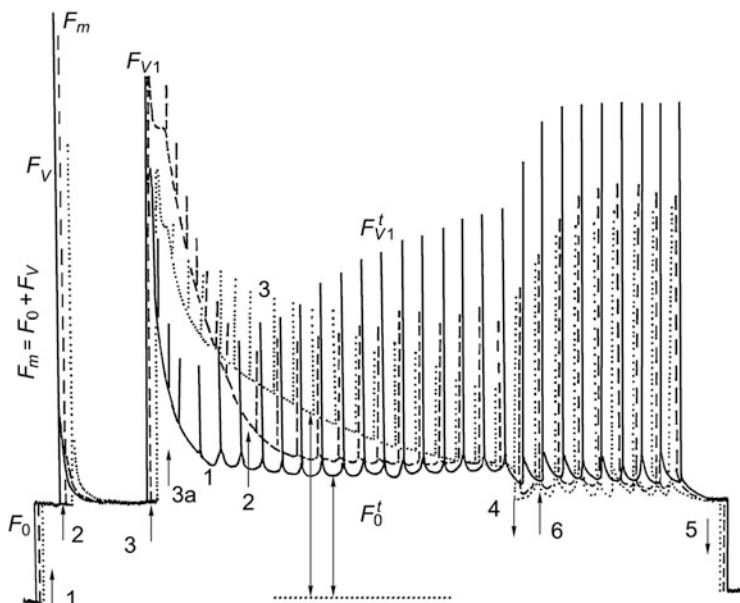


**Fig. 2.3** The character of signal harmonics change in PAMF of a *Nicotiana tabacum* leaf in response to dehydration. *Curves*: 1 control; 2 experiment: dehydration to 45 % of the initial state; 3 dehydration to 30 % of the initial state. *Arrows*: 1 and 5 indicate, respectively, the input and shutdown of the modulating light flux of frequency of 1.6 kHz ( $5 \mu\text{E}/(\text{m}^2 \text{ s})$ ,  $\lambda < 670 \text{ nm}$ ); 2 input of the saturating 1 s impulse of white light ( $2,500 \mu\text{E}/(\text{m}^2 \text{ s})$ ) for finding of  $F_m$  and  $F_V$  values; 3 and 4 input and shutdown, respectively, of actinic light ( $1,200 \mu\text{E}/(\text{m}^2 \text{ s})$ ); 3a input, 30 s later, of 1 s impulses of saturating light against the background of the actinic light for determination of  $F_{V1}^t$  values; 6 input of 1 s impulses of saturating light after shutdown of the actinic light (Saakov 2003a, b; Saakov et al. 2010)

time  $t$ , called “spikes” in the English literature) defined by a low value of coefficient  $q_E$  emphasizes the active utilization of energy in the Calvin cycle and a simultaneous decrease in the membrane proton gradient caused by ATP formation. The suppression of PS-2 activity defined by  $F_V$  suppression is a result of inhibition of the charge transfer between  $P_{680}$  and pheophytin (Pheo), that is, a result of damage localized in PS-2 RCs, which corresponds to earlier-stated ideas.

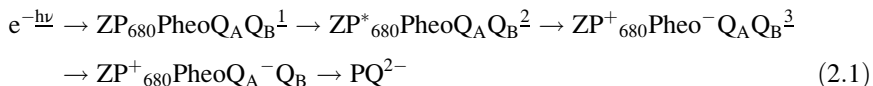
Because the open RC gets energy from antenna chlorophyll, oxidized  $Q_A^+$  acts as the quencher of fluorescence; so in the state  $P_{680}^+Q_A^-$ , the photochemical transformation of energy ( $P_{680}^+Q_A^-$  formation) is a convenient way for de-excitation because the presence of  $Q_A^-P^*$  cannot transfer an electron ( $e^-$ ) to it and the probability of FI emission from the state  $P_{680}^+Q_A^-$  is increased, that is, the RC possesses a high quantum yield of FI. The decrease in  $F_V$  yield is explained by manifestation of the photoinhibition effect. With an increase in influence intensity and aftereffect of EFEs, the  $F_V/F_0$  ratio decreases, which is one more substantial criterion speaking for the damage in PS-2 of ETC and is explained by reduction of the  $P_{680}^+PheoQ_A^-$  link. The  $e^-$  transport in PS-2 RCs starts with charge separation between  $P_{680}$  in the first excited singlet state and pheophytin and is expressed in the

**Table 2.2** The character of changes in the coefficients of modulated fluorescence quenching under the influence of low temperatures<sup>a</sup>

Object	Variant of experiment	Measured coefficient (average of $n = 4, p \leq 0.08$ )										Spikes 5 min (mm)	Spikes 6 min (mm)
		$F_v/F_m$	$F_v^{exp}/F_v^{cont}$	Level of PS-2 reduction (%)	$F_{max}/F_0$	$F_v/F_0$	$F_{v1}/F_v$	$F_{v1}/F_0$	$F_0^5/F_0$	$q_E^{5min}$	$q_q^{5min}$		
<i>Robinia pseudoacacia</i>	Control	0.832	–	93.9	4.34	3.60	0.89	3.2	1.11	0.30	0.94	92	–
	(–10 °C) 2 min	0.652	0.462	43	2.57	1.69	0.814	1.37	1.62	0.27	0.43	21	–
<i>Taxus baccata</i>	Control	0.801	–	91	4.8	3.79	0.93	4.1	1.21	0.32	0.917	68	79
	(–15 °C) 15 min	0.66	0.49	38	3.15	1.79	0.81	1.62	1.67	0.73	0.375	22	36
<i>Fraxinus ornus</i>	Control	0.806	–	92.4	5.17	4.17	0.89	3.71	1.114	0.472	0.92	72	83
	(–13 °C) 13 min	0.736	0.517	52	3.1	2.28	0.854	1.95	1.51	0.801	0.48	26	32
<i>Fagus sylvatica</i>	Control	0.829	–	94.6	5.04	4.05	0.92	3.97	1.13	0.33	0.95	71	80
	(–14 °C) 10 min	0.723	0.64	53	3.12	2.3	0.83	1.9	1.54	0.47	0.46	26	33
<i>Hedera taurica</i>	Control	0.825	–	88	5.6	4.65	0.92	4.28	1.29	0.42	0.89	67	70
	(–12 °C) 20 min	0.694	0.51	32	3.86	2.33	0.86	2.02	1.83	0.72	0.32	12	27
<i>Laurus nobilis</i>	Control	0.817	–	89	5.1	3.83	0.91	3.81	1.22	0.38	0.91	88	93
	(–10 °C) 20 min	0.754	0.488	39	3.21	1.81	0.8	1.54	1.62	0.66	0.39	29	34

<sup>a</sup>The calculation of coefficients  $F_0^5, q_E^{5\min}, q_q^{5\min}$  and values of spike 5 min were performed 5 min after switching the actinic light off; spike 6 min: 6 min after switching the actinic light off

$e^-$  transfer from the secondary donor Z to the primary and secondary acceptors  $Q_A$  and  $Q_B$  of the quinone type, as shown in Eq. (2.1):



When PhIn is induced by intense light, damage to  $e^-$  transport at stages 2 and 3 occurs and is caused by the disorder of charge separation between  $P_{680}^*$  and Pheo. In the state  $P_{680}Q_A^-$ , there is no photochemical transformation of energy. The intermediate Pheo acts as the mediator between  $P_{680}$  and  $Q_A$  and promotes the primary charge separation (forming  $P_{680}^+Pheo^-Q_A^-$ ). It is assumed that  $F_V$  should be “recombinant luminescence” during the transition  $P_{680}^+Pheo^-Q_A^- \rightarrow P_{680}^*PheoQ_A^-$ . Consequently, the decrease in  $F_V$  value directly indicates the suppression of PS-2 activity and the damage of  $e^-$  transport from  $P_{680}$  to  $Q_A^+$  because of inhibition of charge migration between  $P_{680}$  and Pheo. The same follows from observation of the absorption signal at  $\lambda = 540\text{--}560$  nm.

The ratio  $F_V/F_m$  is an indicator of the high efficiency of primary reactions in PS-2, and for intact chloroplasts, it is close to 0.832. Deviation of the experiment value from the control by 0.03–0.04 relative units is considered significant and testifies to the PS-2 response to the influence of external stress factors. A decrease in this ratio emphasizes the existence of a negative reaction of the photosynthetic apparatus to the action of EFEs, which is connected with the PhIn effect (illustrated by the necessary evidence as literature data). The transition from PhIn to the reversible restoration of ETC activity directly correlates with an increase in the ratio  $F_V/F_m$ . A change in  $F_V$  yield is also caused by energy transformation in PS-2 and indicates the presence of minimal non-photochemical processes. As can be seen in Fig. 2.3, the damaging influence of environmental factors on leaves usually reduces the  $F_V$  yield, which speaks for the existence of primary damage and its localization near the PS-2 RCs. A decrease in the ratio of  $F_{V \text{ experiment}}$  to  $F_{V \text{ control}}$  (Table 2.2) also emphasizes the suppression of PS-2 activity in the experiment and corresponds to the earlier-stated proposition (Baranov et al. 1974, 1975; Saakov et al. 1975; Saakov 1987, 1990; Saakov and Leontjev 1988). A high  $F_V$  value (including the  $F_V^t$  value) is connected to a low value of  $q_E$  and high utilization of the energy in the Calvin cycle, correlating with a decrease in the membrane proton gradient due to ATP formation.

After  $F_V$  decrease (3 min), the actinic light flux ( $180\text{--}1,100 \mu\text{E}/(\text{m}^2 \text{ s})$ ) was switched on and induced the  $F_{V1}$  level; after 30 s a number of saturating impulses ( $F_V^t$ ) of 1 s duration were also switched on (Fig. 2.3). These impulses together with actinic light flux promoted complete reduction of the  $Q_A^-$  acceptor and RC closing. The higher the  $F_V^t$  amplitude and the closer it is to the  $F_{V1}$  level, the larger the probability of  $Q_A^-$  pool reduction, of high ETC activity, of a decrease in  $q_E$  value, and activation of the Calvin cycle. It is especially necessary to emphasize the very similar levels of  $F_V^t$  under the influence of temperature and  $\gamma$ -radiation. Because the  $q_E$  value correlates with energizing of the thylakoid membrane, that is, with a light-excited proton gradient, it will be higher for a higher proton gradient and lower ATP

synthesis. The influence an EFE on a leaf results in an increase in  $q_E$  value, together with a decrease in the yield of  $F_V$ ,  $F_{V1}$ , and  $F_V'$  (Fig. 2.3), which proves the existence of primary damage and its localization near PS-2 RCs.

It is possible to speak about the presence of a functional link between the activities of PS-2 and other components of the photosynthetic ETC with a certain degree of confidence; the changes in  $F_V$ ,  $F_{V1}$ ,  $F_V'$ , and  $F_m'$  show the activity of the photosynthesis process as a whole. This supports the idea that increased temperature leads to an electron transport decrease at saturating light flux intensities. The damage to energy transmission between PS-2 and PS-1 is the primary event correlating with electron transport inhibition, termination of photophosphorylation, suppression of reducer formation, and suppression of photosynthesis intensity. The influence or aftereffect of an EFE reduces  $F_V/F_m$  for all investigated objects of different resistance degree, depending on the depth of the damage and efficiency of adaptive reactions at  $F_V$  quenching (Saakov 1971a, b, 1987, 1990, 1993a–d, 1998a, b, 2000a–e, 2001a, b; Baranov et al. 1974–1976; Saakov et al. 1975, 1993; Saakov and Leontjev 1988; Saakov and Baranov 1987; Saakov and Barashkova 1999; Saakov and Shiryayev 2000; van Kooten and Snel 1990a).

We have described the essence of the technique in detail to acquaint the reader from the outset with the principles of the analysis and methods of calculating results. Furthermore, in the course of describing experiments, we will repeatedly but briefly backtrack to features of obtaining and interpreting experimental data; the reader should not consider this to be distrust concerning their understanding of the research.

### **2.2.1 Influence of Negative Temperatures on the Kinetics of Pulse-Amplitude Modulated Fluorescence Parameters ( $F_0$ , $F_m$ , $F_V$ )**

In Russia, plant cell tolerance to the influence of environmental stress factors of anthropogenous and natural origin is a problem of paramount importance because a combination of the very diverse set of climatic zones, soil features, and climatic and technogenic factors of the negative orientation create a constant threat to cultivated and wild plants. To understand the processes of plant green cell tolerance and adaptation, there have been numerous studies of the deep mechanisms at the heart of green cell adaptive reactions to the influence of EFEs.

It is necessary to emphasize and remind that, in speaking of (plant resistance) tolerance and adaptation, it is necessary to (1) differentiate very accurately and carefully between the *energy reactions* and *fermentative–biochemical reactions* of metabolism in chloroplasts; (2) characterize the mitochondrial energy reactions of a protoplasm and its organelles; (3) define the morphological changes in separate bodies of plants; and (4) describe the character of plant productivity as a whole, distinguishing the economic crop and the usual increase in vegetational mass.

We point out that in articles and discussions, all four of the above-listed problems often form a heterogeneous conglomerate of confused theoretical assertions, without division of the primary and secondary processes forming the basis of green cell's

relations with environment, and this results in miscommunication (Schindler and Lichtenthaler 1990) because of uncoordinated positions and confused terminology.

Any theoretical constructions in science that are not characterized by strict mathematical formalization need much and many-sided experimental evidence. From this point of view and due to the attractive universality, the concept of the energetic basis of the *Procarvota* and *Eucaryota* green cell's resistance (Saakov 2000a–e) also needs its evidential value strengthening, especially when considering the influence of negative temperatures on photosynthesizing cells. This problem is important in Russia in connection with spring and autumn morning frosts, when the short-term impact of negative temperature on vegetational bodies and leaves can lead to the death of plants.

The definite answer, which would exclude the possibility of contradictory interpretation of the influence of negative and low positive temperatures on the yield character of signal harmonics of PAMF, was not obtained in vivo (Krause and Somersalo 1989; Schindler and Lichtenthaler 1990; Snel and van Kooten 1990). From this point of view, we began to analyze a number of herbaceous and woody plants, investigating the response of their photosynthetic device to a short influence of negative temperatures in the range  $-7$  to  $-18$  °C, which can be inherent in morning frosts. The work was carried out under late autumn conditions in regions of the Schwarzwald and southern Germany, when in nature and in a botanical garden there were enough objects with unfallen foliage.

Great success in studying the response of green cells of higher and inferior plants to EFE influence became possible due to the development of the pulse-amplitude modulated fluorescence method, allowing results to be obtained about the reaction of the photosynthetic device to the chosen influence type quickly and in field conditions (Schreiber and Bilger 1987; Schreiber 1986; Saakov et al. 1993). The possibility of this research is caused by the existence of chlorophyll *a*, the presence of which unites autotrophic organisms such as *Cyanophyceae* in *Procarvota* and *Vegetalia* in *Eucaryota*.

The stationary ( $F_0$ ), variable ( $F_v$ ), and maximum ( $F_m$ ) fluorescence associated with those *functional* changes of the photosynthetic device, which take place *before structural* changes (Saakov 1993a–d), were registered with the pulse fluorometer Walz 101-103 (Effeltrich, Germany). The convenience of the method and the speed of obtaining results about changes in main measured parameters for an intact leaf were checked in detail in many laboratories of the USA and Europe. The calculation of photochemical ( $q_q$ ), non-photochemical ( $q_E$ ), and other coefficients of fluorescence quenching and the interpretation of their changes were carried out with the help of the accepted technique (Saakov 2000a–e; Schreiber and Bilger 1987; Schreiber et al. 1997a; Saakov et al. 1993). Separation of fluorescence from the much stronger excitation light is attained by the application of primary optical filters transmitting the excitation light ( $\lambda < 670$  nm) and of secondary filters transmitting the long-wave spectral area ( $\lambda > 680$  nm) and protecting the photodetector from parasitic diffused light from the excitation source. Owing to the design features, detectors of the device are insensitive to external light and are recommended for field ecological research because they allow efficient comparison of the influence of many anthropogenous and natural EFEs using only one



characteristic sign. In addition, the received results are easily digitalized and easily entered into information computer systems for further processing.

Objects of research different in tolerance were chosen: leaves of haricot *Phaseolus vulgaris*, tobacco *Nicotiana tabacum*, dandelion *Taraxacum officinale*, acacias *Robinia pseudoacacia*, nettles *Urtica dioica*, ivy *Hedera taurica*, Chinese sumac *Rhus succedanea*, beech *Fagus sylvatica*, yew *Taxus baccata*, monastery *Laurus nobilis*, ash tree *Fraxinus ornus*, etc.

The results of experiments on kinetics of signal harmonic change and the change in corresponding coefficients of fluorescence quenching under the influence of negative temperatures demonstrated functional damage of the photosynthetic device (see Fig. 2.4a–d and Table 2.2). The  $F_0$  level arising after the dark period of leaf adaptation, when photosynthetic membranes are in the non-energized state and all PS-2 RCs are open, is caused by radiation of excited chlorophyll *a* molecules before energy migration into RCs and when the first stable acceptor in PS-2,  $Q_A^+$ , is completely oxidized; at that point, coefficients  $q_q = 1$  and  $q_E = 0$  (Snel and van Kooten 1990; Saakov 2000a–c; Schreiber and Bilger 1987; Schreiber et al. 1986; Saakov et al. 1993).

From the data in Fig. 2.4 and Table 2.2, it follows that the  $F_0$  value ( $F_0'$  is the stationary fluorescence in any interval of time under actinic light influence) significantly increases with the action of negative temperature, which causes the change in the state of PS-2 pigments and leads to photoinhibition. At more intensive influence of the negative temperature or in the aftereffect process,  $F_0$  recession to a level below the stationary value is observed (Fig. 2.4b–d, designated by arrows with an asterisk) that, probably, is the result of the deep inhibition of  $Q_A$  reduction and accumulation of its oxidized store, caused by damage of the  $e^-$  transport to  $Q_B$ . The character of base fluorescence kinetics changes under the influence of negative temperatures after induction with actinic light (Fig. 2.4a–d) and is similar to that seen in response to the influence of ionizing radiation, dehydration, and high temperature (Saakov 2000c).

An impulse of saturating light of 2,500–3,000  $\mu\text{E}/(\text{m}^2 \text{ s})$  induces the maximum fluorescence, that is,  $F_m$  increases and its first increase, the variable fluorescence ( $F_v$ ), corresponds to the reduction  $Q_A^+ \rightarrow Q_A^-$  and results in closing of RCs in PS-2. Imbalance in the sequence of ETC reactions results in the impossibility of light energy capture from the antenna chlorophyll in RCs. Oxidized  $P_{680}^+$  does not catch energy, and the RC is closed and is characterized by the maximum fluorescence yield. Decrease in the  $F_v$  yield is connected with manifestation of the photoinhibition effect. With an increase in intensity of the EFE and its aftereffect, the  $F_v/F_0$  ratio decreases, which is one more substantial criterion speaking for damage in the PS-2 ETC and explained by reduction of the  $P_{680}^+\text{Pheo}Q_A^-$  link. The  $e^-$  transport in PS-2 RCs starts with charge separation between  $P_{680}$  in the first excited singlet state and pheophytin and is expressed in  $e^-$  transfer from the secondary donor Z to primary and secondary acceptors  $Q_A$  and  $Q_B$  of the quinone type. This is shown in Eq. (2.1), to which we will repeatedly return:

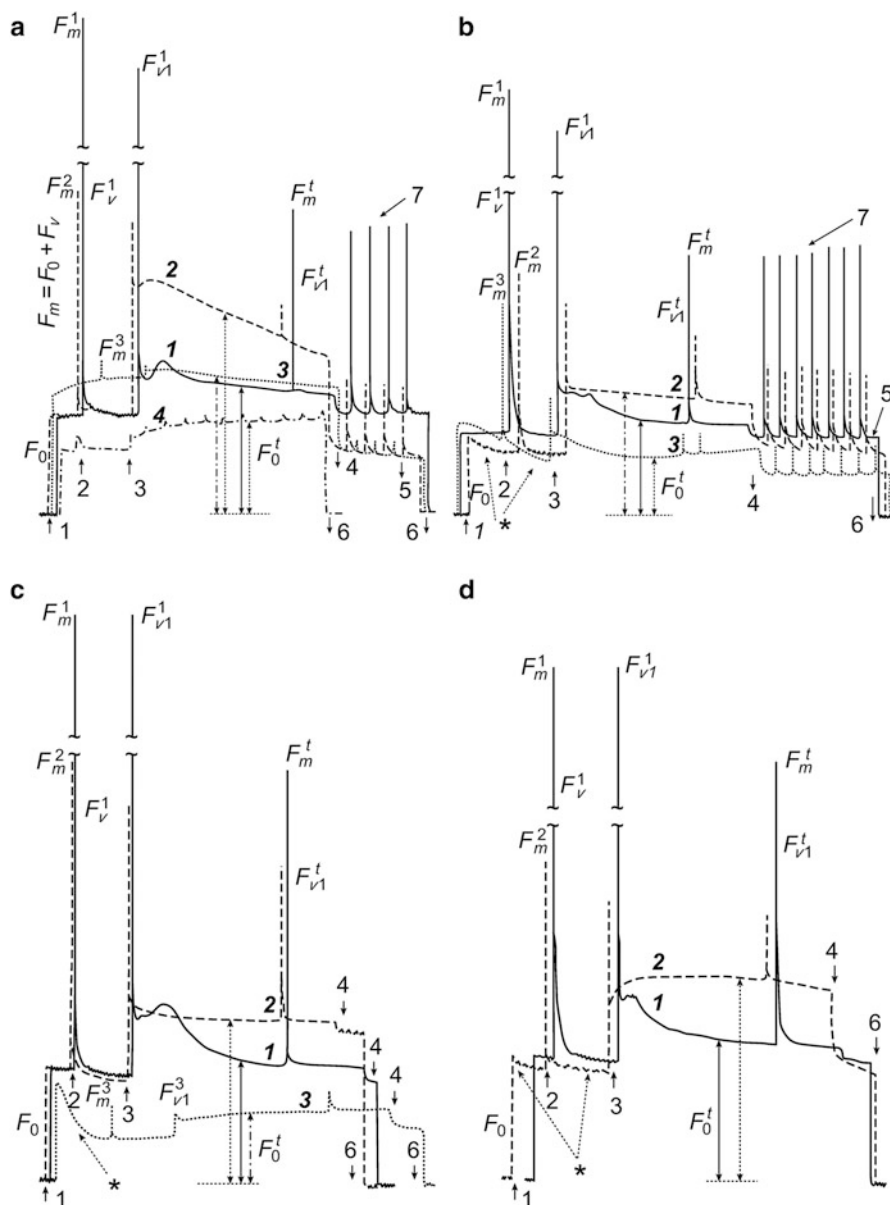
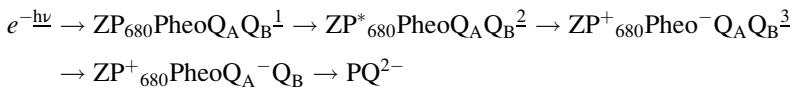


**Fig. 2.4** Character of signal harmonics change in PAMF under the influence of negative temperatures on leaves of (a) *Hedera taurica* ( $-12^{\circ}\text{C}$ ), 20 min; (b) *Fraxinus ornus* ( $-13^{\circ}\text{C}$ ), 13 min; (c) *Fagus sylvatica* ( $-14^{\circ}\text{C}$ ), 10 min; (d) *Robinia pseudoacacia* ( $-10^{\circ}\text{C}$ ), 2 min. Curves: 1 control; 2 experiment; 3 aftereffect of the negative temperature in 2 h; 4 the same, but after a day. The  $F_0$  level decreased almost to the initial value and rudiments of spikes appeared. Arrows: 1 input and 6 shutdown of the modulating light flux of frequency of 1.6 kHz ( $5-6 \mu\text{E}/(\text{m}^2 \text{s})$ ,  $\lambda < 670 \text{ nm}$ ) for determination of the dark base fluorescence  $F_0$ ; 2 input of the saturating impulse of the white light for determination of the  $F_m$  level; 3, 4 input and shutdown of the actinic light ( $1,500 \mu\text{E}/(\text{m}^2 \text{s})$ ); 5 shutdown of impulses of saturating light; 7 the spikes after shutdown of the actinic light. Arrows marked with an asterisk point to  $F_0$  decrease right after shutdown of the modulating light flux of 1.6 kHz, which confirms the damage to the antenna chlorophyll  $a$  pool



When PhIn is induced by intense light, damage to  $e^{-}$  transport at stages 2 and 3 is found and caused by the disorder of charge separation between  $P_{680}^*$  and Pheo. In state  $P_{680}Q_A^{-}$  there is no photochemical transformation of energy. The intermediate Pheo acts as the mediator between  $P_{680}$  and  $Q_A$  and promotes primary charge separation (forming  $P_{680}^+Pheo^{-}Q_A^{-}$ ). It is assumed that  $F_V$  should be “recombinant luminescence” during the transition  $P_{680}^+Pheo^{-}Q_A^{-} \rightarrow P_{680}^*PheoQ_A^{-} \rightarrow P_{680}PheoQ_A^{-}$ . Consequently, the  $F_V$  value decrease shown in Fig. 2.4 directly indicates the suppression of PS-2 activity and damage of  $e^{-}$  transport from  $P_{680}$  to  $Q_A^{+}$  because of inhibition of the charge migration between  $P_{680}$  and Pheo and retardation of the transformation of light energy into the energy of ATP chemical bonds, that is, there is disorder of the phototrophic function in RCs of PS-2, which corresponds to earlier-stated conceptions (Saakov 1976, 1987, 2000a–e; Saakov and Shiryaev 2000).

The ratio  $F_V/F_m$  is an indicator of the high efficiency of PS-2 primary reactions, and for intact chloroplasts, it is close to 0.832. The deviation of the experimental value from the control by 0.03–0.04 relative units is considered to be significant and testifies to the PS-2 response to the influence of external stress factors (Schreiber and Bilger 1993, 1987; Schreiber et al. 1994, 1997a, b). The transition from PhIn to the reversible reduction of ETC activity directly correlates with an increase in  $F_V/F_m$  (Table 2.2) and indicates the high efficiency of charge separation (Genty et al. 1989). A decrease in the ratio  $F_{V \text{ experiment}}/F_{V \text{ control}}$  (Table 2.2) also emphasizes the suppression of PS-2 activity in experiment, which corresponds to the earlier-stated proposition on localization of the EFE damaging influence (Saakov 1976, 1987, 2000c; Saakov and Shiryaev 2000). A high  $F_V$  value (including the  $F_V^t$  value, designated in English-language literature as “spikes”; Fig. 2.4, Table 2.2) is connected to a low  $q_E$  value. The high utilization of energy in the Calvin cycle correlates with a decrease in the membrane proton gradient due to ATP formation. The higher the  $F_{V1}^t$  amplitude and the closer it is to  $F_{V1}$ , the larger is the probability of a more complete  $Q_A^{-}$  pool reduction, of high ETC activity, of a  $q_E$  value decrease, and Calvin cycle activation. It is especially necessary to emphasize the very similar levels of  $F_V^t$  under the influence of negative temperatures and other EFEs (Saakov 2000c; Saakov and Shiryaev 2000). Because the  $q_E$  value correlates with the thylakoid membrane energizing (i.e., with the light-excited proton gradient), it will be higher for a higher proton gradient and lower ATP synthesis. The low level of PS-2 reduction unambiguously indicates its damage (Table 2.2). The influence of an EFE on a leaf results in an increase in  $q_E$  value, together with a decrease in the yield of  $F_V$ ,  $F_{V1}$ , and  $F_V^t$  (Fig. 2.4), which proves the existence of primary damage and its localization near to PS-2 RCs. The  $q_E$  relaxation is accompanied by the simultaneous activation of the Calvin cycle, coupled with ATP usage and a proton gradient decrease. The quick decrease in  $q_q$  in the first minutes of light exposure occurs due to ETC reduction. The change in

this coefficient by 0.03–0.04 relative units is significant and indicates the response of the photosynthetic device (Schreiber and Bilger 1993, 1987; Schreiber et al. 1997a, b). In the stationary state,  $q_q$  is usually approximately 0.8–0.9 relative units. When  $q_q = 0$ , there is no light energy transformation, and at  $q_q = 1$ , it is optimal. The increase in  $q_q$  takes place because of *re-oxidation* of  $Q_A^-$ . The low level of  $q_q$  shows the accumulation of electrons in the acceptor part of PS-2 and shows the high level of  $Q_A^-$  reduction and of the  $PQ^{2-}$  pool, that is, ETC rupture (Table 2.2, experimental variants). The high  $q_q$  value for well-illuminated plants indicates high levels of electron transport, NADPH/ $H^+$ , and intensity of photosynthesis (Table 2.2, controls). With the damaging influence of negative temperatures,  $q_q$  decreases, emphasizing suppression of the ETC activity, increase in the proton current, and  $e^-$  accumulation in the acceptor part of PS-2.

For a long time, there have been ambiguous ideas concerning the influence of low temperatures and frosts on the character of PAMF kinetics change (Snel and van Kooten 1990; Schreiber and Bilger 1987). Data presented in Fig. 2.4 and in Table 2.2, and also the results of our previous works (Saakov 2000a, b; Saakov and Shiryaev 2000), give grounds to suggest the similarity of damage mechanisms in ETC links in the region  $P^+_{680} \text{Pheo}^- Q_A^- \rightarrow P^*_{680} \text{Pheo} Q_A^- Q_B$  under the impact of negative temperatures and other EFEs of natural and technogenic origin. It allows us to reliably eliminate from discussion the statement on the exclusive PAMF invariance with the action of low temperatures and frosts, and to remove the problem of EFE damage specificity for separate components of PS-2 RCs. Serious support to our concepts was given by a work (Bukhov et al. 2001a) in which, with a method similar to ours, similar data were obtained on the change in variable fluorescence in spinach (*Spinacia oleracea*) under the influence of a scale of low positive and negative temperatures. There was a difference between our results and those of Bukhov et al. (2001a) only in the kinetics of the base, dark fluorescence values, which remained at the initial dark level with small fluctuations, whereas we observed  $F_0$  changes under the influence of actinic light. Probably there were also distinctions in experimental conditions because in the work of Bukhov and colleagues, measurements of FI kinetics were carried out against a background of temperatures (duration of thermal exposure was not specified) in the presence of the herbicide diuron, which impeded  $Q_A^+$  re-oxidization by the secondary acceptor  $Q_B$ . At the same time, rather numerous measurements performed in different laboratories (Snel and van Kooten 1990; Schreiber and Bilger 1987; Schreiber et al. 1997a, b) emphasized the high lability of the  $F_0$  level under EFE influence of natural and anthropogenous origin. The correct explanation for the found discrepancies demands additional experimental support.

Thus, in the described work, after investigation of a large variety of plant material, reliable data were obtained on the change in PAMF kinetics under the influence of negative temperatures. They can be taken as the basis for the diagnostics of green cell resistance to the impact of an extreme factor. The presented material gives an additional proof of rightness of the stated reasons concerning the primacy of the energetic basis for the resistance of *Procaryota* and *Eucaryota* green cells to extreme environmental effects and also about localization of the

damage induced by negative temperatures in PS-2 RCs (Saakov 2000a–e). The data presented can, to a certain degree, serve as the methodological management for works on selection of cultivars of cultivated plants tolerant to negative temperatures by analyzing the stability of their photosynthetic device, especially when using genetic engineering approaches.

### 2.2.2 Association of High Temperature Stress to the Signal Harmonics Change in Pulse-Amplitude Modulated Fluorescence ( $F_0$ , $F_m$ , $F_v$ )

To discover the possible localization of thermal influence in the system of interactions between photosystems and ATP synthesis (Weis 1981a, b), we carried out research on herbaceous and woody plants that were different in resistance to the influence of physiologically high temperatures. Our task was the profound application of the PAMF method for demonstration in vivo of the localization of stress-induced damage in a link of the ETC of photosystems. It should be noted that the great sensitivity of isolated preparations of PS-2 to EFEs is beyond doubt. It is necessary to emphasize that early experiments assessing the stability of photosystems were not performed in vivo (i.e., with a leaf) but with fragmentary preparations isolated as a result of a differential centrifugation of a chloroplast suspension.

We relied on earlier research (Semikhatova and Saakov 1962) and investigated the character of signal harmonic change in PAMF in the range of temperatures +35 to +45 °C. The registration of parameters  $F_0$ ,  $F_m$ , and  $F_v$  was carried out using the fluorometer Walz 101-103 (Effeltrich, Germany) (van Kooten and Snel 1990a; Schreiber et al. 1997). The method was proven in leading laboratories of Europe and the USA as accurate and fast for obtaining results about changes in the key measured parameters of an intact leaf or of suspensions of chloroplasts or algae. The calculation of photochemical ( $q_q$ ), non-photochemical ( $q_E$ ), and other coefficients of fluorescence quenching and the interpretation of their changes were performed using the accepted technique (van Kooten and Snel 1990b; Schreiber et al. 1997a, b). Detectors of the analytical device are insensitive to external light, and therefore, the device is recommended for field ecological research because it allows comparison of the influence of many technogenic and natural EFEs after analysis of only one characteristic feature. Obtained results are easily digitalized, which provides their easy input into computer systems for further processing. We performed experiments in Europe, because at that time there were stagnation and disorganization of this scientific area in Russia.

Objects of research were chosen to simultaneously compare leaves resistant and intolerant to high temperatures: the cultivar Saratovskaya 29 of wheat (*Triticum vulgare*), known for its resistance to drought and thermal influence; haricot *Phaseolus vulgaris*; tobacco *Nicotiana tabacum*; acacia *Robinia pseudoacacia*;

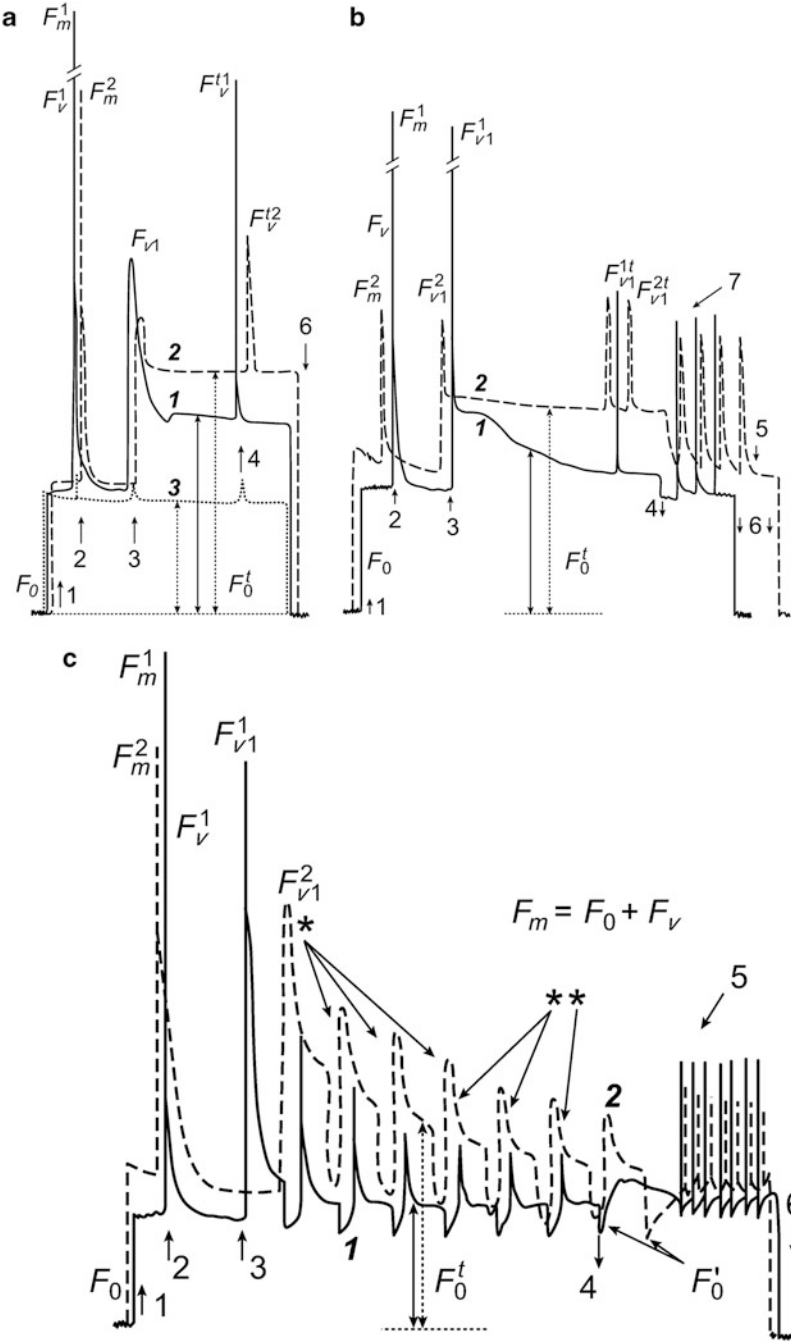
nettle *Urtica dioica*; pea *Pisum sativum*; bay laurel *Laurus nobilis*; ash *Fraxinus ornus*; clover *Trifolium* sp.; oak *Quercus robur*; etc.

In Figs. 2.5a–c and 2.6 and in Table 2.3, the block of data on features of PAMF change and coefficients of fluorescence suppression under the influence of physiologically high temperatures is presented.

The level of base dark fluorescence  $F_0$  is characterized by the open RC state before migration of electrons into open RCs due to excited chlorophyll *a* emission and further reduction of the first stable acceptor of PS-2  $Q_A^+ Q_A^-$ ; at this time, thylakoid membranes of the leaves adapted to darkness are in a non-energized state.

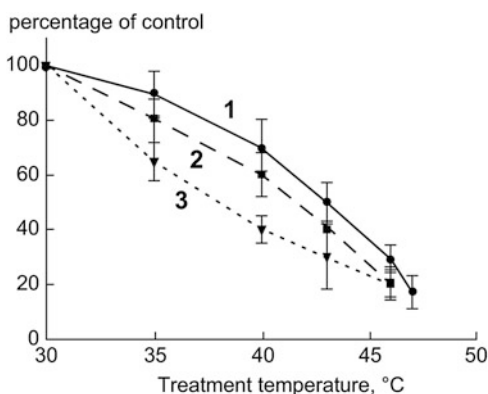
The initial saturating light impulse of 1 s duration and intensity of 2,500–3,000  $\mu\text{E}/(\text{m}^2 \text{ s})$  (Figs. 2.5 and 2.6) leads to an increase in maximum fluorescence ( $F_m$ ). Its first increase, the variable fluorescence ( $F_V$ ), corresponds to the level of  $Q_A^-$  reduction (Table 2.3) and is accompanied by RC closing. The change in  $F_V$  yield is caused by energy transformation in PS-2 and points to minimal non-photochemical processes (Snel and van Kooten 1990; Schreiber et al. 1997a, b). The intermediate Pheo works as the mediator between  $P_{680}$  and  $Q_A$  and promotes the primary charge separation (forming  $P_{680}^+ \text{Pheo}^- Q_A^-$ ). It is assumed that  $F_V$  should be a “recombinant luminescence” during the transition  $P_{680}^+ \text{Pheo}^- Q_A^- \rightarrow P_{680}^* \text{Pheo} Q_A^-$ . From this, the decrease in  $F_V$  directly indicates the suppression of functional activity of RCs of PS-2 and the damage of  $e^-$  transport from  $P_{680}$  to  $Q_A^+$ , coupled with the inhibition of charge migration between  $P_{680}$  and Pheo. This can be explained as follows: The quantum yield of the linear electron transport depends on the concentration of the RCs of opened PS-2, on the efficiency of acceptance of excitation energy by these open centers, and on the usage of the accepted excitation energy by the PS-2 complexes.

As follows from Figs. 2.5 and 2.6, the damaging impact of high temperature on leaves usually reduces the  $F_V$  yield, that is, indicates the existence of primary damage and its localization in PS-2 RCs (Snel and van Kooten 1990; Schreiber et al. 1997a, b). The decrease in the ratio  $F_{V \text{ experiment}}/F_{V \text{ control}}$  (Table 2.3) also emphasizes suppression of PS-2 activity in experiment. With a certain degree of confidence, it is possible to speak about the existence of a functional link between the activity of PS-2 and other photosynthetic ETC components; therefore, the changes in  $F_V$ ,  $F_{V1}$ , and  $F_{V'}^I$  are coupled to changes in the photosynthesis process activity as a whole (Fork et al. 1985; Snel and van Kooten 1990). In favor of this statement is the fact that increased temperature results in a decrease in the electron transport at saturating intensities of light flux. The damage to energy transfer between PS-2 and PS-1 is the primary event correlating with inhibition of electron transport, termination of photophosphorylation, suppression of reducer formation, and photosynthesis intensity (Armond et al. 1978; Monson et al. 1982; Saakov 2000a–e). The value of the ratio  $F_V/F_m$  is extremely important and is considered to be an indicator of photosynthetic function. It fluctuates for intact chloroplasts around 0.83 relative units (Snel and van Kooten 1990; Schreiber et al. 1997). A deviation of this coefficient from the control by 0.03–0.04 relative units significantly emphasizes the existence of a negative reaction of the photosynthesis machinery to external influences, as illustrated by the data in Table 2.3. The effect



Legend to Fig. 2.5 see p.70

**Fig. 2.6** Dynamics of the change in  $F_m$  (curve 1,  $n = 12$ ),  $F_{V1}$  (curve 2,  $n = 8$ ), and  $F'_V$  (curve 3,  $n = 8$ ) for *Nicotiana tabacum* leaves relative to control in response to a change in the influencing temperature. *Abscissa*: temperature in degrees; *ordinate*: percentage decrease relative to control



or aftereffect (Saakov 1999, 2000a–e) of high temperature reduces  $F_V/F_m$  for all investigated objects, differing in tolerance degree, depending on the depth of damage and effect of adaptive reactions at  $F_V$  quenching.

Suppression of the RC activity in PS-2 determined from  $F_V$  suppression is linked, first of all, with inhibition of the charge transfer between  $P_{680}$  and pheophytin (Saakov 2000a, b, 2001a, b; Saakov and Shiryayev 2000), that is, with the primary change in excited energy distribution between PS-1 and PS-2 during thermal influence, which is localized in RCs of PS-2. This moment is especially emphasized because we, for the first time, connected the *functional stability* of the photosynthetic device with the *activity* of the RCs and *damageability* of their link in the area  $P_{680}^+Pheo^-Q_A^-P_{680}^*PheoQ_A^-Q_B$ . This idea corresponds to the conceptions stated earlier (Saakov 2000a, b, 2001a, b; Saakov and Shiryayev 2000). Moreover, the  $F_V$  value of the control (including values of variable fluorescence at any time  $t = F_V^t$ , designated in English-language literature as “spikes”) and the index  $F'_m$  (Schreiber et al. 1997a, b) interrelated with the change in  $q_E$  value indicate the active utilization of energy in the Calvin cycle and simultaneous decrease in the membrane proton gradient interfaced to ATP formation (Saakov 2000c). From Table 2.3, it is seen that

**Fig. 2.5** (continued) Character of signal harmonics change in PAMF during the influence of high temperature on leaves of (a) *Solanum lycopersicum*, (b) *Robinia pseudoacacia*, and (c) *Laurus nobilis*. *Curves*: 1 control, 2 experiment for (a) +42 °C, 7 min; (b) +43 °C, 5 min; (c) +45 °C, 5 min. *Arrows* for a–c: 1 and 6, respectively, input and shutdown of the modulating light flux of frequency 1.6 kHz ( $0.5\text{--}0.6 \mu\text{E}/(\text{m}^2 \text{ s})$ ,  $\lambda \leq 670 \text{ nm}$ ); 2 input the saturating 1 s impulse of white light ( $2,500 \mu\text{E}/(\text{m}^2 \text{ s})$ ) for determination of  $F_m$  and  $F_V$  values; 3 and 4 (except a), respectively, input and shutdown of the actinic light ( $600 \mu\text{E}/(\text{m}^2 \text{ s})$ ); for a: 4 input of the 1 s impulse of the saturating light against actinic light; 6 simultaneous shutdown of the actinic and modulating light fluxes; for b: 5 shutdown of 1 s impulse of white light ( $2,500 \mu\text{E}/(\text{m}^2 \text{ s})$ ); 7 the level of 1 s spikes at switched shutdown of actinic light; for c: 3 and 4, respectively, input and shutdown of the actinic light with periods of light/darkness of 60/20 s ( $800 \mu\text{E}/(\text{m}^2 \text{ s})$ ); 5 the level of 1 s spikes after shutdown of the actinic light. *Arrows*: single asterisk indicates the start, double asterisks the development and recession of the slow component (Saakov 2000a–e, 2001a, b, Saakov et al 2012/2013), noticeable in b in the form of spike bifurcation.  $F_0$  is the base  $F_0$  level right after shutdown of the actinic light



**Table 2.3** Effects of high temperature (43°, 10 min) treatment on quenching coefficients of PAM fluorescence from leaves of various species<sup>a</sup>

Species	Experimental conditions	Coefficient (mean value; $n = 4-5$ , $p \leq 0.08$ )											
		$F_v/F_m$	$F_v^{exp}/F_v^{cont}$	PS-2 reduction (%)	$F_{max}/F_0$	$F_v/F_0$	$F_{v1}/F_v$	$F_{v1}/F_0$	$F_0^5/F_0$	$q_E^{5min}$	$q_q^{5min}$	Spikes 5 min (mm)	Spikes 6 min (mm)
<i>T. vulgore</i> cultivar Saratovskaya 29	Control	0.827	0.893	94	5.1	3.57	0.93	4.30	1.10	0.326	0.940	91	102
	Exp	0.802		83	4.5	2.70	0.82	2.70	1.24	0.52	0.830	83	89
<i>U. dioica</i>	Control	0.817	0.477	91	5.2	3.79	0.89	3.70	1.24	0.40	0.912	77	83
	Exp	0.679		72	3.15	1.90	0.79	1.90	1.70	0.72	0.715	45	53
<i>P. sativum</i>	Control	0.835	0.521	92.7	4.9	4.10	0.92	3.80	1.03	0.37	0.930	79	84
	Exp	0.737		76	3.7	3.10	0.81	1.95	1.63	0.79	0.770	49	51
<i>N. tobacum</i>	Control	0.812	0.534	89.3	5.3	4.60	0.88	3.71	1.11	0.47	0.888	81	86
	Exp	0.694		64	4.3	3.40	0.77	1.87	1.57	0.81	0.645	43	59
<i>Trifolium</i>	Control	0.832	0.645	92.4	5.2	4.05	0.92	3.90	1.07	0.42	0.930	75	81
	Exp	0.656		72	4.1	2.70	0.75	1.89	1.48	0.73	0.715	46	52
<i>Solanum lycopersicum</i>	Control	0.841	0.783	90.3	5.0	4.65	0.90	3.92	1.21	0.39	0.900	79	88
	Exp	0.779		80.1	4.3	3.40	0.79	2.21	1.32	0.52	0.801	63	69
<i>R. pseudoacacia</i>	Control	0.821	0.672	94	4.8	3.70	0.89	3.30	1.09	0.38	0.940	88	94
	Exp	0.784		56	3.6	1.90	0.78	1.88	1.50	0.49	0.570	46	71
<i>Fraxinus excelsior</i>	Control	0.819	0.691	89	5.4	4.2	0.91	3.74	1.12	0.41	0.891	78	83
	Exp	0.767		72	4.6	3.5	0.85	2.20	1.41	0.56	0.725	43	67
<i>Q. robur</i>	Control	0.824	0.911	88	4.9	3.95	0.87	3.90	1.20	0.40	0.884	76	83
	Exp	0.795		80	4.3	2.70	0.79	2.66	1.37	0.52	0.810	53	73

<sup>a</sup> $F_0^5$ ,  $q_E^{5min}$ ,  $q_q^{5min}$  and spike 5 min were calculated 5 min after switching the actinic light on; spike 6 min—6 min after switching the actinic light off

with an increase in the intensity of the influence of extreme factors, the  $q_E$  value also increases and points to suppression of the Calvin cycle activity. The  $F_V/F_0$  ratio decreases, which is one more criterion proving the damage in ETC of PS-2 and is a result of the reduction in the link  $P_{680}^*PheoQ_A^-$  (Weis 1981; Saakov 2000c). Simultaneously, the level of PS-2 reduction (Table 2.3) decreases.

Switching on the actinic white light flux of intensity  $1,100 \mu E/(m^2 s)$  induces the FI  $F_{V1}$  level arising after  $F_V$  recession, and the ratios  $F_{V1}/F_V$  and  $F_{V1}/F_0$  (Table 2.3) seem to be reliable indicators characterizing the activity of RCs of PS-2 ETC (Saakov and Shiryaev 2000). The higher the amplitude of  $F_V^t$  impulses and the closer it is to the  $F_{V1}$  level, the higher the probability of more complete reduction of the  $Q_A^-$  pool and the high activity of ETC and the Calvin cycle. The calculation of the FI coefficient at the fifth minute of the PAMF signal harmonics registration, when the most significant difference in  $F_0$  and  $F_0^{5(t)}$  levels appears, gives the  $q_E$  value in control and experiment (Table 2.3), which also indicates a decrease in the Calvin cycle activity with EFE influence.

From the figures and Table 2.3, it follows that, with an increase in the negative impact of external factors, the coefficient  $F_0^{5(t)}/F_0$  increases, that is, the  $F_0^{5(t)}$  level (to the fifth minute of the measurement of PAMF signal harmonics) becomes significantly higher than  $F_0$ . In close connection with the value of coefficient,  $F_{V1}$  is the change in  $F_V^{5(t)}$  (the value of spikes at the fifth minute) induced by the saturating light impulse against the actinic light flux (Figs. 2.5, 2.6 and Table 2.3) or after switching off the actinic light flux (spikes at sixth minute). The  $F_V^t$  value is sensitive to thermal processing and is already suppressed in response to 70 % relative humidity and  $\gamma$ -radiation (Monson et al. 1982; Saakov 2000a, c). The effect and aftereffect of  $\gamma$ -radiation correlate with the influence of temperature, fumigation, dehydration, and herbicides (Snel and van Kooten 1990; Schreiber et al. 1997a, b; Saakov 2000c), which reduce  $F_V^t$  and  $q_E$  levels, that is, decrease the activity of the Calvin cycle and  $q_q$ . This  $F_V^t$  change demonstrates the depth of the time-evolved damage of energy links of PS-2 RCs. Thus, the manifestation of non-specificity of the kinetics of the change in PAMF signal harmonics to the impact of various EFes, and features of the changes in coefficients  $F_m$ ,  $F_V$ ,  $F_{V1}$ ,  $F_V^t$ ,  $F_0$ , and  $F_0^t$  point to the relation of the found disorders to damage of specific components of PS-2 RCs (Saakov 2001a, b).

The high  $F_V$  value (including spikes at  $F_V^t$ ) is defined by the low  $q_E$  value and high utilization of energy in the Calvin cycle. The high temperature leads to an increase in  $q_E$  (to 0.6–0.75) that causes the  $F_V^t$  decrease and an energized thylakoid membrane. In this case, ETC inhibition occurs, probably when the Calvin cycle is unable to work as an electron acceptor. The  $q_E$  relaxation is accompanied by simultaneous switching on of the Calvin cycle and the ATP use coupled to it and by a decrease in the proton gradient. At thermal processing, the  $q_E$  relaxation is suppressed (Table 2.3), testifying to restriction of the Calvin cycle activity. This restriction probably precedes damage at the level of PS-2 RCs and is expressed as an increase in  $F_0$ ,  $F_V^t$  reduction, and  $F_m^t$  decrease with a corresponding increase in  $q_E$ .

It is reasonable that EFE influence affects the orientation of the photosynthesis carbon metabolism, but these are already stages of secondary reactions because the initial non-specificity is defined by primary reactions of the damage of the ETC RC functional state, arising ATP deficiency, and coupled accumulation of ADP and orthophosphate in chloroplasts. It is possible to prevent these phenomena by introduction of exogenous ATP in a suspension of chloroplasts. Earlier we wrote about pre-lethal increasing of the respiration intensity together with a simultaneous decrease in photosynthesis in a leaf (Saakov 1994) in response to radiation damage. Probably, it is defined by the intake of phosphoglyceric acid funds into the cytoplasm, and during the processes of glycolysis and respiration, these funds form pools of phosphoenolpyruvate and pyruvic acid, the synthesis of which is connected to ATP formation. These reactions couple together the metabolic and energy pathways of photosynthesis and respiration. The known activation of the intensity of glycolysis and respiration in response to a decrease in illumination correlates well with the increase in respiration in response to radiation impact on plants and also under the influence of other EFEs (Saakov and Shiryaev 2000) and can be considered as a special compensatory replacement of the ATP deficiency that arises with a break in the photosynthetic ETC.

From this point of view, the role of glycolysis is more significant. With an increase in the intensity of the influence of EFEs, glycolysis becomes the dominating ATP supplier, suppressing the role of oxidative phosphorylation. The manifestation of alternative pathways of energy supply in a cell under EFE influence has important biological value, because it allows maintenance of cellular energy resources at a stationary level during the midday depression of photosynthesis and under the influence of other environmental factors (Semikhatova and Saakov 1962). This implies the biological expediency of activation of energy processes in mitochondria and cytoplasm to supply damaged chloroplasts with ATP funds for the realization of carbon metabolism reactions in the Calvin cycle. Data on the use of exogenous funds of ATP and its penetration in chloroplasts has already become axiomatic material and does not raise doubts.

Thus, the presented results and some of our other works (Saakov 2000a–c, 2001a, b; Saakov and Shiryaev 2000) and reviews of European literature (Havaux 1988; Heber and Santarius 1973; Fork et al. 1985; Gounaris et al. 1983; Monson et al. 1982; Schreiber et al. 1997) are aligned in that the tolerance and reparation reactions of a green cell to the effect of high temperature depend, mainly, on primary damage to the chain  $P_{680} Q_A Q_B P Q^{2-}$  in the link  $P^+_{680} Pheo^- Q_A^- P^*_{680} Pheo Q_A^-$ . This conclusion is of general meaning in the sense that it interfaces the formation of ATP, formation of the reducer, and activity of the Calvin cycle, damages to which are secondary. Available data also suggest the possibility of close interrelation of vegetational cell resistance and the energy chain of mitochondria. The presence of chlorophyll *a* defining the FI yield of blue-green algae (*Cyanobionta*, *Procaryota*) suggests that ETC disorder mechanisms in response to the damaging influences of environmental factors of natural and technogenic origin are similar to those in *Phycobionta* and *Embryobionta* (*Vegetalia* from *Eucaryota*) and also in *Procaryota*.

Thus, there is the high probability that any factor influencing the efficiency of the excitation energy capture by RCs of open PS-2 will affect the speed of the electron transport through the PS-2 centers and be manifested as changes in FI parameters  $F_m$  and  $F_v$ . The conclusion about the primacy of damage to the link  $P_{680}^+Pheo^-Q_A$   $P_{680}^*PheoQ_A^-$  of the PS-2 RCs under the influence of an EFE can be used in practice for the selection of cultivars genetically modified with polygene systems and with transformed electron transport systems according to the tolerance of the considered characteristic.

### ***2.2.3 The Coupling of Mechanisms of Green Cell Resistance to Changes in the Pulse-Amplitude Modulated Fluorescence Parameters Under the Influence of Atmospheric Drought***

The ways that plants adapt to conditions of soil and atmospheric drought are very various. It is necessary to remember the coupling of the influence of atmospheric drought with, as a rule, a simultaneous temperature increase in a lamina and accompanying overheating and dehydration (Saakov 2002a–c). The point of view of researchers on the drought resistance of plants changed with developments in the methodological basis for experimental studies and with scientific successes in adjacent areas of the physiology and biophysics of plants. In this regard, in this section we will focus on changes in the functional reactions of a native leaf in connection with the main processes of light energy transformation into the energy of chemical bonds, that is, with the performance of or damage to the phototrophic reactions inherent in all green cells (Saakov 1993a–d, 2000a–e, 2001a, b). Emphasis will be placed on the assessment of the possibility and primacy of damage to the electron transfer link in the system  $P_{680} \rightarrow Q_A$ , since the results of earlier research suggested that this is the link most subjected to EFEs of natural and anthropogenous origin (Schreiber et al. 1997a, b; Saakov 2000a–e, 2001a, b, 2002a–c).

During short atmospheric drought, the considered functional reactions can be defining. Considering the connection between changes in the parameters of PAMF signal harmonics and the processes of carbonic acid fixation by a leaf, there was an attempt to connect the known midday minima of photosynthesis intensity with the processes of damage to the activity of the ETC, arising as a result of dehydration of a lamina. We considered the variant of *acute* (coming quickly and lasting for a short time) atmospheric drought, when radical changes in cell metabolism processes and in the synthetic activity of a green cell have not yet occurred, and the regulation and restoration of changes are still possible through repair of ETC energetics with formation of ATP and a reductant.

As objects of research, we chose leaves different in their tolerance to atmospheric drought: the cultivar Saratovskaya 29 of wheat (*Triticum vulgare*), a barley mutant lacking chlorophyll *b* (*Hordeum vulgare*, cultivar Donaria №. 3613), oak (*Quercus robur*), bay laurel (*Laurus nobilis*), tomato (*Lycopersicon esculentum*),

nettle (*Urtica dioica*), acacia (*Robinia pseudoacacia*), clover (*Trifolium* sp.), haricot (*Phaseolus vulgaris*), tobacco (*Nicotiana tabacum*), and some others.

The specifics of the change in the character of stationary dark FI ( $F_0$ ), the maximum FI at saturating pulse light flash ( $F_m$ ), variable FI ( $F_v$ ), FI in response to the action of actinic light ( $F_{v1}$ ), and in a combination of actinic light with a saturating light impulse ( $F'_{v1}$ ) in response to atmospheric drought were registered with the pulse fluorometer Walz 101-103 (Effeltrich, Germany). We consider it necessary to note the great convenience of this method, the speed of obtaining data on changes in key measured parameters of an intact leaf, and the possibility after a specified time interval to come back to registration of *repeated* characteristics of this leaf. The calculation of photochemical ( $q_q$ ), non-photochemical ( $q_E$ ), and other coefficients of FI quenching and the interpretation of their changes were carried out by the accepted technique described earlier.

We generally follow the nomenclature for signals of PAMF suggested by van Kooten and Snel (1990a) and supported by other experts (Schreiber and Bilger 1993, 1997). The separation of the FI signal from the much more intensive excitation light is achieved by the application of primary optical filters with the excitation light transmission ( $\lambda < 670$  nm) and secondary filters with transmission in the long-wave spectral area ( $\lambda > 680$  nm) to protect the photodetector from parasitic diffused light from the excitation source. Owing to design features, the detectors of the device are insensitive to external light. The device is recommended for field ecological researches because it allows comparison of the influence efficiency of many technogenic and natural EFEs using *only one parameter*. In addition, obtained results are easily digitalized and entered into information computer systems for further processing. The performance of large-scale and easily comparable research in different laboratories on all continents is possible, thanks to the existence of chlorophyll *a*, the presence of which unites autotrophic organisms, such as *Cyanophyceae* in *Procaryota* and *Vegetalia* in *Eucaryota*.

The measurement of photosynthesis intensity was carried out with a radiometric method using  $^{14}\text{CO}_2$  (Saakov 1959, 1987) and in some cases with the Warburg method using vessels designed to allow introduction of the fiber-glass cable of the Walz 101-103 device directly into the vessel (Saakov and Shiryaev 2000). During the period of influence of a warm air current and a “dry wind,” the leaves were kept in the dark. After a 1 s impulse of light, they were irradiated with actinic light or by a combination of the actinic light with a subsequent series of 1 s impulses of white light (Saakov 1993a–d). As a result, the relative number of light quanta effectively used in PS-2 by virtue of ETC saturation and active reduction of  $Q_A^+$  and  $Q_B^+$  increases. Experimental plants reacted to the influence of the dry wind by moisture reduction in leaf tissues, which was registered as a percentage of the initial weight of the leaf (Table 2.4). The plants reacted differently; most significant moisture loss was from *U. dioica*, *Trifolium* sp., and *N. tabacum*, with smaller water loss from *L. nobilis* and *Q. robur* (Table 2.4). Results of the experiments are presented in Figs. 2.7, 2.8, 2.9, and 2.10 and in Table 2.4.

**Table 2.4** Effect of atmospheric drought (10 min) on the changes in coefficients of quenching of PAM fluorescence<sup>a</sup>

		Coefficient (mean value; $n = 4-5, p \leq 0.01$ )											Spikes 5 min (mm)	Spikes 6 min (mm)		
		% of leaf humidity in exp.	$F_v/F_m$	$F_{v1} \ h/2$ (mm)	$F_v \ exp/F_{v \ cont}$	PS-2 reduc. (%)	$F_m/F_0$	$F_v/F_0$	$F_{v1}/F_v$	$F_{v1}/F_0$	$F_0^5/F_0$	$q_E^{5min}$			$q_q^{5min}$	
Object		Control	0.827	5		0.893	90	5.1	3.57	0.91	4.30	1.10	0.426	0.880	92	101
	<i>Q. robur</i>	70	0.812	16			77	4.5	2.90	0.83	2.90	1.24	0.53	0.810	82	87
<i>L. nobilis</i>		Control	0.817	9		0.827	89	5.2	3.79	0.87	3.70	1.23	0.40	0.90	77	85
	73		0.779	14			72	4.1	2.06	0.79	2.90	1.72	0.48	0.725	66	65
<i>T. vulgore</i> № 29		Control	0.835	4		0.791	87	4.9	4.10	0.94	4.10	1.13	0.37	0.880	78	87
	69		0.797	15			73	3.9	3.29	0.79	2.80	1.23	0.49	0.760	69	56
<i>L. esculentum</i>		Control	0.841	5		0.778	90.3	4.9	4.56	0.88	3.92	1.21	0.39	0.900	76	88
	61		0.789	18			68	4.1	2.96	0.72	2.41	1.32	0.64	0.70	66	73
<i>R. pseudoacacia</i>		Control	0.821	6		0.664	92	4.7	3.92	0.87	3.50	1.09	0.41	0.920	88	92
	45		0.789	20			56	3.2	2.10	0.72	1.78	1.50	0.49	0.575	54	73
<i>Ph. vulgaris</i>		Control	0.819	7		0.691	89	5.2	4.37	0.86	3.74	1.12	0.46	0.891	79	85
	40		0.758	19			62	3.7	2.35	0.72	2.20	1.65	0.66	0.625	44	65
<i>H. vulgare</i> № 3613		Control	0.815	9		0.622	84	5.1	3.1	0.89	3.9	1.37	0.37	0.79	80	96
	42		0.770	19			59	3.6	1.8	0.67	3.21	1.47	0.71	0.50	63	71
<i>N. tobacum</i>		Control	0.812	8		0.544	87	5.2	4.62	0.88	3.71	1.12	0.47	0.818	81	96
	39		0.578	21			46	3.4	2.32	0.70	1.67	1.57	0.81	0.645	40	57
<i>U. dioica</i>		Control	0.814	7		0.561	88	4.9	3.95	0.83	3.90	1.22	0.40	0.884	72	89
	34		0.656	25			50	3.2	1.70	0.66	1.66	1.87	0.68	0.690	49	72
<i>Trifolium</i> sp.		Control	0.830	8		0.545	90	5.1	4.05	0.92	3.94	1.18	0.42	0.910	73	87
	36		0.645	24			61	3.0	1.53	0.61	1.79	1.56	0.74	0.700	42	49

<sup>a</sup> $F_0^{5\min}$ ,  $q_E^{5\min}$  and spike 5 min were calculated 5 min after switching the actinic light on; spike 6 min—6 min after switching the actinic light off

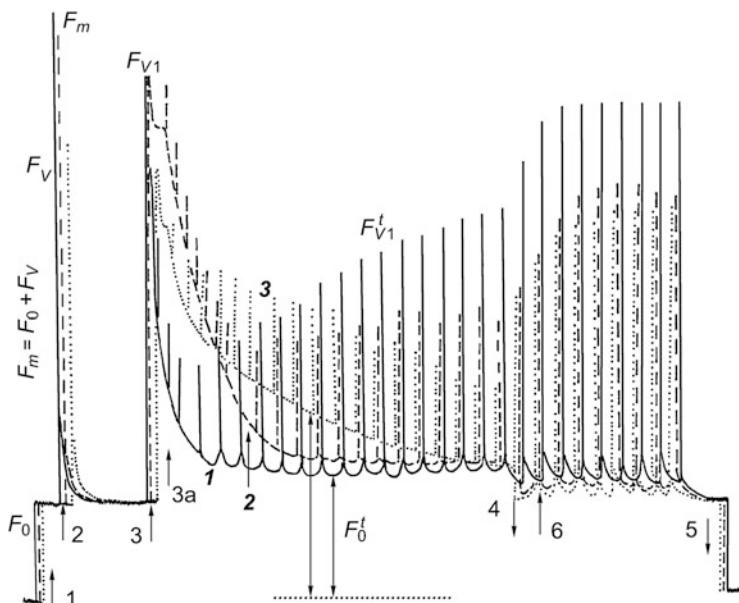


**Fig. 2.7** The character of signal harmonics change in PAMF of a leaf of *Nicotiana tabacum* in response to dehydration. *Curves*: 1 control; 2 experiment: dehydration to 45 % of the initial state; 3 dehydration to 30 % of the initial state. *Arrows*: 1 and 5, respectively, input and shutdown of the modulating light flux of frequency of 1.6 kHz ( $5 \mu\text{E}/(\text{m}^2 \text{ s})$ , with  $\lambda < 670 \text{ nm}$ ); 2 input of the saturating 1 s impulse of white light ( $2,500 \mu\text{E}/(\text{m}^2 \text{ s})$ ) for determination of  $F_m$  and  $F_V$  values; 3 input, 4 shutdown of the actinic light ( $1,200 \mu\text{E}/(\text{m}^2 \text{ s})$ ); 3a input after 30 s of 1 s impulse of the saturating light against the actinic light for determination of  $F_V^t = F_V^t$  values; 6 input of the 1 s impulses of the saturating light after shutdown of the actinic light

It is necessary to remember that the parameters and PAMF configuration are substantially defined by the physiological features of a leaf and depend on its genotypic and phenotypic features. The PAMF method enables the same leaf to be used to compare PAMF contour changes caused by the EFE effect or aftereffect in control and experimental conditions. One such induced PAMF contour change is the change in band half-width, described by the height of  $F_{V1}$  and course of the descending curve  $F_0$  ( $F_0^t$ ), induced by actinic light flux under the influence of the stress factor (Saakov 1993a–d, 2000a–e).

We can see the characteristic change in the considered coefficient ( $F_{V1} h/2$ ) under the influence on the green leaf of  $\gamma$ -radiation, high and low temperatures, and also under the influence of excess  $\text{Na}^+$ ,  $\text{Cl}^-$ , and  $\text{SO}_4^{2-}$  ions (Saakov 1993a–d, 2000a–e, 2001a, b, 2002a–c; Saakov and Shiryaev 2000). We can recommend with a high degree of confidence the coefficient  $F_{V1} h/2$  as a criterion to characterize the level of damage of the photosynthetic device of a green cell under the influence of EFEs of natural or technogenic origin.

The  $F_0$  level of base (dark) FI indicates the openness of RCs of PS-2 before electron migration into open RCs under the influence of the light impulse and the

**Fig. 2.8** The character of signal harmonics change in PAMF of a leaf of

*Lycopersicon esculentum* in response to dehydration.

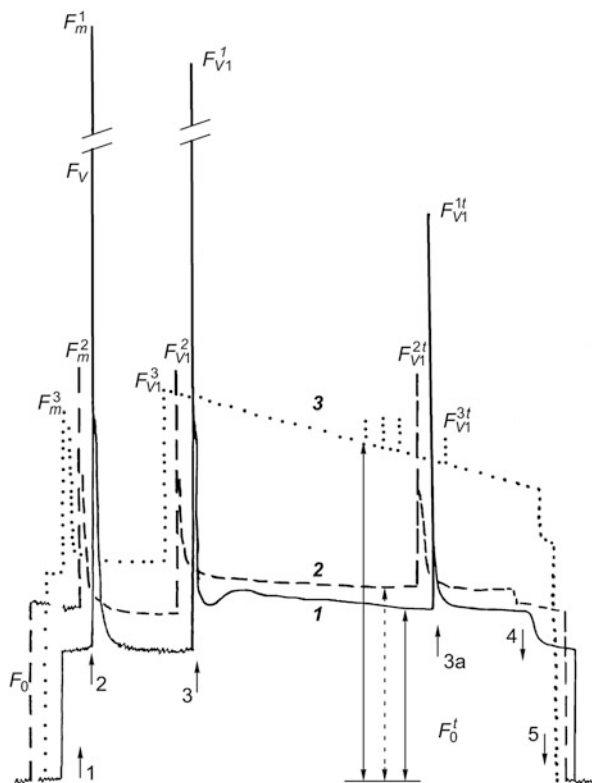
Curves: 1 control;

2 experiment: dehydration to 55 % of the initial state;

3 experiment, dehydration to 38 % of the initial state

(17 min of the “dry wind” influence. Arrows: 1, 2, 3,

3a, 4, 5, 6 as in Fig. 2.7



emission of excited chlorophyll *a* and before the reduction of the first stable acceptor  $\text{PS-2 } \text{Q}_\text{A}^+ \rightarrow \text{Q}_\text{A}^-$  caused by this migration.  $F_0$  quenching corresponds to a decrease in the absorbed light energy directed to PS-2. From the data in Table 2.4 and the figures, it follows that, with an increase in the negative influence of the dry wind, the value of coefficient  $F_0^5/F_0$  increases, that is, the height of  $F_0^5$  after the cell damage tends to increase, emphasizing PS-2 inactivation accompanied by increasing  $F_0(F_0^t)$ . In this regard, there is a direct dependence between the increase in coefficient  $F_{V1} h/2$  and coefficient  $F_0^5/F_0$ .

The dependence of the  $F_0^5$  height on the dose of  $\gamma$ -radiation impacting on the photosynthetic device (Saakov 1993a–d, 2000a–e) was confirmed for the influence of atmospheric drought. Taking into account data on the influence of fumigation and herbicides (Saakov 1993a–d), there is a high probability of the reliable application of coefficient  $F_0^5/F_0$  for characterization of the openness state of RCs of PS-2 and the *oxidization degree*. The ratio  $F_m/F_0$ , similarly to the ratio  $F_V/F_m$ , allows conclusions to be made about PS-2 activity. For undamaged (control) plants,  $F_m/F_0$  is approximately four to five times as in experiment much (Table 2.4); for slightly damaged plants, the coefficient  $F_m/F_0$  on average is reduced by 15–22 % compared with controls; and for the damaged plants, it decreases by 30–40 % (Table 2.4).



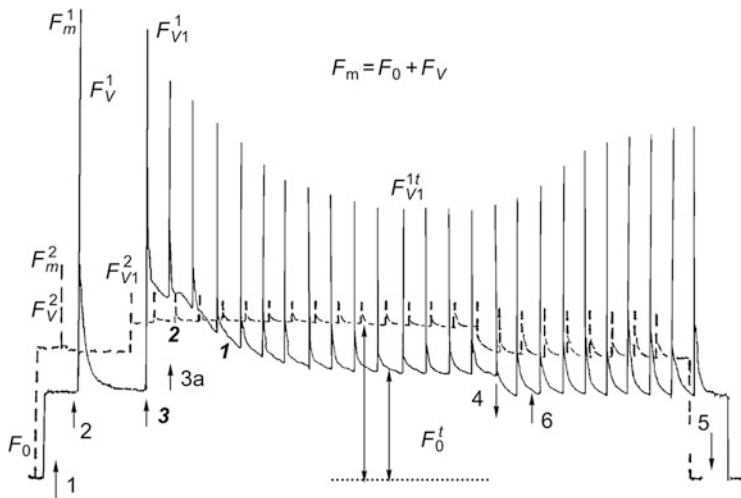


**Fig. 2.9** The character of signal harmonics change in PAMF of a leaf of *Laurus nobilis* in response to dehydration. Curves: 1 control; 2 experiment: dehydration to 65 % of the initial state; 3 experiment: dehydration to 33 % of the initial state (25 min of the “dry wind” influence). Arrows: 1, 2, 3, 4, 5, 6 as in Fig. 2.7

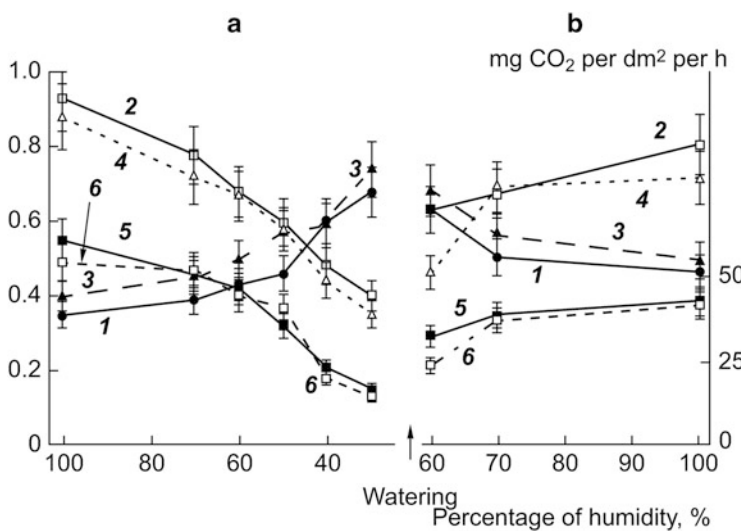


**Fig. 2.10** The dynamics of change in (a)  $q_q$  and  $q_E$  coefficients and (b) in the photosynthesis intensity ( $\text{mg CO}_2/\text{dm}^2 \text{ h}$ ) during the “dry wind” period and at the tidal drop in water level for *Phaseolus vulgaris* (curve 5) and *Robinia pseudoacacia* (curve 6). Curves: 1 and 2, respectively, demonstrate the dynamics of  $q_q$  and  $q_E$  for *Ph. vulgaris* and 3 and 4 for *R. pseudoacacia*. Left ordinate: coefficient change in relative units; right ordinate: values of the photosynthesis intensity

Variable FI,  $F_V$ , defines the level of  $Q_A^-$  reduction and is accompanied by RC closing. Research experience shows that the damaging influence of an EFE reduces the  $F_V$  level. This decrease indicates disorder of energy transformation in PS-2 and the incompleteness of RC closing, with partial damage of their function of light energy conversion into chemical potential. The inhibition of energy transmission between PS-2 and PS-1 is the primary event induced by dry wind and results in imbalance of the reaction ensemble of electron transfer in the link  $P_{680}^* \rightarrow Q_A^+ \rightarrow Q_B^+$ . This is caused by photophosphorylation damage and interruption of the phototrophic function of the leaf. There are bases for the belief that suppression of PS-2 activity is connected with suppression of the  $F_V$  value and is caused by inhibition of charge transfer between  $P_{680}$  and Pheo (Schreiber and Bilger 1993; Schreiber et al. 1997a, b; Saakov 2001a, b, 2002a–c), that is, directly by damage to the function of PS-2 RCs. The  $F_V$  value (especially important, the  $F_V$  level at any time  $t$  is  $F_{V1}^t$ , which is the same as  $F_{V1}'$ , designated in the literature as “spikes”) is coupled with fluctuations in the coefficient  $q_E$ . The low value of  $q_E$  emphasizes a decrease in the proton gradient interfaced to ATP formation and simultaneous active use of the energy in the Calvin cycle. The correctness of this statement is illustrated by data in Table 2.4, from which it follows that an increase in the dry wind impact on a leaf results in an increase in the value of the coefficient  $q_E$ . At the same time, the ratio  $F_V/F_0$  decreases, which is also evidence for ETC damage connected with a reduction of the link  $P_{680}^* \text{Pheo} \bar{Q}_A^+ \rightarrow P_{680}^* \text{Pheo} \bar{Q}_A^- \bar{Q}_B$  (Saakov 2000a–e).

A decrease in the ratio  $F_{V \text{ experiment}}/F_{V \text{ control}}$  also indicates suppression of PS-2 activity (Table 2.4). Obtained results on the influence of atmospheric drought correlate well with published data (Saakov 2000a–e) and are additional evidence for the link between the photosynthetic device stability and RC activity, and the damageability of their link at the stage  $P_{680}^* \text{Pheo} \bar{Q}_A^- \rightarrow P_{680}^* \text{Pheo} \bar{Q}_A^- \bar{Q}_B$  (Saakov 2000a–e, 2001a, b, 2002a–c).

From the figures it follows that, after the decrease in  $F_V$ , the actinic light generates the FI signal  $F_{V1}$ . Experience shows that the ratio  $F_{V1}/F_V$  and coefficient  $F_{V1}/F_0$  (Table 2.4) can be considered as reliable indicators of PS-2 ETC activity (van Kooten and Snel 1990a; Saakov et al. 1992; Saakov 1993a–d; Schreiber and Bilger 1993, 1994). The higher the amplitude of impulses  $F_{V1}^t = F_{V1}'$  and the closer they are to  $F_{V1}$ , the more significant is the probability of complete reduction of the  $Q_A^+$  pool and of high activity of ETC and the Calvin cycle.

As can be seen from Table 2.4, in parallel with the increase in coefficient  $q_E$ , the coefficient  $q_q$  decreases. Values of  $q_q$  receding from 1 to 0 emphasize the decrease in light energy conversion and disorder of leaf phototrophic ability. A value of  $q_q = 1$  indicates high levels of electron transfer, photosynthesis intensity, and  $\text{NADPH}/\text{H}^+$ . Figure 2.10 presents the dynamics of changes in  $q_q$  (curves 2 and 4) and  $q_E$  (curves 1 and 3) as a function of the decrease in leaf water content under the influence of a dry wind, together with the dynamics of  $\text{CO}_2$  absorption intensity change (curves 5 and 6). After a tidal drop in water level, the opposite effect is seen. Simultaneously with a decrease in coefficient  $q_q$  and increase in  $q_E$ , the intensity of

photosynthesis falls off and reaches a minimum at the minimum water content in a leaf; the respiration intensity increases 2.5- to 4-fold. We reported earlier on the change in PAMF parameters, photosynthesis, and respiration in response to  $\gamma$ -radiation for similar dehydration of a leaf (Saakov 1987, 1993a–d). The presented data correlate well with the described results of spectrophotometric research on the damage and regeneration of functional and structural features of thallomes of the red alga *Porphyra perforata* in the case of its predrying and a tidal drop in water level (Saakov 1987; Fork and Hiyama 1973).

Here it is possible to include the character of change in the photosynthetic processes of bryophytes (bryophytes are poikilohydric plants) when adapting to inconstancy of the water content in the surrounding environment. Among the most known consequences of drying for these plants is the termination of photosynthesis if the water content is lower than the critical level; this phenomenon is characteristic for a large number of liverworts (Tuba et al. 1994). A decrease in photosynthesis intensity is accompanied by an excess of light energy that cannot be transformed through ETC and leads to photoinhibition, suppression of PS-2, and non-photochemical quenching. The decrease in PS-2 activity under these conditions can be explained by the inability of RCs to carry out photochemical quenching. Scientists assume the existence of mechanisms protecting the photosynthetic device from photoinhibition in the period of dehydration. The xanthophyll zeaxanthin has been considered as such a possible quencher of the non-radiating dissipation energy, appearing under the influence of light on violaxanthin together in the process of its reduction through antheraxanthin (Schindler and Lichtenthaler 1996). The contribution of non-radiating energy transformations is rather great; its intensity decrease is caused by the acceptor–donor properties of the pigment system and a quencher. The quencher serves as an electron acceptor and the pigment system as the electron donor. However, the exact mechanism of such photoprotection is not known, and a number of facts place the reality of this hypothesis in the category of insufficiently convincing and not at all the only one possible (Saakov et al. 1993; Schindler and Lichtenthaler 1996). Moreover, in many publications describing the protective role of zeaxanthin (see Chap. 1), researchers fail to mention the numerous works and reviews of the 50–60 years of work by H. Claes, G.W. Cohen-Bazire, M. Griffiths, R.Y. Stanier, T. W. Goodwin, and N.I. Krinsky on the protective role of carotenoids in response to an excess of light (see Chap. 1).

We consider the increased respiration noted above and the decreased photosynthesis at deep dehydration to be a result of the manifestation of the *compensatory replacement* of cellular energy systems under the extreme life conditions discussed by us earlier (Saakov 2000a–e). We explained the manifestation of compensatory replacement by the possibility of cytoplasmic intake of phosphoglyceric acid funds that, under the influence of an EFE (dehydration) and via processes of glycolysis and respiration, form pools of phosphoenolpyruvate and pyruvic acid, the synthesis of which is connected with ATP formation. It is not excluded that a similar increase in respiration is coupled with the formation of glyoxalic and glycolic acids and

glycolaldehyde. These substances are inherent in chloroplasts and mitochondria and also in animal cells. It is probable that, with an increase in dehydration, the role of glycolysis is more significant and it becomes the general supplier of endogenous ATP. These reactions show the *link between photosynthesis and respiration* under extreme living conditions, during the attempt to maintain the energy resources of the cell during the midday depression of photosynthesis, and under the influence of an EFE in its broadest terms. Obviously, in a green cell, there are mechanisms for certain oxidation–reduction reactions of metabolism that occur with light participation in chloroplasts to be replaced by the dark reactions of mitochondria. The specified reactions show the biological expediency of the activation of processes separated in space, that is, the energy processes in mitochondria and cytoplasm that supply damaged chloroplasts with ATP to guarantee the reactions of the Calvin cycle.

Thus, the results of the present section and of previous works (Schreiber et al. 1997; Saakov and Shiryaev 2000; Saakov 2000a, b, 2001a, b) provide material for a reliable conclusion about the primary influence of an EFE on the damage to the ETC at light energy conversion between  $P_{680}$  and  $Q_A$ . Existing data allow us to speak about localization of the damage at the link  $P_{680}^+Pheo^-Q_A^- \rightarrow P_{680}^*PheoQ_A^-$ . The dependence of photosynthesis intensity on the character of the dynamics of changes in  $q_q$  and  $q_E$  is shown and offers a possible explanation for the link between the midday depression of photosynthesis and increased dehydration of leaf tissue. The considered regularities could be general for a wide range of representatives of *Vegetalia* from *Eucaryota*. They should be taken into account during target selection of genetically modified cultivars for zones suffering from atmospheric drought. The material presented shows the correctness of our ideas about the cooperative interaction of three factors (Saakov 2000a–e) providing the necessary adaptation and resistance of a green cell to the influence of stress factors of natural and anthropogenous origin and coupled with structurally functional features of the photosynthetic device.

### 2.2.3.1 Coefficient Dynamics of Pulse-Amplitude Modulated Fluorescence Under the Long-Term Influence of Soil Drought and High Temperature

Different points of view of researchers on the nature of the stability of vegetational organisms determine the strategic outlook of scientists and are the basis for further development of experiments in different areas of physiology and biotechnology. At the same time, for many years the level of studies of plant tolerance to EFEs and the mechanisms explaining it fluctuated from extremely average to catastrophic (G.V. Udovenko) in their artificiality. The reason was both the methodology used and the very mediocre methodological and intellectual basis (potential). An example of a typical report on scientific activities in the field of research of plant resistance is the collection edited by G.V. Udovenko 1976. The content of this

collection is shameful for science of the end of the 1970s. It dramatically contrasts with the well-grounded statements of P.A. Henckel (1954). Regretfully, under the pressure of the administration of the Institute of Plant Industry and for reasons of an unscientific nature, one of authors of this book had to publish twice his own theoretical and methodological developments, the coauthor of which was the scientific editor of that collection. It appears that European researchers are also familiar with analogous situations.

The statement that the primary localization of damaging influences of EFEs of natural and anthropogenous origin is in the RCs of photosystems was published by us in 1974–1975 on the basis of studies of *structural* changes in the photosynthetic device by methods of high-order derivative spectrophotometry (Baranov et al. 1974; Saakov et al. 1975; Saakov 1976; Saakov and Leontjev 1988). The harbinger of these works was research performed on mutant collections of green algae *Scenedesmus* and *Chlamydomonas*, which possess varying sensitivity to light and differ in nutrition type (Baranov et al. 1975).

The above-mentioned material was reported at a number of international and all-USSR forums with international participation. Works on the investigation of structural changes in the photosynthetic device under the influence of EFEs emphasized that primary damages of this mechanism are connected, not with quantitative disorders of pigment content, but with the qualitative reorganization caused by damage to chloroplast's autotrophic ability to convert light energy into the energy of ATP chemical bonds. Serious support for these conclusions followed from research on the character of fluorescence change under the influence of EFEs (Krause and Weis 1984; Lichtenthaler 1996a, b).

The introduction in leading laboratories of the world of the method of registration of the harmonics of pulse-amplitude modulated fluorescence (PAMF) (Schreiber and Bilger 1987) and the conclusions of leading European experts unequivocally showed the interconnection of PAMF signal changes induced by EFEs with functional damage of PS-2 RCs. The development of ideas about the localization of EFE damaging influences at a qualitatively new stage of research on the functional activity of the photosynthetic device is summarized in reviews (Lichtenthaler 1988a; Lichtenthaler and Rinderle 1988; Lichtenthaler 1988b, 1996a, b; Schreiber and Bilger 1987; Bolhar-Nordenkamp et al. 1989) and completely agrees with conceptions stated by us earlier. Plus, a strong point of European research consists in the speed of realization of new methodological advantages, so the wide range of various experiments covers a variety of EFEs and specific particular characteristics of biological objects.

The new material on the influence of various EFEs on vegetational objects different in their tolerance level allowed us to formulate the theory of the energetic basis of green cell tolerance to EFE impact (Saakov 2000a–e), which was further developed into the theory of energetic basis of the stability of phototrophic cells of *Prokaryota* and *Eucaryota* to the influence of abiotic factors of the environment (Saakov 2004). As the basis of the green cell tolerance, energy theory was a complex of research such as ours and that of a number of European authors on

changes in both the *structural* state of the chlorophyll–protein complex (ChPC) of RCs and its *functional* activity under the EFE influence. In formulating these theses, the main emphasis was on the existence of the most sensitive links in the ETC connected with the transformation of light energy into the energy of ATP chemical bonds. The deficiency of the latter does not say anything about the Calvin cycle activity or about other ways of further synthesis of endocellular products.

Thus, the disorder of light energy *conversion* into the energy of ATP chemical bonds is *primary* and is typical under the influence of various types of stress, that is, it is *nonspecific*. Changes in the content of other cellular metabolites (quantity of pigments, sugars, proteins, etc.) are *secondary* and demonstrate the time process of deeper functional damage induced by EFEs in an autotrophic cell (Saakov 2004). The plentiful material presented in reviews (Krause and Weis 1984; Schreiber and Bilger 1987; Lichtenthaler 1988a, 1996a, b; Bolhar-Nordenkamp et al. 1989), and also our own data, gave assurance during creation of these theories and supported our ideas on the identity of chloroplast ETC responses to the influence of various EFEs. This corresponds to the thesis of the well-known biochemist Prof. E.M. Kreps that “nature seldom invents new biochemical mechanisms; it widely uses earlier created functional systems, combining them in different variants throughout evolution” (Kreps 1976).

The mass application of the PAM method by known schools of Western Europe and the USA defined the readiness of the scientific audience to understand and interpret the obtained results. There were also plenty of skeptics, but it is almost impossible to oblige *urbi et orbi*. At the end of the twentieth century, there was a bulk of correct research in the field of physiology and biophysics on the stability of the photosynthetic device. This material was a result of the PAM method being able to provide *in vivo* data acquisition about the functional state of the photosynthetic device, allowing use of the same leaf to investigate *in situ* the long-term dynamics of the primary reactions of photosynthesis in connection with damage to the light energy conversion processes.

We investigated for the first time the reaction of the same phototrophy tissues of a set of plants differing in degree of tolerance to the influence of high temperature and drought, at increasing levels of EFE influence over a long interval of time. This response was estimated with the change in dynamics of the photochemical ( $q_q$ ) and non-photochemical ( $q_E$ ) coefficients of fluorescence quenching.

The specifics of PAMF change was measured with the Walz 101-103 device (Effeltrich, Germany) (Schreiber and Bilger 1987; Bolhar-Nordenkamp et al. 1989; Lichtenthaler 1996a, b). Unfortunately, the realities of life are such that we could get access to modern equipment only by working in Europe. The positive features of the method are defined, in particular, by its exclusively high sensitivity, and specialties of the interpretation of registered data are described in reviews (Krause and Weis 1984; Lichtenthaler 1988a; Schreiber and Bilger 1987; Bolhar-Nordenkamp et al. 1989).

The experimental points obtained at 7–9 min of PAMF registration and presented in Figs. 2.11, 2.12, 2.13, and 2.14 show the average values of studied

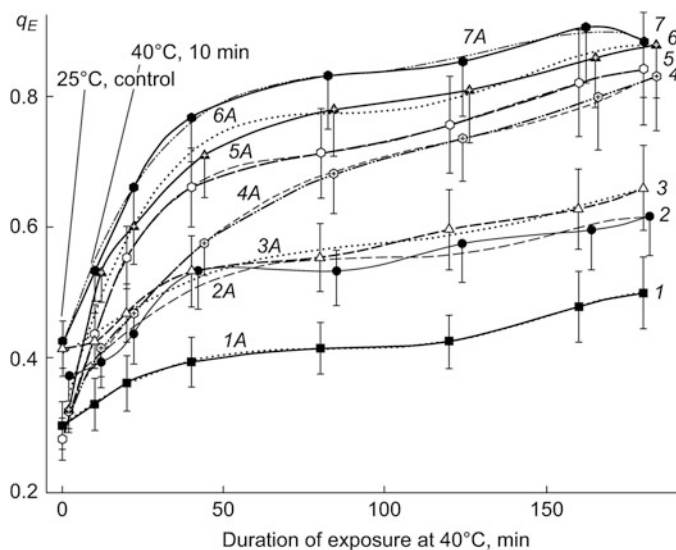


**Fig. 2.11** The dynamics of change in the  $q_E$  coefficient of energy quenching of PAMF in response to increasing duration of a thermal influence of 40°C for different types of plants: 1 *Artemisia* sp., 2 *Laurus nobilis*, 3 *Quercus robur*, 4 *Phaseolus vulgaris*, 5 *Nicotiana tabacum*, 6 *Trifolium* sp., 7 the mutant № 3613 of *Hordeum vulgare*, lacking chlorophyll *b*, the cultivar Donaria. Curves 1A–7A, corresponding to curves 1–7, are nonlinear regressions of the fifth order

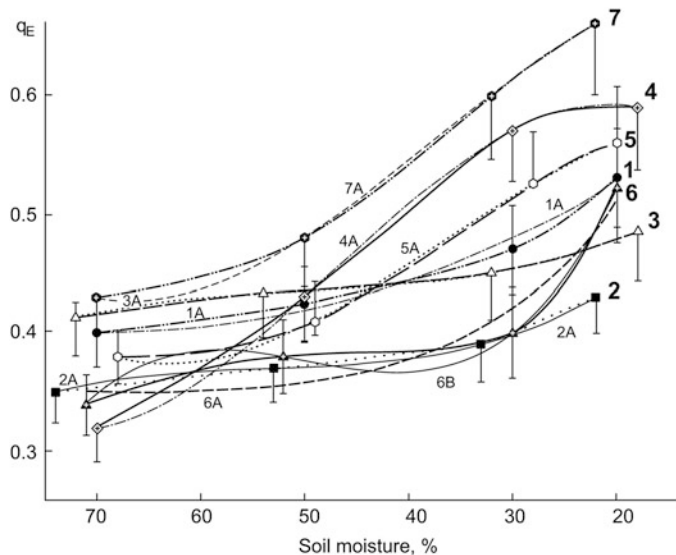
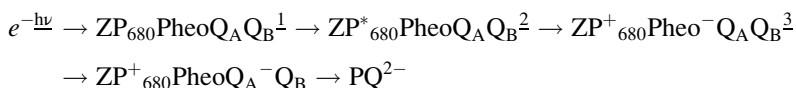


**Fig. 2.12** The dynamics of change in the  $q_E$  coefficient of energy quenching of PAMF in response to increasing soil drought for plants: curves 1–5 and 7 areas in Fig. 2.11; 6 *Triticum* sp. the cultivar Saratovskaya 29. 1A and 6A are nonlinear regressions of the second order for curves 1 and 6, respectively; 2A–5A, 6B, and 7A are nonlinear regressions of the third order for curves 2–7, respectively. Abscissa: the decrease in soil humidity



coefficients of 9–12 parallel experiments. Processing and visualization of data and regression curves were carried out with the software package *SigmaPlot* 2000.

From the previous works, it follows that the level of base fluorescence,  $F_0$ , arising after the dark adaptation of a leaf, when all RCs are open, membranes are in the non-energized state, and the first stable acceptor of PS-2 ( $Q_A^+$ ) is completely oxidized, corresponds to  $q_q = 1$  and  $q_E = 0$ . The influence or aftereffect of EFEs results in an increase in  $F_0^t$  (in any time interval  $t$ ) and to the simultaneous change in the state of PS-2 pigments, inhibition of  $Q_A$  reduction, and accumulation of its oxidized funds caused by the rupture of the electron transport onto  $Q_B$ , that is, by the destruction of RCs of PS-2. An increase in intensity of the EFE influence reduces the  $F_V/F_0$  ratio ( $F_V$  is variable FI, indicating the change in  $q_E$  of the non-photochemical quenching), which is one more significant criterion speaking for the damage of the ETC of PS-2 and occurs due to reduction of the link  $P_{680}^* \text{Pheo} Q_A^-$ . The  $e^-$  transport in RCs of PS-2 starts from the charge separation between  $P_{680}$  in the first excited singlet state and pheophytin and represents the  $e^-$  transfer from the secondary donor Z to primary and secondary acceptors  $Q_A$  and  $Q_B$  of the quinone type. To illustrate our line of reasoning, we again show Eq. (2.1) of the ETC:



At the photoinhibition induced by intensive light, damage to the  $e^-$  transport at stages 2 and 3 is found, that is, disorder of charge separation between  $P_{680}^*$  and Pheo. In the state  $P_{680} Q_A^-$ , there is no photochemical transformation of energy. The intermediate Pheo works as a mediator between  $P_{680}$  and  $Q_A$ , promoting the primary charge separation (forming  $P_{680}^+ \text{Pheo}^- Q_A^-$ ). The scientists suppose that  $F_V$  should be the “recombinant luminescence” at the transition  $P_{680}^+ \text{Pheo}^- Q_A^- \rightarrow P_{680}^+ \text{Pheo}^- Q_A^- \rightarrow P_{680}^* \text{Pheo} Q_A^-$ . From here, the decrease in  $F_V$  value directly indicates the suppression of PS-2 activity and the damage of the  $e^-$  transport from  $P_{680}$  to  $Q_A^+$ , caused by the inhibition of charge migration between  $P_{680}$  and Pheo and retarding the light energy transformation into the energy of ATP chemical bonds, that is, damage to the phototrophic function in PS-2 RCs occurs. The EFE influence on a leaf reduces the yield of  $F_V$ ,  $F_{V1}$ , and  $F_{V1}^t$  and increases the  $q_E$  value, which proves the existence of the primary damage and its localization close to RCs of PS-2 (Krause and Weis 1984; Lichtenthaler 1988a, b; Schreiber and Bilger 1987; Bolhar-Nordenkamp et al. 1989; Lichtenthaler 1996a, b; Saakov 2000a–e, 2004). In this case, it is necessary to carefully distinguish between the reduction of the specified coefficient and the  $F_0$  increase (Bolhar-Nordenkamp et al. 1989).



Figures 2.11 and 2.12 show the dynamics of the coefficient  $q_E$  value change depending on the intensity of chosen EFEs. From consideration of Fig. 2.11, the following conclusion can be made: The dynamics of curves 1–7 is approximated by lines of the nonlinear regression of the fifth order (curves 1A–7A) and can be reconstructed with the corresponding equations provided by the program.

The chosen objects can be divided into two groups according to the character of their  $q_E$  dynamics (curves 1–3 and 4–7) and to the initial inclination angles of curve dynamics. The  $q_E$  increase is accompanied by a decrease in the activity of dark reactions. On the basis of ETC activity invariance, it is possible to draw a conclusion on the degree of tolerance of object leaves to the prolonged influence of high temperature. Taking into account that wormwood and laurels can be considered as thermosteady objects, the character of  $q_E$  dynamics is no surprise. In this case, RCs of PS-2 subjected to EFE impact turn into fluorescence quenchers, but also, probably, trap excitons and convert the accepted energy into thermal radiation,  $q_E$ . The increase in dissipation of the excited thermal energy reduces the primary photosynthetic efficiency and the activity of ETC. The  $q_E$  value corresponds to the *trans*-thylakoid  $\Delta pH$ . From consideration of the dynamics regularity of the difference  $1 - q_E$ , it follows that a decrease in the yield of fluorescence is defined by an accumulation of protons in thylakoids.

Different dynamics of  $q_E$  change is observed in the case of prolonged soil drought (Fig. 2.12). In the experiment, the same objects were chosen as in the case of high temperature influence, but tolerant wheat Saratovskaya 29 was added. Curves 2A–7A (Fig. 2.12) are approximated by the nonlinear regression of the third order, and curve 1A is of the second order. They can also be reconstructed using the corresponding equations. It follows from the  $q_E$  dynamics that the barley mutant 3613, tobacco, and haricot suffer the effects of soil drought comparatively much worse than laurel and oak; wormwood and Saratovskaya 29 were intermediate. At 30 % soil drought, laurel, Saratovskaya 29, wormwood, and oak showed values of coefficient  $q_E$  only 10–20 % different from the initial reference level (70 %). The value of  $q_E$  for Saratovskaya 29 especially increased (jump-like) at the transition to 20 % soil humidity. For other objects, essential differences in  $q_E$  values in comparison with the control were registered in the interval between 40 and 30 % soil drought. Thus, the prolonged influence of high temperature and soil drought led to an increase in non-photochemical quenching of FI caused by accumulation of reduced Pheo<sup>-</sup>, decrease in the quantum yield, and inactivation of the Calvin cycle. Data on the  $q_E$  dynamics under the EFE influence increasing in time correspond well to results of researchers Schreiber and Neubauer (1990).

The dynamics of  $q_q$  under the prolonged influence of high temperature and soil drought is presented in Figs. 2.13 and 2.14, respectively. The data of Fig. 2.13 shows that the chosen objects can be subdivided into two groups

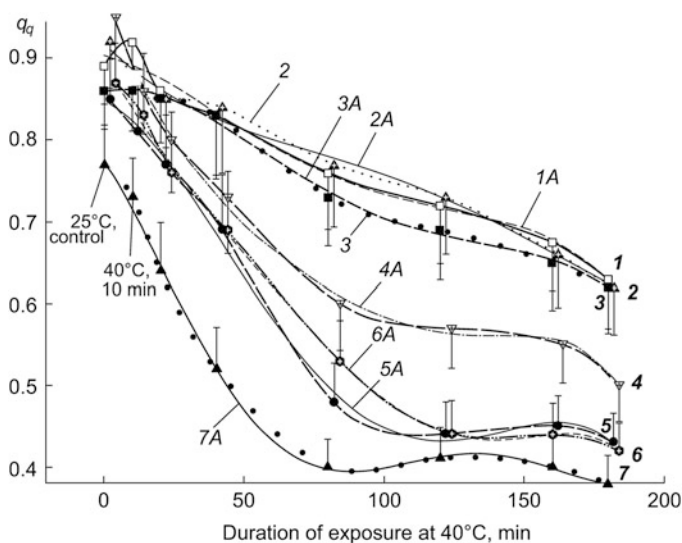


**Fig. 2.13** The dynamics of change in the PAMF photochemical quenching coefficient  $q_q$  in response to increasing duration of the thermal influence of 40°C for plants: curves 1, 4–7 are as in Fig. 2.11; 2 *Q. robur*; 3 *L. nobilis*. 1A–3A nonlinear regressions of the fourth order for curves 1–3, respectively; 4A–7A nonlinear regressions of the fifth order for curves 4–7, respectively

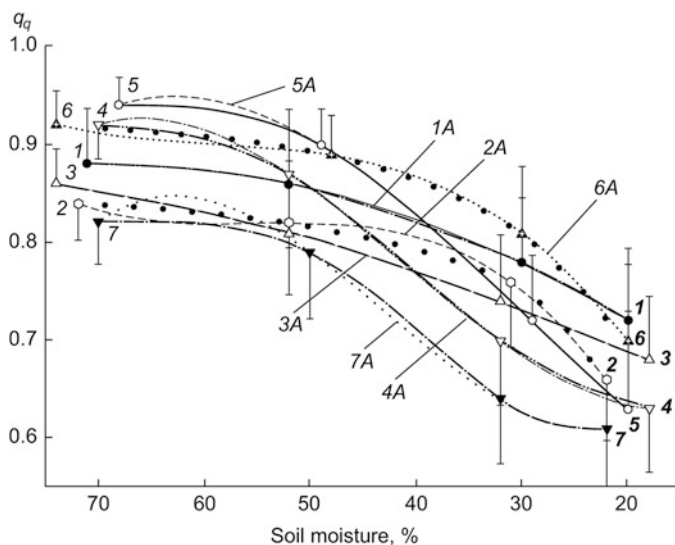


**Fig. 2.14** The dynamics of the PAMF photochemical quenching coefficient  $q_q$  at the growing soil drought. 1–5, 7 as in Fig. 2.11; 6: *Triticum* sp., the cultivar Saratovskaya 29. Curves 1A–7A are, respectively, nonlinear regressions of the third order for curves 1–7. Abscissa: decrease in the soil humidity

(curves 1–3 and 5–7). Objects of the first group manifested higher tolerance to temperature influence compared with the second group. Haricot is intermediate, but, possibly, is closer to the second group.

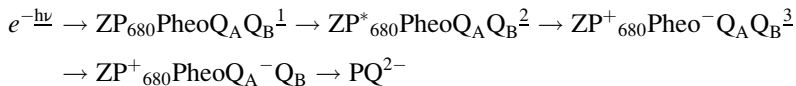
In Fig. 2.13, the dynamics of curves 1–3 is approximated by lines of nonlinear regression of the fourth order (curves 1A–3A); at the same time the dynamics of curves 4–7 is approximated by lines of nonlinear regression of the fifth order (curves 4A–7A). The decrease in  $q_q$  values observed in all variants emphasizes the increasing reduction of ETC (the primary acceptor is  $Q_A^-$ ; the difference  $1 - q_q$  points at the relative level of the  $Q_A$  reduction). The reduction of  $PQ^{2-}$  is coupled with the increase in the proton current, showing energy accumulation (electrons) in the acceptor part of PS-2, and the inhibition of ETC re-oxidation. These data correlate with results on  $CO_2$  fixation obtained earlier.

The other dynamics of  $q_q$  can be seen under the increasing influence of soil drought (Fig. 2.14). Sharp differences in  $q_q$  values between the experiment and the control start in the region of 40 % soil humidity, reaching a maximum at 25–20 %. In this regard, wormwood, oak, and the wheat Saratovskaya 29 possess similar and higher  $q_q$  values, whereas haricot, tobacco, and the barley mutant 3613 are all in the group with much lower  $q_q$ . Laurels were intermediate, although it is necessary to emphasize that the relative recession of  $q_q$  values compared with the control point (70 %) is not lower than in the first group of objects. Curves 1, 3, and 7 of  $q_q$  dynamics are approximated by the nonlinear regression of the second order (curves 1A, 3A, 7A), whereas curves 2, 4, 5, and 6 are approximated by the nonlinear regression of the third order (curves 2A, 4A, 5A, and 6A). Unlike the data in Fig. 2.13, the results in Fig. 2.14 indicate the differentiated change in  $q_q$  within several days for the same objects during increasing soil drought and the corresponding reduction in the  $PQ^{2-}$  pool. Such work was performed for the first time, and its results reliably emphasize the ability of the PAM method to make numerous measurements of  $q_E$  and  $q_q$ , and, consequently, monitor the oxidation–reduction state of the chloroplast's energy status using the same vegetational material in situ.

Earlier, we found the identity of  $q_q$  and  $q_E$  changes for leaves when dehydration was induced by  $\gamma$ -irradiation and atmospheric drought, with analogous parameters for algae with changeable water content (poikilohydric). The same concerns the short-term influence of high temperatures. Data, brought to the reader's attention in this book, from studies of the long-term dynamics of  $q_E$  and  $q_q$  change correspond well to material obtained for drying mosses and lichens. Rehydration of these objects restores photochemical transformation of the energy, causes fluorescence growth, increases the  $q_q$  value, and leads to  $q_E$  relaxation (Heber et al. 2001).

The considered  $q_E$  and  $q_q$  dynamics are tightly interfaced to the change in other coefficients of fluorescence quenching. The level of base fluorescence ( $F_0$ ) arising after dark adaptation of a leaf, when all RCs are open, membranes are in the non-energized state, and the first stable acceptor of PS-2— $Q_A^+$  is completely oxidized, corresponds to  $q_q = 1$  and  $q_E = 0$ . The influence or aftereffect of EFEs results in an increase in  $F_0^t$  (in any time interval  $t$ ) and to a simultaneous change in the state of PS-2 pigments, inhibition of  $Q_A$  reduction, and accumulation of its oxidized funds caused by rupture of the electron transport onto  $Q_B$ , that is, by

destruction of PS-2 RCs. An increase in the intensity of EFE influence reduces the  $F_V/F_0$  ratio ( $F_V$  is variable FI, indicating the change in  $q_E$  of the non-photochemical quenching), which is one more significant criterion speaking for the damage of PS-2 ETC and occurs due to reduction of the link  $P_{680}^*PheoQ_A^-$ . The  $e^-$  transport in PS-2 RCs starts from the charge separation between  $P_{680}$  in the first excited singlet state and Pheo and represents the  $e^-$  transfer from the secondary donor (Z) to the primary and secondary acceptors  $Q_A$  and  $Q_B$  of the quinone type (see Eq. (2.1), shown again here for convenience):



During photoinhibition induced by intense light, damage to the  $e^-$  transport at stages 2 and 3 is found, that is, at the disorder of charge separation between  $P_{680}$  and Pheo. In the state  $P_{680}Q_A^-$ , there is no photochemical transformation of energy. The intermediate Pheo works as a mediator between  $P_{680}$  and  $Q_A$ , promoting the primary charge separation (forming  $P_{680}^+Pheo^-Q_A^-$ ). It is supposed that  $F_V$  should be the “recombinant luminescence” at the transition  $P_{680}^+Pheo^-Q_A^+ \rightarrow P_{680}^+Pheo^-Q_A^- \rightarrow P_{680}^*PheoQ_A^-$ . A decrease in  $F_V$  value directly indicates suppression of PS-2 activity and damage of  $e^-$  transport from  $P_{680}$  to  $Q_A^+$ , caused by inhibition of charge migration between  $P_{680}$  and Pheo and retarding of the transformation of light energy into the energy of ATP chemical bonds (i.e., damage to the phototrophic function in PS-2 RCs occurs). The EFE influence on a leaf reduces the yield of  $F_V$ ,  $F_{V1}$ , and  $F'_{V1}$  and increases the  $q_E$  value, which proves the existence of the primary damage and its localization close to RCs of PS-2 (Krause and Weis 1984; Lichtenthaler 1988a, b, 1996a, b; Schreiber and Bilger 1987; Bolhar-Nordenkamp et al. 1989; Saakov 2000a–e, 2004). In this case, it is necessary to carefully distinguish between the reduction of the specified coefficient and the  $F_0$  increase (Bolhar-Nordenkamp et al. 1989).

Thus, the functional mechanism of the light energy conversion created by nature simultaneously defines the tolerance of phototrophic cells to EFE influence, which corresponds to the position of academician E.M. Kreps (1976) and to the idea of interpenetration of all evolutionary processes on the Earth and their involvement in a uniform and eternal energy flux of life existence that assumes different shapes.

Our experiments and the data of European scientists using the PAM method provide a new orientation to the development of research on plant tolerance to the influence of various EFEs, connecting these studies with target works on biotechnology for use in the process of selection of tolerant cultivars genetically modified by polygene systems.

At the end of this section, the authors consider it their pleasant duty to express great thanks to Prof. Dr. Hartmut Lichtenthaler (University of Karlsruhe) and to Prof. Dr. H. Bolhar-Nordenkamp (University of Vienna) for the fruitful discussion on questions discussed in the section.

### **2.2.4 The Influence of $\text{Na}^+$ , $\text{Cl}^-$ , and $\text{SO}_4^{2-}$ Ions on the Change in Pulse-Amplitude Modulated Fluorescence Kinetics. Resistance Features of the Phototrophic Function of Photosystem 2 at Salification**

The salt tolerance of photosynthesizing green cells is linked to features of ion flux changes in higher and lower organisms and takes a special place in the development of the resistance theory of *Prokaryota* and *Eucaryota* because of the existence of a special physiologically unique group of halophytes. Despite long-term study of the causes and effects of salt tolerance, the variety of works ascertaining the appearance of secondary effects as a result of the salt stress do not mention the primary, deep reactions of the salt tolerance mechanism. Because of methodological insufficiency, cornerstone questions arise about the interrelation between ionic transport and its influence on the realization of general energy processes in a green cell.

European experiments of the last 70 years performed at the appropriate methodological level with spinach chloroplasts have provided assumptions about the association of activity of the PS-2 RCs with primary electron transfer and with the aggravation of competition between primary oxidizing equivalents in response to salt stress (Diner 1974). Meanwhile, an increase in the fluorescence yield of chloroplast suspensions was shown, indicating disorder of ETC activity in response to salification, in many respects similar to the influence of the herbicide diuron. As a working hypothesis, the authors assumed inhibition of the RCs by salification, which they noted for  $\text{Mg}^{2+}$  ions (Malkin and Siederer 1977). McSwain et al. (1976) came to similar conclusions. They showed the kinetics of change in levels “O” and “P” of the Kautsky curve under the joint influence of  $\text{Na}^+$  and  $\text{Mg}^{2+}$  ions on the RCs of PS-2 and the energy distribution between the two photosystems. By investigating membranes of fragments of blue-green alga *Nostoc muscorum*, they found inhibition of reductant formation. These data were supported by the work of Wydrzynski et al. (1975), who also determined the decrease in levels “O” and “P” of the Kautsky curve of spinach chloroplasts. On the basis of changes in the amplitude ratio  $F_{695}/F_{685}$ , a conclusion was made about the influence of ionic agitation on PS-2 RCs. At the same time, for the halophyte green alga *Dunaliella tertiolecta*, the tolerance of thylakoid membrane preparations under the NaCl influence (1.5 M) was manifested as an increase in oxygen outflux, that is, as the effective work of photosynthetic ETC (Aoki et al. 1986). Studies on rice (*Oryza sativa*) with the *codA* incorporated gene for choline oxidase from the bacteria *Arthrobacter globiformis* and able to synthesis glycine betaine showed that this transgenic plant is more tolerant to photoinhibition and quicker to adapt to salt stress (Sakamoto et al. 1998, 1999). Transgenic cells of the rice mutant exhibited tolerance in 150 mM NaCl solution, whereas the control manifested complete disorder of PS-2 activity (Hoshida et al. 2000). Similarly, transgene cells of the *Synechocystis* sp. mutant PCC603 with damage to the mono-unsaturated fatty acid content lose

PS-2 activity in comparison with the wild type in the presence of 0.5 M NaCl or LiCl (Allakhverdiev et al. 1999).

Thus, analysis of literature suggests that damage to the physiological functions of green cells under salt stress is probably caused by inhibition of the energy processes. We have previously published a review of structural changes in leaf chloroplasts under the influence of salt stress (Udovenko and Saakov 1976).

For the successful adaptation of a green cell to stress, our data (Saakov 2000c, 2001a, 2002a, b) indicate the necessity for the combination and cooperative interaction of three features:

1. An optimum structural state of the chlorophyll *a*-protein complex
2. The ETC activity inherent in the object and photophosphorylation
3. The activity of fermentative systems providing the habitual volume of CO<sub>2</sub> fixation and the activity of the Calvin cycle

From the above-cited material, it seems that, until recently, a number of studies were carried out with chloroplast fragments or other preparative structures. The conclusions drawn from them about the higher PS-2 lability became axiomatic, although they could not fully describe the true functional reactions and physiological processes in vivo. In this regard, we would like to rebuff with all clarity the statements about the lack of novelty of in vivo experiments with a leaf or integral suspensions of algae in comparison with those on chloroplasts.

Such a position only emphasizes the misunderstanding of some researchers of the experimental essence of a study carried out with contactless methods and *without damage* to the structure inherent in the intact photosynthetic device. Furthermore, contactless methods allow the researcher to come back after a specified time interval to the same leaf and to again obtain information on the course of its physiological processes. One such method is that of PAMF, which was acknowledged as possessing important informativeness, speed, and short response time. Since the end of the 1980s, this method has proved itself in leading laboratories of Germany, the USA, and France, but due to financial difficulties, it is only minimally available in Russia (Saakov 2000b, 2001a, 2002a).

In spite of that, details of the method have been published (Saakov 2000c, 2001a, 2002a), and it is necessary to describe some of its features.

The stationary, dark FI ( $F_0$ ) (or as it is sometimes called the base FI) and the variable FI ( $F_v$ ), showing the activity of PS-2 at reduction  $Q_A^+ \rightarrow Q^-$  and leading to closing of PS-2 RCs, can be registered with the impulse fluorometer Walz 101-103 (Effeltrich, Germany). The peculiarity of this device is the possibility of separation of an experimentally induced FI signal from the significantly more intense excitation light, which is possible due to the application of primary ( $\lambda < 670$  nm) and secondary ( $\lambda > 680$  nm) optical filters. The latter protect the photodetector from the diffused light of the excitation source. Emission detectors and the selective amplifier allow fluorescence measurements to be carried out *in the light*. This feature of the device promotes its active application in ecological field research studying the influence of a variety of stress factors of natural and technogenic character. If necessary, the data digitalization or their input in packages

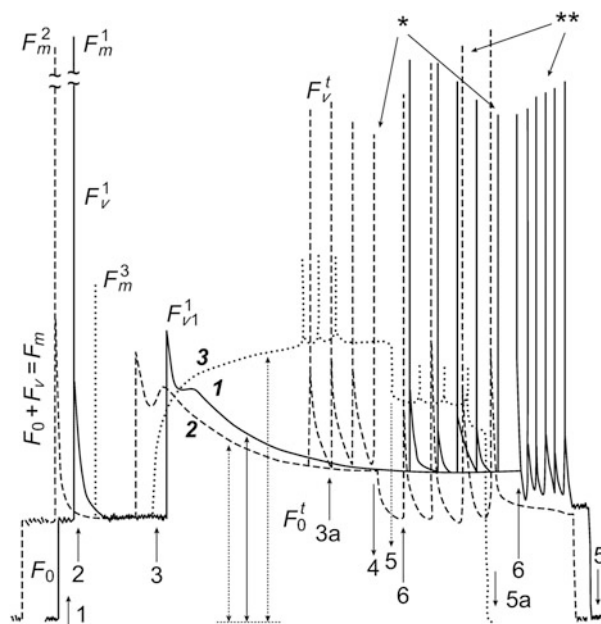


**Fig. 2.15** The character of PAMF signal harmonics change for native cells of halophyte *Dunaliella salina* in response to salt stress. Curves: 1 control; 2 experiment: influence of 2.5 %  $\text{MgSO}_4$  solution for 20 min; 3 experiment: the same as 2, but showing the influence of 6 h of exposure. Arrows: 1 and 5, respectively, input and shutdown of the modulating stream of light flux of frequency of 1.6 kHz ( $5 \mu\text{E}/(\text{m}^2 \text{ s})$ ,  $\lambda < 670 \text{ nm}$ ); 2 input of the saturating 1 s impulse of white light ( $2,500 \mu\text{E}/(\text{m}^2 \text{ s})$ ) for determination of  $F_m$  and  $F_v$  values; 3 input and 4 shutdown of the actinic light ( $600 \mu\text{E}/(\text{m}^2 \text{ s})$ ); 3a input of 1 s impulse of the saturating light against the actinic light for determination of  $F_v^t$  values; 6 input of 1 s impulses of the saturating light after shutdown of the actinic light. Arrows with one asterisk show the  $F_v$  level recession; two asterisks indicate the growth of “spikes 6 min” (Saakov 2000b, 2001a, b, 2002a–c) after shutdown of the actinic light

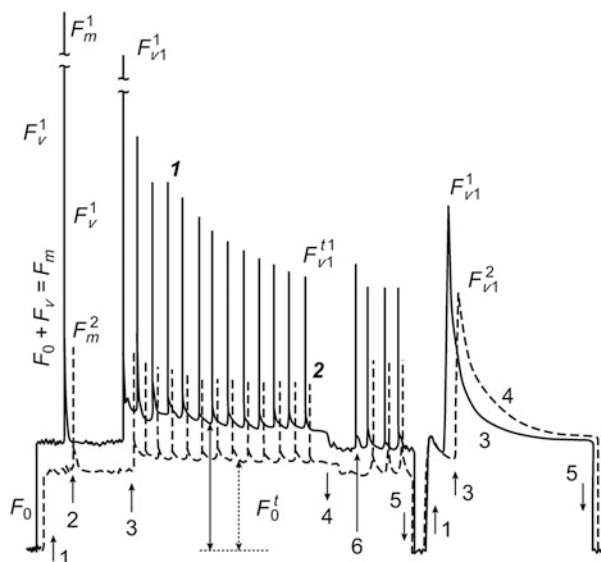
Photoshop CS3 or Origin 6.0–8.0 can be performed with the help of the program Graph Digitizer 2.14 according to N. Rodionov (see <http://nick-gd.chat.ru>).

The choice of research objects was dictated by the desire to investigate vegetational cells of various plant systematics and plants that were either salt tolerant or easily damaged by this factor. As experimental plants, we used suspensions of a halophyte alga *Dunaliella salina*, clover leaves (*Trifolium* sp.), tobacco (*Nicotiana tabacum*), haricot (*Phaseolus vulgaris*), beech (*Fagus sylvatica*), acacia (*Robinia pseudoacacia*), etc. Salt solutions of necessary concentration were introduced into the culture or infiltrated in a leaf.

Figures 2.15, 2.16, 2.17, and 2.18 and in Table 2.5 show the results of experiments on the influence of salification on the change in PAMF signal harmonics and the corresponding coefficients of FI quenching. From the provided data, it can be seen that salt stress causes a change in  $F_0$  and  $F_0^t$  levels ( $F_0^t$  is the  $F_0$  value in any interval of time  $t$ ). It is necessary to remember that  $F_0$  arising under the influence of a modulating flux of 1.6 kHz ( $5 \mu\text{E}/(\text{m}^2 \text{ s})$ ,  $\lambda < 670 \text{ nm}$ ) is characterized by the open



**Fig. 2.16** The character of PAMF signal harmonics change for *Trifolium* sp. leaves in response to salt stress. Curves: 1 control; 2 experiment: effect of a solution of 0.5 %  $\text{MgSO}_4$  for 15 min; 3 induction of  $F_{V1}^1$  of the control; 4 the same experiment ( $F_{V1}^2$ ) under the influence of only actinic light. Arrows 1, 2, 4, 5 as in Fig. 2.15. Arrow 3 for curves 1 and 2: the simultaneous input of actinic light and the 1 s pulse light. Arrow 3 for curves 3 and 4: input of only actinic light



RC state before migration of electrons into open RCs due to excited chlorophyll  $a$  emission and further reduction of the first stable acceptor of PS-2  $\text{Q}_A^+ \text{Q}_B^-$ . At this time, thylakoid membranes of leaves are in a non-energized state and coefficient  $q_q = 1$  and  $q_E = 0$  (Saakov 2000c, 2001a, 2002a).

The prolonged influence of salification is accompanied by an increase in the  $F_0^t$  level. There is considerable similarity between the  $F_0$  dynamics observed and the influence of other factors of extreme impact (Saakov 2000c, 2001a, 2002a). The induction of the maximum FI ( $F_m$ ) and its component (the variable  $F_V$ ) by an impulse of saturating light is accompanied by RC closing. The decrease in the  $F_V$  yield corresponds to manifestation of the photoinhibition effect and shows the impossibility of capture of light energy from the antenna chlorophyll in RCs. With the increase in the impact of the influencing factor, and especially in the process of the aftereffect, a decrease in the ratio  $F_V/F_0$  occurs that can be considered as the significant feature characterizing damage to the  $\text{P}_{680}^* \text{PheoQ}_A^+$  reduction process. Intermediate Pheo acts as the mediator between  $\text{P}_{680}$  and  $\text{Q}_A$  and promotes the primary charge separation, with the formation of  $\text{P}_{680}^* \text{PheoQ}_A^-$ . It follows that the decrease in the  $F_V$  level shown in Figs. 2.15, 2.16, 2.17, and 2.18 (experimental curves 2 and 3) suggests the suppression of PS-2 activity. More exactly, there is suppression of its link  $\text{P}_{680}^* \text{PheoQ}_A^+ \rightarrow \text{P}_{680}^* \text{PheoQ}_A^-$  connected with the  $e^-$  transfer that promotes the inhibition of the light energy into the energy of ATP chemical bonds. As a consequence, there is a significant change in the ratios  $F_V/F_m$  and  $F_m/F_V$ , indicating damage to PS-2 activity and its response to the influence of salt stress (Table 2.5). The specified values are widely used to explain the adaptive mechanisms during photoinhibition. However, discussion of the large amount of literature on this matter is beyond the scope of this book.



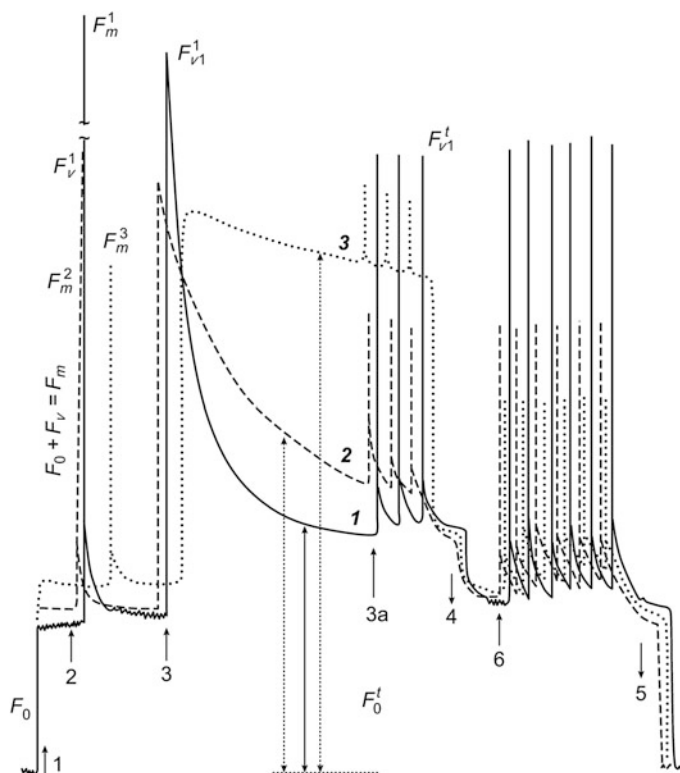


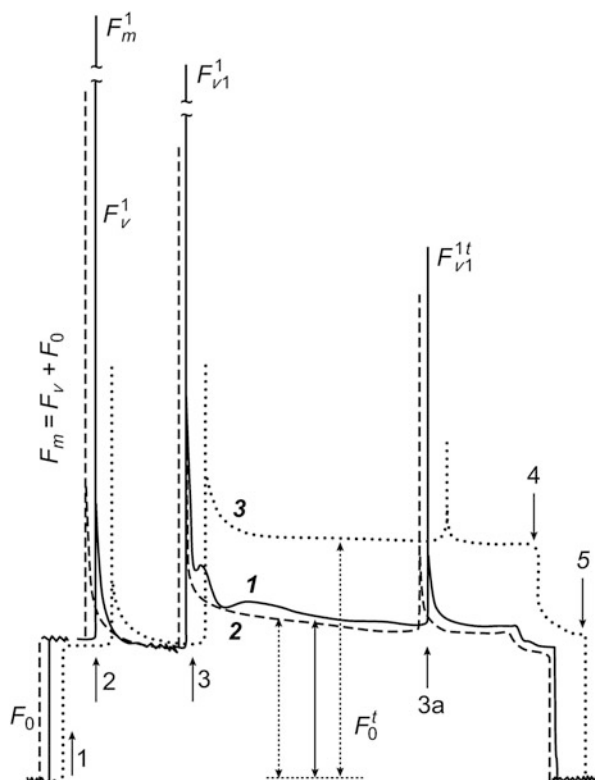
**Fig. 2.17** The character of the signal harmonics change in PAMF for haricot leaves in response to salt stress. Curves: 1 control; 2 experiment: influence of 1.4 % NaCl solution for 15 min; 3 experiment: under the same influence after 24 h. Arrows: 1, 2, 3, 3a, 4, 5, 6 as in Fig. 2.15

The significant decrease in the ratio  $F_{V \text{ experiment}}/F_{V \text{ control}}$  similarly indicates the suppression of PS-2 activity in the experimental variant and corresponds well to the earlier-stated reasons about the place of localization of the damaging influence of EFEs in RCs of PS-2 (Saakov 2000c, 2001a, 2002a).

The experimental curves in Figs. 2.15, 2.16, 2.17, and 2.18 show the reliable change in  $F_{V1}$  amplitude (including the  $F_{V1}^t$  amplitude) that is accompanied by a simultaneous increase in the value of  $q_E$ , which indicates the suppression of energy utilization in the Calvin cycle during the corresponding increase in the proton gradient coupled with a decrease in intensity of ATP store formation. The low value of the level of PS-2 reduction (Table 2.5) also testifies convincingly to its damage.

Thus, the yield decrease in  $F_V$ ,  $F_{V1}$ , and  $F_{V1}^t$  in response to salt stress is similar to the change in these PAMF parameters in response to diverse extreme influences (Saakov 2000c, 2001a, 2002a) and rather reliably points to the existence of primary damage and its localization in the RCs of PS-2. This means that, obviously, the

**Fig. 2.18** The character of the signal harmonics change in PAMF for *Fagus sylvatica* leaves in response to salt stress. Curves: 1 control; 2 experiment: influence of 1.5 % NaCl solution for 15 min; 3 experiment: under the same influence after 24 h. Arrows: 1, 2, 3, 3a, 4, 5, as in Fig. 2.15



inhibition of energy transmission in the links of PS-2 RCs is the primary event damaging electron transport, uncoupling of photophosphorylation, and formation of a reductant. The integrity of exactly this link can be the defining factor during an assessment of adaptive and tolerant reactions of the photosynthetic device under the influence of stress.

In the steady state of photosynthesis, the value of coefficient  $q_q$  is close to 0.8–0.9, and its change by 0.03–0.04 relative units reliably proves the response of the photosynthetic device (Saakov 2001a). At  $q_q = 0$ , there is no transformation of light energy into the energy of chemical bonds, and at  $q_q = 1$ , this transformation is optimal. The fast decrease in the  $q_q$  value during the initial moments of illumination of the object is caused by ETC reduction, and the increase in this coefficient indicates  $Q_A^-$  re-oxidization. The low level of  $q_q$  is the result of electron accumulation in the acceptor part of PS-2 and the high level of reduction of  $Q_A^-$  and  $PQ^{2-}$  pools.

In other words, low values of  $q_q$  indicate the functional damage of ETC (Table 2.5, experimental variants), and a high  $q_q$  value emphasizes the active transport of electrons and a high level of  $NADPH/H^+$ .

Stress arising under the influence of  $Na^+$ ,  $Cl^-$ ,  $Mg^{2+}$ , and  $SO_4^{2-}$  ions naturally induces changes in the reactions of carbon metabolism and in the synthesis of

**Table 2.5** The pattern of salinization-induced changes in the quenching coefficients of modulated fluorescence<sup>a</sup>

Object	Variant of experiment	Measured coefficient, arithmetic mean of $n = 6$ , $p < 0.085$										Spikes 5 min (mm)	Spikes 6 min (mm)
		$F_V/F_m$	$F_V^{exp}/F_V^{contr}$	PS 2 reduction (%)	$F_m/F_0$	$F_V/F_0$	$F_{V1}/F_V$	$F_{V1}/F_0$	$F_0^5/F_0$	$q_E^{5min}$	$q_q^{5min}$		
<i>Dunaliella salina</i>	Control	0.841		94	4.44	3.57	0.87	3.3	1.15	0.38	0.94	94	106
	2.5 % Na <sub>2</sub> SO <sub>4</sub> , 15 min	0.811	0.935	91	4.1	3.45	0.81	3.15	1.12	0.40	0.91	92	101
<i>Trifolium sp.</i>	Control	0.839		89	4.8	3.61	0.84	4.1	1.23	0.33	0.89	67	87
	0.5 % Na <sub>2</sub> SO <sub>4</sub> , 15 min	0.673	0.802	58	3.12	1.86	0.73	2.0	1.54	0.73	0.42	34	37
<i>R. pseudoacacia</i>	Control	0.824		91	5.1	3.78	0.91	4.2	1.21	0.41	0.93	72	89
	0.6 % NaCl, 10 min	0.675	0.819	67	2.9	1.52	0.68	2.89	1.62	0.68	0.66	33	34
<i>Artemisia sp.</i>	Control	0.826		90	4.7	3.71	0.90	3.71	1.23	0.42	0.91	72	87
	1 % NaCl, 20 min	0.805	0.503	88	4.6	3.65	0.88	3.68	1.21	0.51	0.89	70	85
<i>Artemisia sp.</i>	Control	0.829		94	5.14	4.06	0.92	3.92	1.13	0.35	0.94	74	85
	1 % NaCl, 6 h	0.661	0.804	49	3.12	2.3	0.72	1.57	1.65	0.67	0.49	25	33
<i>Fagus sylvatica</i>	Control	0.817		89	5.1	3.83	0.93	3.84	1.20	0.38	0.90	89	93
	0.8 % NaCl, 25 min	0.665	0.813	41	3.24	1.71	0.82	1.64	1.63	0.67	0.42	31	36
<i>Solanum lycopersicum</i>	Control	0.826		91	5.19	4.27	0.891	3.72	1.14	0.46	0.921	72	83
	1.3 % NaCl, 15 min	0.727	0.880	52	3.71	2.28	0.754	1.93	1.31	0.78	0.48	36	33
<i>Fraxinus ornus</i>	Control	0.825		87	5.5	4.71	0.88	4.34	1.3	0.39	0.87	73	75
	0.8 % Na <sub>2</sub> SO <sub>4</sub> , 15 min	0.634	0.768	39	3.12	2.63	0.76	2.1	1.87	0.76	0.40	29	34
<i>Nicotiana tabacum</i>	Control	0.816		90	4.7	3.81	0.94	3.83	1.17	0.34	0.90	78	89
	0.4 % NaCl, 20 min	0.799	0.979	37	2.75	1.78	0.77	11.4	1.43	0.73	0.375	24	37

<sup>a</sup>  $q_E^{5\min}$ ,  $q_q^{5\min}$  and spike 5 min were calculated 5 min after switching the actinic light on; spike 6 min—6 min after switching the actinic light off

proteins, pigments, and other components of a cell. However, these are the stages of deeper, secondary reactions of *adaptation processes* or of a lethal outcome, whereas the *primary processes* of damage to the functional state of PS-2 RCs define the *non-specificity* of the reactions inherent in *Procaryota* and *Eucaryota*.

In the course of manuscript preparation, we became aware of the work by Chauhan et al. (2001), the results of which are indicative. The mutant of blue-green alga *Anabaena variabilis* is tolerant to NaCl influence, characterized by slow inclusion of  $\text{Na}^+$  ions and also by the high content of glycine betaine (Sakamoto et al. 1999), and showed inhibition of the  $\text{Na}^+$  ion flux under the influence of diuron. This allowed us to interpret the results of the work (Chauhan et al. 2001) as the evidence of connection between the ion transport and the PS-2 energetics. The inhibition of the  $\text{Na}^+$  ion flux was found under the influence of KCN, dinitrophenol, and sodium azide. The effect of the last two inhibitors suggests a link between the  $\text{Na}^+$  ion flux and the photophosphorylation activity. At the same time, the authors of the work (Chauhan et al. 2001) suggested the possibility of utilization of oxidative phosphorylation energetics for the regulation of the  $\text{Na}^+$  flux, which corresponds to the point of view of our work on the existence of compensatory replacement of energy funds under the influence of stress (Saakov 2002a). On the other hand, we showed earlier the destructive effect of inhibitors of photosystems, of uncouplers of photophosphorylation, and of KCN on structures of the ChPC (Saakov 1973). From this point of view, the restriction of the  $\text{Na}^+$  flux can be explained by the damage to ChPC integrity, which is the necessary condition of ETC functioning and of normal adaptation of a green cell to a stress.

We have not yet clarified the dependence of the suppression of  $F_m$ ,  $F_v$ , and  $F_{v1}^t$  on the anion valency. However, from the data in Table 2.5 and Figs. 2.15 and 2.16, it is possible to suppose a larger decrease in the ratio  $F_m/F_v$  in the case of  $\text{SO}_4^{2-}$  ions. This position corresponds well to the data in the work by Jajoo et al. (one of the authors, Govindjee, is a known expert in fluorescence analysis), in which the generalization was made that the valency increase in an anion row ( $\text{Cl}^-$ ,  $\text{SO}_4^{2-}$ ,  $\text{PO}_4^{3-}$ ) reduces the ratio  $F_m/F_v$  and the electron transport in PS-2 and adequately increases the energy flux in PS-1 (Jajoo et al. 1998).

Thus, the material of the present work together with a literature analysis (Diner 1974; Malkin and Siederer 1977; Wydrzynski et al. 1975; McSwain et al. 1976; Udovenko and Saakov 1976; Aoki et al. 1986; Allakhverdiev et al. 1999; Sakamoto et al. 1999; Chauhan et al. 2001) allows us to make a conclusion about the primary localization of the negative influence of ions  $\text{Na}^+$ ,  $\text{Cl}^-$ ,  $\text{Mg}^{2+}$ , and  $\text{SO}_4^{2-}$ , substantially defining the manifestation of a salt stress, in the link of PS-2 RCs connected with the energy transfer  $\text{P}_{680}^*\text{PheoQ}_A^+ \rightarrow \text{P}_{680}^*\text{PheoQ}_A^-$ . The generality of the presence of chlorophyll *a* in *Procaryota* and *Eucaryota* and also data from the above-discussed works (McSwain et al. 1976; Aoki et al. 1986; Allakhverdiev et al. 1999; Chauhan et al. 2001) confirm our statement on the close interconnection of tolerance and reparation reactions of a green cell and the functional stability of the link  $\text{P}_{680} \rightarrow \text{Q}_A \rightarrow \text{Q}_B \rightarrow \text{PQ}^{2-}$  and expand the idea of the energetic basis for green cell tolerance to the influence of stress factors.

The ideas stated by us (Saakov 2000c, 2002a) about the change in the qualitative orientation of works on the target-intensive selection of cultivars genetically modified by polygene systems, transformed in their systems of electron transport in PS-2, have found support in studies of tolerant transgenic plants (Allakhverdiev et al. 1999; Sakamoto et al. 1998, 1999; Hoshida et al. 2000; Chauhan et al. 2001), although it is still necessary to specify the role of glycine betaine in salt tolerance.

### ***2.2.5 The Concept of the Energetic Basis of Green Cell Resistance to the Influence of Extreme Environmental Factors***

The working hypothesis suggested by us about the localization of damaging influences of environmental factors in the RCs of photosystems and in the centers of pigment biosynthesis in the photosynthetic device (Baranov et al. 1974; Saakov et al. 1975; Saakov 1976; Saakov and Leontjev 1988) was supported by European works on fluorescence changes under the influence of EFEs of natural and anthropogenous origin (Krause and Weis 1984; Lichtenthaler 1988a; Briantais et al. 1986). Subsequent years promoted the accumulation of facts in support of the put-forward hypothesis (Saakov 1987; Saakov 1990, 1992, 1996). Successes in this direction were connected first of all with the improvement in electron-optical methods of diagnostics of the stability of chloroplasts and cells, especially after introduction of the PAM fluorescence method (Lichtenthaler 1988a), which manifested as a stream of works in specialized journals and monographs (Lichtenthaler 1988a). Experimental data of the recent past (Saakov 1993a–d, 2000a–e; Saakov and Shiryayev 2000) supported our position and the conclusions of European researchers (Lichtenthaler 1996b, 1988b; Lichtenthaler and Rinderle 1988; Schreiber et al. 1994; Schreiber and Bery 1977) and gave confidence about the correctness of the chosen research direction.

Our task consisted in the comparative study of PAM kinetics under the influence of  $\gamma$ -radiation, temperature, drought, fumigation, and herbicides to obtain information on the *specificity* or *non-specificity* of the response of the ETC of the photosynthetic device to the impact of chosen EFEs. We emphasize the use of simultaneous comparative investigation of different factors using the same objects in a specified time interval.

The work was carried out with the help of a PAM fluorometer (Walz 101-103; Effeltrich, FRG) by the signal harmonics registration method tested in different countries. The calculation of photochemical ( $q_p$ ), non-photochemical ( $q_E$ ), and other coefficients of FI quenching and the interpretation of their changes were performed by the accepted technique (Krause and Weis 1984; Briantais et al. 1986; Snel and van Kooten 1990; Lichtenthaler 1996a, b), and the results are presented in Table 2.6. As objects of research, we used the leaves of plants *Phaseolus vulgaris* L., *Robinia pseudoacacia* L., and *Nicotiana tabacum* L., which are different in tolerance.

**Table 2.6** Effects of environmental stressors on quenching coefficients of PAM fluorescence from leaves of various species<sup>a</sup>

Species and actinic light intensity	Stressor	Coefficient (mean value; $n = 4, p < 0.05$ )										Spikes 5 min (mm)	Spikes 6 min (mm)
		$F_v/F_m$	$F_v/F_v \text{ control}$	Degree of PSII restoration (%)	$F_v/F_0$	$F_{v1}/F_v$	$F_{v1}/F_0$	$F_0^5/F_0$	$F_{v1} h/2 \text{ (mm)}$	$q_E^{5 \text{ min}}$	$q_q^{5 \text{ min}}$		
<i>Robinia</i> , 185 $\mu\text{E}/\text{m}^2 \text{ s}$	Control	0.823	—	61	4.96	0.95	4.7	1.31	5	0.786	0.70	25	117
	Irradiation 8 kGy	0.804	0.880	28	4.24	0.935	3.96	2.16	45	0.45	0.26	20	74
	2 h after irradiation 8 kGy	0.800	0.880	42	4.0	0.935	3.96	1.93	27	0.62	0.40	21	68
	Low humidity (30 % of the normal)	0.808	0.827	14	4.29	0.877	3.77	2.26	18	0.74	0.117	5	28
	5 % $\text{SO}_2$ for 3 h	0.8	0.830	49	4.3	0.930	3.8	1.8	18	0.7	0.31	17	97
<i>Phaseolus</i> , 185 $\mu\text{E}/\text{m}^2 \text{ s}$	Control	0.837	—	86	5.32	0.848	4.5	1.29	4	0.612	0.843	54	125
	Irradiation 3.5 kGy	0.83	0.927	74	5.1	0.88	4.51	1.5	17	0.64	0.71	38	94
	117 h after irradiation 3.5 kGy	0.789	0.703	54	3.74	0.922	3.45	2	16	0.43	0.53	34	93
	Heat stress (45 °C for 10 min)	0.751	0.751	25	3.45	0.958	3.31	1.68	14	0.74	0.212	7	41
<i>Nicotiana</i> , 590 $\mu\text{E}/\text{m}^2 \text{ s}$	Control	0.850	—	62	5.7	0.906	5.16	1.46	5	0.842	0.46	15	91
	17 h after irradiation at 0.6 kGy	0.811	0.754	59	4.3	0.837	5.16	1.87	6	0.577	0.49	26	97
	200 h after irradiation at 0.6 kGy	0.821	0.807	29.4	4.33	0.949	4.3	2.6	20	0.51	0.24	16	102
	$5 \times 10^{-3} \text{ g/l}$ methyl viologen	0.837	0.933	32.4	5.16	0.831	4.29	1.70	4.5	0.786	0.29	10	61

<sup>a</sup> $F_0^5$ ,  $q_E^{5 \text{ min}}$ ,  $q_q^{5 \text{ min}}$  and spike 5 min were calculated 5 min after switching the actinic light off; spike 6 min—6 min after switching the actinic light off

Results of experiments on the kinetics of the change in PAMF signal harmonics under the influence of and during the aftereffect of various EFEs are presented in Figs. 2.19 and 2.20.

The  $F_0$  level of the base dark FI characterizes the open RC state before electron migration into the open RC due to the excited chlorophyll *a* emission and, therefore, before reduction of the first stable acceptor PS-2  $Q_A^+ \rightarrow Q_A^-$ . At this time, the thylakoid membranes of leaves *adapted for darkness* are in the non-energized state. The  $F_0$  quenching shows the decrease in the absorbed energy directed to PS-2. Even the first saturating impulse of light of 1 s duration and  $3,000 \mu\text{E}/(\text{m}^2 \text{ s})$  intensity (Figs. 2.19 and 2.20, point 2) leads to an increase in maximum FI ( $F_m$ ). Its first increase, the variable FI ( $F_V$ ), defines the degree of  $Q_A^-$  reduction (Table 2.6) and is accompanied by RC closing.

The  $F_V$  yield change corresponds to the energy transformation in PS-2 and points to the stay at minimal non-photochemical processes (Krause and Weis 1984; Briantais et al. 1986; Saakov and Shiryaev 2000). It follows from Figs. 2.19 and 2.20 that the damaging EFE influence on thylakoids usually reduces the  $F_V$  yield, which proves the existence of the primary damage and its localization close to the RCs of PS-2 (Lichtenthaler 1988a, b, 1996a, b; Saakov 1993a, b; Snel and van Kooten 1990). The decrease in the ratio  $F_{V \text{ experiment}}/F_{V \text{ control}}$  (Table 2.6) also emphasizes the suppression of PS-2 activity in the experiment. With a certain level of confidence, it is possible to speak about the existence of a functional link between the PS-2 activity and other components of the photosynthetic ETC and the change in  $F_V$ ,  $F_{V1}$ , and  $F_V^t$  coupled to changes in the activity of the photosynthesis process as a whole (Krause and Weis 1984; Lichtenthaler and Rinderle 1988; Briantais et al. 1986; Lichtenthaler 1988a, b, 1996a, b; Saakov 1993a, b, 2000c).

This is supported by the fact that increased temperature leads to a decrease in electronic transport with the increased intensity of the saturating light flux. The disorder of energy transmission between PS-2 and PS-1 is the primary event correlating with the inhibition of electron transport, termination of photophosphorylation, suppression of reducer formation, and suppression of photosynthesis intensity (Saakov 1976, 1996; Krause and Weis 1984; Lichtenthaler and Rinderle 1988; Briantais et al. 1986; Lichtenthaler 1988a, b, 1996a, b; Saakov et al. 1993).

The value of coefficient  $F_V/F_m$  is extremely important because it is considered to be an indicator of photosynthetic function and is equal to 0.832 relative units for intact chloroplasts (Krause and Weis 1984; Lichtenthaler and Rinderle 1988; Briantais et al. 1986; Lichtenthaler 1988a, b, 1996a, b; Saakov 1993a, b, 2000c). The deviation of this coefficient from the control value by 0.03–0.04 relative units is considered significant and emphasizes the existence of a negative reaction of the photosynthetic device to the external influence (as illustrated by the data in Table 2.6). The effect or aftereffect of EFEs reduces  $F_V/F_m$  for all investigated objects (of different levels of resistance), depending on the depth of damage and the effect of adaptive reactions at  $F_V$  quenching.

It is known that the suppression of PS-2 activity (as defined by the  $F_V$  suppression) is coupled with inhibition of the charge transfer between  $P_{680}$  and Pheo

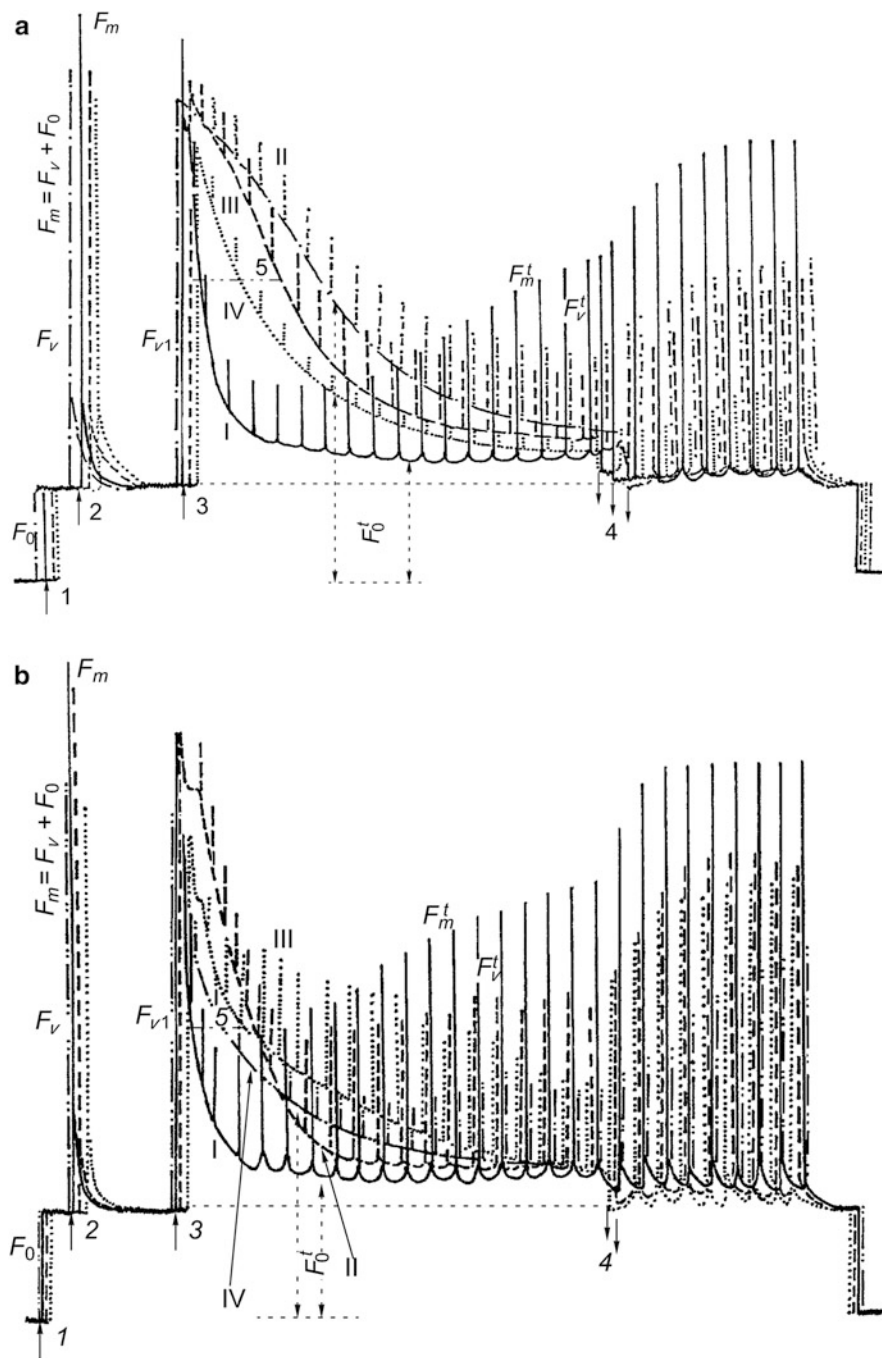
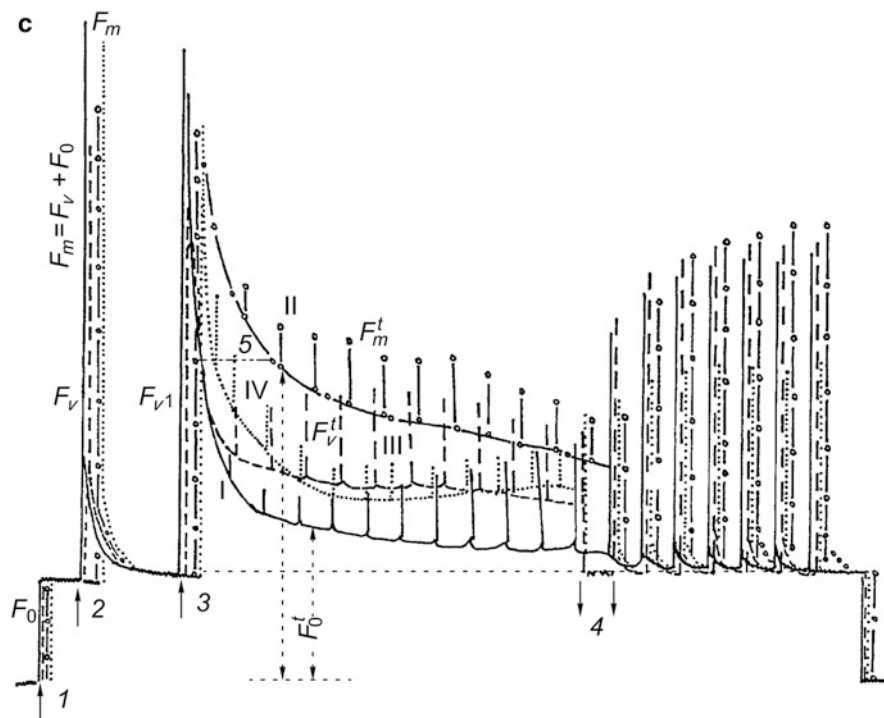


Fig. 2.19 (continued)





**Fig. 2.19** The character of signal harmonics change in PAMF for the chlorophyll *a* of leaves adapted to darkness: (a) *Robinia* under the influence of  $\gamma$ -radiation and dehydration. Curves: I control; II influence of a  $\gamma$ -radiation dose of 8 kGy; III 2 h of the aftereffect of  $\gamma$ -radiation dose of 8 kGy; IV influence of 30 % relative humidity; (b) *Phaseolus* under the influence of  $\gamma$ -radiation and high temperature. Curves: I control; II influence of a  $\gamma$ -radiation dose of 3.5 kGy; III 117 h of the aftereffect of the  $\gamma$ -radiation dose of 3.5 kGy; IV influence of the temperature 45 °C for 10 min; (c) *Nicotiana*, the aftereffect of a  $\gamma$ -radiation dose of 0.6 kGy and methyl viologen (paraquat). Curves: I control; II 200 h of the aftereffect of a  $\gamma$ -radiation dose of 0.6 kGy; III influence of a  $\gamma$ -radiation dose of 0.6 kGy; IV influence of methyl viologen (solution concentration 5 mg/L). For determination of  $F_0^t$  and  $F_v^t$  values, a combination was used (for a and b) of a 1 s impulse of white light flux (1,100  $\mu\text{E}/(\text{m}^2 \text{ s})$ ) and 40 s of actinic light (185  $\mu\text{E}/(\text{m}^2 \text{ s})$ ); for c, the actinic light influence was 590  $\mu\text{E}/(\text{m}^2 \text{ s})$  for 60 s, followed by a 1 s impulse of white light (1,100  $\mu\text{E}/(\text{m}^2 \text{ s})$ ). Arrows: 1 input of the modulating light flux of frequency of 1.6 kHz ( $\sim 5 \mu\text{E}/(\text{m}^2 \text{ s})$ ,  $\lambda \leq 680 \text{ nm}$ ,) for determination of the dark (base) fluorescence value  $F_0$ ; 2 input of the saturating white light impulse (3,000  $\mu\text{E}/(\text{m}^2 \text{ s})$ ); 3 input of the actinic light flux of frequency of 100 kHz and after 30 s input of the white light impulses (1,100  $\mu\text{E}/(\text{m}^2 \text{ s})$ ) for induction of spikes ( $F_v^t$  is the variable fluorescence during the time  $t$ ); 4 shutdown of the actinic light flux for determination of  $F_0^{11-12 \text{ min}}$  values and at the same time input of the light flux of frequency 1.6 kHz; 5 the value  $F_{v1} h/2$  introduced by us (Saakov 1993a) and characterizing the  $F_0^t$  level at the half-height  $F_{v1}$  and the distance  $F_0^t$  from  $F_{v1}$  (in millimeters or seconds)

(Krause and Weis 1984; Briantais et al. 1986; Saakov and Shiryaev 2000; Lichtenthaler 1988a, b, 1996a, b), that is, with the localization of damage as being in the RCs of PS-2, which corresponds to ideas stated by us earlier (Baranov

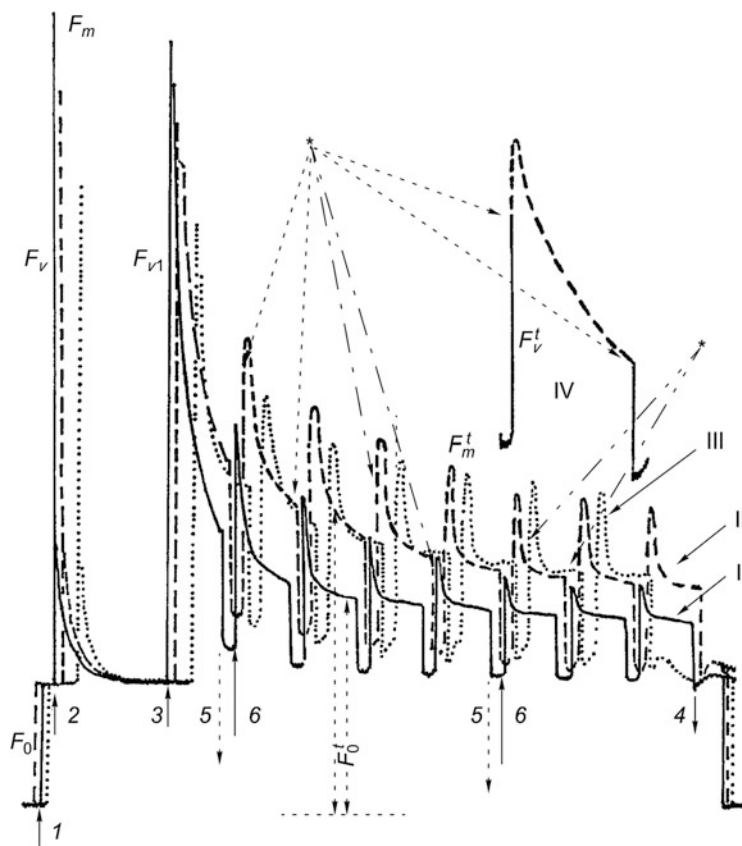


**Fig. 2.20** The character of PAMF signal harmonics change for *Phaseolus* leaves adapted to darkness during cycles of light/darkness (80 s/20 s) and light impulses of 1,100  $\mu\text{E}/(\text{m}^2 \text{ s})$ . Curves: *I* control; *II* influence of  $\gamma$ -radiation of 1.3 kGy; *III* influence of temperature of 45 °C for 10 min; *IV* closeup view of the impulse 80 s/20 s with the expressed slow component arising in kinetics of PAMF signal harmonics for damaged leaves. Arrows with asterisks specify the start of appearance and the termination of the slow component; 5 input and 6 shutdown of the 80 s light impulse. Arrows 1–4 and other designations as in Fig. 2.19

et al. 1974; Saakov 1976, 1990, 1996; Saakov and Leontjev 1988). Moreover, the  $F_v$  value (including values of variable fluorescence at any time  $t$ ,  $F_v^t$ , designated in English literature as “spikes”) connected with the low  $q_E$  value indicates the active utilization of the energy in the Calvin cycle and the simultaneous decrease in the membrane proton gradient coupled with the ATP formation (Krause and Weis 1984; Saakov and Leontjev 1988; Lichtenthaler 1996a, b). From Table 2.6, it can be seen that during the increasing intensity of influence and aftereffect of extreme factors, the ratio  $F_v/F_0$  decreases, which is one more criterion speaking for the damage in ETC of PS-2 caused by the reduction of the link  $\text{P}_{680}^* \text{PheoQ}_A^-$  (Saakov and Shiryayev 2000).

After the  $F_V$  decrease, switching on an actinic white light flux of intensity  $1,100 \mu\text{E}/(\text{m}^2 \text{ s})$  induces the level of FI  $F_{V1}$  and  $F_{V1}/F_V$ , as well as  $F_{V1}/F_0$  (Table 2.6), which seem to be reliable indicators for characterizing the activity of PS-2 ETC (Saakov et al. 1992; Lichtenthaler 1988a, b, 1996a, b; Saakov and Shiryaev 2000). The higher the amplitude of the  $F_V^t$  impulse and the closer it is to the  $F_{V1}$  level, the higher the probability of more complete reduction of the  $\text{Q}_\text{A}^-$  pool, and higher activity of ETC and the Calvin cycle.

In this work, the calculation of the coefficient FI after 5 min of PAMF signal harmonics registration is performed, when there is the most distinction between  $F_0$  and  $F_0^5$ . By this time, an increased initial  $q_\text{E}$  value in the control is noted (Table 2.6), as defined by that after dark exposure (6–24 h); the photosynthesis process has not yet passed the light adaptation; and the stationary activity of the Calvin cycle has not increased. This is emphasized by the corresponding changes in  $q_\text{E}^{11-12}$  and  $q_\text{q}^{11-12}$  after 11–12 min of PAMF signal harmonics registration of control leaves (Fig. 2.19a, curve I 0.54–0.52 and 0.86–0.85; Fig. 2.19b, curve I 0.44–0.42 and 0.9–0.905; Fig. 2.19c, curve I 0.758–0.776 and 0.763–0.756), that is, showing complete de-epoxidation of the xanthophyll cycle (Saakov et al. 1992; Saakov 1993a–d), and confirmed by the degree of the PS-2 reduction in the control, the level of which decreases in the damaged objects.

From Figs. 2.19 and 2.20 and Table 2.6, it follows that, with the increase in the negative impact of external factors, the ratio  $F_0^5/F_0$  increases, that is, the  $F_0^5$  level (after 5 min of PAMF signal harmonics measurement) becomes significantly higher than  $F_0$ . The change in  $F_{V1} h/2$  introduced by us (Lichtenthaler 1988a, b; Saakov 1993a) correlates well with this indicator and is characterized by the band half-width of the PAMF signal harmonic contour, which is described by the  $F_{V1}$  height and the course of the  $F_0^t$  curve induced by the actinic light flux (Fig. 2.19, point 5). The units of this coefficient can be expressed in seconds or in millimeters. From Table 2.6 and Fig. 2.19, it can be seen that  $F_{V1} h/2$  in a certain way corresponds to the level of the reaction of the photosynthetic device caused by the damaging effect of the influencing factor. Earlier we determined the dependence of  $F_0$  or  $F_0^t$  on the radiation dose (Saakov et al. 1993; Saakov 1993b). Our obtained results allow us to extend this dependence to the influence of high temperatures, dehydration and fumigation levels, and also herbicide concentration (methyl viologen, diuron, etc.) and agree well with European data (van Kooten and Snel 1990a, pp. 199–211; 241–248; 279–293).

In close connection with the value of coefficient  $F_{V1}$ , there is a change in  $F_V^5$  (the value of “spikes 5 min”) induced by the saturating light impulse superimposed with the actinic light flux (Fig. 2.19, Table 2.6) or at shutdown of the latter (“spikes 6 min”). The  $F_V^t$  value is sensitive to thermal processing and is already suppressed by 70 % relative humidity and  $\gamma$ -radiation (Saakov et al. 1993; Lichtenthaler 1996a, b; Saakov and Shiryaev 2000). The effect and aftereffect of  $\gamma$ -radiation correlate with the influence of temperature, fumigation, dehydration, and herbicides and decrease the  $F_V^t$  and  $q_\text{E}$  levels (i.e., reduce the Calvin cycle activity and  $q_\text{q}$ ). This change in  $F_V^t$  corresponds to the damage depth of PS-2 energy links that develops in time. It is noted that with an increase in the actinic light flux intensity from 185 to

590  $\mu\text{E}/(\text{m}^2 \text{ s})$ , the value of the spikes (equal to  $F_V^t$ ) decreases. Separately, we wish to draw attention to research on the kinetics of changes in  $F_V^t/F_0^t$  (Saakov 1993a), because this parameter is also closely coupled with the damage to PS-2 energetics and changes from 3 to 6 relative units for the control and from 1.3 to 0.1 relative units for the experiment (Saakov et al. 1992; Lichtenthaler 1996a, b; Saakov and Shiryaev 2000).

Thus, there is a clear manifestation of the *non-specificity* of the kinetics of PAMF signal harmonics in response to the influence of various EFEs, and features of the change in the coefficients  $F_m$ ,  $F_V$ ,  $F_{V1}$ ,  $F_V^t$ ,  $F_0$ , and  $F_0^t$  indicate the interconnection of determined disorders with the damage to components of PS-2 RCs.

The high  $F_V$  value (including spikes at  $F_V^t$ ) is a result of the low  $q_E$  value and the high utilization of energy in the Calvin cycle. High temperatures result in increased  $q_E$  (to 0.6–0.75), which indicates  $F_V^t$  decrease and energizing of the thylakoid membrane. In this case, ETC inhibition occurs, probably when the Calvin cycle is unable to work as an acceptor of electrons and the suppression of its activity is much more probable than the inhibition of ATPase. The  $q_E$  relaxation is accompanied by the simultaneous switching on of the Calvin cycle, coupled ATP use, and decrease in the proton gradient. At thermal processing the  $q_E$  relaxation is suppressed, testifying to the restriction of Calvin cycle activity. This restriction probably precedes the damage at the PS-2 level and is expressed as an increase in the  $F_0$  level,  $F_V^t$  reduction, and  $F_m^t$  decrease at the simultaneous growth of  $q_E$ . So the low  $q_E$  value (0.3–0.4 relative units) indicates the high activity of the carbon cycle reactions. Increases in  $q_E$  will not be observed after addition of uncouplers of the proton gradient. Also, after addition of methyl viologen (the electron acceptor PS-1), ATP and NADPH/ $\text{H}^+$  will not be formed because methyl viologen is a better electron acceptor that directly or indirectly influences the proton gradient and  $\text{CO}_2$  fixing.

The fast decrease in coefficient  $q_q$  in the first minutes of light exposure indicates ETC reduction. The change in this coefficient by 0.03–0.04 relative units is significant (Krause and Weis 1984; Lichtenthaler and Rinderle 1988; Briantais et al. 1986). The increase in  $q_q$  is caused by re-oxidization of  $\text{Q}_\text{A}^-$ . At values  $q_q = 0$ , there is no transformation of light energy, and at  $q_q = 1$ , it is optimal. In the steady state,  $q_q$  is usually approximately 0.8–0.9 relative units. The high  $q_q$  value for well-lit plants indicates high levels of electron transport, NADPH/ $\text{H}^+$ , and photosynthesis. Before the leaf falls under the negative influence of environmental factors (Table 2.6),  $q_q$  decreases, pointing to suppression of the ETC activity (Krause and Weis 1984; Lichtenthaler and Rinderle 1988; Briantais et al. 1986; Lichtenthaler 1988a, b, 1996a, b; Snel and van Kooten 1990). The high reduction of the  $\text{PQ}^{2-}$  plastoquinone pool is accompanied by a low  $q_q$  value (Lichtenthaler 1988a, b). The  $q_q$  decrease to 0.4 indicates ETC reduction, with subsequent re-oxidization and increase in  $q_q$  value to 0.9; the decrease in  $q_q$  is also accompanied by an increase in the proton current and shows the accumulation of electrons in the acceptor part of PS-2 (Briantais et al. 1986; Lichtenthaler 1988a, b).

The unusual form of spikes obtained during the light/darkness cycles of 80 s/20 s allows tracking of the process of PS-2 reduction with a great degree of reliability

and to take notice of the *two-phase* or sometimes *three-phase* structure of spikes for damaged leaves (Saakov 1993a–d; Saakov and Shiryaev 2000; Rubin 1987, 1997, 2000a, b, 2004) when the initial fast  $F_V^t$  increase slows (Fig. 2.20, point 5) and then starts to decrease smoothly, showing the transition from  $F_V$  to  $F_{V1}$ . The presence of three components in such a signal was also observed by other researchers (Bukhov et al. 2001b; Egorova et al. 2001). Shutdown of the actinic light flux reduces  $F_V^t$ . We suppose that the fast component of PAMF signal harmonics demonstrates the  $Q_A^-$  quenching, because  $Q_A^+$  acts as a FI quencher and in the state  $P_{680}^*PheoQ_A$  the transformation of photochemical energy (i.e., formation of  $P_{680}^*PheoQ_A^-$ , of the integral part of RCs) is a convenient opportunity for the de-excitation (Saakov and Shiryaev 2000). The second, short and slower, component (Fig. 2.20, arrows with asterisks) shows the delay of  $Q_A^+$  reduction due to the electron transfer from  $P_{680}$  to Pheo. The third, slow, component suggests that ETC damage arises during the  $e^-$  transfer from  $Q_A^-$  to  $Q_B^+$  (Krause and Weis 1984; Lichtenthaler and Rinderle 1988; Briantais et al. 1986; Lichtenthaler 1988a, b, 1996a, b; Snel and van Kooten 1990). Such a many-component decrease in the fluorescence coefficient underlines the complexity of mechanisms and pathways of  $Q_A^-$  re-oxidization. The slow component possibly corresponds to the inhibition (as under the influence of diuron) of the  $e^-$  transfer between  $Q_A^-$  and  $Q_B^+$  or  $PQ^{2-}$  that leads to the  $q_q$  decrease, because all quenchers of FI are reduced and the subsequent re-oxidization is absent. This is supported by the gradual decrease (relaxation) of the slow component after input of the actinic light flux. Shutdown of the light flux results in the fast re-oxidization of  $Q_A$  and  $Q_B$  and in the  $e^-$  transfer to PS-1 and the FI signal decrease to  $F_0^t$ .

Acquaintance with the literature (Lichtenthaler and Rinderle 1988; Briantais et al. 1986; Lichtenthaler 1988a, b, 1996a, b; Snel and van Kooten 1990) and our own data (Saakov 1976, 1987, 1990, 1993a, b, 2000a–e; Saakov and Shiryaev 2000; Saakov et al. 1993) allow the conclusion to be made that the influence of natural EFEs (intensive light exposure, high and low temperatures, dehydration, ionic deficiency, flooding, salification ( $Na^+$ ,  $Cl^-$ ,  $SO_4^{2-}$ ), pathogenic viruses and bacteria) and anthropogenous stressors (herbicides, fungicides, fumigation ( $SO_2$ ,  $NO$ ,  $NO_2$ ), ozone and photochemical smog, active oxygen (radicals and peroxides), photo-oxidizers, acid rains, fogs, acid pH soils and the related deficiency of  $K^+$ ,  $Mg^{2+}$ ,  $Ca^{2+}$ ,  $Mn^{2+}$  ( $4-7+$ ), and  $Zn^{2+}$ ; surplus of nitrogen and  $NH_4^+$ , heavy metals, UV and  $\gamma$ -radiation, and high concentration of  $CO_2$ ) is coupled in overwhelming majority to the primary influence on the state of PS-2 RCs, which manifests as changes in the coefficients of PAMF signal harmonics quenching and in the suppression of the re-oxidization of  $e^-$  transfer links in PS-2 RCs. This is illustrated by the following scheme, the vertical arrows of which emphasize the possible sites of the influence of various EFEs on PS-2 RCs:



### ***2.2.6 Additional Material for Substantiation of the Energetic Basis of the Theory of Procaryota and Eucaryota Phototrophic Cell Tolerance to the Influence of Abiotic Environmental Factors***

#### **2.2.6.1 Problems of Chloroplast Resistance**

In the 1980s and 1990s, there was mass development of works on the PAMF of chlorophyll, which allowed registration in vivo of the dynamics of the leaf state in direct sunlight and of the photosynthetic primary reactions. This directed the interest of researchers to biophysical aspects of assessment of the electronic transport efficiency and of photosynthesis regulation in situ, because they correspond to the chloroplast's functional activity under various ecological conditions of the plant state (Briantais et al. 1986; Bolhar-Nordenkamp et al. 1989; Schreiber and Bilger 1993; Mohammed et al. 1996; Schreiber et al. 1997a, b). The nomenclature of FI levels and coefficients of FI quenching, and also ways of their calculation and formulae for assessment of the PS-2 quantum yield, have been established (Schreiber and Bilger 1993; Schreiber et al. 1997a, b; van Kooten and Snel 1990a; Snel and van Kooten 1990). These have proved useful for the practical application of this technique in various areas of biophysics, physiology, and plant ecology under the influence of stress on a vegetational cell regardless of its systematic origin. The main factor is the presence of chlorophyll *a*. The stress influence of the EFE does not necessarily lead to a long-term decrease in the photosynthetic activity (Semikhatova and Saakov 1962), which also can be determined after analysis of the coefficients of FI quenching.

Thanks to the regulatory mechanisms of compensatory replacement, adaptive repair of the process occurs and neutralizes the influences of stress and the induced photoinactivation (photoinhibition, PhIn), that is, the decrease in the photosynthetic activity in response to light excess (Saakov 2003a, b). Study of PAMF signal harmonics is useful for the quantitative assessment of characteristics of the photosynthesis change in response to light excess under the conditions of EFE stress on a cell. From the previous sections, it is seen that the ratio  $F_v/F_m$  ( $F_v$  is the variable FI and  $F_m$  the maximum FI) is a reliable indicator for assessment of the PS-2 quantum yield, which decreases at PhIn. With photoinhibition, the ability of PS-2 to manage the electron flux is broken, and the active RCs become photochemically inactive, dissipating the de-excitation energy in the form of heat. The research on non-photochemical quenching ( $q_E$ ) opened the way for a wide range of investigations into adaptive and protective mechanisms against the stress influence of EFEs. Low-temperature FI is applicable for study of theoretical aspects of the fluorescence phenomenon, such as the change in the excitation energy distribution between PS-1 and PS-2 and for the analysis of changes in the system of photosynthetic pigments caused by EFEs (Briantais et al. 1986; Bolhar-Nordenkamp et al. 1989). Still, it is important to note that the physiological interpretation of obtained practical data would be impossible without works in this direction. At room temperature, most of



the fluorescence is emitted by PS-2, whereas at  $-196^{\circ}\text{C}$  there is a significant contribution of PS-1 to the far red spectral area.

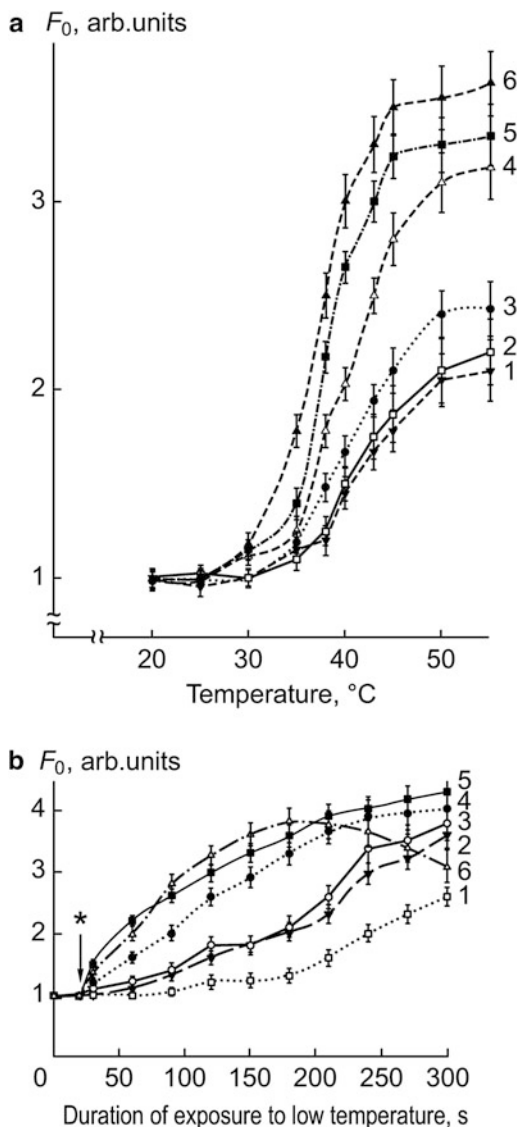
Thus, there are two types of possible research into FI, theoretical and practical. Until now, theorists treat practical conclusions deduced from the analysis of coefficients of FI quenching with a certain snobbery. However, FI measurement gives useful practical information on the state of cultured and wild plants and on algae and their communities in the ocean. Progress in the development and in the breadth of application of the method is possible due to the close connection of theoretical interpretation with practical conclusions about the functional state of an organism. Their combination with precision methods such as spectrophotometry *in vivo* also allows conclusions to be made about damage to the structural organization of the photosynthetic device (Saakov 1993a–d, 2002a–c, 2003a, b). The large volume of the world literature, partially summarized in reviews (Briantais et al. 1986; Bolhar-Nordenkamp et al. 1989; Schreiber and Bilger 1993; Mohammed et al. 1996; Schreiber et al. 1997a, b), gives severe rebuff to theorists haughtily looking at the practical use of the PAM method and at the conclusions made on the basis of its application.

It is necessary to emphasize that the Ministry of Agriculture and Sciences of Austria sponsored an international research program for the comparative assessment of the equipment made by different firms and for the assessment of their possibilities for the rapid diagnosis of plant states in field conditions when damage to biological objects is not yet visually detectable (Bolhar-Nordenkamp et al. 1989). Due to the high practical advantage of FI research, many European firms produce various highly demanded models of fluorometers, the comparative analysis of which (Briantais et al. 1986; Bolhar-Nordenkamp et al. 1989; Mohammed et al. 1996) showed their high precision and good reproducibility of results and accented the prospective applications. This experience should doubtlessly be adopted not only for Russian scientific institutions; but the PAMF method could also be used by the Ministry of Emergency Situations and other State services in cases of ecological terrorism and technogenic accidents. The long experience of Russian experts working abroad in this direction is, as usual, unclaimed in Russia.

As in the majority of published works, the influence of different factors on different objects was studied with the use of different equipment and different conditions of measurements. In the present work, we summarize the experience of registration of PAMF signal harmonics changes under influence of various EFEs in one laboratory, in approximately the same season, and with the same device (101-103 Walz, Effeltrich, FRG) (Saakov 1993a–d, 2000a–e, 2002a–c, 2003a, b; Saakov et al. 1993). The calculation of quenching coefficient  $q_E$  and the photochemical coefficient  $q_q$  was carried out at 7–8 min of PAMF registration. We again emphasize that the analysis of  $q_q$  and  $q_E$  is of great diagnostic value because it helps to localize the biological link of EFE influence (Saakov 1993a–d; Saakov et al. 1993; Saakov and Shiryaev 2000). In this section, we limited ourselves to a review of high and low thermal influence on the character of the dynamics change in  $F_0$ ,  $q_q$ , and  $q_E$  (Figs. 2.21, 2.22, 2.23, and 2.24) as a function of the stress factor



**Fig. 2.21** (a) The character of the change in base fluorescence  $F_0$  dynamics under the influence (15 min) of increased temperature for woody and herbaceous plants different in resistance. 1 laurel (*Laurus nobilis*); 2 wheat Saratovskaya 29 (*Triticum* sp., the cultivar Saratovskaya 29); 3 barley (*Hordeum* sp.); 4 clover (*Trifolium pratense*); 5 nettle (*Urtica dioica*); 6 barley mutant № 2807 lacking chlorophyll *b* (*Donaria* cultivar). *Abscissa*: the influencing temperature. *Ordinate*: relative  $F_0$  values. (b) The character of the change in base fluorescence  $F_0$  dynamics under the influence of low temperature ( $-5^\circ\text{C}$ ) for woody and herbaceous plants different in resistance. 1 burdock (*Arctium* sp.); 2 laurel (*Laurus nobilis*); 3 plum (*Prunus domestica*); 4 clover (*Trifolium pratense*); 5 nettle (*Urtica dioica*); 6 barley mutant № 2807 lacking chlorophyll *b* (*Donaria* cultivar). *Abscissa*: duration of thermal influence; *ordinate*: relative  $F_0$  values. The asterisk indicates the  $F_0$  value at  $20\text{--}22^\circ\text{C}$



impact. The latter became possible due to the ability of the PAM technique to repeatedly measure the functional characteristics of an object *in vivo* (Mohammed et al. 1996; Saakov 2003a, b).

Usually in the experiment, 8–12 leaves were taken for one variant, and the value for each point (Figs. 2.21a, b and 2.22a, b) represents the average of the response of the object to the influence of the EFE, which corresponds to recommendations and our research experience (Bolhar-Nordenkamp et al. 1989; Mohammed et al. 1996). European researchers investigated plants that were

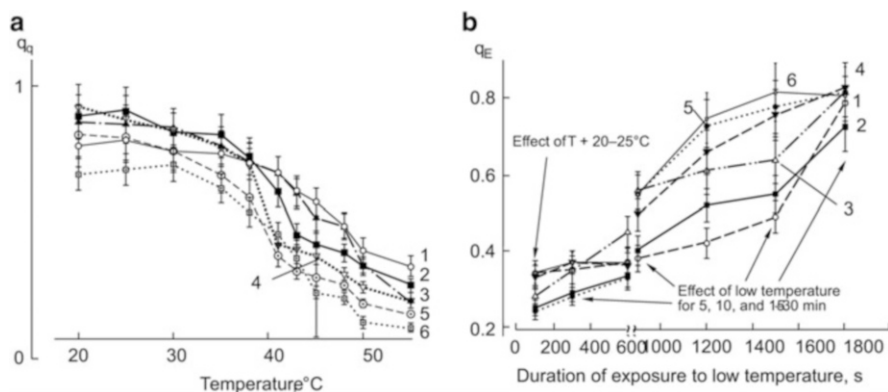


**Fig. 2.22** (a) The dynamics of the change in PAMF photochemical quenching coefficient ( $q_q$ ) under the influence (15 min) of high temperatures for woody and herbaceous plants: 1 oak (*Quercus robur*); 2 laurel (*Laurus nobilis*); 3 Sakhalin buckwheat (*Polygonum sachalinense*); 4 clover (*Trifolium pratense*); 5 nettle (*Urtica dioica*); 6 barley mutant № 2807 lacking chlorophyll *b* (*Donaria cultivar*). *Abscissa*: duration of thermal influence; *ordinate*: relative  $q_q$  values. (b) The dynamics of the change in PAMF non-photochemical quenching coefficient ( $q_E$ ) under the influence of low temperature ( $-4^{\circ}\text{C}$  for 10 min) for woody and herbaceous plants. 1 ivy (*Hedera helix*); 2 oak (*Quercus robur*); 3 Sakhalin buckwheat (*Polygonum sachalinense*); 4 barley (*Hordeum* sp.); 5 barley mutant № 2807 lacking chlorophyll *b*; 6 clover (*Trifolium pratense*)

already adapted for higher summer temperatures owing to the climatic conditions of the countries. In this regard, we tried to perform experiments during the early autumn period.

The constant FI after the *dark period* of object adaptation when all PS-2 RCs are open is designated as  $F_0$  (the minimum FI yield), which is induced by a modulated light beam ( $\lambda \leq 670$  nm) of flux of  $0.1 \mu\text{E}/(\text{m}^2 \text{s})$ ; its intensity is small enough to change the oxidation–reduction potential of the primary acceptor of  $Q_A$  and leaves it in the  $Q_A^+$  state (Saakov et al. 1993; Saakov and Hoffmann 1974; Schreiber et al. 1997a, b; Saakov 2003a, b). The  $q_q$  value is maximum and equal to 1.0. The  $F_m/F_0$  ratio between the maximum yield of FI (in this case  $Q_A^-$  is reduced) and the minimum yield of FI ( $Q_A^+$  is oxidized) fluctuates approximately from 5 to 6 relative units. The  $F_0$  increase occurs at the damage of PS-2 RCs and the disorder of the light energy transfer from antenna complexes. It is shown that the  $F_0$  change can be used for determination of the critical borders of phototrophy realization in *Prokaryota* and *Eucaryota*, depending on the influence of high and low temperatures, radioactivity, and other EFEs (Mohammed et al. 1996). The ratio  $F_0/F_m$  indicates the temperature tolerance of PS-2 when cultivating plants at high temperature. The increase in  $F_0$  under increased thermal impact correlates with the irreversible thermal influence on leaf tissue (Schreiber and Bilger 1993; Schreiber et al. 1997; Saakov 2003a, b). The soft influence of temperature does not cause the irreversible damage to tissues that is noted at midday depressions of photosynthesis. In this regard, we observed the change in  $F_0$  over a wide range of physiological temperatures, but they were lower than those resulting in tissue

necrosis (Fig. 2.21a, b); this caused the significant complexity of the present work and its difference from many European publications.

When analyzing  $F_V/F_m$ , it is especially necessary to take into consideration and to distinguish the  $F_0$  level increase from the  $F_V$  reduction. The change in the  $F_0$  level alters the usual ratio  $F_V/F_0$  (3.1–3.5 relative units), reducing it to 0.9–1.0 relative units. The  $F_0$  value increase characterizes the destruction of PS-2 RCs, whereas the decrease in  $F_V$  is coupled with the  $q_E$  change; PhIn causes both these changes (as illustrated by the data in Figs. 2.21 and 2.22). From Fig. 2.21, it follows that the changes in  $F_0$  with increasing temperature are of an S-shaped character and already start to manifest in the region 35–38 °C. Exactly this area of temperature was determined by us many years ago (Semikhatova and Saakov 1962). A further increase in temperature results in a jump-like change in  $F_0$  values. These data correlate well with studies of the suppression of photosynthesis intensity under similar conditions (Semikhatova and Saakov 1962; Schreiber and Bilger 1987; Schreiber and Neubauer 1987; Saakov 2001a, b). A conclusion about the possibility to distinguish the resistance of objects to the influence of high temperature by the change in their  $F_0$  (Fig. 2.21a, curves 1, 2, 3 and the group of curves 4, 5, 6) is not excluded. The final validity of this conclusion demands the study of a wide set of plants different in stability and high statistics.

The stress influence of low temperatures also leads to an increase in  $F_0$  (Fig. 2.21b). The degree of the  $F_0$  increase directly depends on duration of the thermal influence. It should be noted that under the soft influence of low temperature, there is no reduction in the  $F_0$  level, which was registered by us and other authors in the case of a shock influence of low temperature in the process of its aftereffect (Mohammed et al. 1996; Saakov 2001a, b), resulting in tissue necrosis. In rough leaves of *Arctium* sp. and also in woody leaves of stiff-leaved *Laurus nobilis* and *Prunus domestica*, the  $F_0$  changes are smoother and less intensive than in herbaceous plants. At the same time, for the mutant of № 2807, which is the least resistant to thermal influence (Fig. 2.21b, curve 6), a rather early tendency for  $F_0$  decrease was noted.

Serious and methodologically competent works established the satisfactory correlation between the level of CO<sub>2</sub> assimilation, O<sub>2</sub> exhalation, and the coefficient  $q_q$  (Schreiber and Bilger 1993; Schreiber et al. 1994, 1997a, b). With the increase in  $q_q$ , oxygen release linearly increases; the reduction of the coefficient  $q_q$  is accompanied by an increase in  $F_0$  and  $q_E$ , and a decrease in  $F_V$ . The data obtained by us on the  $q_q$  dynamics as a function of the thermal stress influence are presented in Fig. 2.22a. The decrease in  $q_q$  corresponds to an increase in  $q_E$  (Fig. 2.22b) induced by other EFEs. Note that the obvious  $q_q$  decrease starts in the area (38–40 °C) of positive temperature influence. This agrees with data earlier obtained by us on the change in the photosynthesis intensity under the thermal influence (Semikhatova and Saakov 1962) and correlates with the opposite character of the  $F_0$  change presented in Fig. 2.21. The suggested explanation for the  $q_q$  decrease is the high level of the PQ<sup>2-</sup> reduction, the increased protonation, and the accumulation of electrons in the acceptor part of PS-2. Under the conditions of the reduced PQ<sup>2-</sup> pool, the electron accessibility of the Q<sub>B</sub><sup>+</sup> acceptor is strongly limited, and the overall performance of the ETC of photosynthesis is broken. Thus, the obstacle to

$Q_A^-$  re-oxidization appears. In this state, the probability of FI emission from the state  $P_{680}^+Q_A^-$  increases.

From the data in Fig. 2.22b, it follows that the constant increase in the effect of the low-temperature influence leads to the increase in  $q_E$  values. In the steady state of the photosynthetic device, the fluctuation of this coefficient is in the range of 0.25–0.4 relative units. In damaged plants, the  $q_E$  level increases and points to inhibition of the ATP synthesis, an increase in the membrane proton gradient, and disorder of the Calvin cycle activity. Removal of the EFE promotes the relaxation of  $q_E$  values to 0.3–0.4, a decrease in the membrane proton gradient, and activation of dark reactions of the Calvin cycle and of the ATP use correlating with them.

Coefficients  $q_E$  and  $q_q$  are very sensitive parameters to the EFE influence, and their change is accompanied by structural damage in the photosynthetic device, which is registered with the help of the derivative spectrophotometry method (see below Sect. 2.2.9). In contrast to  $F_0$  and  $F_v$ , the recovery of these coefficients requires a longer time after removal of the EFE, which was observed for drought (Saakov 2003a, b).

Thus, in this section, using leaves that varied in their level of EFE resistance, the dynamics of stationary values of  $F_0$ ,  $q_q$ , and  $q_E$  as a function of the intensity of the stress influence was investigated, and statistically valid limits of their change under the influence of low and high temperatures were determined. We showed that changes in  $q_q$  and  $q_E$  appear a little earlier than changes in  $F_0$  and  $F_v$ . The results of our previous investigation of the dynamics of  $F_m$  and  $F_v$  as a function of the high temperature influence (Saakov 2002a–c) do not contradict the results of this work.

This experimental work was the first of this kind to be reported in the world scientific literature. We invite any skeptic to perform control measurements and to enjoy the labor intensity of such measurements.

The accepted interpretation (Briantais et al. 1986; Bolhar-Nordenkamp et al. 1989; Schreiber and Bilger 1993; Mohammed et al. 1996; Schreiber et al. 1997a, b) of PAMF suppression coefficients indicates the link between these coefficients and the stability of phototrophy systems of a green cell. Together with the material published earlier (Saakov 1993a–d, 2000a–e, 2002a–c, 2003a, b), the results of this section support the correctness of the point of view about the primacy of the damage to the link  $P_{680}^+Pheo^-Q_A^- \rightarrow P_{680}^+PheoQ_A^-$  and the interrelation of processes responsible for the *Procaryota* and *Eucaryota* green cell tolerance to EFE influence, with the optimization of the conversion of light energy into the energy of ATP chemical bonds.

## 2.2.7 Features of the Fluorescence Change in $F_0$ and $F_m$ in Response to Dithiothreitol Inhibition of Zeaxanthin Formation

The xanthophyll cycle (sometimes called the “violaxanthin cycle”) (see Chap. 1) is a complex reaction system consisting of the light-induced de-epoxidation of

violaxanthin to zeaxanthin (Zea) via the monoepoxide antheraxanthin and of the reversible epoxidation of the latter, lower in speed and occurring in response to the photon flux density limiting the CO<sub>2</sub> fixing (Yamamoto 1995; Yamamoto et al. 1962; Saakov 1963, 1965). Considerable information has accumulated on the properties of the xanthophyll cycle and on the association of these reactions with photosynthesis and photophosphorylation processes (Saakov 1971a, b; Baltscheffsky 1971; Saakov and Hoffmann 1974; Saakov et al. 2013). The interrelation between the stability of the cycle activity and the stability of the plant plastid device system has been shown (Saakov 1973). Over a number of years, there has been active discussion on the correlative dependence between the Zea content and the type of chlorophyll FI quenching in response to photoinhibiting stress, when FI is characterized by a decrease both in the minimum dark stationary FI ( $F_0$ ) and in the maximum FI ( $F_m$ ) at the different photon flux density (Demming-Adams 1990; Demming-Adams and Adams 1990, 1992, 1996; Demming-Adams et al. 1987, 1989, 1990). The authors supposed that Zea is involved in the process of non-radiative dissipation of energy, which takes place in the complex of chlorophyll molecules and allows transfer of the excited chlorophyll into its ground state by means of thermal emission. The  $F_0$  quenching is the key point of the dissipation process coupled with Zea, that is, in the absence of a change in Zea, changes in  $F_0$  should not be observed.

At the same time, the first data were published (Foyer et al. 1990a, b) that showed the ambiguity of such an interpretation and were further developed in later works (Saakov et al. 1993; Richter et al. 1994).

In this section, we will concentrate on the research into the dependence of the FI change on the Zea content. For this purpose, we used the inhibition of the Zea formation reaction with dithiothreitol (DTT) according to the work of Demming-Adams et al. (1990).

As the investigated object, the compound leaves of *Robinia pseudoacacia* L. and *Taraxacum officinale* L. were used. Their choice was defined by the possibility of the selection of physiologically homogeneous leaflets. After cutting, the leaves were left for 24 h in the dark, on water. This allowed a stationary level of Zea and  $F_0$  to be reached in leaves adapted to darkness, when the RCs of PS-2 are completely open. Unlike previous methods of DTT introduction (Demming-Adams et al. 1990), we softly infiltrated the inhibitor solution (3 or 6 mM) in the half-light (Saakov 1965, 1971a, b). Control leaves were infiltrated with water. The measurement of fluorescence was carried out by means of the pulse-amplified modulated method (Schreiber 1986), using the PAM fluorometer M-101-103 (Walz, Effeltrich, Germany). We emphasize that the method of FI registration applied by us was identical to the published method (Demming-Adams 1990; Demming-Adams and Adams 1990, 1992). The top part of the leaflet was placed on the frontal part of the light guide, which delivered both the white actinic light and the excitation red light ( $\lambda \approx 670$  nm) to the leaf, and passed the fluorescence emission to the photodiode detector protected by a filter ( $\lambda = 700$  nm). The selective amplifier perceived only pulse signals of FI induced by the excitation light. Upon

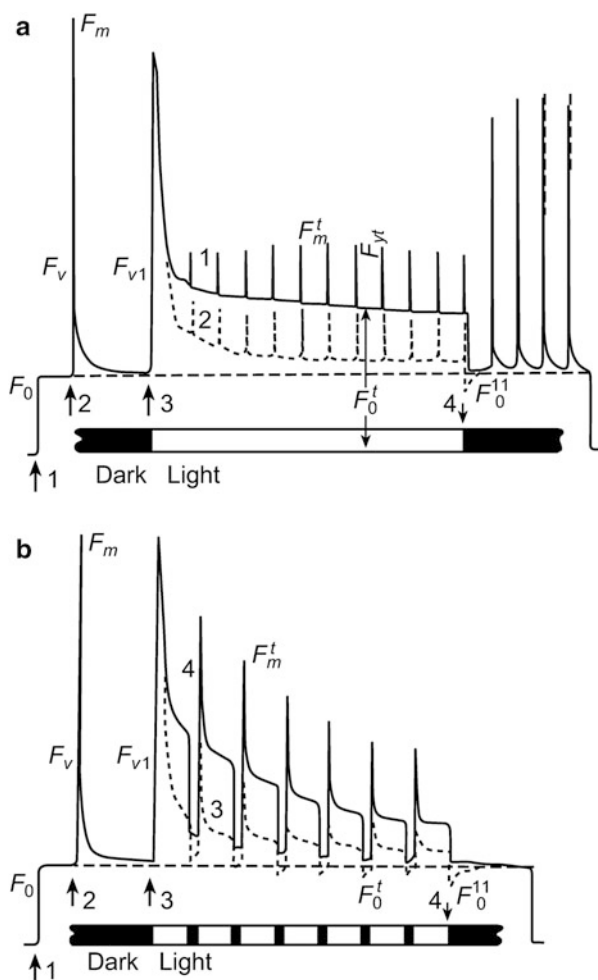


**Fig. 2.23** The character of the change in modulated fluorescence harmonics for the chlorophyll *a* of *Robinia* leaflets adapted to the darkness and infiltrated with water (curves 2 and 3) or with 6 mM DTT solution (curves 1 and 4) in response to light exposition of 11 min. (a) The combination of a 1-s saturating white light impulse ( $3,000 \mu\text{E}/(\text{m}^2 \text{ s})$ ) followed by 60 s of darkness and then by 11 min of actinic light of  $590 \mu\text{E}/(\text{m}^2 \text{ s})$  and frequency 100 kHz for the determination of  $F_m^t$  values. (b) Seven cycles of 80 s light (non-saturating light impulses)/20 s darkness for the  $F_0^t$  determination at the start of dark periods. The used actinic light was  $1,550 \mu\text{E}/(\text{m}^2 \text{ s})$ . Arrows: 1 input of modulating light of frequency of 1.6 kHz for the determination of the  $F_0$  level of the minimum dark fluorescence; 2 the saturating light impulse ( $3,000 \mu\text{E}/(\text{m}^2 \text{ s})$ ); 3 input of actinic light of frequency of 100 kHz; 4 shutdown of the actinic light for the  $F_0^{11}$  determination.  $F_0$  the minimum dark fluorescence of leaves adapted to the darkness;  $F_m$  the maximum fluorescence;  $F_v$  the variable fluorescence ( $F_v = F_m - F_0$ );  $F_0^t$  the minimum fluorescence at the start of the 20-s dark period;  $F_0^{11}$  the minimum fluorescence at shutdown of the actinic light of 100 kHz

termination of the exposure, the leaf material was fixed with liquid nitrogen and analyzed using high pressure liquid chromatography (Saakov et al. 1993).

Results on the character of the change in FI yield harmonics after the DTT processing of leaves were obtained under conditions of actinic light radiation ( $590 \mu\text{E}/(\text{m}^2 \text{ s})$ ) with a 1 s red light impulse and a dark interval of 60 s (Fig. 2.23a). A second approach used a light/dark cycle of 80 s/20 s and actinic light intensities of 560 and  $1,550 \mu\text{E}/(\text{m}^2 \text{ s})$  (Fig. 2.23b). The second approach is optimum because of the different speeds of the light and dark reactions of the xanthophyll cycle and also due to the re-oxidization of acceptors  $Q_A$ ,  $Q_B$ , and PQ.

From the data in Fig. 2.23, it follows that DTT does not significantly influence the  $F_V/F_m$  ratio (usually 0.825–0.830), and its high value emphasizes the increase in the PS-2 reduced state and the RC closing. At the moment of maximum dark FI ( $F_m$ ), the coefficient of the FI photochemical quenching  $q_q=0$  and non-photochemical processes are minimized (i.e.,  $q_E=0$ ). The  $F_m$  level after DTT addition increased for both investigated objects, pointing to an increase in the variable FI,  $F_V$ , ( $F_m - F_0 = F_V$ ). When exposing leaves to cyclic lighting (80 s/20 s), it follows that the 80-s non-saturating impulse does not significantly influence the  $F_m^t$  change. At the same time, the illumination of plants by actinic light considerably changes  $F_0$ , which suggests the incomplete work of the cycle of re-oxidization of electron acceptors in RCs of PS-2. The change in the ratio  $F_m/F_0$  emphasizes the increase in the PS-2 reduction state. The high level of  $F_0 + F_V^t$  corresponds to the small  $q_E$  value and points to activation of the energy utilization in the Calvin cycle. Further, from the data of Fig. 2.23, it follows that  $F_0^t$  values ( $F_0$  in the specific interval of time  $t$ ) increase in the presence of DTT. In response to DTT infiltration, the increase in  $F_0$  correlates well with the coefficient  $F_{V1} h/2$ , characterizing the half-width of the FI harmonic contour band and described by the height  $F_{V1}$  and the run of the curve  $F_0^t$  (Saakov 1993a–d), induced by the actinic light. The  $F_0^t$  level reached after 11 min of light exposure in the experiment after shutdown of the light was lower than the initial  $F_0$  of the leaves adapted to darkness in the absence of DTT. So both approaches to the lighting of samples yielded identical results that agreed with the data (Demming-Adams 1990; Demming-Adams and Adams 1992; Demming-Adams et al. 1990).

In the absence of DTT, the character of the dynamics of the content change in the xanthophyll cycle components at pulse lighting (80 s/s) did not differ from the well-known dynamics (Yamamoto et al. 1962; Saakov 1963, 1965; Demming-Adams and Adams 1990, 1992, 1996). DTT infiltration inhibited Zea formation (Fig. 2.24, curve 3), in agreement with reported data (Demming-Adams et al. 1987, 1989, 1990).

At the same time, we found inhibition of violaxanthin de-epoxidation (Table 2.7). Other pigments of chloroplasts do not react to DDT infiltration.

The results presented in Fig. 2.24a, b show the considerable distinction between the kinetics of  $F_0$  curves and the Zea content. The first curve ( $F_0$ ) reaches the

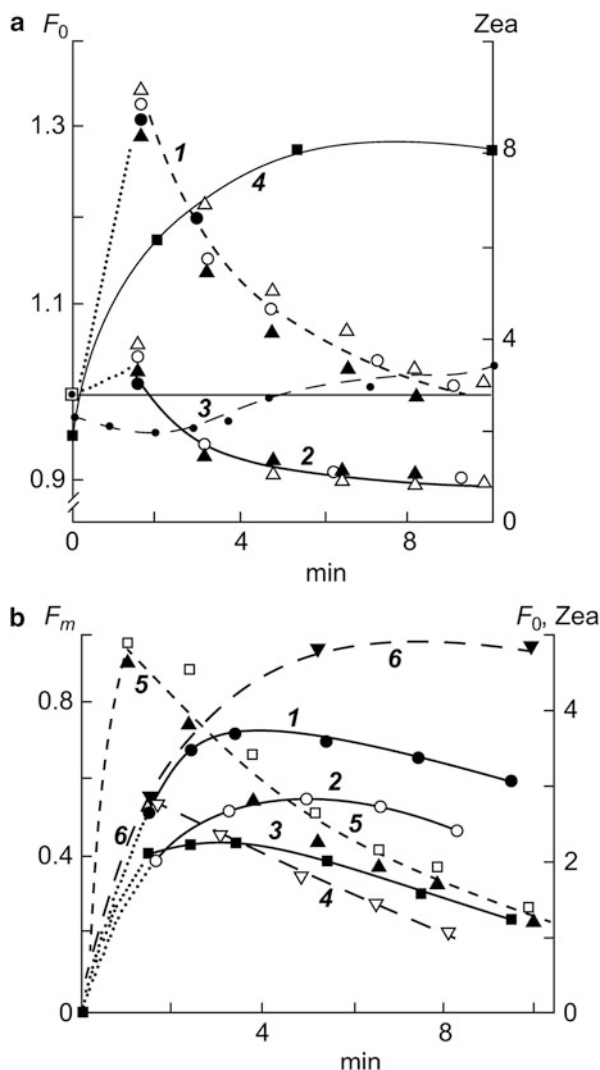


**Fig. 2.24** (a) The kinetics of the change in the ratio  $F_0^t/F_0$  and of the zeaxanthin content in *Robinia* leaves infiltrated with the DTT solution (6 mM) (curve 1  $(F_0^t/F_0)^{+DTT}$ ; 3  $Zea^{+DTT}$ ) and in the *Robinia* control leaves (curve 2  $(F_0^t/F_0)^{-DTT}$ ; 4  $Zea^{-DTT}$ ) at light/dark illumination of 80 s/20 s with actinic light of 1,550  $\mu E/(m^2 s)$ . Abscissa: time of light exposure in minutes; left ordinate relative units for curves 1 and 2; right ordinate Zea content in mol/100 mol of chlorophyll *a*. Symbols on curves 1 and 2 show data for separate leaflets of the *Robinia* compound leaf. (b) The dynamics of  $F_m$  fluorescence quenching (curves 1–3), fluorescence  $F_0$  (curve 4) of the additional fluorescence  $F_0^t$  (curve 5) at the DTT infiltration and in the presence of the additional quantity of the formed Zea (curve 6) in the absence of DTT. Abscissa: time in minutes; left ordinate for curves 1–3  $(F_m^{t(+DTT)}/F_m^{t(-DTT)}) - 1$ ; right ordinate for curve 4  $(F_0^{t(+DTT)}/F_0^{t(-DTT)}) - 1$ ; curve 5  $(F_0^t/F_0)^{+DTT} - (F_0^t/F_0)^{-DTT}$ , all in relative units; curve 6  $Zea^{-DTT} - Zea^{+DTT}$ , in mol/100 mol of chlorophyll *a*. Curves 1 and 3 correspond to actinic light of 1,550 and 590  $\mu E/(m^2 s)$ , respectively (as in Fig. 2.23a), in combination with saturating impulses. Curve 2 pulse period 80 s/20 s with actinic light of 1,550  $\mu E/(m^2 s)$  (as in Fig. 2.23b). Data are averaged for 2–3 leaves



**Table 2.7** Inhibition of de-epoxidation of violaxanthin (mol/100 mol chlorophyll *a*)

Inhibitor	Violaxanthin content			
	Dark	Light (min)		
		2	5	10
–DTT	10.1	4.6	3.4	2.5
+DTT	9.75	9.3	8.0	7.0

maximum in 80 s of the light period, and the Zea content becomes maximal after three light periods (see curves 2 and 4). The difference curves for the kinetics  $(F'_0/F_0)^{+DTT} - (F'_0/F_0)^{-DTT}$  and for the Zea content ( $Zea^{-DTT} - Zea^{+DTT}$ ) are presented in Fig. 2.24b and demonstrably illustrate the discrepancy between the maxima of the curves for  $F_0$  and Zea.

From data in Fig. 2.24, it follows that the intensity of the  $F_0$  change induced in the presence of DTT (curve 1) is much higher than in the absence of DTT (curve 2). The very insignificant Zea content increase corresponds to the  $F'_0$  yield increase at 8–10 min (curve 3). Note the mirror course of curves 2 and 4, which could be interpreted by some stretch of imagination as the existence of a correlation between the  $F_0$  quenching and the increase in Zea quantity, although the positions of their maxima are different in time. Thus, under these experimental conditions, the  $F'_0$  yield increase *does not correlate* with the Zea content increase.

So the illuminated *Robinia* leaves adapted to darkness are characterized by differing kinetics of the  $F_0$  quenching and of Zea accumulation. Different time intervals were determined for the curves to reach the maximum in the range from 80 to 240 s. The data allowed us to come to the conclusion that the  $F_0$  change develops quicker than Zea formation as a result of violaxanthin de-epoxidation and quicker than the  $F_m$  quenching (Fig. 2.24b). This suggests small probability that, after the transfer of leaves adapted to the darkness to the light, Zea acts as a *quencher* of  $F_0$  induced in the presence of DTT.

The different character of the  $F_0$  and  $F_m$  quenching kinetics suggests the existence of various mechanisms of their quenching. In the assumption that the DTT influence on photosynthetic membranes is limited to Zea formation, our data would mean that the  $F_0$  quenching is *not caused* by the Zea emergence. At the same time, considering the modulation of  $H^+$ -ATPase by DTT and the sensitivity of PS-2 protease to DTT, it is possible to assume that the  $F_0$  effective quenching is the consequence of the DTT influence and is not related to the inhibition of Zea formation.

The presented materials demand that caution is taken in accepting the unambiguity of conclusions in the works of Demming-Adams and colleagues (Demming-Adams 1990, Demming-Adams and Adams 1992; Demming-Adams et al. 1990) about the role of Zea in the quenching of the excited chlorophyll fluorescence.

### **2.2.8 *Specifics of $\gamma$ -Radiation Influence on the Stability of Energetics and the Pigment System of the Photosynthetic Device***

Despite plentiful publications concerning the resistance of vegetational and animal organisms to the influence of environmental factors, for many years the theoretical aspect of the problem was not established and required additional experimental data about the energetic part of the resistance and the development of new approaches (Saakov 1976, 1987).

A confused picture is also observed regarding the influence of ionizing radiation on the photosynthetic device of higher plants and algae. This is of special concern for atomic proving grounds and accident situations at nuclear power stations and other technogenic sites (Gonzalez and Moreno 1983; Ignacimuthu and Babu 1989).

Analysis of incidents has shown the absence of appropriate methods. Obtained results were considered as the model for further research on the reliable diagnostics of the flora photosynthetic device state after exposure to ionizing radiation (USSR State Committee on the utilization of atomic energy: the accident at the Chernobyl nuclear power plant and its consequences. Working document for the IAEA post-accident review meeting, Vienna, 1986. P. 101; Gesellschaft für Reaktorsicherheit (GRS): Neuere Erkenntnisse zum Unfall im Kernkraftwerk Tschernobyl. GRS-S-40 (Februar, 1987). ISBN 3-923875-13-4. P. 74; Gesellschaft für Strahlen und Umweltschutz: Umweltradioaktivität und Strahlenexposition in Südbayern durch Tschernobyl-Unfall. Bericht des Instituts für Strahlenschutz. München, Nueherberg: GSF-Bericht, 1986. Bd.16/86. S. 76.; International Atomic Energy Agency: Summary report on the post-accident review meeting on Chernobyl accident. IAEA safety ser. № 75- INSAG-1. Vienna, 1986. P.96.)

The tragic case at Fukushima demonstrated that appropriate conclusions from the Chernobyl accident were not made.

The method of pulse-amplitude modulated fluorescence (Schreiber 1983) was successfully used for the assessment of the damage to the photosynthetic device caused by temperature and radiation of radar devices (Rinderle et al. 1988; Schreiber and Bilger 1987). Taking into account the convenience of the method, we applied the modification of this method for characterization of the damage level of the photosynthetic device under the influence of high doses of  $\gamma$ -ionizing radiation using smaller doses of radiation. It is necessary to emphasize the significant difference in the order of effective dose values for vegetational and animal cells (Timofeev-Ressovsky et al. 1981). This was taken into consideration in choosing the radiation doses.

As objects of study, we chose the leaves of acacia (*Robinia pseudoacacia* L.) and haricot (*Phaseolus vulgaris* L.). The source of  $\gamma$ -radiation was a shielded capsule containing the isotope  $^{57}\text{Co}$ . During the experiment, the source power was 670 Gy/h. PAMF spectra were recorded with the Walz 101-103 device (Effeltrich, Germany). Absorption spectra of intact leaves were registered with

the spectrophotometer DW-2000 (Aminco, Germany). The computer built into the device carried out the calculation of derivative spectra.

The data in Figs. 2.25 and 2.26 show the comparative influence of different doses of  $\gamma$ -radiation on the yield and contours of the PAMF signal. In Table 2.8 the calculated coefficients on the change in initial ( $F_0$ ), variable ( $F_V$ ), and maximum ( $F_m$ ) fluorescence are presented along with data on the photochemical ( $q_q$ ) and non-photochemical ( $q_E$ ) coefficients of the fluorescence quenching.

The fluorescence arising after the dark period of adaptation ( $F_0$ ), when all RCs of PS-2 are open, is the emission of molecules of excited chlorophyll *a* taking place before the energy migration in RCs and when the first stable acceptor of PS-2, namely,  $Q_A$ , is oxidized.  $F_0$  is defined at the input of the measured light flux of  $0.1 \mu\text{E}/(\text{m}^2 \text{ s})$ . The  $F_0$  level depends on the EFE influence that causes the change in the state of PS-2 pigments. Thermal influence and photoinhibition lead to an increase in the  $F_0$  level.

Low temperatures do not cause such a sharp change (in the opinion of Schreiber and Bilger 1987). The data in Fig. 2.25 and Table 2.8 show that the influence of ionizing radiation significantly changes the  $F_0$  level after the induction with light ( $F_0^{10}$ ). After the measurement of  $F_0$ , a saturating light flux impulse ( $3,000\text{--}3,500 \mu\text{E}/(\text{m}^2 \text{ s})$ ) was applied for the determination of  $F_m$ . Its level defines the reduction of the primary electron acceptor  $Q_A$ . After the  $F_V$  decrease (2–3 min), actinic light ( $180\text{--}1,100 \mu\text{E}/(\text{m}^2 \text{ s})$ ) was turned on to induce the  $F_{V1}$  level. After 30 s, a number of saturating impulses (1 s duration, light flux of  $3,000 \mu\text{E}/(\text{m}^2 \text{ s})$ ) were fed, with intervals between impulses of 20–60 s. This set of impulses in addition to the actinic light promotes the complete reduction of the acceptor  $Q_A$ . The higher the amplitude of these induced impulses, that is, the closer they are to the  $F_{V1}$  value, the larger is the quantity of the reduced acceptor  $Q_A$ . The ratio  $F_V/F_m$  is considered to be an indicator of the photosynthetic function, and for intact chloroplasts, the value of this ratio fluctuates as approximately 0.8–0.85. A deviation of 0.03–0.04 is considered significant and points to the response of the photosynthetic device to the external influence (Schreiber and Bilger 1987).

From Table 2.8, it follows that a dose of 3.5–4 kGy is boundary; exceeding that value leads to considerable changes in photosynthetic function.

It is established that the  $q_E$  value correlates with the energization of thylakoid membranes, that is, with a light-excited proton gradient (Schreiber and Bilger 1987). The  $q_E$  value will be the higher, the higher the proton gradient and the lower the ATP synthesis. The high activity of dark reactions reduces the  $q_E$  value. Under the EFE influence,  $q_E$  usually increases. At the same time, in response to the radiation of objects with 12 kGy, the  $q_E$  value decrease suggests the pre-lethal surge of ATP synthesis caused, probably, by the critical increase in respiration intensity (James 1953). The low  $q_q$  level indicates the accumulation of electrons in the acceptor part of PS-2 and the high level of reduction of  $Q_A$  and of the PQ pool, also as the value  $1 - q_q$  characterizes the level of PS-2 reduction.

After accumulation of research experience with this method, we introduced a new parameter, which was not considered earlier in the scientific literature, namely,

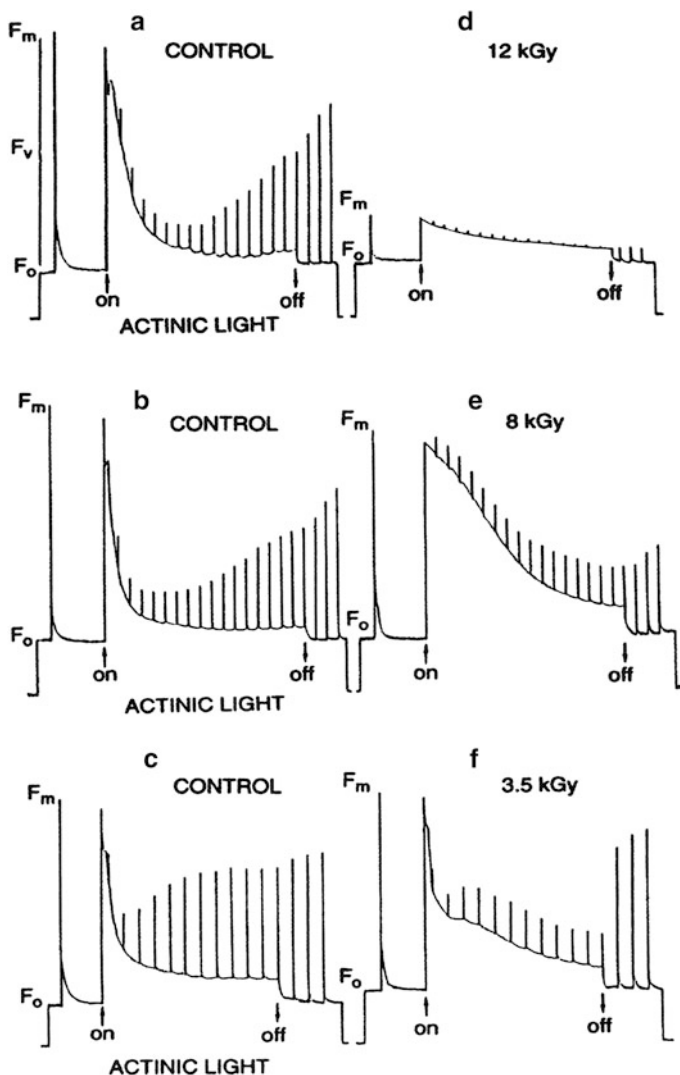


**Fig. 2.25** Influence of  $\gamma$ -radiation of 12, 8, and 3.5 kGy (d–f) on the PAMF spectra change of *Phaseolus* leaves compared with the corresponding controls (a–c).  $F_0$  initial stationary fluorescence;  $F_m$  maximal fluorescence;  $F_V$  variable fluorescence;  $F_{V1}$  fluorescence induced by actinic light;  $F_0^{10}$   $F_0$  level after 10 min of actinic light influence. Arrows indicate the input (on) and shutdown (off) of the actinic light

$F_{V1} h/2$  (see Fig. 2.19), characterizing the half-width of the contour band of the PAMF spectrum (SPF), which is described by the height  $F_{V1}$  and the run of the curve  $F_0$  induced by the actinic light. From the data in Table 2.8 it can be seen that this parameter describes, to a certain degree, the level of damage to the photosynthetic device caused by the influence of ionizing radiation.

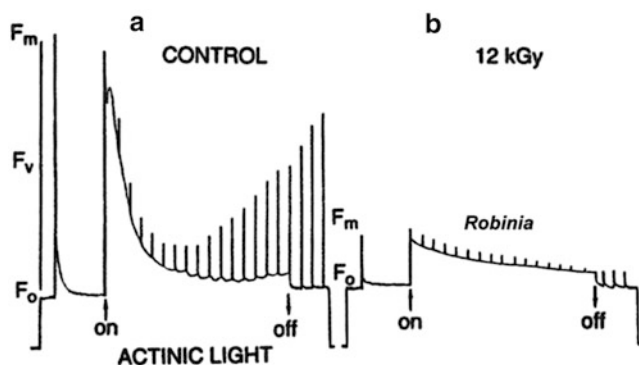


**Fig. 2.26** The influence of gamma-radiation of 12 kGy on PAMF spectra change of *Robinia pseudoacacia* L. compared with corresponding control. Robinia has leaves with more xeromorphic structure

**Table 2.8** Determination of borders of photosynthetic malfunction

Coefficient	Control	Experimental levels of irradiation, kGy, $p < 0.05$					
		12	8	4	3.5	2.5	1.3
<i>Robinia</i>							
	$n = 14$	$n = 4$	$n = 2$	$n = 4$	$n = 3$	$n = 3$	$n = 3$
$F_{\sqrt{}}/F_{\text{m}}$	0.823	0.776	0.776	0.791	0.817	0.801	0.809
$q_{\text{E}}$	0.695	0.250	0.660	0.670	0.710	0.857	0.710
$q_{\text{q}}$	0.839	0.080	0.530	0.786	0.772	0.860	0.859
$1 - q_{\text{q}}$	0.161	0.917	0.470	0.191	0.228	0.170	0.140
$F_0^{10}/F_0$	1.130	2.660	1.670	1.220	1.270	1.210	1.142
$F_{\sqrt{1}} h/2$	8.7	98.5	44.0	5.0	15.0	10.5	8.0
<i>Phaseolus</i>							
	$n = 4$	$n = 2$	$n = 4$		$n = 5$	$n = 4$	$n = 3$
$F_{\sqrt{}}/F_{\text{m}}$	0.826	0.47	0.79		0.788	0.79	0.792
$q_{\text{E}}$	0.552	0.68	0.66		0.714	0.67	0.485
$q_{\text{q}}$	0.847	0	0.53		0.727	0.90	0.861
$1 - q_{\text{q}}$	0.153	1	0.47		0.273	0.10	0.139
$F_0^{10}/F_0$	1.139	1.285	1.67		1.31	1.2	1.216
$F_{\sqrt{1}} h/2$	11	35–60	32–44		15	8.5	12

Thus, the change in coefficients calculated on the basis of SPF characterizes the damage to the energetics of the photosynthetic device and points to the damage localization in the RCs, resulting in damage to the coordinated character of reactions of components of the ETC of photosynthesis. This thesis can be also extended to the influence of other EFes.

At the same time as SPF registration, the changes in the intensity of photosynthesis and respiration were assessed. Five hours after irradiation of haricot with 8 kGy, the photosynthesis intensity reduced by 75 %, and in 10 h it was 80% less or

one fifth than the control. Correspondingly, the intensity of respiration sharply *increased* 11- and 18-fold. A smaller dose of radiation (3.5 kGy) at once reduced the intensity of photosynthesis to 0.34 of initial value and 0.14 of initial value after 5 days; the respiration intensity increased 6.1 times, and 5 days later, it fell and was only 1.6 times higher than the control. It is probable that the drop in respiration intensity corresponds to the attempt at compensatory replacement of the basic energy system of cells with the accessory system. We wrote earlier about such replacement.

It is possible to suppose, but not to state, that this phenomenon is the manifestation of the beginning of the repair of the photosynthetic device activity.

For irradiated leaves, but not cut off from plants, the characteristic feature is their water loss. At 24 h after a dose of 8 kGy, leaves contained 60 % less water than the control and 20 % less at 5 days after a dose of 3.5 kGy. After irradiation (8–12 kGy), acacia leaflets easily fall from a leaf stalk and dry up 30–50 min later; it is remarkable that they do not lose green color. In the experiment and in the control, the content of pigments *did not significantly differ*. It, apparently, masks changes in the *qualitative* state of the pigment complex of the photosynthetic device.

The *in vivo* research on derivative absorption spectra of control and irradiated leaves did not reveal considerable distinctions between the experiment and the control. Also, there was no hypsochromic shift of the red maximum inherent in the disaggregation of the chlorophyll–protein complex. Only the analysis of spectra with help of derivatives of higher orders (Fig. 2.27) allowed discovery of

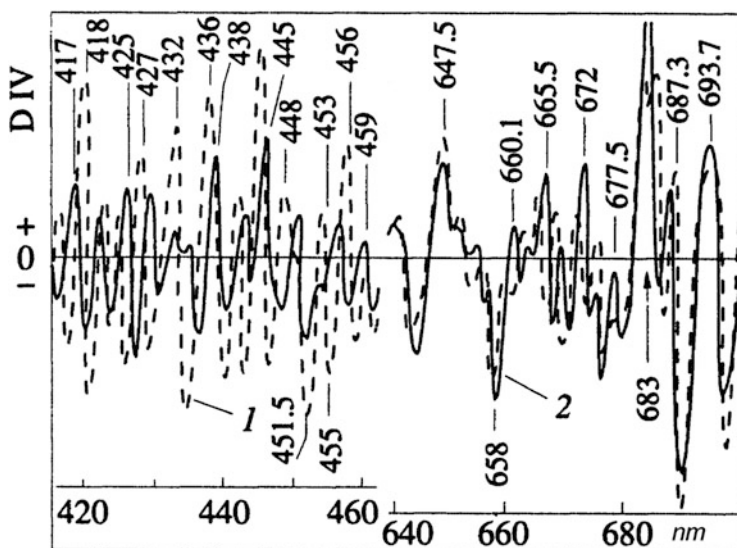


**Fig. 2.27** The course of change in the fourth derivative ( $D^{IV}$ ) of the absorption spectrum of intact leaves under the influence of  $\gamma$ -radiation (12 kGy). 1 experiment; 2 control. Numbers indicate the positions of maxima

characteristic shifts in the absorption spectrum of the fourth derivative ( $D^{IV}$ ) of intact irradiated leaves, more localized in the blue spectral area (namely, in the Soret band) and in the area of carotenoid absorption. In the red part of the spectrum, distinctions were insignificant and manifested, mainly, as changes in the positions of the spectrum of short-wave forms of the chlorophyll–protein complex. The analysis of spectra of the eighth derivative and the twelfth derivative did not reveal significant new additions about the character of damage to the chlorophyll–protein complex under the conditions of this experiment.

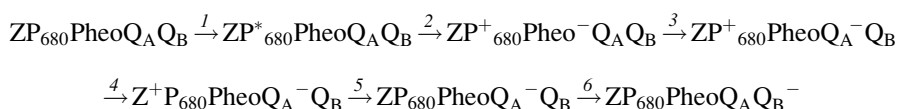
The set of native forms of chlorophyll is a system of energetically interacting elements participating in electron transfer. Even small changes in the spectral curve induced by ionizing radiation correspond to the disorder of stationary transitions of the energetic step. It is not excluded that ionizing radiation breaks the link of the electron transfer from  $P_{680}$  to the neighboring Pheo and thus prevents  $Q_A$  reduction. This can be extended to the long-term impact of powerful radar systems on the environment.

The material presented in this section indicates that the PAMF method can be considered a prospective technique for assessment of radiation damage to the photosynthetic device. We have presented data on the targeting of radiation damage to RCs of PS-2. The separate moments of spectral changes of the photosynthetic device induced by extreme influences are considered in more detail in the following sections. These results support our concept (Saakov 1976) of the interrelation of the resistance of a plant cell to EFE influence with the stability of RCs and the primary non-specific localization of the damage in the energy links of the photosynthetic device (Saakov 1987, 1996; Saakov and Leontjev 1988).

### ***2.2.9 Features of the Structural Stability of the Light-Harvesting Complex of Photosystem 2 Under the Influence of $\gamma$ -Radiation***

In more recent years, we began research on the coupling of the changes in the structure and function of the photosynthetic device under the influence of  $\gamma$ -radiation (Saakov 1992; Saakov 1993a–c, 1996). It was shown that the impact of high doses of  $\gamma$ -radiation reduces the intensity of photosynthesis, promotes the manifold increase in respiration intensity, but for a long time does not visibly changes the structural state of the chlorophyll–protein complex of the in vivo leaf, as assessed by the method of derivative spectrophotometry of high orders ( $D^{IV}$ ,  $D^{VIII}$ ,  $D^{XII}$ ) (Saakov 1993a). In the process of the *aftereffect* of  $\gamma$ -radiation (see Sect. 2.2.8), the gradual dehydration of leaf tissues manifests, the processes of lamina growth (Saakov et al. 1993) are damaged, and the S-shaped suppression of the activity of the violaxanthin de-epoxidation cycle takes place (Saakov 1993a, b). It was noted that old leaves and leaves with a pronounced xeromorphous structure

distinguished themselves by higher radioresistance (Saakov et al. 1992; Saakov 1993a). Further investigations showed the dependence of the photosynthetic function on the state of the ETC, in particular on the damage to the electron transfer links of PS-2; when the energy reaches the complex of the PS-2, the pigment P<sub>680</sub> initiates the primary transfer of an electron into the RCs of PS-2 (Saakov and Shiryaev 2000). Here we again recall the electron transport scheme at the first stages of photosynthesis:



The electron appearing at oxidization of water is transferred through the secondary donor (Z), through the pigment P<sub>680</sub> and the primary acceptor of an electron, Pheo, to the acceptor of the quinone type Q<sub>A</sub>. In stages 1 and 2, Q<sub>A</sub> and Q<sub>B</sub> are open; in stages 4 and 5, Q<sub>B</sub> is open (Saakov 1993a; Saakov and Shiryaev 2000); and in stage 5, Q<sub>A</sub> is again open. Components of Eq. (2.1) are known as integral parts of PS-2 RCs. When Q<sub>A</sub><sup>−</sup> is reduced, the RC is closed, and the electron transport and the ETC functioning are broken.

The high functional radioresistance of plant cells and of their protein-synthesizing systems (Saakov et al. 1992; Goncharova and Sheverdov 1993), and also the weak variability of ChPC in vivo under the influence of high doses of γ-radiation, promoted us to investigate the radioresistance of its separate components, namely, protein structures (Saakov 2000a–e), aromatic amino acids (Saakov 1993a–d, 1994, 1998a, b), and a number of pigment solutions (Saakov 1993a, b). The simple elements of the ChPC structure, taken apart, possess lower radioresistance than the compound biological ChPC of chloroplasts in vivo providing the basis of the photosynthetic device.

In this section, the influence of high doses of γ-radiation on the antenna light-harvesting complexes of PS-2 extracted from the plants *Phaseolus vulgaris* L. and *Spinacia oleracea* L., with differing radioresistance, is considered.

For the extraction of antenna light-harvesting complexes, we used the method of Bassi and Machold (Bassi et al. 1985), modified according to our objects of research. Leaves (2–3 g) were homogenized in 25 mL of cool medium (250 mM sorbitol; 42 mM HEPES buffer, pH 7.5; 15 mM MgCl<sub>2</sub> solution; 10 mM sodium ascorbate; 8 mM NaCl; 28 mass% polyvinylpyrrolidone 15). The homogenate was mixed with 10 mL of cooled hexane and filtered through nylon tissue. The filtrate was centrifuged for 3 min at 500 × g; the supernatant was again centrifuged for 5 min at 12,000 × g. The precipitate was resuspended in the wash medium (300 mM sorbitol; 50 mM HEPES buffer, pH 7.5; 10 mM NaCl) and was again centrifuged at 12,000 × g. The precipitate was subjected to osmotic shock in distilled water, centrifuged for 10 min at 40,000 × g, and resuspended in water. Samples of volume of 350–400 μL containing approximately 300 μg of chlorophyll were frozen and kept in liquid nitrogen. For the experiment, samples were defrosted and mixed with



Triton X-100 for 5 min on a shaker (the ratio of chlorophyll to Triton X-100 was 1:30 by weight using 2 % Triton X-100) and again centrifuged for 10 min at  $40,000 \times g$ . The supernatant was added to polyacrylamide gel plates containing digitonin (0.5 mass%) and subjected to electrophoresis. The antenna light-harvesting complexes of PS-2 were washed from the plates using tricine buffer (50 mM, pH 7.8). The  $\gamma$ -radiation and spectrophotometry of samples were carried out as described previously (Saakov 1993a–d, 1994, 1996, 1998a, b, 2000a, b). Spectra were processed with the *Graph Digitizer 1* program, digitalized, and, where necessary, differentiated with smoothing of the next to last derivative with the help of the Microcall *Origin 5.0* program (Saakov 2000a, b).

It can be seen from the kinetics of change in optical density (OD) values in absorption spectra of the antenna light-harvesting complexes of PS-2 that within 24 h of exposure to dispersed light (control), there is a decrease of 6–10 % (Fig. 2.27). The  $\gamma$ -radiation of preparations of the light-harvesting complexes of PS-2 promotes a gradual decrease in the kinetics of the OD value change, and at high doses of  $\gamma$ -radiation, this reduction does not exceed 30 % in 24 h. Thus, the influence of  $\gamma$ -radiation on the light-harvesting complexes of PS-2 is a little deeper in comparison with a native leaf (Saakov et al. 1993; Saakov 1993a). The short-term influence of temperature on a complex causes considerably greater change in the OD values in comparison with  $\gamma$ -radiation, and their additive influence quickly destroys the antenna complex of PS-2. The total extract of pigments is notable for the lowest resistance to the influence of  $\gamma$ -radiation (Fig. 2.28).

So the antenna light-harvesting complex (Saakov 1994) shows significantly higher resistance than its separate constituent components of protein or pigment nature (Saakov 1993a, 1998a, b, 2000a, b). The consecutive simplification of ChPC or of its components inevitably leads to the loss of functional properties of the chloroplast system responsible for the energy supply of the photosynthetic device. In this regard, the antenna light-harvesting complex of PS-2 occupies an intermediate place in the resistance to  $\gamma$ -radiation, converging closer to the resistance of the native ChPC.

The data shown in Figs. 2.29a, b and 2.30 reveal fine changes in the spectral structure of the light-harvesting complex of PS-2, manifested as the influence of  $\gamma$ -radiation on the red and blue areas of its spectrum. Figure 2.29a shows, for the first time, the eighth derivative of the absorption spectrum ( $D^{VIII}$ ) of a native leaf of haricot and clearly shows specific changes in the spectral structure that arise during extraction of the complex. The hypsochromic shift of the main maximum of absorption ( $\lambda = 682$  nm) is specific to simpler structures or for ChPC *in vivo*, exposed to EFE influence. The fine structure of spectra  $D^{IV}$  and  $D^{VIII}$  allows confirmation of the data in Fig. 2.29a, b on the OD decrease and also connects this OD reduction with specific bands of the spectrum range of the antenna light-harvesting complex of PS-2. First of all, one can distinguish the more stable bands of the spectrum of the complex, unchanging during its extraction ( $\lambda = 641.2$ , 655.3, 666–667.1, 671–672, 676.6, 681.2–682, 692.7, and 694.7 nm), and the spectral bands of high instability ( $\lambda = 659.8$ , 674.2, 687.7, and 691.6 nm). At  $\gamma$ -irradiation, the location of spectral bands changes only a little, but OD decreases at  $\lambda = 641.2$ , 648.3, 652, 655.3, 658.3, 662.4, 666, 669.6–672, 676.6, 681.2, 690.8, and

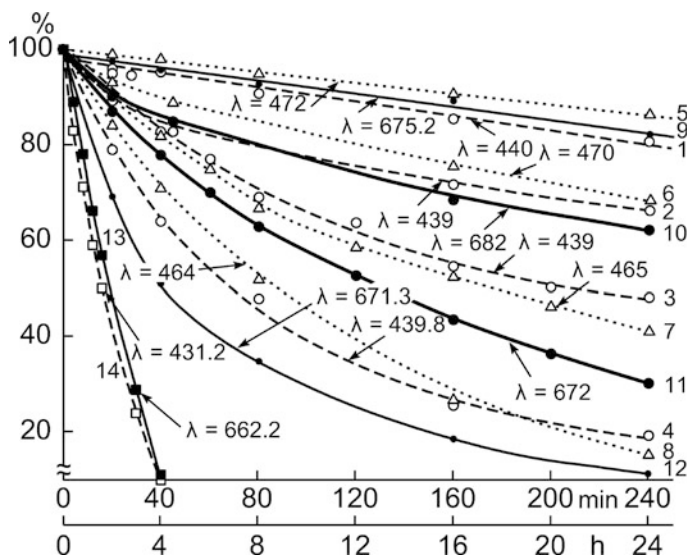


**Fig. 2.28** Kinetics of change in OD value in absorption spectra of the antenna light-harvesting complex under the influence of  $\gamma$ -radiation (630 Gy/h) and temperature (55 °C, 6 min). Curves: 1, 5, 9 control samples (1  $\lambda$  = 440, 5  $\lambda$  = 472, 9  $\lambda$  = 675.2 nm); 2, 6, 10  $\gamma$ -irradiated preparations (2  $\lambda$  = 439, 6  $\lambda$  = 470, 10  $\lambda$  = 682 nm); 3, 7, 11 thermally processed preparations (3  $\lambda$  = 439, 7  $\lambda$  = 465, 11  $\lambda$  = 672 nm); 4, 8, 12 under the simultaneous influence of temperature (6 min) and  $\gamma$ -radiation doses as in 2, 6, 10 (4  $\lambda$  = 439.8, 8  $\lambda$  = 464, 12  $\lambda$  = 671.3 nm); 13, 14 the same for the acetone extract of pigments from samples of light-harvesting complexes after their processing by  $\gamma$ -radiation (13  $\lambda$  = 431.2, 14  $\lambda$  = 662.2 nm). Ordinate: OD as a percentage of control value. Abscissa: time of action of  $\gamma$ -radiation or temperature aftereffect (bottom abscissa for curves 1–3, 5–7, 9–11; upper abscissa for curves 4, 8, 12–14)

694.7 nm. For some spectral bands, OD increases after  $\gamma$ -irradiation ( $\lambda$  = 652, 655.3, 666, and 672 nm). The OD increase in listed bands is coupled both with hypsochromic and with bathochromic shifts of initial bands of the spectrum of the light-harvesting complex. The general decrease in OD depends more on the OD value of the band  $\lambda$  = 681.2 nm.

The data obtained for haricot are supported by results of the  $\gamma$ -radiation impact on the antenna light-harvesting complex of PS-2 of spinach (Fig. 2.29b). The extraction of the antenna complex from *Spinacia oleracea* also leads to hypsochromic shift of the main maximum of absorption ( $\lambda$  = 682.5 nm). Spectral bands that do not change during the extraction of the antenna light-harvesting complex are  $\lambda$  = 636.4, 642.2, 645.6, 657, 667.6, 671.3, 674, 678.3, 687.5, and 693.6 nm. There are significant changes in the position of spectral bands  $\lambda$  = 657.4, 660.8, 664.7, 674, 678.3, 685, and 689 nm. The  $\gamma$ -radiation results in an increase in the differentiation of spectral bands, sometimes in the OD increase

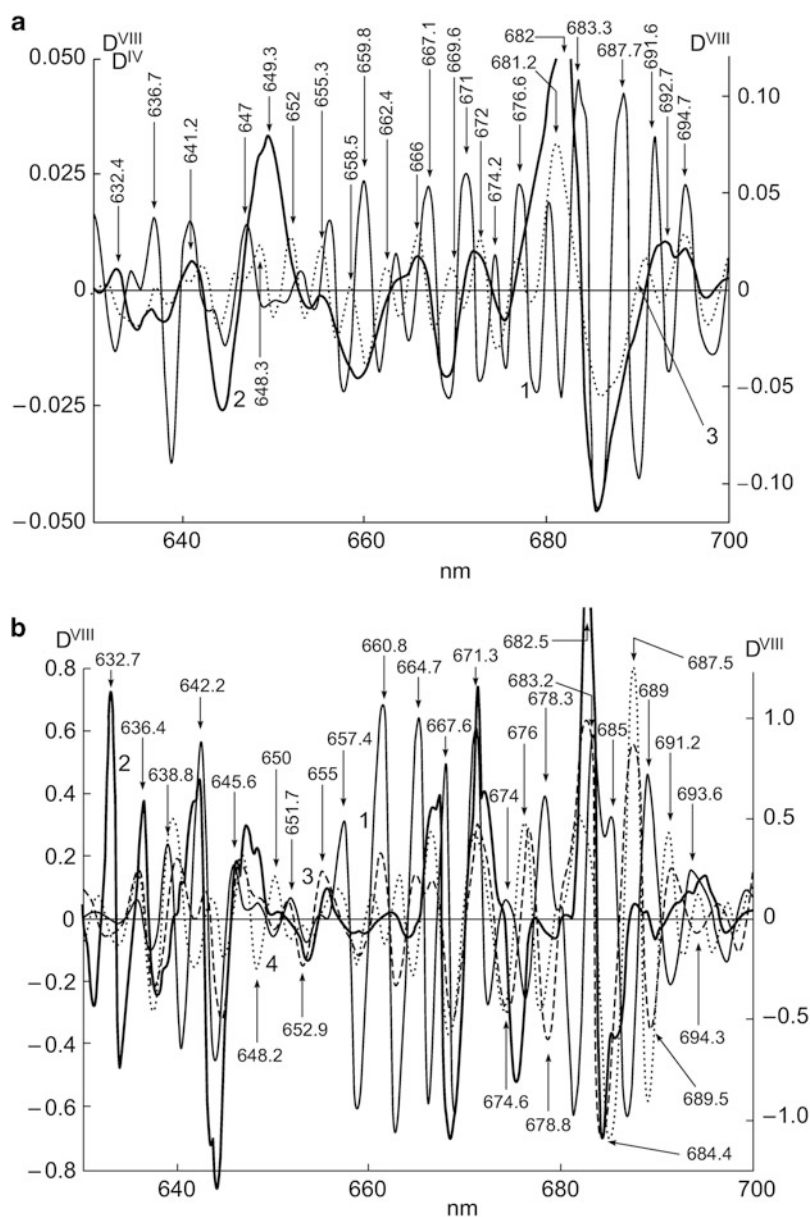


**Fig. 2.29** Changes in the red area of the absorption spectrum of the antenna light-harvesting complex of PS-2 for *Phaseolus vulgaris* (a) and for *Spinacia oleracea* (b) in response to  $\gamma$ -irradiation. (a) 1 The eighth derivative of the absorption spectrum ( $D^{VIII}$ ) of the intact leaf of *Ph. vulgaris* (control); 2 the fourth derivative of the absorption spectrum ( $D^{IV}$ ) of the sample of the antenna light-harvesting complex of PS2 (control); 3  $D^{VIII}$  of the light-harvesting complex of PS2 after irradiation by 24 kGy. Left ordinate: OD relative units for curves 2 and 3; right ordinate: the same for the curve 1. (b) 1  $D^{VIII}$  of the intact leaf *S. oleracea* (control); 2  $D^{VIII}$  of the sample of the antenna light-harvesting complex of PS2 from spinach leaves (control); 3  $D^{VIII}$  of the antenna light-harvesting complex of PS2 after  $\gamma$ -irradiation by 2.8 kGy; 4 the same as 3 after 12 kGy. Right ordinate:  $D^{VIII}$ , OD relative units for curve 1; left ordinate: the same for curves 2, 3, and 4

and very frequently in the hypsochromic shift in areas  $\lambda = 648.2, 650, 660.8\text{--}664.7, 674.6\text{--}678.8, 689.5, \text{ and } 694.3 \text{ nm}$ , with appearance of minima. The most stable bands of the spectrum of the antenna light-harvesting complex of PS-2 of spinach at  $\gamma$ -irradiation were  $\lambda = 636.4, 645.6, 651.7, 655, 664.7\text{--}667.6, 671.3, 682.5, 687.5\text{--}689, 691.2, \text{ and } 693.6\text{--}694.5 \text{ nm}$ . At  $\gamma$ -radiation, the OD increase is noticed for some bands in the spinach spectrum ( $\lambda = 639, 676, 687.5, \text{ and } 691.2 \text{ nm}$ ).

Summing up the consideration of features of structural changes in the red spectral area of the light-harvesting complex of PS-2, we can separate spectral bands common for considered objects, some bands are resistant and others are non-resistant to the influence of  $\gamma$ -radiation.

In Fig. 2.30 changes in the blue area of the spectral structure of the PS-2 antenna complex of *S. oleracea* in response to the influence of  $\gamma$ -radiation are shown. In Fig. 2.30 it is seen that a dose of 2.5–2.6 kGy induces only about 10 % of damage to the kinetics of the change in OD values and that these changes can serve as an additional control for assessment of the influence of high doses of  $\gamma$ -radiation. The extraction of the antenna light-harvesting complex leads to disappearance of spectral bands  $\lambda = 441.8, 459.6, 463.5, 479.5, \text{ and } 489.5 \text{ nm}$ . Bands at  $\lambda = 408.4, 448.3, 450.9, 476.6, \text{ and } 487.5 \text{ nm}$  on the curve  $D^{\text{IV}}$  (curve 2) are not sufficiently resolved. Under the influence of  $\gamma$ -radiation, the most stable bands are still  $\lambda = 404.4, 408.4, 411.7, 420, 424.5, 429, 433.6, 444.3, 448.3, 454.8, 461.5, 465.5, 481, 487.5, \text{ and } 495 \text{ nm}$ . Similarly to the red area, the OD increases for some spectral bands ( $\lambda = 404, 411.7, 415, 420.8, 424.5, 429, 444.3, 448.3, 450.9, 451.4, 454.8, 461.5, 465.5, \text{ and } 487.5 \text{ nm}$ ). An increase in the dose of  $\gamma$ -radiation to 12 kGy does not reduce the OD of spectral bands  $\lambda = 411.7, 415, 444.3, 448.3, 454.8, 461.5, 476.6, 487.5, \text{ and } 495 \text{ nm}$ .

The data presented lead to the conclusion that there is a higher radioresistance of spectral bands of the blue region in the structure of the spectrum of the antenna light-harvesting complex of PS-2. The stability of the Soret band and of carotenoids is especially outstanding. Lower stability characterizes the spectral bands interfaced to the violaxanthin de-epoxidation cycle in the area  $\lambda = 467\text{--}476.6 \text{ nm}$ ; the same is also characteristic of the influence of high temperatures and inhibitors of ETC of the photosynthetic device. Data from previous work (Saakov et al. 1978) allow us to conclude that changes in bands of the spectrum of the light-harvesting complex of PS-2 at  $\lambda = 411.7, 415, 419, 427\text{--}429, 433.6, \text{ and } 444.3 \text{ nm}$ , and also of the bands absent in Fig. 2.30 ( $\lambda = 515\text{--}516, 518\text{--}521, 540\text{--}541, 547\text{--}550, \text{ and } 566\text{--}569 \text{ nm}$ ), and in the red spectral region (Fig. 2.29) ( $\lambda = 623\text{--}625, 632\text{--}635, \text{ and } 663\text{--}666\text{--}669.6 \text{ nm}$ ) correspond to damage in the state of the submicroscopic structure of the pheophytin complex.

Changes in spectral bands  $\lambda = 623\text{--}625, 632\text{--}636, \text{ and } 664\text{--}669.6\text{--}672 \text{ nm}$  are closely coupled with changes in spectral bands at  $\lambda = 678.3\text{--}682.5 \text{ nm}$  and indicate the localization of the damage of interaction in elements of the submicroscopic

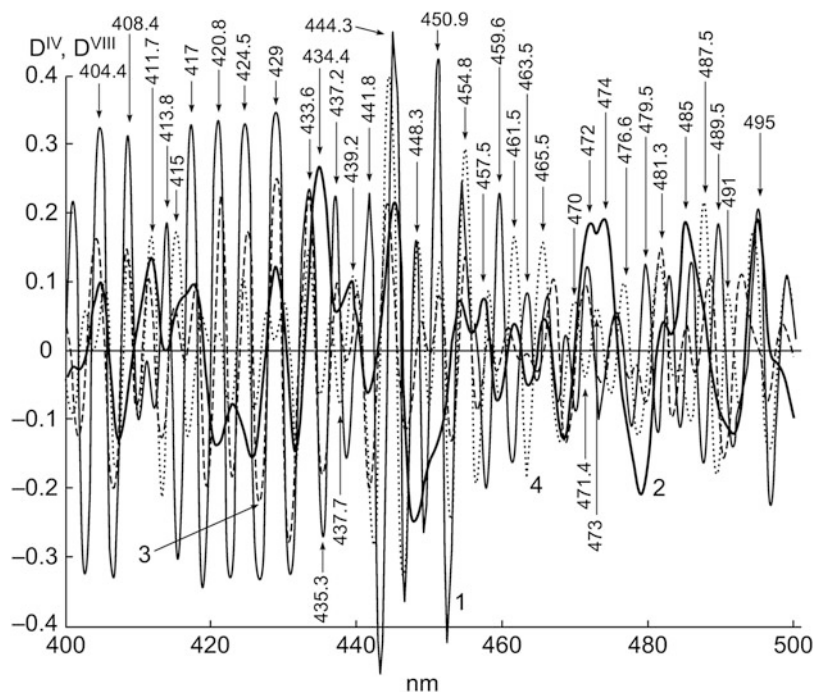


**Fig. 2.30** Changes in the blue area of the absorption spectrum of the antenna light-harvesting complex of PS-2 extracted from *Spinacia oleracea* after  $\gamma$ -irradiation by 2.6 and 12 kGy. 1 The eighth derivative of the absorption spectrum ( $D^{VIII}$ ) of the intact spinach leaf (control 1); 2 the fourth derivative of the absorption spectrum ( $D^{IV}$ ) of the preparation of the antenna light-harvesting complex of PS-2 (control 2); 3 changes in  $D^{VIII}$  of the PS2 complex under the influence of 2.6 kGy; 4 the same as 3, but under the influence of  $\gamma$ -radiation (12 kGy). The ordinate for  $D^{IV}$  and  $D^{VIII}$  is OD relative units

structure of PS-2 RCs (the complex  $P_{680}\text{Pheo}$  with acceptors  $Q_A$  and  $Q_B$ ; see Eq. (2.1)) under the influence of  $\gamma$ -radiation, which also agrees with the published point of view (Saakov and Shiryaev 2000). Complexes of xanthophylls with chlorophyll require deeper study (Peterman et al. 1997). Forms of lutein ( $\lambda = 494$  nm) and neoxanthin ( $\lambda = 486$  nm) combine in the complex with chlorophyll ( $\lambda = 675$  nm), causing quenching of the chlorophyll triplet state in the light-harvesting complex of PS-2. Spectral bands with  $\lambda = 670$ – $672$  nm are known as a manifestation of the presence of ChPC monomeric forms and correspond to the formation of the chlorophyll–violaxanthin complex. Possibly, under the influence of  $\gamma$ -radiation, the changes in the spectral structure in this area are caused by damage to the protective function of the xanthophyll cycle (Saakov 1998a, b) at the non-radiative dissipation of the light energy and the transfer of the excited chlorophyll to its ground state by means of thermal emission.

Thus, in this section we have presented for the first time comparative research on the antenna light-harvesting complexes of PS-2 from plants that differ in

radioresistance. We have described their native spectra  $D^{\text{VIII}}$ , the set of spectral bands stable at the extraction of the complex, and the similarity of some bands for different objects. We have also established that the influence of high doses of  $\gamma$ -radiation on the antenna light-harvesting complex of PS-2 induces considerably smaller changes in the OD value kinetics than a short-term temperature shock or their combined impact. We found a set of stable spectral bands that are uncoupled from hypsochromic or bathochromic shifts under the influence of  $\gamma$ -radiation. We described the lower resistance of the antenna light-harvesting complex of PS-2 to the influence of  $\gamma$ -radiation than that of the native ChPC. We found spectral bands that corresponded to the realization of functional properties of ChPC during the energy transformation in RCs of ETC, which are aligned with the spectral characteristic of the link  $P_{680}\text{Pheo}$  (see Eq. (2.1)) in ETC of the photosynthetic device. The higher radioresistance of the functionally active ChPC in comparison with the resistance of its constituent structural elements was also emphasized.

### ***2.2.10 New Data on the Development of the Hypothesis on the Localization of Damaging EFE Influences in a Green Leaf; After-effect of $\gamma$ -Radiation on the Energetics of Chloroplasts***

In the previous sections, we considered material in favor of the hypothesis on the existence of centers of localization of the EFE damaging influence in chloroplast thylakoids, the activity of these centers defining the level of leaf resistance to the EFE impact. It was supposed that these centers coincide with centers of pigment biosynthesis and with the RCs of photosystems (Baranov et al. 1974; Saakov et al. 1975; Saakov 1976). Further research provided additional material for developing ideas about coupling of the resistance of the plant photosynthetic device with the entirety of its ETC and with the photophosphorylation process (Saakov 1987, 1992, 1996; Saakov and Baranov 1987; Saakov and Leontjev 1988). Our point of view was also developed abroad (Schreiber and Bilger 1987; Krause 1988; Krause and Weis 1991, 1984; Dietz et al. 1985).

Research on the influence of  $\gamma$ -radiation and of its aftereffect is a convenient approach for studying the damage and reparation of energy links of the photosynthetic device and assessing the localization of this damage (Saakov 1993a, b; Saakov et al. 1993). Because biological systems respond with a delay to the influence of an EFE, the assessment of the influence of the *aftereffect* of  $\gamma$ -radiation is connected with the prognosis of situation development.

The objects of our researches were 2- to 3-week-old leaves of *Phaseolus vulgaris* and *Nicotiana tabacum* and compound leaves of *Robinia pseudoacacia*. We used the new methodological possibilities of the pulse fluorescence to look at the aftereffect of  $\gamma$ -radiation on the change in PAMF signal harmonics registered

with the fluorometer Walz 101–103 (Effeltrich, Germany). The experimental technique is described in Sect. 2.2 (Fig. 2.3). Simultaneously with PAMF registration, we used the Warburg method to measure, at the same time, the intensities of photosynthesis and respiration. Of the 20 vessels of the device, two served as thermobarometers, nine for determination of photosynthesis intensity, and nine shielded vessels for assessment of respiration intensity. We obtained individual illumination of the leaf cuttings by the introduction of fiber-glass optical light guides in each vessel and were thus able to avoid the thermal influence of a light source on the object. The light flux from halogen lamps was transferred through the system of condenser lenses and the divider to an entrance end face of an optical bundle, which was fastened on the top part of a vessel with a Teflon gasket, creating a light flux within the range 180–1,400  $\mu\text{E}/(\text{m}^2 \text{ s})$ . The chosen method of lighting allowed the simultaneous measurement of the intensities of photosynthesis and respiration with the same device. To obtain correct data on the fluorescence intensity, the fulfillment of a number of conditions is necessary (Saakov 1960, 1961).

The formulae concerning theoretically expected areas of saturating concentrations of  $\text{CO}_2$  when using Warburg's buffers for any geometry of a vessel are presented here.

Considering the interacting system “liquid–gas,” let  $\Delta n$  be the number of molecules evaporating from the liquid in the time  $\Delta t$ ; then

$$\Delta n = S \cdot V \cdot \Delta t \cdot n_g$$

where  $S$  is the area of the phase contact surface,  $V$  the speed of molecules in the liquid, and  $n_g$  the initial concentration of the gas in the liquid. Analogically, the number ( $\Delta n'$ ) of molecules returned back to the liquid is

$$\Delta n' = S \cdot V' \cdot \Delta t \cdot n$$

where  $n$  is the concentration of the gas molecules above the liquid and  $V'$  the speed of molecules in the gas. Suppose that the number of evaporating and returned molecules in a unit time are equal to each other, and  $V = V'$ . Then the comprehensive change in the number of molecules is described as

$$\Delta N = \Delta n' - \Delta n = S \cdot V \cdot \Delta t \cdot (n - n_g)$$

At  $\Delta t \rightarrow 0$ , we will get the following system of equations:

$$\begin{cases} N'_g = S \cdot V \cdot (n - n_g) \\ N'_g = -N' \end{cases}$$



But  $n_g = N_g/V_1$ , where  $V_1$  is the volume of liquid and  $N_g$  is the number of molecules in the liquid. Similarly,  $n = N_c/V_c$ , where  $V_c$  is the volume of the upper space and  $N_c$  is the number of gas molecules in the upper space. Then the system becomes

$$\begin{cases} n'_g = \frac{S \cdot V \cdot (n - n_g)}{V_1} \\ n'_g V_c = -n'_g \cdot V_1 \end{cases} \quad (2.2)$$

Solving this system and adding  $E$ , the comparison error, we find the time  $t$  of the achievement of equilibrium of gas partial pressure in the system to be

$$t = \frac{\ln \left| \left( \frac{E}{n_g(0) - n(0)} \right) \right|}{-S \cdot V \cdot \left( \frac{1}{V_c} + \frac{1}{V_1} \right)}$$

and  $E \rightarrow -0+$ .

Thus, the formula for determination of equalization time of gas concentrations in the buffer system for any geometry of Warburg's vessel is deduced. This allows avoidance of mistakes connected with the time of gas phase saturation during determination of photosynthesis intensity. Besides, it is necessary to find the optimum size of a lamina to maintain the constancy of carbon dioxide concentration in the vessel volume, predefined by the chosen buffer mix.

The results of performed experiments are presented in Fig. 2.31a, b, c and 2.32 and also in Table 2.9, which show the character of changes in key parameters and in coefficients characterizing the fluorescence intensity during the aftereffect of  $\gamma$ -radiation. The  $F_0$  level corresponding to the dark, base FI, when photosynthetic membranes are in the non-energized state, is characterized by the emission of the excited antenna chlorophyll  $a$  before the migration of excitation in the open RCs. At this time, the first stable acceptor of PS-2,  $Q_A^+$ , is completely oxidized,  $q_q = 1$ , and  $q_E = 0$ . In response to an impulse of light or the actinic light flux, the maximum FI ( $F_m$ ) increases, and  $F_v$  shows the  $Q_A^-$  reduction that leads to closing of the PS-2 RCs ( $q_q$  and  $q_E$  equal to 0). The  $F_v$  level shows that all non-photochemical quenching processes are at a minimum (Schreiber and Bilger 1987; Krause 1988; Krause and Weis 1984). The suppression of  $F_v$  is coupled to the suppression of PS-2 activity and damage to the electron transport from  $P_{680}$  to  $Q_A^+$ , connected with the inhibition of the charge transfer between  $P_{680}$  and Pheo (Figs. 2.30 and 2.31; Table 2.9). The same follows from the analysis of the absorption signal at  $\lambda = 540$ –560 nm (Saakov 1976, 1987, 1992, 1996).

The ratio  $F_v/F_m$  is an indicator of the high efficiency of primary reactions of PS-2 and for intact chloroplasts is close to 0.832. The experimental deviation from the control by 0.03–0.04 is considered significant and points to the PS-2 response to



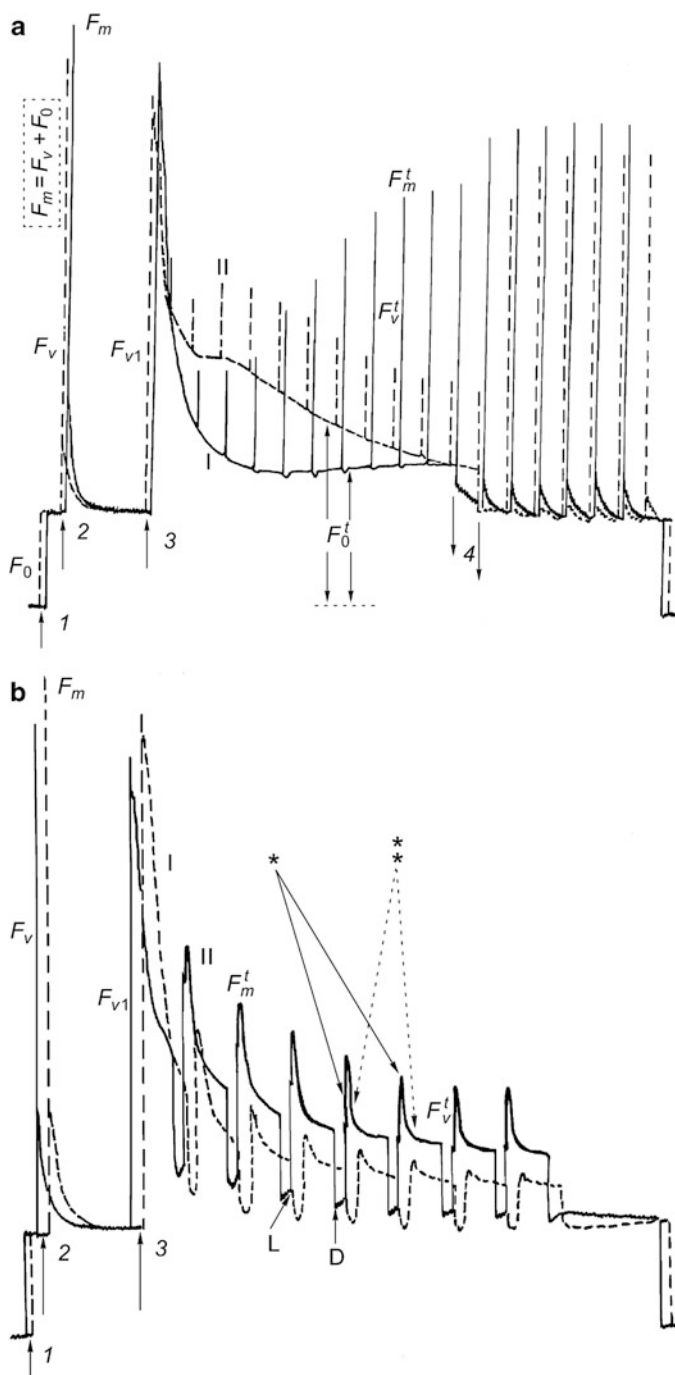
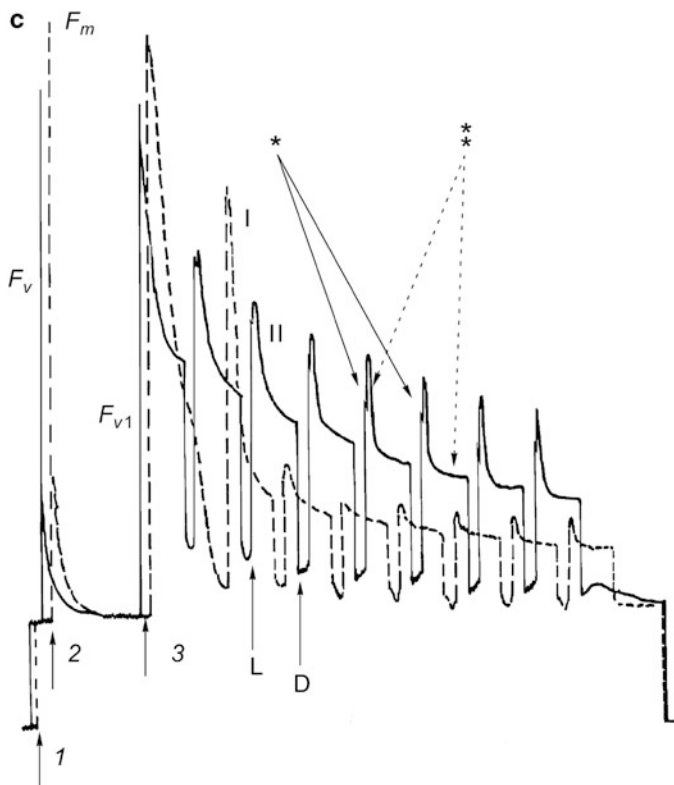
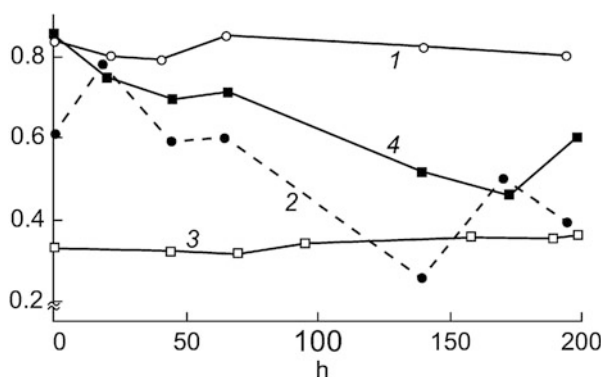


Fig. 2.31 (Continued)



**Fig. 2.31** The character of PAMF harmonics change for the chlorophyll *a* of *Phaseolus vulg. Forti* leaves adapted to darkness, in the process of the  $\gamma$ -radiation after-effect. (a) 20 hours after the influence of 3.5 kGy; input of 1-s saturating white light impulse ( $1,100 \mu\text{E}/(\text{m}^2 \text{ s})$ ) followed by 60 s of darkness and then by actinic light of  $590 \mu\text{E}/(\text{m}^2 \text{ s})$  and frequency 100 kHz for the determination of  $F_0^t$  and  $F_v^t$ . (b) The kinetics of PAMF change in response to cycles of light (L)/dark (D) of 80 s/20 s. The actinic light used was  $1,100 \mu\text{E}/(\text{m}^2 \text{ s})$  (40 h of the after-effect of 0.6 kGy). (c) The same as b, but 200 h of the after-effect of 0.6 kGy. With the increase in duration of the after-effect, the kinetics of the slow FI component manifests more clearly. Single asterisk indicates the increase and double asterisks the decrease in the slow component. I experiment; II control. Arrows: 1 input of the modulating light of 1.6 kHz ( $6 \mu\text{E}/(\text{m}^2 \text{ s})$ ,  $\lambda = 660 \text{ nm}$ ) for the determination of the level of the minimum (base) dark FI,  $F_0$ ; 2 the saturating impulse of light ( $3,000 \mu\text{E}/(\text{m}^2 \text{ s})$ ), causing the reduction of the acceptor  $Q_A$ ; 3 input of actinic light of frequency of 100 kHz; 4 shutdown of actinic light of 100 kHz for the determination of the  $F_0^{11-12 \text{ (min)}}$  value and input of light of 1.6 kHz; C input of actinic light for 80 s; T shutdown of actinic light for 20 s of darkness.  $F_0$  minimum dark FI;  $F_v$  variable FI;  $F_{v1}$  variable FI at input of actinic light of 100 kHz;  $F_v^t$  variable FI (spikes values) during  $t$ . The course of PAMF harmonics for *Robinia pseudoacacia* and *Nicotiana tabacum aurea* is similar



**Fig. 2.32** The dynamics of the change in coefficients of fluorescence quenching in the process of the aftereffect of  $\gamma$ -radiation (3.5 kGy) for *Robinia*. 1 The change in the coefficient  $q_q$ , photochemical quenching, control; 2 the same, experiment; 3 the change in the coefficient  $q_E$ , non-photochemical quenching, control; 4 the same, experiment (indicates a decrease in the activity of dark reactions of the Calvin cycle). Ordinate: relative units; abscissa: the aftereffect time in hours

the EFE influence and to photoinhibition (Schreiber and Bilger 1987; Krause 1988; Krause and Weis 1984; Dietz et al. 1985) (Table 2.9).

EFEs and PhIn cause a decrease in  $F_V$ , indicating the existence of the primary damage and its localization close to PS-2 RCs (Schreiber and Bilger 1987; Krause 1988; Krause and Weis 1984; Dietz et al. 1985), which corresponds to the statement earlier formulated by us (Baranov et al. 1974; Saakov et al. 1975; Saakov 1976, 1987; Saakov and Baranov 1987).

The high  $F_V$  value (including values of spikes at  $F_V^t$ ) is coupled with the low  $q_E$  value and indicates the high utilization of energy in the Calvin cycle and the decrease in the membrane proton gradient due to ATP formation (Schreiber and Bilger 1987; Krause 1988). After the  $F_V$  decrease (3 min), the light flux ( $1,100 \mu\text{E}/(\text{m}^2 \text{ s})$ ) inducing the  $F_{V1}$  level is switched on. After 30 s, there is an additional input of a number of saturating impulses of 1 s duration and flux of  $3,000 \mu\text{E}/(\text{m}^2 \text{ s})$  (Fig. 2.31a). These impulses in combination with the actinic light flux promote the complete reduction of  $\text{Q}_\text{A}^-$  and RC closing. The higher the amplitude of these impulses and the closer they are to the  $F_{V1}$  value, the higher the quantity of the reduced acceptor  $\text{Q}_\text{A}^-$ , and the higher the probability of high ETC activity, decreased  $q_E$  value, and Calvin cycle activation. The aftereffect of  $\gamma$ -radiation correlates with the influence of high temperature, reducing values of  $F_V^t$  and increasing the  $q_E$  value.

This phenomenon precedes the damage at the PS-2 level and is accompanied by the  $F_0^t$  increase and  $F_V^t$  decrease. The impulse of saturating light, as well as in the case with  $F_0$ , leads to closing of PS-2 RCs. Fluorescence  $F_0$  depends on the EFE influence (except at low temperature) (Schreiber and Bilger 1987; Krause 1988; Krause and Weis 1984; Dietz et al. 1985). Earlier we found that the levels of  $F_0$  or  $F_0^t$  (the base FI at the input of actinic light flux for the separate time  $t$ ) changed as a

**Table 2.9** The character of changes in the quenching of FI of photosynthesis and respiration intensities in the process of aftereffect of  $\gamma$ -irradiation of *N. tabacum aurea*

Variant	Measured parameter	Value of control $n = 4$	Immediately after irrad, 0 h $n = 3$	Aftereffect of $\gamma$ -irradiation (time, h), $p < 1\%$							
				20–24 $n = 3$	40–44 $n = 3$	68–72 $n = 3$	138–140 $n = 3$	160–170 $n = 2$	190–200 $n = 2$		
I 0.6 kGy	Int. of ph. synth. (mg CO <sub>2</sub> /dm <sup>2</sup> h)	42	29	32	33	37	26	27	13		
	Int. of respirat. (cm <sup>3</sup> CO <sub>2</sub> /dm <sup>2</sup> h)	0.6	0.9	0.7	0.9	0.9	1.9	2.8	3.1		
	$F_v/F_m$	0.843	0.815	0.805	0.816	0.785	0.740	0.735	0.720		
	$F_0^{10}/F_0$	1.220	1.322	1.656	1.870	2.250	2.453	2.551	2.620		
	$q_q$	0.808	0.705	0.525	0.517	0.472	0.463	0.431	0.390		
	$q_E$	0.431	0.482	0.644	0.595	0.681	0.746	0.776	0.812		
	$F_{v1} h/2$	24	30	36	42	120	146	156	224		
II 1.3 kGy	Int. of ph. synth. (mg CO <sub>2</sub> /dm <sup>2</sup> h)	45	27	29	25	21	16	12	9		
	Int. of respirat. (cm <sup>3</sup> CO <sub>2</sub> /dm <sup>2</sup> h)	0.8	1.0	1.6	1.8	2.3	2.8	4.2	5.6		
	$F_v/F_m$	0.891	0.842	0.810	0.787	0.743	0.716	0.711	0.690		
	$F_0^{10}/F_0$	1.120	1.320	1.390	1.732	1.923	2.541	2.634	2.742		
	$q_q$	0.827	0.693	0.681	0.593	0.560	0.482	0.459	0.438		
	$q_E$	0.430	0.671	0.613	0.690	0.746	0.873	0.879	0.889		
	$F_{v1} h/2$	18	29	37	56	129	138	178	236		
III 2.5 kGy	Int. of ph. synth. (mg CO <sub>2</sub> /dm <sup>2</sup> h)	39	18	27	23	12	8	–	–		
	Int. of respirat. (cm <sup>3</sup> CO <sub>2</sub> /dm <sup>2</sup> h)	0.6	1.3	1.9	3.0	5.6	7.8	–	–		
	$F_v/F_m$	0.836	0.792	0.800	0.810	0.760	0.681	0.661	0.660		
	$F_0^{10}/F_0$	1.280	1.380	1.667	2.232	2.345	2.675	2.696	0.273		
	$q_q$	0.863	0.800	0.814	0.606	0.511	0.390	0.370	0.320		
	$q_E$	0.462	0.656	0.671	0.683	0.774	0.821	0.863	0.900		
	$F_{v1} h/2$	22	36	48	59	126	152	192	243		

function of the radiation dose (Saakov 1992; Saakov et al. 1992). The ratio  $F_0^{10}/F_0$  serves as one indicator of damage to the photosynthetic device (Fig. 2.31, Table 2.9). This means that a rise in  $F_0'$  corresponding to the increase in the aftereffect of  $\gamma$ -radiation shows the depth of the radiation damage to PS-2 RCs evolving in time. We pay attention to the prospects of more detailed study of  $F_V'/F_0'$  because it is closely coupled with the damage to PS-2 energetics and with the change in ratio values from 3–6 to 1.4–0.1 relative units (Saakov 1992).

The data in Fig. 2.31b, c show, for the first time, the influence of the aftereffect of  $\gamma$ -radiation on the change in signal amplitude in response to periods of light and dark (80 s/20 s). From these data, it can be seen that input of the light flux for 80 s causes the amplitude of the induced signal of  $F_V'$  to split into three components. The first, fast, component is connected with the so-called Q quenching, that is, the oxidized  $Q_A^+$  acts as an FI quencher because in the state  $P_{680}^* \text{Pheo}Q_A$  the transformation of the photochemical energy (i.e., the formation of  $P_{680}^* \text{Pheo}Q_A^-$  of the integral part of RCs) is a convenient opportunity for the de-excitation (Klimov and Krasnovskii 1981). The second component is short and slower (Fig. 2.31b, c, arrows with an asterisk) and emphasizes the delay in  $Q_A$  reduction due to the link damage of the transfer of  $e^-$  from  $P_{680}$  to the proximate Pheo (Saakov 1993a–d). The third, slow, component (SC) noted in FI signals of damaged plants (Fig. 2.31b, c, curve II) most likely demonstrates damage in ETC arising during the  $e^-$  transfer from  $Q_A^-$  to the secondary acceptor  $Q_B^+$  (the part of RCs) (Krause 1988; Krause and Weis 1984). The equilibrium  $Q_A^- Q_B^+ = Q_A^+ Q_B^-$  can exist when the plastoquinone  $PQ^{2+}$  pool is completely oxidized (Schreiber and Bilger 1987; Krause and Weis 1984). Probably, the SC indicates the inhibition (as in the case with diuron) of  $e^-$  transport to the acceptor part of PS-2 between  $Q_A$  and  $Q_B$ , which leads to the  $q_q$  decrease (Table 2.9, Fig. 2.31), because all quenchers of FI are reduced and there is no subsequent re-oxidization. In favor of this is the gradual decrease in the SC at the input of light flux (Fig. 2.31b, c, arrows with two asterisks). The shutdown of the light flux results in fast re-oxidization,  $e^-$  transfer to PS-1, and a decrease in the FI signal to the  $F_0'$  level. The gradual decrease in the SC shows the kinetics of  $q_q$  noted in response to pulse lighting, which is explained by the beginning of ETC reduction. The high  $q_q$  value (0.8–0.9) emphasizes the active work of ETC, the high level of NADPH/ $H^+$ , and the active assimilation of  $CO_2$  (Fig. 2.31). The decrease in  $q_q$  before the leaf falls is coupled with ETC suppression (Schreiber and Bilger 1987; Krause and Weis 1984). The high reduction of the PQ pool is accompanied by the low  $q_q$  value, and  $PQ^+$  re-oxidization leads to its increase.

Thus, the decrease seen in curve 2 in Fig. 2.32 specifies that the aftereffect of  $\gamma$ -radiation results in the impossibility of PQ re-oxidization and in the accumulation of electrons in the acceptor part of PS-2. The  $q_E$  increase occurs due to the increase in the proton gradient on membranes and the decrease in ATP synthesis. According to the change in  $q_q$  and  $q_E$  (Table 2.9), the intensity of photosynthesis changes. With its decrease during the aftereffect, the dynamics of the respiration intensity increases in agreement with the conformity noted before (Saakov 1992; Saakov et al. 1993).

The provided results underline the similarity of damage to ETC energy links under the influence of various EFEs on a chloroplast and indicate that the most vulnerable areas of ETC are links of the  $e^-$  transfer chain to primary and secondary acceptors of PS-2 RCs.

The data presented in the section show, for the first time, that in the process of the aftereffect of  $\gamma$ -radiation, there is an increase in  $F_0$  and a decrease in the level of spikes  $F_V^t$  and in the ratio  $F_V/F_m$ . The change in coefficient of FI quenching indicates the damage to the dark reaction of the Calvin cycle, the decrease in photosynthesis intensity, and the increase in respiration intensity. The discussed data confirm our hypothesis about the localization of EFE damaging influences in the energy link of the photosynthetic ETC responsible for the reduction of primary and secondary acceptors of PS-2 RCs. It allows the supposition that thermal stress (Schreiber and Bilger 1987; Krause and Weis 1984), dehydration (Saakov et al. 1993; Schreiber and Bilger 1987), salification, various regimes of  $\text{CO}_2$  and  $\text{O}_2$  (Schreiber and Bilger 1987), intense light, and  $\gamma$ -radiation are characterized by identical mechanisms of the damaging influence on the redox state of  $Q_A$  of the ETC of photosynthesis.

### ***2.2.11 Specifics of Change in the Coefficients of Pulse-Amplitude Modulated Fluorescence Quenching ( $q_q$ and $q_E$ ) During the after-effect of $\gamma$ -Irradiation***

At the modern level of research, green cell resistance to the influence of an EFE, identification of resistance mechanisms, and elucidation of the mechanisms for reparation and adaptation of the phototrophic ability are all closely connected to the choice of objects (within the possibilities of the biotechnological experiment) during the target selection of cultivars genetically modified by polygene systems (Saakov 2002a). There is a large volume of European literature, partially considered in reviews (Briantais et al. 1986; Schreiber et al. 1986, 1997a,b; 1998; Bilger et al. 1988; Schreiber and Bilger 1987; Bolhar-Nordenkamp et al. 1989; Mohammed et al. 1996), on the results and interpretation of experiments using various ways of studying the FI character change for leaves, suspensions of chloroplasts, and algae under the influence of the wide set of natural and anthropogenous EFEs.

In European works, together with the modern techniques and competent theoretical interpretation of obtained data, there is a common fault. The effect of only one, and occasionally two, stress factor is considered rather than combining the sets of results for chloroplasts to separate influences in a unifying concept that describes the universal character of the damage to the phototrophic reaction ensemble in a green cell. Most strikingly, this is manifested in the identity of fluorescence changes, especially of PAMF harmonics under the influence of various EFEs

(Schreiber et al. 1986; Schreiber et al. 1975, 1994, 1997a,b; Bilger et al. 1988; Schreiber and Bilger 1987; Bolhar-Nordenkamp et al. 1989; Mohammed et al. 1996). A good analytical approach has led to the statement of facts and to the explanation of separate findings that summarizes, without creation of new theoretical constructions, the complex of appeared knowledge in a new way that is applicable to the requirements of studying the tolerance of plant cells and the problems of biotechnology of transgene samples.

We have summarized the results of our research, linking them together in the concept of the energetic basis of the resistance of the phototrophic ability of prokaryotic and eukaryotic cells to the influence of various EFEs (Saakov 2000a–e). One EFE is the impact of  $\gamma$ -radiation, the effects of which on green (phototrophic) cells were reported at a conference at the Joint Institute for Nuclear Research, Dubna, Russia, 2000 (website [http://www.jinr.ru/drrr/Timofeeff/conference/index\\_r.html](http://www.jinr.ru/drrr/Timofeeff/conference/index_r.html) and <http://www.jinr/news00.html>). Thus, the hypothesis about the localization of EFE damaging influences in the RCs of photosystems was further developed (Saakov 1987, 1990, 1996).

We consider it necessary to emphasize that during formulation of the energetic basis of the theory of green cell tolerance, we always considered the variety of earlier accumulated knowledge of European colleagues (Briantais et al. 1986; Schreiber et al. 1986; Schreiber et al. 1975, 1994, 1997a,b; Bilger et al. 1988; Schreiber and Bilger 1987; Lichtenthaler 1988a,b; 1992, 1996a,b; 1998a,b; 2000; Bolhar-Nordenkamp et al. 1989; Bolhar-Nordenkamp 1997; Mohammed et al. 1996), whose experimental and theoretical approaches were trustworthy.

Theoretical positions on the energetic basis for the resistance of phototrophic cells to EFE influence were formulated by us on the basis of the set of experimental research on the localization of damaging influences and *structural* changes of the chlorophyll–protein complex in RCs (Saakov 1987, 1990, 1993a–d, 2000a–e, 2002a–c), and also of investigations of the *functional* damage to ETC activity (Saakov 1972, 1973, 1975, 2001a, b, 2000a–e, 2004; Bilger et al. 1988; Schreiber and Bilger 1987). This research indicated the most sensitive points of the ETC connected with the transformation of light energy into the energy of chemical bonds. Our own material and the works of other groups gave confidence during the development of our theoretical concepts, especially the similarity of chloroplast reactions to the influence of the most diverse EFEs on taxonomically various phototrophs of *Procaryota* and *Eucaryota*. Such a similarity of reactions allowed us to state the idea about the adequacy of primary mechanisms of chloroplast RC damage under the influence of an EFE set (Saakov 1987, 1990, 1996, 2000a–e, 2001a, b, 2002a–c, 2003a, b, 2004).

The introduction of modern experimental techniques for the determination of the FI yield and the subsequent emergence of new theoretical constructions was not always met with positivity. For the purpose of verification of both new types of technical decisions and scientific recommendations on the basis of experiments, programs were set up in different countries to find the optimum conditions suitable for practical application with simultaneous economy of material resources (Bolhar-Nordenkamp et al. 1989). It is very regretful that in Russia, except for declarations

on the necessity of modernization of the experimental technique, no real steps towards such modernization were taken.

It should be noted that investigation of the influence of the EFE, in particular of  $\gamma$ -radiation or temperature, is closely coupled with the manifestation of its aftereffect, which is a convenient approach for investigation of the damage and reparation of the energy links of the photosynthetic device and assessment of the localization of this damage. The aftereffect is defined by the fact that biological systems respond to the EFE influence with some delay and, therefore, the assessment of aftereffect, in particular of  $\gamma$ -radiation, is conveniently connected with the prognosis of the development of adaptable or lethal situations during realization of the phototrophic function in a green leaf. For this purpose, we, for the first time in the world, analyzed changes in the PAMF coefficients over time for a long period, after the radiation influence and before the lethal outcome and possible necrosis of tissues.

The research on the influence of ionizing radiation allowed us to establish that PAMF changes in response to the impact of different doses of radiation (including lethal doses) are not accompanied by radical structural changes in the ChPC at the initial stages of EFE influence. References to these works are available in the bibliographic database of the National Center for Biotechnology Information USA or the Institute for Scientific Information (ISI) (<http://www.ncbi.nlm.nih.gov/>; <http://wokinfo.com/>) or, for example, on the site [http://bashedu.ru/str\\_n\\_col/vestnic/magaz1\\_2/S1\\_31/html](http://bashedu.ru/str_n_col/vestnic/magaz1_2/S1_31/html).

It is important to assess the processes of the aftereffect of  $\gamma$ -radiation doses by trying to track the possible reparation of the biological system or the occurrence of a lethal outcome and to assess the mechanisms of reactions. For this purpose, in this section, we first analyzed our own data on changes in PAMF coefficients over time for a long period, after the radiation influence. The aftereffect of  $\gamma$ -radiation on the specifics of the PAMF change was measured as earlier with the Walz 101-103 device (Effeltrich, Germany) (Saakov 1993a–d, 2000a–e).

Positive aspects of the method and features of the interpretation of obtained data are described in detail in reviews (Briantais et al. 1986; Lichtenthaler 1988a, b; Lichtenthaler and Rinderle 1988; Schreiber et al. 1986, 1994, 1997a,b; Schreiber 1983, 1986, 1998; Bolhar-Nordenkamp et al. 1989; Lichtenthaler 1996a, b).

The overwhelming amount of correct research of the end of the twentieth century in the field of resistance physiology is connected with the application of the PAMF method. This method provides the acquisition of data in vivo about the functional state of the photosynthetic device and allows, in the same leaf over a long time period, the investigation and comparison of the in situ dynamics of the processes connected with the damage to the primary reactions of photosynthesis induced by EFEs. It also allows tracking of the reparation processes or the death of an object. In our first works on the assessment of the influence of irradiation on phototrophic cells, we successfully applied this method (Saakov 1993a–d; Saakov et al. 1993) and obtained results that were repeatedly proved later. These results were taken as basis of our ideas on the energetic nature of the resistance of phototrophic tissues to EFE influence.



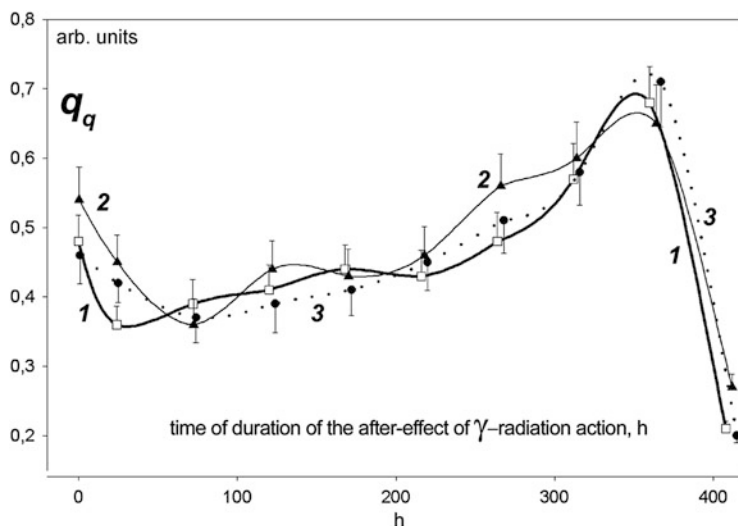


**Fig. 2.33** The dynamics of the change in the coefficient  $q_E$  of the PAMF energetic quenching after the influence of  $\gamma$ -radiation of 0.3 kGy on leaves of 1 haricot; 2 pea; and 3 oak. Ordinate:  $q_E$  values, relative units; abscissa: the time of aftereffect of  $\gamma$ -radiation, in hours

The objects of the present research were 2-week-old plants of haricot (*Phaseolus vulgaris* L.) and pea (*Pisum sativum*) and oak seedlings (*Quercus robur*). The choice of objects was defined by radiation conditions in the experiment and by the need for assessment of the long-term aftereffect of  $\gamma$ -radiation. In the experiment, we took 8–10 leaves of one variant, and the data in Figs. 2.33, 2.34, 2.35, and 2.36 correspond to the average value of the variability induced by the radiation. The isotope  $^{57}\text{Co}$  was used as the source of  $\gamma$ -radiation. The power source in experiments was 670–650 Gy/h. The design of the isotope chamber allowed us to bring objects in pots down to the  $\gamma$ -source and then to lift them out after exposure.

Two main types of FI quenching are distinguished, the photochemical quenching ( $q_q$ ) caused by the light energy transformation in the energy of chemical bonds in PS-2 RCs and non-photochemical quenching ( $q_E$ ), representing other non-radiative ways of the de-excitation by means of the dissipation of energy and the activity of the xanthophyll and Calvin cycles. Results of experiments are presented in Figs. 2.33, 2.34, 2.35, and 2.36 and show the dynamics of the change in  $q_q$  and  $q_E$  during the aftereffect of various doses of irradiation. The calculation of the specified coefficients was based on the knowledge of a number of FI parameters. The level of the dark, base FI ( $F_0$ ), is theoretically the FI emission when all RCs are open, the  $q_q$  value is maximal (i.e.,  $q_q = 1$ ), and the primary acceptor  $\text{Q}_\text{A}^+$  is oxidized. Just the  $F_0$  level provides the basis for calculation and standardization of other signals and of FI coefficients. The  $F_0$  level is not constant; its increase occurs in response to damage of PS-2 RCs and disorder of the excitation energy transfer from antenna complexes to RCs. In this regard, the correct determination of

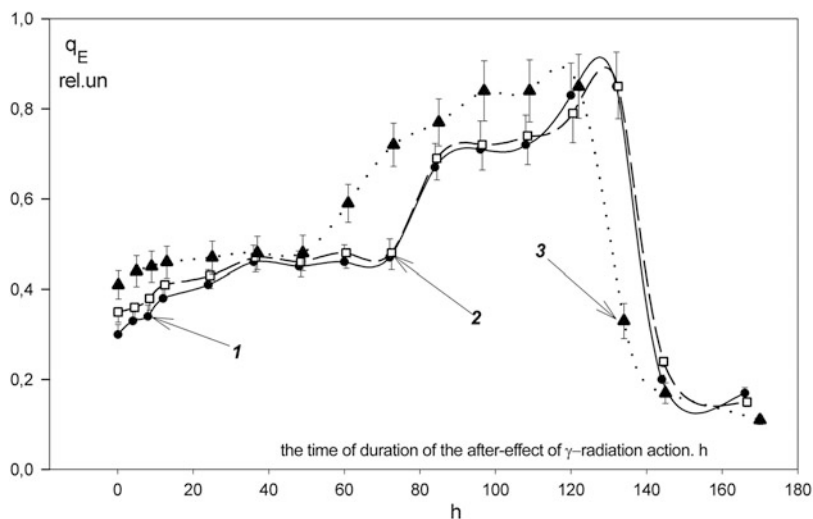


**Fig. 2.34** The dynamics of the change in the coefficient  $q_q$  of the PAMF photochemical quenching as aftereffect of the influence of  $\gamma$ -radiation of 0.3 kGy on leaves of 1 haricot; 2 pea; and 3 oak. *Ordinate*:  $q_q$  values, relative units; *abscissa*: time in hours

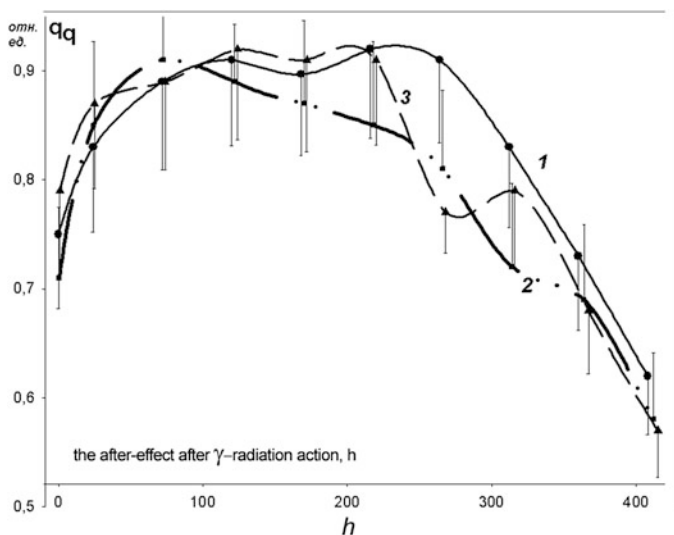


**Fig. 2.35** The dynamics of the PAMF coefficient  $q_E$  change as aftereffect of the influence of  $\gamma$ -radiation of 2.5 kGy on leaves of 1 haricot; 2 pea; and 3 oak. *Ordinate*:  $q_E$  values, relative units; *abscissa*: the time of aftereffect of  $\gamma$ -radiation, in hours

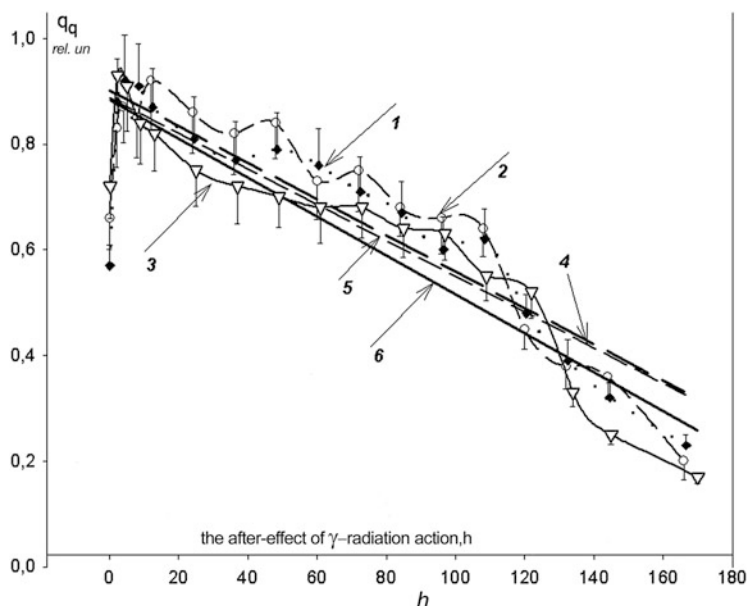


**Fig. 2.36** The dynamics of the coefficient  $q_q$  change after the influence of  $\gamma$ -radiation of 2.5 kGy on leaves of 1 oak, 4 the regression line of the first order of the curve 1,  $q_q = 0.845$ ; 2 haricot, 5 the regression line of the 1st order of the curve 2,  $q_q = 0.947$ ; 3 pea, 6 the regression line of the first order of the curve 3,  $q_q = 0.924$ . Ordinate:  $q_q$  values, relative units; abscissa: the time of aftereffect of  $\gamma$ -radiation, in hours

$F_0^t$  values induced by EFEs requires the initial alignment of  $F_0$  in the experiment and a control at input of the modulating beam of 1.6 kHz. The highest point of FI ( $F_m$ ), induced by a light impulse of  $3,000 \mu\text{E}/(\text{m}^2 \text{ s})$ , corresponds to the complete reduction of the primary acceptor  $Q_A^-$ , and the photochemical quenching of FI is equal to zero (i.e.,  $q_q = 0$ ). At this point, there is maximal closing of RCs and of traps of the excitation energy. The difference between  $F_m$  and  $F_0$  is defined by the variable component  $F_v$ . In this regard, close attention to the change  $F_v = F_m - F_0$  is necessary.

The ratio  $F_v/F_m$  is a sensitive parameter of the state when a leaf is subjected to EFEs. After the  $F_v$  decrease (2–3 min), actinic light ( $1,100$ – $1,800 \mu\text{E}/(\text{m}^2 \text{ s})$ ) inducing the  $F_{v1}$  level was put in. After 30 s, a number of saturating impulses (1 s duration, light flux of  $3,000 \mu\text{E}/(\text{m}^2 \text{ s})$ ) were put in (Bolhar-Nordenkamp et al. 1989; Mohammed et al. 1996; Saakov 1987, 1993a–d, 2000a, b, 2001a, b, 2002a–c, 2003a, b, 2004). These impulses added to the actinic light to promote the complete reduction of the acceptor  $Q_A$ . To obtain correct data on the  $q_q$  and  $q_E$  values, identically determined around the world (Saakov 1987–2004; Briantais et al. 1986; Schreiber et al. 1986, 1994, 1997a,b; Schreiber 1983, 1986, 1998; Bolhar-Nordenkamp et al. 1989; Mohammed et al. 1996), it is necessary to distinguish precisely and carefully between the increase in the  $F_0$  value and the

decrease in the  $F_V$  value. The increase in  $F_0$  is characteristic of the destruction of PS-2 RCs, whereas the decrease in  $F_V$  shows the change in energetic quenching and depends on the accuracy of the  $F_0$  determination. For all measurements of FI coefficients, we used 7–9 min of PAMF signal harmonics, when the efficiency of the xanthophyll cycle reached the maximum.

The energy-dependent quenching of  $q_E$  (Fig. 2.34) is explained by the internal protonation of thylakoids, and its increase shows the increased energization of membranes, defined by the low speed of ATP utilization. For some time, the value of coefficient  $q_E$  remains at a plateau. Then, it increases and there is a short plateau with a further premortal peak in the  $q_E$  value. The increase in  $q_E$  to 0.5–0.6 indicates inactivation of the Calvin cycle. The secondary changes in the ChPC structural organization are less manifested (Saakov 2001a, b, 2003a, b). Specifically, because some defects of the photosynthetic device can be found only by analysis of FI quenching coefficients, we investigated, for the first time, changes in the  $q_q$  and  $q_E$  dynamics in the process of the long aftereffect of  $\gamma$ -radiation (Figs. 2.33, 2.34, 2.35, and 2.36).

It is necessary to emphasize that the analysis of FI quenching is essential and, at the qualitatively new level, supplements data on gas exchange to provide information on the specific sites of RC exposure to the stress influence.

The following conclusions result from the data in Figs. 2.33, 2.34, 2.35, and 2.36:

1. The initial stages of the curves specify that after removal of the radiation source, there is a tendency for the coefficient of FI quenching to go to the level inherent in the intact plant (i.e., a decrease in  $q_E$  values and an increase in the coefficient  $q_q$ ).
2. The process of influence of the aftereffect of  $\gamma$ -radiation starts when, for seemingly healthy plants, the level of  $q_q$  and  $q_E$  is similar to that of non- $\gamma$ -irradiated plants, that is, the visible reparation of phototrophy functions previously suppressed by the influence of  $\gamma$ -radiation can be supposed. A similar phenomenon was noted earlier (Saakov 1996, 2000a–e).
3. This process is functionally connected with the influence dose.
4. For a seven- to eightfold increase in the dose of radiation, the time to lethal outcome is halved.
5. An increase in the dose of  $\gamma$ -radiation causes irregularity in the level change in  $q_E$ . The sharper increase and decrease in curve 3 in Fig. 2.33 show the lower resistance of pea leaves.
6. At radiation in high doses, the decreased dynamics of coefficient  $q_q$  values reduces by the law of the 1st-order regression.
7. The influence of rather small doses causes a plateau zone (Fig. 2.33, 50–80–150–200 h) in the dynamics of coefficient  $q_q$ . This plateau can be interpreted as the attempt of objects to maintain the normal level of functional reactions of phototrophy. In this case, the level of the PS-2 reduction is close to the control. This period coincides in time with the course of the curves in Fig. 2.33. Two plateaus in the dynamics of coefficient  $q_q$  probably reflect the pre-lethal state of the object.

The relaxation of curves in Fig. 2.35 indicates that the aftereffect of  $\gamma$ -radiation leads to the impossibility of the re-oxidization of  $PQ^{2-}$  and to the accumulation of

electrons in the acceptor part of PS-2. Further, the decrease in all curves shows the death of plants and is accompanied by the drying of laminae, but not their necrosis. In this case, the lethal reaction of objects to the aftereffect of  $\gamma$ -radiation is identical to the reaction of leaves to high doses of irradiation of approximately 8–12 kGy (see our publications in the databases of NCBI Pub Med, ISI, Google).

Earlier we showed the high functional radioresistance of green cells and their protein-synthesizing systems, and small structural changes in various ChPC that differed in the complexity of their structural organization. Simplification of the ChPC structure resulted in damage to its radioresistance.

Thus, the influence of high doses of  $\gamma$ -radiation led to a considerable decrease in the photosynthetic intensity and a sharp increase in the level of respiration. Research on the influence of atmospheric drought and high temperatures (Saakov 2003a, b, 2004) revealed the correlation between the decrease in photosynthetic intensity and the reduction in  $q_q$  and increase in  $q_E$ .

The interpretation of these data allowed us to find the correlation between the reparation of photosynthetic intensity in response to watering and during a decrease in the day temperature.

Simultaneously, the close link between the decrease in coefficients  $F_m$ ,  $F_{V1}$ , and  $F'_V$ , the damage to the ETC functional activity, and the drop in  $\text{CO}_2$  fixing was shown. The data in Figs. 2.33, 2.34, 2.35, and 2.36 on the influence of the aftereffect of  $\gamma$ -radiation on the dynamics of the change in FI quenching coefficients confirm the early works studying the influence of other EFEs (Saakov 1993a–d, 2000a–e, 2001a, b, 2002a–c, 2003a, b, 2004) and allowed us to develop the assumption of the adequacy of mechanisms of response to the damage and the reparation of leaf autotrophy.

Scientists suppose that  $F_V$  should be “recombinant luminescence” during the  $\text{P}^+_{680}\text{Pheo}^- \text{Q}_\text{A}^- \rightarrow \text{P}^*_{680}\text{PheoQ}_\text{A}^-$  transition. The decrease in  $F_V$  or  $F'_V$  values under the influence of  $\gamma$ -radiation or its aftereffect is coupled with the changes in  $q_q$  and  $q_E$  and indicates the suppression of PS-2 RC function and of the  $e^-$  current from  $\text{P}_{680}$  to  $\text{Q}_\text{A}^+$ . Similar to the case of the influence of other EFEs, the phototrophy function of the photosynthetic device during the influence of the aftereffect of  $\gamma$ -radiation is connected with the RC activity and damage to the ETC in the link  $\text{P}^+_{680}\text{Pheo}^- \text{Q}_\text{A}^- \rightarrow \text{P}^*_{680}\text{PheoQ}_\text{A}^- \text{Q}_\text{B}$ , which is accompanied by a decrease in the level of PS-2 reduction. Thus, the specifics of the long-term dynamics of coefficients  $q_q$  and  $q_E$  are a convincing criterion for identification of the functional state of phototrophic systems when visual signs of damage to a green cell are absent. This should be taken into consideration in the case of ecological accidents of anthropogenous origin.

### **2.2.12 *The Specifics of the Fine Structural Changes in the Photosynthetic Device Under the Influence of $\gamma$ -Radiation***

#### **2.2.12.1 The Character of the Changes in the Derivative Spectra of a Green Leaf In Vivo in the Red Spectral Area**

Pigment–protein complexes of chloroplasts are responsible for the absorption of light energy and its transformation and conversion to other forms of energy, in particular, into the energy of chemical bonds. Significant progress in understanding the organization of photosynthetic membranes of eukaryotes and cyanobacteria (prokaryotes) responsible for the specified processes of energy transformation occurred after research on the ChPC composition by modern methods of the analysis (Green and Durnford 1996). The pigment complex consists of two photosystems, possessing a number of cofactors necessary for the charge separation and for the electron transfer. The organization and composition of the pigment complexes are rather conservative both for higher and lower eukaryotes and for prokaryotic cyanobacteria (Green and Durnford 1996). The state and functional activity of pigment complexes define the phototrophic ability of a leaf and correspond to its resistance to the EFE influence.

For the earlier assessment of the functional state of the photosynthetic device under the influence of an EFE, we used the method of PAMF (Saakov et al. 1993; Saakov 1993a–d, 1996). These studies allowed us to reveal the very peculiar character of the damage to the activity of the xanthophyll cycle, that is, some shifts in the character of derivative spectra in blue and red spectral areas (Saakov 1993a–d, 1996) indicating structural damage of the pigment complex. The improvement in research methods and the possibility of application of computer equipment for the processing of spectrophotometric research in vivo have allowed us to return, at a qualitatively new stage, to questions regarding the study of structural damage to the photosynthetic device under extreme influences (Saakov 2002a–c).

In this section we investigate features of the change in derivative absorption spectra of high orders in red and dark blue spectral areas using a native leaf under the influence of high doses of  $\gamma$ -radiation. Previous research showed that green cells of plants and algae are distinct in their rather high radioresistance, without essential disorder of their phototrophy function, and are much more tolerant to the influence of  $\gamma$ -radiation than animals (Saakov et al. 1992; Saakov 1993a, b, 1996).

As objects of research, we used the leaves of acacia (*Robinia pseudoacacia* L.), haricot (*Phaseolus vulgaris* L.), tobacco (*Nicotiana tabacum*), and the barley *Hordeum vulgaris* L. variety Donaria mutant № 2807 lacking chlorophyll *b*. The source of  $\gamma$ -radiation was the isotope  $^{57}\text{Co}$  mounted into a lead chamber with a sliding glass for the placement of vessels with leaves inside. The power source for the period of the experiment was equal to 670 Gy/h. Absorption spectra of intact leaves were registered with the spectrophotometer DW-2000 (Aminco, Germany). In some cases, spectra were recorded by the UV-VIS-Specord device (Carl Zeiss, Jena,

Germany) supplied with a differentiating facility (Saakov 2000a–e; Saakov et al. 2012/2013). The digitalization of spectral curves was carried out with the *Graph Digitizer* 2.14 program according to N. Rodionov (see <http://nick-gd.chat.ru>). Further processing of the digital material to obtain derivative spectra of the fourth ( $D^{IV}$ ) and the eighth ( $D^{VIII}$ ) orders was performed with the help of programs *Spectra Calc* and *Origin* 5.0-8 (Saakov 2000a, b; Zhukovskii and Saakov 2002). The reproducibility of results was proved or not proved by the record of five to seven parallel spectra. The available software easily allows the calculation of derivatives of high orders and determination of the integral of the area of a peak and on this basis to make conclusions about the change in the quantitative composition of components (*Peak Explorer* 1.0; *PeakFit* v.4), to perform statistical calculations (*SigmaPlot* 2000), to modify the view of any spectra to a uniform scale, and to carry out the addition of several spectra and calculate the average spectrum.

For more precise determination of substances possessing spectra found in registered spectral curves of native leaves (Figs. 2.39 and 2.40), we carried out careful purification of solutions of chlorophyll *a* and Pheo with the help of the technique (Saakov et al. 1978) described in Chap. 3 and performed the graphic presentation of their spectral properties with the corresponding derivative curves (Fig. 2.37).

Derivative spectra of high orders for Pheo are shown for the first time, as well as the eighth derivative of the absorption spectrum of chlorophyll *a*. In the spectral area *D* with  $\lambda \approx 530$  nm for the spectrum  $D^{VIII}$  Pheo, there are six bands (from 522.7 to 539.5 nm); in the area with  $\lambda \approx 565$  nm (from 556 to 576 nm), there are also six bands; in the area with  $\lambda \approx 600$  nm (from 585 to 620.5 nm), there are nine bands; in the main maximum of Pheo absorption of  $\lambda = 653$  nm (from 629.1 to 678.2 nm), 13 bands can be distinguished. The advantages of registration of  $D^{VIII}$  spectra are revealed when, on curve 4, bands appear with  $\lambda = 529.9$  and 552.6 nm; peak bifurcation at 560.7, 568.8, 576.30, and 586.7 nm; the shoulder at 592.5 nm; and peaks at 612.80, 632.40, 648.80, and 652.2 nm. The registration of Pheo derivative spectra of higher orders is inexpedient and can be only defined by special research, which should be accompanied by an essential increase in the recording scale of the abscissa axis. The location of spectral bands of the  $D^{VIII}$  chlorophyll *a* spectrum substantially coincides with bands of the  $D^{VIII}$  Pheo spectrum, although sometimes bands have bathochromic or hypsochromic shifts along the abscissa. A number of bands do not show such coincidences:  $\lambda = 650.4, 652.3, 658.8, 668.1, \text{ and } 671.20$  nm.

To have the possibility to obtain information about the presence or absence of changes in the red area of the registered fine spectral structure of the ChPC for leaves *in vivo* subjected to radiation, we used the known selectivity of derivative spectrophotometry of higher orders. We also used properties of difference derivative spectra of the fourth ( $\Delta D^{IV}$ ) order (Figs. 2.38 and 2.39).

Because the set of ChPC forms is a system of energetically interacting elements participating in the electron transfer, even small changes in the spectral curve of a native leaf induced by ionizing radiation correspond to the disorder of stationary transitions of the step-like pathway and of the conversion of light energy into the energy of chemical bonds. Earlier, we supposed that ionizing radiation can break the function of the electron transfer link from  $P_{680}$  to Pheo and so prevent  $Q_A$

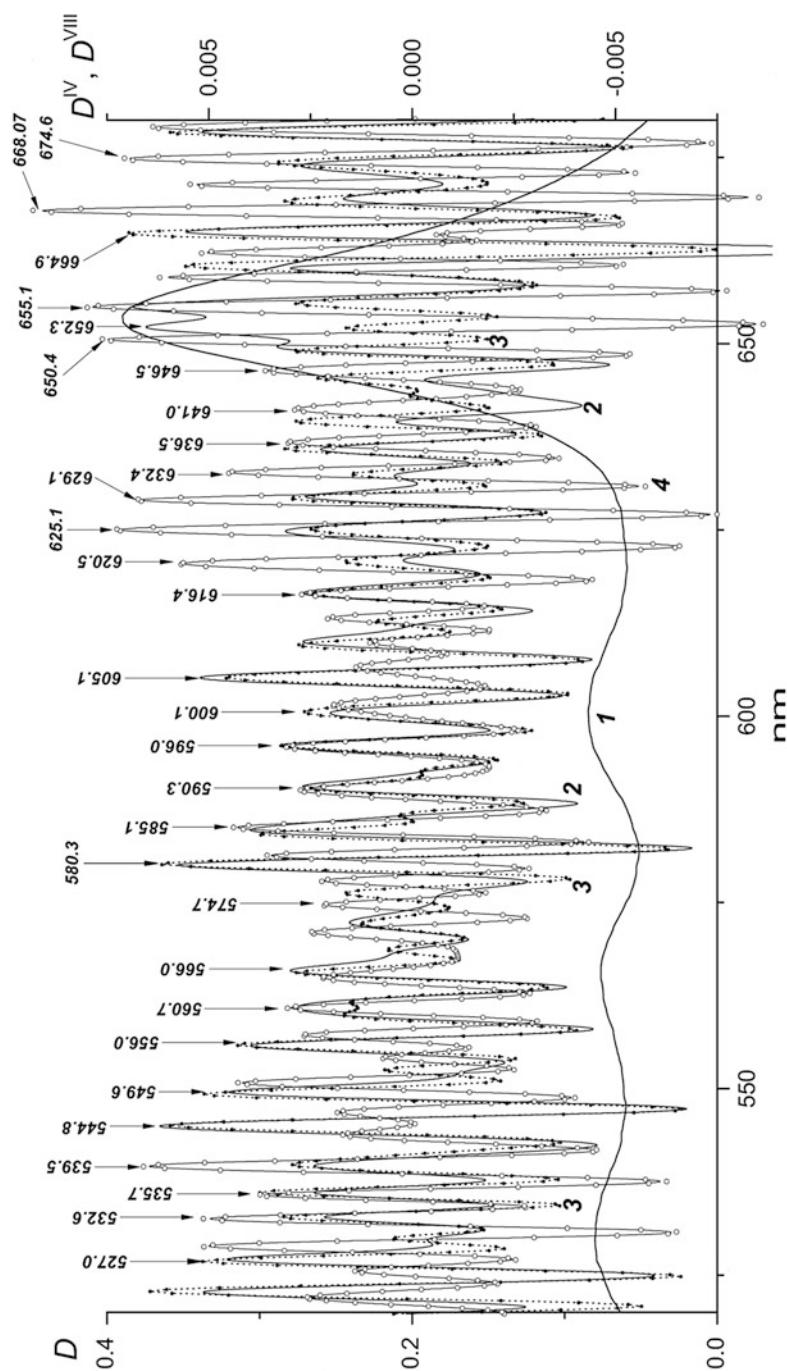
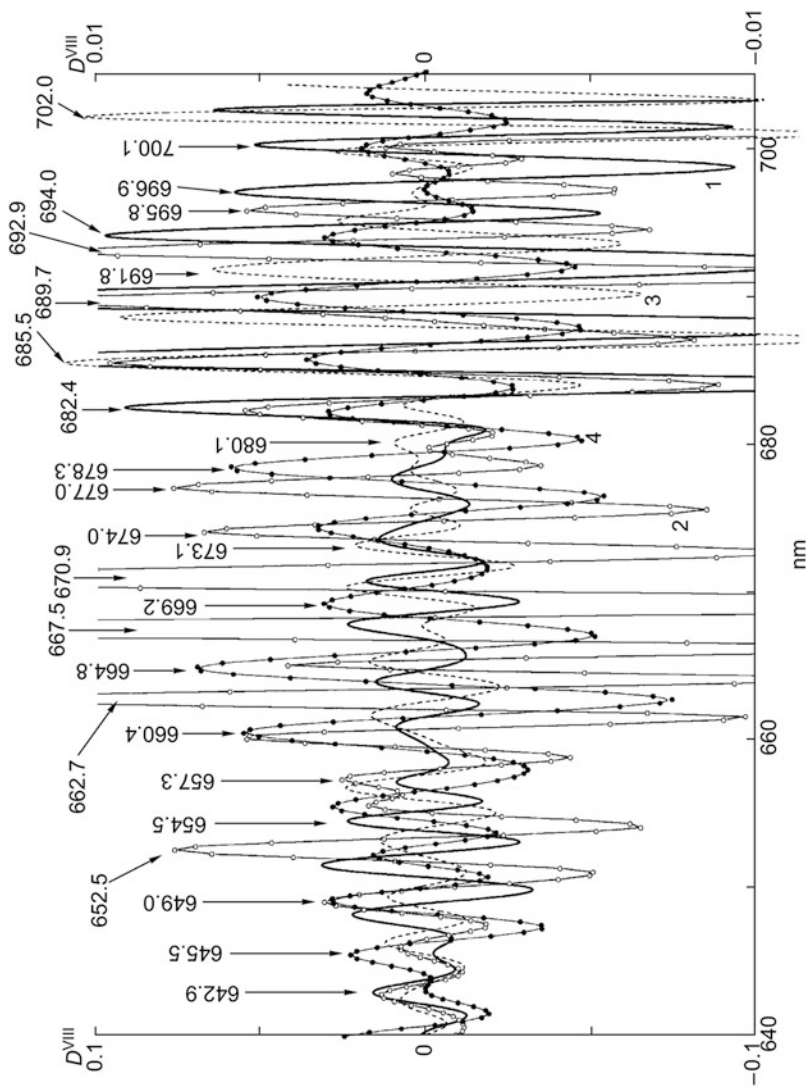
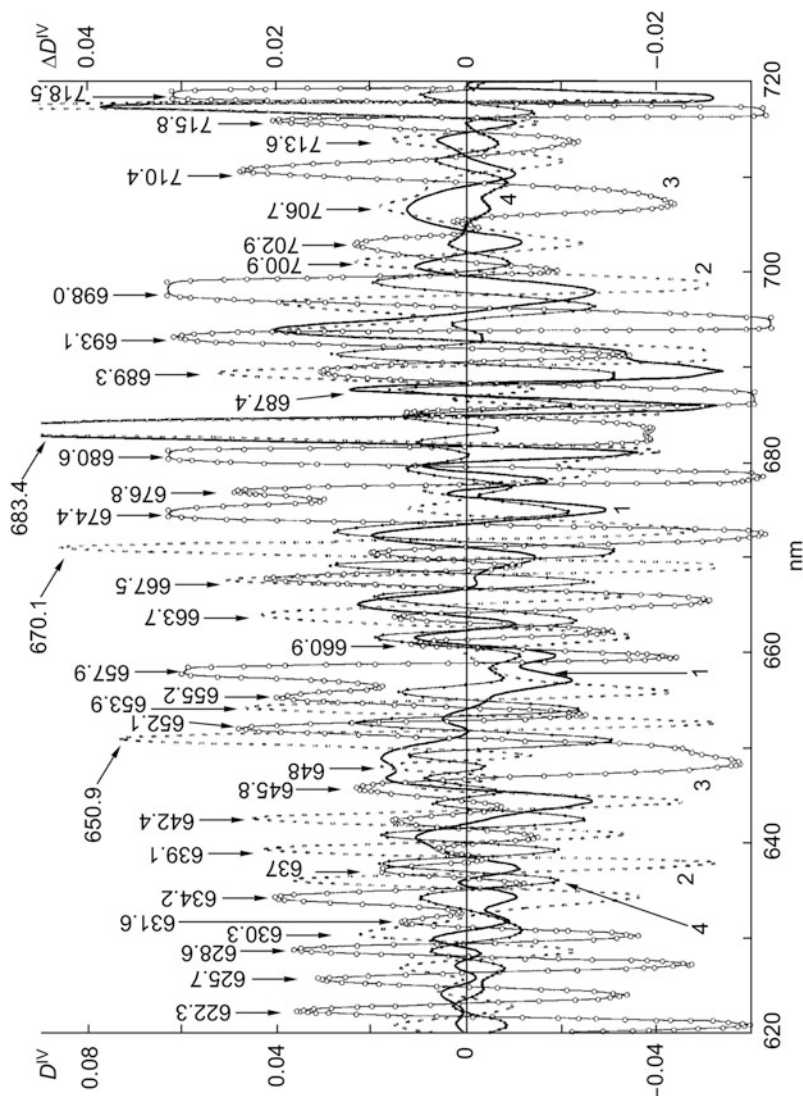


Fig. 2.37 The absorption spectrum of the pheophytin solution (1) and its fourth (2) and eighth derivatives (3). The eighth derivative of the absorption spectrum of chlorophyll in ethanol (4). Preparations passed fourfold chromatographic purification





**Fig. 2.38** The character of the change in the eighth derivative of the absorption spectrum of a native leaf of the barley mutant № 2807 lacking chlorophyll *b* (1) and under the influence of chloro carbonyl cyanide phenylhydrazone (2) or potassium cyanide (3). The eighth derivative of Pheo solution (4)



**Fig. 2.39** The specifics of the fourth derivative change in the absorption spectrum of a native leaf of *Robinia pseudoacacia* under the influence of 8 kGy  $\gamma$ -radiation. 1 control; 2 the experiment after 8 kGy irradiation; 3 the difference spectrum ( $\Delta D^IV$ ) "control minus experiment"; 4  $D^IV$  of the Pheo solution

reduction (Saakov 1993a–d, 2000a–e). In assessing the functional damages to ETC caused by ionizing radiation and other EFEs, this situation was the subject of rather serious argumentation (Saakov 2000a–e, 2002a–c, 2003a, b; Bukhov et al. 2001a, b). The experiment showed that the short-term influence of EFEs, followed by the reparation of functional reactions of the photosynthetic device or the adaptation of the object to the influence of the EFE, is not necessarily accompanied by a quantitative change in the pigment content (Saakov 1993a–d; Semikhatova and Saakov 1962). From this point of view, the detection of minor changes in the state of the fine structure of the photosynthetic device becomes of significant value.

For the determination of separate spectral bands that are not disguised by the presence of chlorophyll *b* and can be with a high degree of reliability considered as a ChPC of chlorophyll *a*, we plotted the spectral curves of an *in vivo* leaf of the barley mutant № 2807 lacking chlorophyll *b* (Fig. 2.38). For this purpose, we digitalized graphic data from earlier years (Saakov 1973) and made the necessary operations of further differentiation to obtain the derivative spectra of the eighth order. This allowed us to conclude with sufficient confidence that the bands of positive extrema ( $\lambda^{\text{DVIII}}_{\text{max}}$ ) presented in Fig. 2.38 (curve 1) are not caused by the contribution of absorption bands of chlorophyll *b*, and therefore they can be attributed to the absorption of native complexes of chlorophyll *a*. The absorption bands  $\lambda^{\text{DVIII}}_{\text{max}}$  of the Pheo *a* solution (Fig. 2.38, curve 4) make it easier to understand the changes in the spectral structure of a leaf under the influence of chloro carbonyl cyanide phenylhydrazone (CCCP) and potassium cyanide (KCN).

With a high level of confidence, it is possible to say that the shifts of positive extrema of spectral bands (Fig. 2.38, curves 2 and 3) are also not caused by the contribution of absorption bands of chlorophyll *b*. There are bases to assume that the extrema  $\lambda^{\text{DVIII}}_{\text{max}}$  induced by the influence of CCCP and KCN can be attributed to the absorption of new compounds formed after destruction of chlorophyll *a* complexes. Data presented in Fig. 2.38 on the influence of CCCP and KCN on the structural state of ChPC enable detection of new components with much higher accuracy than in previous work (Saakov 2003a, b). At the same time, these data confirm the correctness of measurements performed 30 years ago (see Saakov et al. 2013, p. 245, Fig. 4.22 and p. 254, Fig. 4.26).

The little-changed experimental design is significant because of the choice of the more informative technique for observation of phenomena. The harmonics of  $D^{\text{VIII}}$  spectra under the influence of CCCP and KCN (Fig. 2.38, curves 2 and 3) allows two conclusions to be made. First, in chloroplasts an increased content of pheophytinized products is formed from the ChPC composition, which was supported by bringing the optical densities of variants in the experiment to the same scale.

Second, the part of aggregated funds of chlorophyll *a* essentially decreases, and the part of short-wave forms with  $\lambda_{\text{max}} = 677, 670.9, 667.5$ , and  $662.7$  nm increases. The presented data create preconditions for the comparison of damage to the ChPC fine structure caused by the influence of chemical agents and radiation. The peak with  $\lambda_{\text{max}} = 650$  nm in the spectrum  $D^{\text{II}}$ , induced by KCN, was decomposed into bands with  $\lambda_{\text{max}} = 649.3$  and  $653.1$  nm. The CCCP impact induced the appearance of peaks in the spectrum  $D^{\text{VIII}}$  with  $\lambda_{\text{max}} = 649.0, 652.5, 655.5, 657.3, 659.9, 662.7$ ,

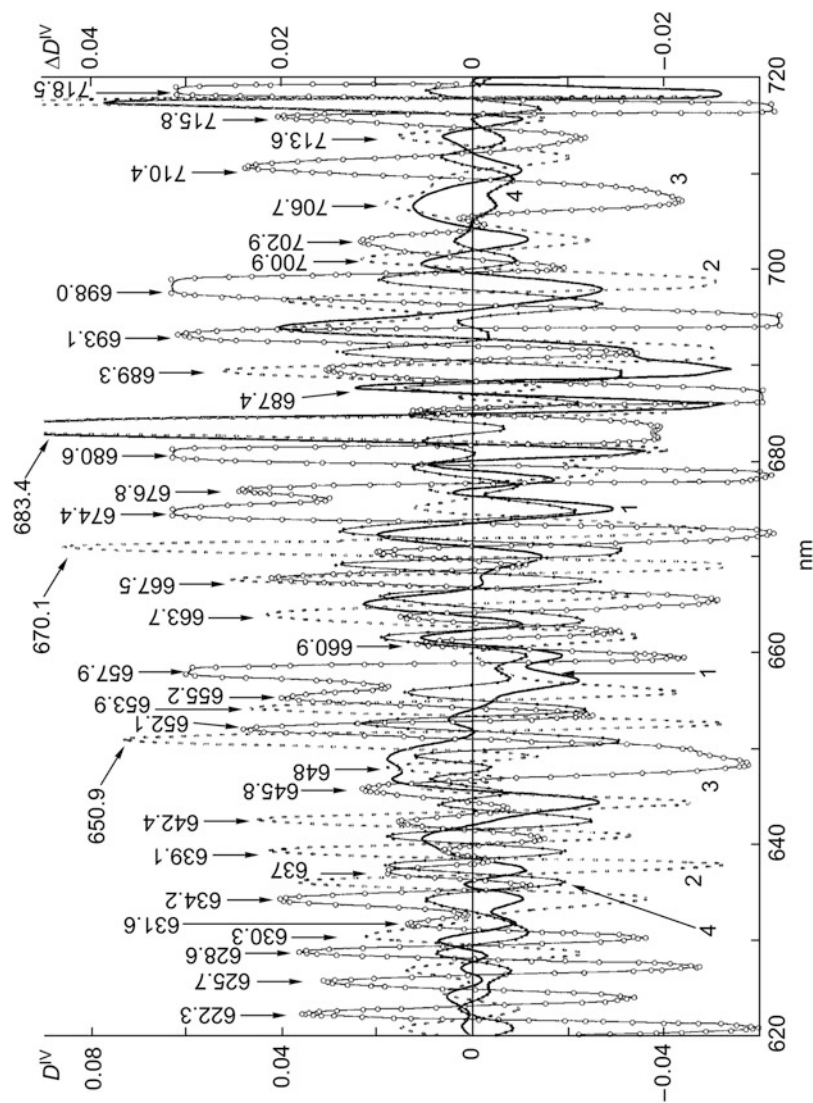


**Fig. 2.40** Features of the fourth derivative change in the absorption spectrum of a native leaf of *Phaseolus vulgaris* under the influence of 12 kGy  $\gamma$ -radiation. 1 control; 2 the experiment just after 12 kGy irradiation; 3 and 4 curves the difference spectrum ( $\Delta D^IV$ ) "control minus experiment" 24 h after termination of irradiation

665.0, and 667.5 nm, the location of which was not revealed in the spectrum  $D^{\text{II}}$ . The hypsochromic shift of maxima relative to the control was found at  $\lambda_{\text{max}} = 674.0, 677.0, 682.1, 685.4, 692.9, 695.8, \text{ and } 698.2 \text{ nm}$ .

Figures 2.39 and 2.40 present results on the influence of high doses of  $\gamma$ -radiation on the change in the ChPC structure in in vivo leaves of *R. pseudoacacia* and *Ph. vulgaris*. From the data in Fig. 2.39, it follows that the influence of  $\gamma$ -radiation leads to the formation of new absorption bands, namely,  $\lambda_{\text{max}} = 620.7, 623.9, 627.2, 635.70, 653.7, \text{ and } 687.0 \text{ nm}$ , and that these maxima are hypsochromically shifted relative to initial bands, the control. Bands with  $\lambda_{\text{max}} = 630, 648.1, \text{ and } 665.2 \text{ nm}$  have the bathochromic shift. A number of new extrema have no or very insignificant shift, but in them the domination of the hyperchromic effect is detectable: 632.4, 635.7, 643.8, 648.1, 650.4, 653.7, 655.9, 659.4, 662.1, 665.2, 669.2, 672.3, 678.3, 687, and 694.5 nm. The manifestation of this effect (e.g., for protein structures) suggests the formation of a less-ordered structure than the initial one, and it is also the criterion of the denaturation degree, that is, of the transition of ChPC protein molecules to the unfolded state (Rozengart and Saakov 2002). In favor of this idea is the hyperchromia of bands with  $\lambda = 678.3 \text{ and } 672.3 \text{ nm}$ , which correspond to non-aggregated ChPC forms. The difference between non-irradiated and irradiated leaves manifests very clearly in the difference spectrum “control minus experiment” (Fig. 2.39, curve 3). Because the same leaf is often used as both control and experimental object, the difference spectrum shows the difference in the structural state of a leaf *before and after irradiation*.

It is necessary to remember that, according to the basic rule of difference spectrophotometry, the orientation of difference spectra cannot coincide with the orientation of the initial spectra, and, as a rule, values of  $\lambda_{\text{max}}$  of difference spectra are not equal to  $\lambda_{\text{max}}$  of absorption spectra; the appearance of new extrema in positive and negative areas is possible. This is illustrated with curve 3 in Fig. 2.39. To the found hyperchromia in the experimental variant correspond negative extrema on this curve at  $\lambda = 620.95, 624.2, 627.4, 635.7, 643.7, 640.7, 648.50, 653.5, 659.6, 662.2, 665.5, 672.2, 678.5, 686.9, 682.9, \text{ and } 694.7 \text{ nm}$ . Taking into account the fact that the location of positive extrema of curve 1 in Fig. 2.39 substantially coincides with the position of positive extrema of curve 1 in Fig. 2.38, it is possible to attribute the absorption band with  $\lambda_{\text{max}} = 644.7, 651.3, 654.7, 659.3, 664.4, 669.39, 672.3, 675.3, 683.4, 688.0, 692.0, \text{ and } 694.2 \text{ nm}$  to bands of chlorophyll *a*.

In the experiments carried out earlier, the bathochromic shift of the main maximum of Pheo during the transition from the polar to nonpolar solvent was equal to 16–17 nm (Saakov and Hoffmann 1974). With a certain level of probability, it is possible to assume that a similar shift of Pheo absorption bands takes place in vivo. Then, it is possible to suppose that a number of extrema of curve 3 in Fig. 2.39 are caused by the formation of Pheo. For example, the band 678.3 in vivo probably corresponds to the in vitro band of the Pheo solution 660.1 nm and the band 672.3 in vivo to 665 nm of the solution. However, the initial polycomponent media in vivo points to necessary carefulness in the final conclusions, although these conclusions are very tempting.

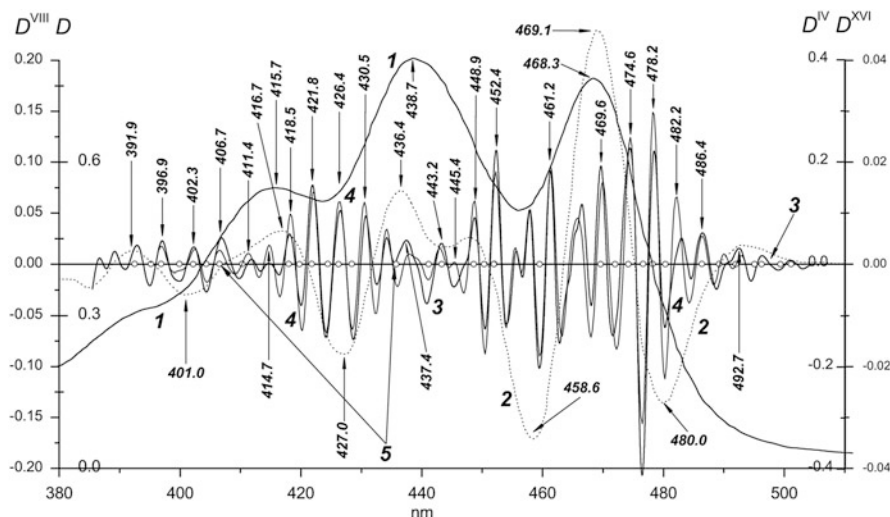


**Fig. 2.41** Derivative spectra of sixfold purified and saponified solutions of violaxanthin in acetone of the 4th (2), 8th (3), and 16th (4) orders; 1 the absorption spectrum; 5 points of intersection of the zero axis by the  $D^{VII}$  of the absorption spectrum are shown on the zero axis. *Ordinates*: OD in relative units; *abscissa*: wavelength in nanometers

With the increase in the dose of  $\gamma$ -radiation (Fig. 2.41, curve 2), we specified the level of the change in ChPC separate bands for haricot leaves. It is necessary to emphasize that  $\gamma$ -radiation promoted high dehydration of the lamina and an increase in respiration (Saakov et al. 1993; Saakov 1993a–d, 2002a–c). We could expect functional and structural changes of the photosynthetic device, inherent in the response to atmospheric drought (Saakov 1973). Probably, the high dehydration of a leaf also promotes the manifestation of the hyperchromic effect, which manifests in the OD increase in spectral bands with  $\lambda_{\max} = 620.8, 624.5, 630.3, 636.1, 639.1, 642.4, 645.7, 648, 650.9, 653.9, 659.9, 663.7, 667.5, 670.1, 675.09, 677.1, 683.4, 689.3, 696.8, 700.9, \text{ and } 706.7 \text{ nm}$ . For one band, the OD at 693.60 remained invariable; the hypsochromic effect was found for bands  $\lambda = 679.8 \text{ and } 703.1 \text{ nm}$ .

Thus, there should be no doubts about the hyperchromia induced by radiation, with appearance of the less-ordered structure and domination of non-aggregated ChPC forms. The course of the curve 3  $\Delta D^{IV}$  in Fig. 2.40 testifies to this as does the orientation of its extrema.

At the same time, not all extrema of the experimental curve 2 in Fig. 2.40 have the corresponding hypsochromic shift, the presence of which also points to ChPC de-aggregation. For example, bands 630.3, 650.9, 653.9, 659.8, and 696.7 nm have manifested bathochromic shift. Bands 620.8, 626.9, 636.0, 648.0, 667.5, 677.0, 683.4, 693.8, 700.9, 706.7, and 713.6 nm possess neither hypsochromic nor bathochromic shifts. Manifestation of the aftereffect starts 24 h later, accompanied by a reduction in OD values for the majority of bands of curves 2 and 3 down to

values close to or even below the values of the initial control (Fig. 2.40, curve 4). At the same time, for bands with  $\lambda_{\max} = 622.7, 628.7, 634.10, 637.65, 640.7, 644.1, 646.8, 649.0, 650.9, 652.4, 655.7, 658.3, 661.5, 665.9, 669.1, 672.6, 679.1, 682.1, 684.7, 687.5, 691.2, 698.9, 702.9, 711.7, \text{ and } 718.5 \text{ nm}$ , residual hyperchromia is observed that substantially coincides with extrema of curve 3. Simultaneously, during the aftereffect of radiation, the hypochromic effect of the OD decrease manifests for separate spectral bands  $\lambda = 620.8, 626.7, 630.7, 636.0, 639.2, 642.45, 648, 653.9, 663.0, 667.3, 670.5, 674.8, 676.3, 683.3, 688.8, 696.4, 700.8, 709.2, 713.1, \text{ and } 716.6 \text{ nm}$ . The location of the bands is sometimes accompanied by the bathochromic shift, showing the complexity of the structure.

In other words, during the aftereffect of radiation, the mirror course of curves 2 and 4 is observed in a quite large number of bands. It is improbable to expect the complete coincidence of the reversible dynamics of extrema positions on the specified curves. But the existence of such a fact, repeatedly registered in experiments, attracts attention and requires further experimental investigation and theoretical grounds. Due to its complexity, the final solution of the question about the possibility of the regenerative aggregation of ChPC during the aftereffect of radiation will be the subject of further research.

Thus, the material presented in this section allows us to draw certain conclusions. Under the influence of  $\gamma$ -radiation on intact leaves, the destruction of the photosynthetic device takes place, and this process is in many respects similar to that taking place under the influence of inhibitors of photosystems, many of which are known herbicidal substances. The structural damage to the photosynthetic device is in many respects similar to disorders arising in response to the impact of deep atmospheric drought (Saakov 2003a, b) and differs only slightly from the damage caused by temperature shock. Obviously, both in the case of the effect of inhibitors (Saakov 1973) and under the influence of ionizing radiation, the coupling of the energy transfer to and migration through ChPC forms is damaged. The appearance or the prevalence of some ChPC intermediate forms over others increases their acceptor properties at the expense of donor properties, which leads to decoupling of the energy conversion chain. The appearance of newly formed absorption bands cannot be unequivocally explained by the formation of pheophytin or of other products of chlorophyll transformation. The presence of the hyperchromic effect and of the hypsochromic shift in a number of bands reliably indicates the presence of mechanisms of de-aggregation and simplification of the structure of the chlorophyll–protein complex. As a result of the registration of derivative spectra of high orders, it became possible to consider the change in separate bands of the ChPC structure and to suggest ways of their repairation. The presented data are the evident illustration of the statement about the close interrelation between the structure and function of the photosynthetic device during the conversion of light energy into chemical potential energy and emphasize the correctness of our early ideas on the generality of primary reactions of photosynthetic device damage under the influence of EFes. In our work, the eighth derivatives of absorption spectra of chlorophyll *a* and of pheophytin are presented for the

first time, which is interesting for further investigation of their analytical biochemistry and physiological properties.

### 2.2.12.2 Features of the Influence of $\gamma$ -Radiation on the Fine Structure of the Photosynthetic Device; the Assessment of the Character of In Vivo Damage in the Blue Spectral Area by Means of Derivative Spectra of High Orders

The correlation between the structure and function of the photosynthetic device is the cornerstone of the elucidation of plant phototrophic function. It especially manifests under extreme influences of the environment coupled with natural or anthropogenous stress. Earlier, we found features of structural change in the photosynthetic device of barley mutants lacking chlorophyll *b* under the impact of inhibitors of photosystems and herbicides (Saakov and Nazarova 1972; Saakov 1971a, b, 1973, 2001a, b; Saakov and Hoffmann 1974). The data pointed to links between structural changes in the photosynthetic device, the activity of the xanthophyll cycle, the ETC activity, and ATP synthesis during the photophosphorylation process (Saakov 1971a, b, 1973; Saakov and Hoffmann 1974). The development of research on the assessment of functional damage under the influence of natural and technogenic stress suggested that the reason for this damage is damage to the ETC link in the area  $P_{680}^+Phe^-O_A^- \rightarrow P_{680}^*PheQ_A^- \rightarrow P_{680}^*PheQ_A^-Q_B$  (Saakov 2000a–c, 2002a–c). The inhibition of the phototrophic function of leaves and earlier registered changes in the fine structure of the photosynthetic device were shown (Saakov et al. 1993; Saakov 1994). It was proved that the photoinhibition of the phototrophic function of leaves begins earlier than registered changes in the fine structure of the photosynthetic apparatus (Saakov et al. 1993; Saakov 1994). The creation of conditions of artificial heterotrophy over a long time period does not result in significant changes in the structural organization of the pigment–protein complex of the photosynthetic apparatus (Saakov 1972).

The ambiguous picture in research on the influence of ionizing radiation on states of photosynthetic devices of *Procaryota* and *Eucaryota*, and also the analysis of accidents of technogenic origin, showed the insufficient reliability of the material on changes arising in the fine structure of the photosynthetic device under the irradiation of green cells of plants and algae. In this regard, in our work we decided to investigate the influence of ionizing radiation on live intact leaves at a statistically reliable level using the new possibilities of derivative spectrophotometry of high orders in combination with the computer analysis of obtained curves. We investigated the change in the fourth to eighth ( $D^{IV}$  and  $D^{VIII}$ ) derivatives of absorption spectra of intact leaves for the possibility to judge about the change in the fine structure of the photosynthetic device in the blue spectral area manifested as damage of the Soret band of the chlorophyll and absorption bands of the oxidization–reduction cycle of xanthophylls (Saakov 1971a, b, 1973; Saakov and Hoffmann 1974). We also compared the obtained data with the results of previous



sections of this chapter and with results obtained by application of the PAM method. Works of such type are unknown in experimental practice.

The objects of research were intact leaves of haricot (*Phaseolus vulgaris* L.) and barley (*Hordeum vulgaris* L., the Donaria variety, the mutant № 3613 lacking chlorophyll *b*). As the source of  $\gamma$ -radiation, a capsule containing the isotope  $^{57}\text{Co}$ , of radiation power of 670 Gy/h, and shielded with lead was used. The absorption spectra of intact leaves were registered with the spectrophotometer DW-2000 (Aminco, Germany) with a built-in computer and also with the spectrophotometer UV-VIS Specord (Carl Zeiss, Jena, Germany), supplied with an analogue differentiating device (Saakov et al. 1987). Solutions of pigments were measured in the spectrophotometer Specord-40 (Carl Zeiss, Jena, Germany). If necessary, the digitalization of spectral curves of pigments or intact leaves was carried out with the help of the *Graph Digitizer* 2.14 program, according to N. Rodionov (see <http://nick-gd.chat.ru>). Further processing of the digital material was performed in *Spectra Calc* and *Origin* 8.0 programs.

In order to obtain information about the presence or absence of changes in the fine structure of the native chlorophyll–protein complex of irradiated leaves, we used the known selectivity of higher orders of derivative spectrophotometry and also the properties of differential derivative spectra of the fourth ( $\Delta D^{\text{IV}}$ ) order (Figs. 2.43 and 2.44). Here we will break the order of figure citation, and for the sake of logic, we will first refer to higher figure numbers. Because the set of ChPC forms is a system of energetically interacting elements participating in electron transfer, even small changes in the spectral curve of a native leaf, induced by ionizing radiation, correspond to the disorder of stationary transitions of the step-like pathway of the energy. Earlier, we supposed that ionizing radiation can break the function of the electron transfer link from  $\text{P}_{680}$  to Pheo and so prevent  $\text{Q}_\text{A}$  reduction (Saakov 1994). The assessment of functional damage in ETC induced by ionizing radiation and other EFEs supported this statement (Saakov 2000a–e, 2002a–c; Bukhov et al. 2001a, b).

To more exactly refer the studied curves of native spectra of leaves to specific compounds, in particular to the most important component of the xanthophyll cycle, violaxanthin (5,6,5',6'-di-epoxy-3,3'-di-hydroxy- $\beta$ - $\beta$ -carotene) (Viol), the radiochemical purification of violaxanthin preparations and their spectrophotometry in two solvents of opposite polarity (acetone and in carbon tetrachloride) (Figs. 2.41 and 2.42) were performed. The spectral contour of the pigment solution in the nonpolar solvent ( $\text{CCl}_4$ ) mostly corresponds to the spectrum of its native state, which allows consideration of separate bands of the blue spectral area with higher conviction (Figs. 2.42 and 2.43).

From the data (Fig. 2.41, curve 2), it follows that even on the spectrum  $D^{\text{IV}}$  the spectral bands specific to Viol, which are not detected by the usual spectrophotometry and are absent from absorption spectra, are revealed:  $\lambda^{\text{DIV}}_{\text{max}} = 391.9, 416.7, 436.4, \text{ and } 448.9 \text{ nm}$ ; the position of the extremum is specified at 469.1 nm. The measurement of the  $D^{\text{VIII}}$  spectrum (curve 3) shows the existence of additional extrema at  $\lambda^{\text{DVIII}}_{\text{max}} = 386.7, 389.3, 392.7, 396.9, 406.7, 411.4, 414.7, 418.5, 421.8, 430.5, 434.3, \text{ and } 437.4 \text{ nm}$ ; it also decomposes at  $\lambda^{\text{DIV}}_{\text{max}} = 469.1 \text{ nm}$  into four

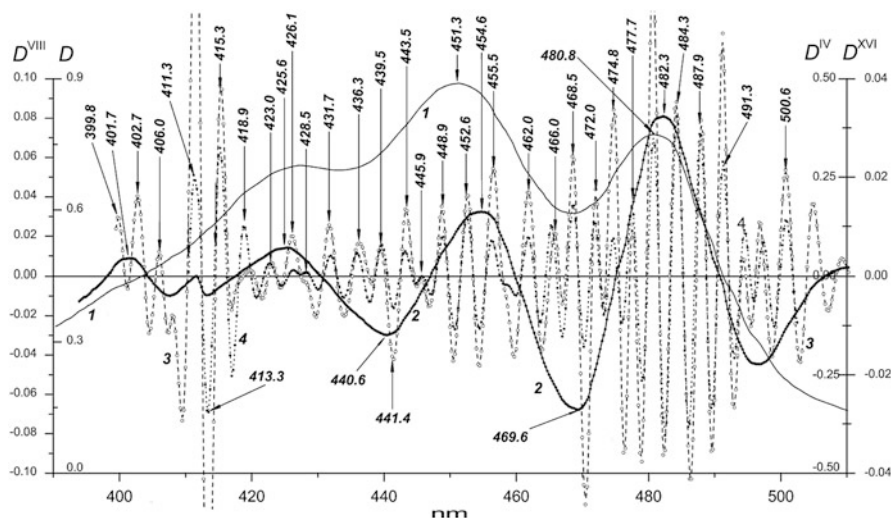
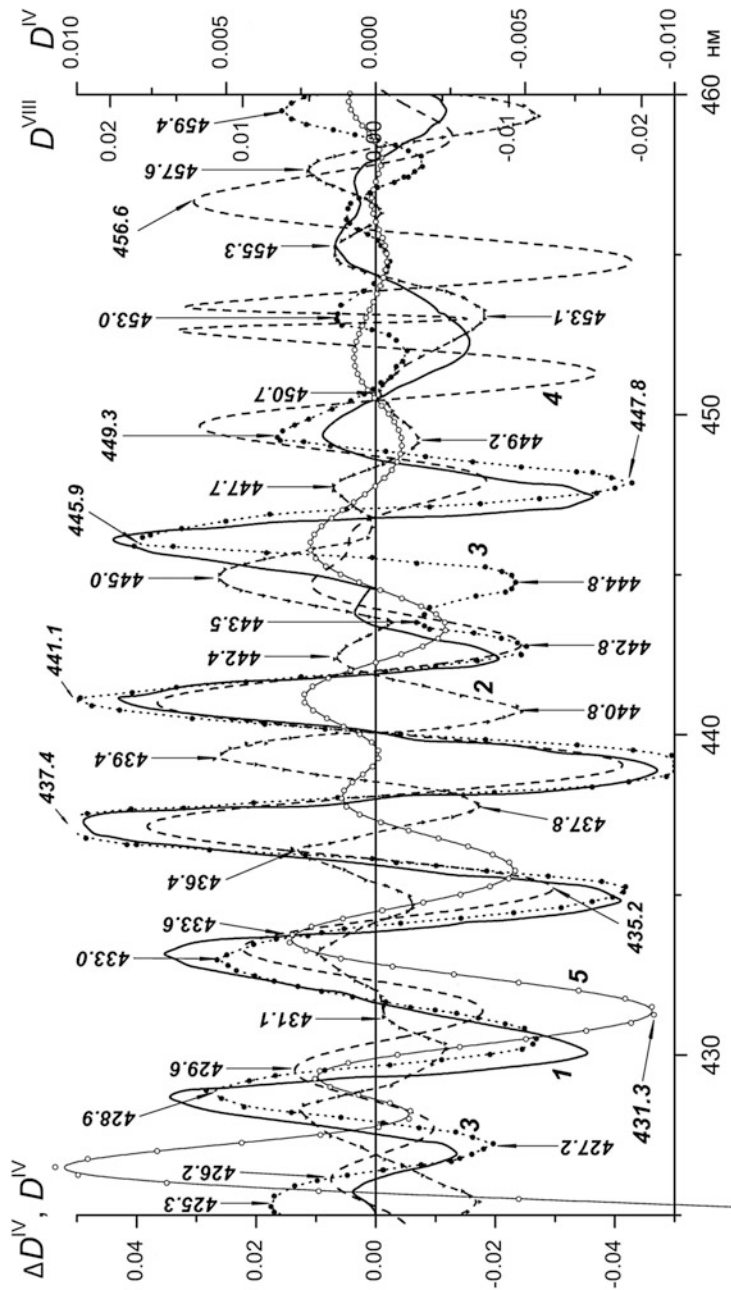


**Fig. 2.42** Derivative spectra of saponified and sixfold purified violaxanthin solution in carbon tetrachloride of the fourth (2), eighth (3), and twelfth (4) orders; 1 the absorption spectrum. *Ordinates*: OD in relative units; *abscissa*: wavelength in nanometers

maxima. At the registration of  $\lambda_{\max}^{D^{XVI}}$  (curve 4), the position of bands 414.7, 438.9–439.5, 445.4, 465.6, 482.2, and 489.9 nm is specified.

The spectra of Viol in  $\text{CCl}_4$  have bathochromic shift comparative to the spectra in acetone (Fig. 2.42, curves 1 and 2). Bands with  $\lambda_{\max}^{D^{IV}} = 401.0$ , 411.5, 425.6, 454.6, and 482.3 nm are found. The double-humped curve in the area 436.4–448.9 nm is characteristic for spectra  $D^{IV}$  of Viol in acetone (noted also in methanol and in ethanol and also for neoxanthin in these solvents) but is absent in  $D^{IV}$  spectra in carbon disulfide. The registration of  $D^{VIII}$  (curve 3) revealed the new harmonics of extrema with  $\lambda_{\max}^{D^{VIII}}$  at 399.0, 402.7, 411.4, 415.3, 419.7, 423.0, 426.1, 431.7, 436.3, 439.5, 443.5, 448.9, 452.6, 455.5, 462.0, 466.0, 468.5, 472.0, 474.8, 477.7, 480.8, 484.3, 487.9, 491.3, 494.6, 497.3, 500.6, and 504.9 nm. We omit the presentation of curves of derivative spectra of 10–14 and 18–22 orders from the illustrative field. For example, spectra of  $D^{XVI}$  differ from spectra  $D^{VIII}$  only by small changes in the curve contour 4 at 426.2–428.5 and 459.3 nm. The consideration of the second ten orders of derivative spectra in this spectral area for the set problems of research does not provide essential additional information. The experimenter can be confined to the eighth order of derivative spectra for sufficient accuracy. Thus, for the first time in the scientific literature, derivative spectra of high orders are described for Viol; their value for the analytical chemistry of carotenoids is shown; and the expediency of restricting the routine analysis to the registration of derivative ranges of the eighth order is proved.

The quantitative content of chlorophylls in the control and in the experiment after  $\gamma$ -irradiation of leaves does not significantly differ. Such a situation,



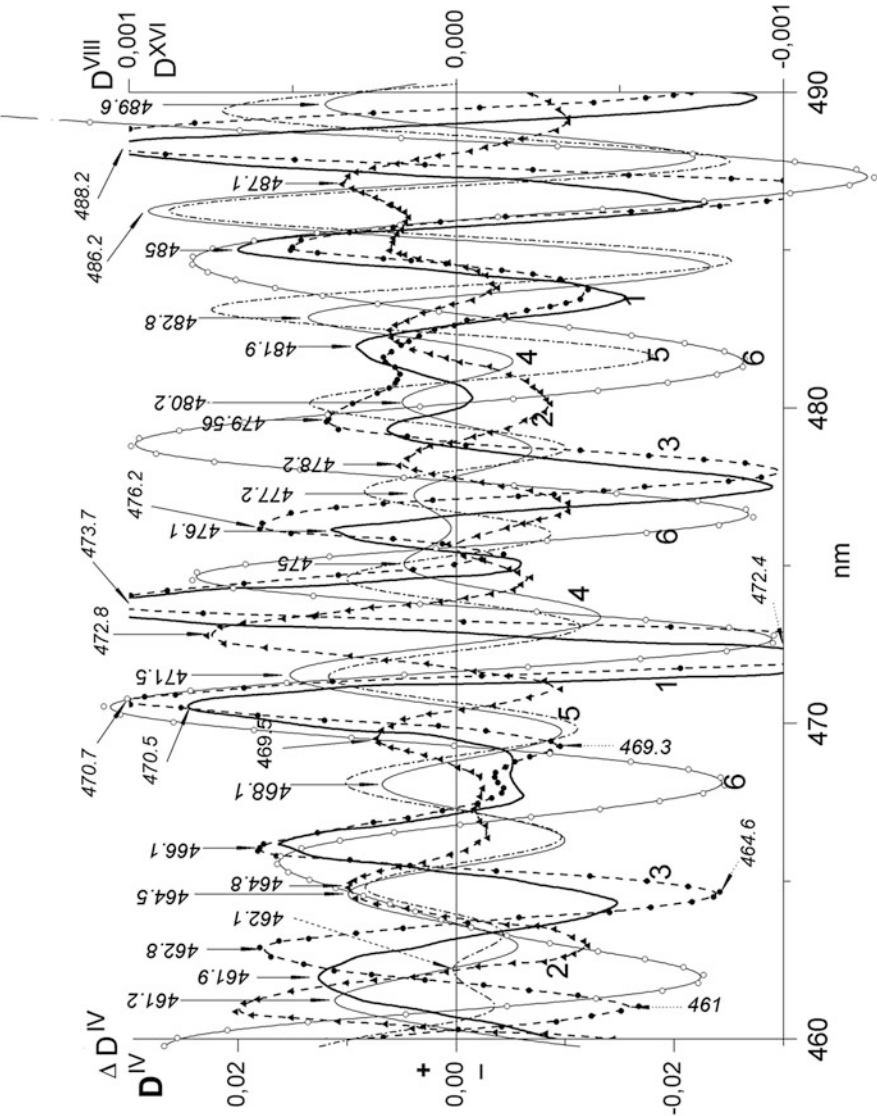


**Fig. 2.44** The influence of  $\gamma$ -radiation (8 kGy) on the structural change in the spectrum of a native leaf of *Phaseolus vulgaris* in the blue area (460–490 nm). Curves: 1 the fourth derivative of the absorption spectrum of a leaf (the control); 2 the influence of  $\gamma$ -radiation (the experiment); 3 the fourth derivative of the difference spectrum “control minus experiment”; 4 the eighth derivative of the spectrum of a native leaf of the *Hordeum* mutant lacking chlorophyll *b*, as described (Saakov 1971a, b; 1973; Saakov and Hoffmann 1974); 5  $D^{XVI}$  spectrum of the native leaf of *Hordeum* mutant treated with chloro carbonyl cyanide phenylhydrazine (CCCCP) as described (Saakov 1973); 6 the fourth derivative of the absorption spectrum of pheophytin solution within the spectral range from 460 to 490 nm

apparently, conceals changes in their *qualitative* state. In experiments with inhibitors, xanthophylls were the most labile pigments (Saakov 1993a–d). It is necessary to especially emphasize that in studies of control and  $\gamma$ -irradiated leaves by methods of registration of the first and the second derivatives of absorption spectra, the reliable differences in the run of spectral curves were not found.

A native leaf has a complex heterogeneous structure of components. In this regard, for the purpose of reliable determination of separate spectral bands that are not masked by the presence of chlorophyll *b* and can be considered as ChPC of the chlorophyll *a*, we have plotted the spectral curves of a leaf of a barley mutant lacking chlorophyll *b* (Figs. 2.43 and 2.44). To do this, we transferred the data on spectral curves  $D^{\text{II}}$  into numerical form by means of their digitalization and performed the necessary operations of differentiation.

We have designated the absorption maxima in derivative spectra of the fourth, the eighth, and further orders, as  $\lambda^{\text{DIV}}_{\text{max}}$ ,  $\lambda^{\text{DVIII}}_{\text{max}}$ , etc. Then the following areas of spectral bands substantially coincide for curves 1 and 4  $D^{\text{IV}}_{\text{max}}$  and  $\lambda^{\text{DVIII}}_{\text{max}}$  in Figs. 2.43 and 2.44: 428.9–429.6, 433.0–433.4, 437.1–437.4, 441.1, 449.3–449.7, 461.2–461.9, 470.5–471.5, 479.6–480.2, and 488.2–489.6 nm. With a certain level of confidence, it is possible to say that the above-listed bands of positive extrema are not caused by the contribution of absorption bands of chlorophyll *b*. It would be excessive to require the absolute coincidence of present data and the results of past years to fractions of nanometers (Saakov 1971a, b). However, it is possible to assume that the specified extrema  $\lambda^{\text{DIV}}_{\text{max}}$  or  $\lambda^{\text{DVIII}}_{\text{max}}$  can be attributed to the absorption of complexes of chlorophyll *a* and carotenoids (Figs. 2.42 and 2.43).

A similar comparison of absorption bands  $\lambda^{\text{DIV}}_{\text{max}}$  of pheophytin solutions (Figs. 2.43 and 2.44, respectively, curves 5 and 6) with  $\lambda^{\text{DIV}}_{\text{max}}$  of curve 1 (Figs. 2.43 and 2.44) reveals close areas of extrema, namely, 426.5, 429.3, 433.6, 438.0, 441.1, 445.9, 451.8, 456.7, 462.1, 465.6, 470.5, 474.7, 478.85, 484.6, and 490.1 nm. One should not expect the complete coincidence of extrema of bands of the considered curves 1, 5, and 6 because the arrangement of spectral bands of the solution is always hypsochromic, that is, they are shifted in the short-wave area relative to spectral bands of native complex structures.

In other words, absorption bands in solution are shifted towards the shorter wavelengths relative to the corresponding spectral bands in complex native structures.

Curve 2 in Figs. 2.43 and 2.44 shows the change in the  $D^{\text{IV}}$  absorption spectrum of a native leaf when it is processed with ionizing  $\gamma$ -radiation. The decrease in optical density (the hypochromic effect) is observed for the majority of registered bands, namely,  $\lambda^{\text{DIV}}_{\text{max}}$ : 425.5, 428.3, 433.2, 436.4, 446.5, 449.2, 453.1, 456.4, 459.3, 469.5, 472.8, 475.6, 477.0, 478.2, 480.1, 482.4, and 485.1–487.1 nm. Some spectral bands manifest hyperchromia coupled with the OD increase, namely,  $\lambda^{\text{DIV}}_{\text{max}}$ : 430.2, 431.1, 434.7, 437.8, 442.4, 444.95, 447.7, 450.7, 456.6, 457.6, 460.9, 464.8, and 467.3 nm. This gives the grounds to suppose that under the influence of  $\gamma$ -radiation, there is the formation of less-ordered structures than for the initial control. Taking into account that we deal with the native structure of

ChPC, we can suppose the formation of its less-ordered structure as a result of denaturation processes induced by the ionizing radiation and the transition of the protein part of ChPC to a new conformational, unfolded state.

The appearance of the hypsochromic shift of spectral bands in the short-wave part under the influence of ionizing radiation, and most EFEs, also indicates the formation of less-ordered ChPC forms. However, sometimes it is difficult to determine whether there was a shift coupled with conformational changes or the formation of new bands under the influence of a studied factor, for example,  $\lambda^{\text{DIV}}_{\text{max}}$ : 431.1, 439.4, 442.4, 447.7, 460.9, 464.8, 472.8, and 478.2 nm.

The run of the curve of the differential spectrum ( $\Delta D^{\text{IV}}$ ) “control minus experiment” (Figs. 2.43 and 2.44, curve 3) supports the above conclusions and demonstrates changes in the fine structure of the ChPC spectrum induced by the ionizing radiation more reliably and demonstrably. These changes concern the following extrema of the curve  $\Delta D^{\text{IV}}$ , namely,  $\lambda^{\text{DIV}}_{\text{max}}$ : 428.9, 433.0, 442.8, 443.5, 445.9, 449.3, 453.0, 459.0, 461.0, 462.8, 464.6, 466.1, 468.4, 470.7, 476.7, 479.6, 481.6, 485.0, and 488.2 nm, and also  $\lambda^{\text{DIV}}_{\text{min}}$ : 427.2, 430.5, 435.1, 439.0, 442.7, 444.8, 447.8, 452.0, 454.9, 457.9, 461.0, 464.6, 467.85, 469.3, 471.4, 475.4, 478.0, 483.8, 486.9, and 490.0 nm.

The listed distinctions between the experiment and the control in Figs. 2.43 and 2.44, with the necessary evidential value emphasize the real impact of the radiation on the structural change in the photosynthetic device. Separately, it is necessary to point to the need to take into account and to consider the basic rule of difference spectrophotometry, according to which the  $\Delta\lambda_{\text{max}}$  of difference spectra, as a rule, does not coincide with  $\lambda_{\text{max}}$  absorption spectra and with their orientation; the appearance of new maxima displaced with respect to initial ones is also probable (Figs. 2.43 and 2.44, curve 3).

However, to draw a conclusion about which elements of the ChPC (the chlorophyll or carotenoids) undergo the greatest damage under  $\gamma$ -irradiation, it is necessary to be careful.

Earlier, the lability of bands of a native spectrum of barley mutants under the influence of inhibitors of photosystems was shown in nanometer areas 428–430, 450, 469–471, and 500 nm (Saakov et al. 1971a, b; Saakov and Nazarova 1972; Saakov 1971a, b, c, 1973; Saakov and Hoffmann 1974), the change of which was explained by the structural damage of ChPC of chlorophyll *a* and carotenoids and also with the suppression of the de-epoxidation reaction of the xanthophyll cycle (Saakov 1971a, b, 1973; Saakov and Hoffmann 1974). The material shown in Fig. 2.43 emphasizes the damage to the ChPC structure in areas of the spectrum 429.6, 432–433, 437–440, and 444–450 nm. Proceeding from the comparison of native spectra of the barley mutant lacking chlorophyll *b*, of spectra of solutions of chlorophyll *a* and pheophytin *a* (Fig. 2.43, curve 4; Fig. 2.44, curve 6), it is possible with a certain degree of confidence to attribute the found changes to structural damage of the native complex of chlorophyll *a*. With sufficient probability, the reason for changes in the bands 428.0, 443.5, 445.9, and 455.0 nm is structural damage to the chlorophyll *b* complex. From the data in Fig. 2.44, a conclusion can be made about the highest lability of the following bands on curve 2: 462.9, 466.5,



468.1, 471.15, 472.8, 475.6, 478.0, 481.1, 483.1, 486.1, and 489.1 nm. The corresponding band shifts on the curve 3 are found in areas 464.6, 468.3, 469.0, 472.4, 475.3, 476.9, 480.6, and 483.7 nm. Taking into account the data of curves 4 and 5 from our previous works (Saakov and Nazarova 1972; Saakov 1973; Saakov and Hoffmann 1974) and presented in the form of derivative spectra of higher orders than earlier, and also the data in Fig. 2.42, it seems possible that the above-specified bands on curves 2 and 3 in Fig. 2.44 belong to the xanthophyll system.

Earlier, we proved the high lability of Viol under the influence of inhibitors of photosystems and herbicides (Saakov 1971a, b, 1973, 2000a–e). The comparison of curves 4 and 5 in Fig. 2.44 reveals hypochromic effects in the courses of curves of native spectra of a barley leaf after the influence of the uncoupler of photophosphorylation CCCP in a range of wavelengths: 461.0, 463.4, 464.8, 469.8, 471.8, 476.0, 477.3, 478.7, 481.7, 486.25, and 487.8 nm. On the contrary, the hyperchromic effect appears in a number of bands: 462.1, 468.15, 474.6, 480.1, 483.1, and 489.4 nm. In bands 474.5, 482.8, and 489.4 nm, the hypsochromic shift caused by the simplification of polymery of structures is noted, and the bathochromic shift is observed in the band 477.3 nm.

Thus, having confirmed at a qualitatively different level the data of the past years, we can attribute the changes in curves 2 and 3 in Fig. 2.44 to damage to the structures of the pigment complex interrelated to the activity of the xanthophyll cycle (Saakov 1971a, b, 2000a–e).

Summing up the material of this chapter, we can draw the following conclusions. For the first time in a native green leaf, the localization of the damaging influence of  $\gamma$ -radiation in the fine structure of the chlorophyll–protein complex is shown. The influence, first of all, concerns the damage to chlorophyll *a* and links of the xanthophyll cycle. Presumably, there is damage to the structure of pheophytin. More detailed proof of this statement is the subject of a separate investigation. As a result of found changes induced by ionizing radiation in the spectral curves of a native leaf, the conclusion about the disorder of stationary transitions of the step-like pathway of light energy and damage to the activity of the photosynthetic ETC follows. The damage to the fine structure of the photosynthetic device takes place later than the change in the functional activity of phototrophy, as determined with the help of the PAMF method described in the previous sections of this chapter. The derivative spectra of high orders for violaxanthin are presented here for the first time and will undoubtedly be interesting during the performance of analytical works on the chemistry and biochemistry of xanthophylls when studying their physiological activity. The presented materials can serve as a reliable diagnostic tool for the assessment of the state of vegetation in the zone of technogenic accidents both on the ground and during the global positioning satellite survey.

The material of this chapter has brought to the attention of the reader the complex biophysical approach to research on the early changes in membrane

structures in the whole functionally active live organisms. From this point of view, it is reasonable to apply two methods for the analysis of two different orientations, functional and structural diagnostics, which allow the intravital registration (on live organisms or objects) of the structural state of biomembranes and their supermolecular complexes. There is the unique possibility to obtain information on the state of chloroplast energetic structures connected with the conversion of light energy to the energy of chemical bonds and evolution of molecular oxygen.

The methodological approaches presented in this chapter can help solve practical problems, for example, those posed by the accident at the nuclear power station in Fukushima. Experts have now found substantial radiation pollution with cesium of vegetation, mushrooms (*Lactarius volemus*), and wheat over a distance of 70–80 km from station. According to the Japanese Ministry of Public Health Services, Work and Social Protection, tea plantations in the provinces Tiba and Saitama and sea plankton are polluted with radioactive cesium. To the north and northwest of the Fukushima station, the crops are polluted with strontium-89. Taking into account the strict territorial limits of Japan, the rational localization of farmland will play a large role. The station continues to pollute coastal waters because of leaking of infected water from accumulation tanks of the station (in 2013, 300 L with radioactivity of 80 million Bq/L; at the beginning of 2014, blowouts of radioactive water with radioactivity of 2.7 million Bq/L were registered). The intravital diagnostics of the state of survival rate of plants and seaweed as a result of the radiation aftereffect can be a defining factor.

The experimental material presented in this section and the analysis of literature on the application of the PAM method allow us to be skeptical about the existing theories, hypotheses, points of view, and, unfortunately, ignorant speculations concerning endocellular mechanisms of *Procaryota* and *Eucaryota* cell resistance to the influence of EFEs of the anthropogenous or natural origin.

In the middle of the twentieth century, one of the first scientists to perform research on this subject at a competent level for that time was P.A. Henckel and coworkers (Henckel 1954). Researches of opposite type existed too (Udovenko 1976).

A review of the state of the problem of studying the resistance of chloroplast membranes with methods of molecular spectroscopy was published by one of authors of this book around the same time (Saakov 1976).

A serious contribution to the formation of biophysical approaches and methods of diagnostics of the vegetative cell state was made by American researchers (Strehler and Arnold 1951). Their studies were developed by the very careful work of B.N. Tarusov, chair of biophysics of Moscow University (Kochetov and Tarusov 1975, 1977; Perelygin and Tarusov 1966; Popov and Tarusov 1964; Tarusov 1966; Tarusov et al. 1962; Dzhanumov et al. 1970; Doskoch et al. 1971; Zakarian and Tarusov 1966). The achievements of the department and its most active scientists are



consolidated in several editions of the textbook *Biophysics* edited by the corresponding member of the Russian Academy of Sciences, A.B. Rubin (2004).

Thus, in discussing the material in this chapter, the authors have tried to underline the high importance of the problem for Russia and its rather superficial and one-sided level of study.

The authors have not mentioned questions of ecological terrorism, the urgency of which has increased in the last decade. However, we consider that this area and subjects are so wide and many-sided in their ecological, political, and economic aspects that it is better to leave them beyond the scope of this book.

We have brought to the attention of the reader our experimental works, their theoretical interpretation, and also the collection of information from European publications leading in the application of the pulse-amplitude modulated fluorescence method.

It is regrettable to acknowledge, but the amplitude and productivity of the use of this method in Europe, and its achieved successes, got the better of Russian science. Attempts by the Saint Petersburg Electrical and Technical University (LETI) to create a Russian device were successful (Saakov et al. 2010). However, an obstruction to its wide introduction in the practice of scientific laboratories was the absence of Russian optic fibers. Costs associated with creation of the device got stuck on the impossibility of buying optic fibers in Europe.

Nevertheless, the method received recognition in Russia, and, with the help of equipment bought in Europe, experiments are now being carried out.

In cells of plants and animals there are two great energetic systems supplying live cells with ATP, NADPH, and NAD. One of these energetic systems is located in chloroplasts and transforms light energy to the energy of chemical bonds; the second system is placed in mitochondria.

With the enough large amount of factual material presented in this chapter we show the role of stability of the electron transport chain (ETC) in chloroplasts and so the role of life activity of a green cells occurs in dependence of functional activity of ETC at transformation of light energy and ATP formation.

The second energetic mechanism is located in cellular mitochondria. This mechanism determines cell survival by producing energy via another system, namely oxidative phosphorylation. By analogy to the activity of photosynthetic ETC in chloroplasts, mitochondrial energetic processes are responsible for cell resistance (including animal cells).

An additional argument in favor of the statements above is the known lethal action of KCN (an inhibitor of oxidative phosphorylation) on the human body and green cells.

Up to the point that factors of extreme intensity suppress the coupled or separate activity of these two energetic systems of a plant cell, it is possible to speak about the repair reactions of an organism.

The present chapter was written to substantiate a thesis about the primacy of energetic stability. The presented material proves that without competent and purposeful selection of plants using the principle of stability of their energetic

systems, all trivial selection turns into long-term shamanism of a different orientation, because it is directed towards a search for casually obtained objects.

Some plant breeders do not analyze the biochemical essence of the main reactions of an organism and blindly waste time on obtaining stable grades. All this is a consequence of aimless chaotic selection of material and absence of real collaborative work with biochemists.

On the other hand, the poverty and weakness of the biochemical base in some selection centers does not promote such collaboration. Besides the steady and competent management of inter-disciplinary collaboration is necessary. Otherwise, good intentions are discussed but not realized.

## References

- Allakhverdiev SI, Nishiyama Y, Suzuki I, Murata N (1999) Genetic engineering of the unsaturation of fatty acids in membrane lipids alters the tolerance of *Synechocystis* to salt stress. *Proc Natl Acad Sci U S A* 96(10):5862–5867
- Aoki K, Ideguchi T, Yamashita J, Horio T (1986) Effects of NaCl and glycerol on photosynthetic oxygen-evolving activity with thylakoid membranes from halophilic green alga *Dunaliella tertiolecta*. *J Biochem* 100(5):1223–1230
- Armond PA, Schreiber U, Bjorkman O (1978) Photosynthetic acclimation to temperature in desert shrub *Larrea divaricata*. II. Light harvesting efficiency and electron transport. *Plant Physiol* 31:411–415
- Baltscheffsky M (1971) Energy transduction in respiration and photosynthesis. Adriatica, Bari, pp 639–648
- Baranov AA, Dorokhov BL, Saakov VS (1974) *Izv Akad Nauk Mold SSR Ser Biol Khim Nauk* (5):29–36
- Baranov AA, Saakov VS, Chunaev AA, Kvitko KV (1975) Reactions of chlorophyll formation and light protection in mutants of green algae studied by absorption spectrophotometry (in Russian). *Sov Physiol Rasteni* 22:702–711
- Bassi R, Machold O, Simpson D (1985) Chlorophyll-proteins of two photosystem I preparations from maize. *Carlsberg Res Commun* 50(3):145–162
- Berman HM, Westbrook J, Feng Z et al (2000) The Protein Data Bank. *Nucleic Acids Res* 28:235–242, [www.pdb.org](http://www.pdb.org)
- Bilger W, Bjorkman O (1980) Role of the xanthophylls cycle in photoprotection elucidated by measurements of light-induced absorbance changes, fluorescence and photosynthesis in leaves of *Hedera canariensis*. *Annu Rev Plant Physiol* 31:491–543
- Bilger W, Bjorkman O (1990) Role of the xanthophyll cycle in photoprotection elucidated by measurements of light induced absorbance changes of fluorescence and photosynthesis in leaves of *Hedera canariensis*. *Photosynth Res* 25:173–185
- Bilger W, Bjorkman O, Thayer SS (1989) Light-induced spectral absorbance changes in relation to photosynthesis and the epoxidation state of xanthophylls cycle components in cotton leaves. *Plant Physiol* 91:542–551
- Bilger W, Heber U, Schreiber U (1988) Kinetic relationship between energy-dependent fluorescence quenching, light scattering, chlorophyll luminescence and proton pumping in intact leaves. *Zt Naturforsch* 43c:877–887
- Bilger W, Johnsen T, Schreiber U (2001) UV-excited chlorophyll fluorescence as a tool for the assessment of UV-protection by the epidermis of plants. *Plants under stress Special issue. J Exp Bot* 52:2007–2014

- Bolhar-Nordenkampf HR (1997) Rapid light curves. A new method to determine light stress in the field. In: Stress of life congress, 1–5 July 1997, Budapest, Hungary, Abstract N D 4-5, p 117
- Bolhar-Nordenkampf HR, Long SP, Öquist C et al (1989) Chlorophyll fluorescence as a probe of the photosynthetic competence of leaves in the field. A review of current instrumentation. *Funct Ecol* 3:497–514
- Bradbury M, Baker NR (1981) Analysis of the slow phases of the in vivo chlorophyll fluorescence induction curve. Changes in redox state of photosystem II electron acceptors and fluorescence emission from photosystem I and II. *Biochim Biophys Acta* 635:542–551, Куда пропала эта ссылка
- Briantais JM, Vernotte C, Krause GH, Weis E (1986) Chlorophyll *a* fluorescence of higher plants: chloroplasts and leaves. In: Govindjee, Ames J, Fork D (eds) *Light emission by plant and bacteria*. Academic, Orlando, pp 539–583
- Bukhov NG, Heber U, Shuvalov VA (2001a) Energy dissipation in photosynthesis: quenching of chlorophyll fluorescence in reaction centers and antenna complexes. *Planta* 212:749–758
- Bukhov NG, Heber U, Shuvalov VA, Carpentier R (2001b) Non-photochemical dissipation of excited states in photosystems 1 and 2 in chloroplasts: mechanisms of protection from photoinhibition. *Vestnik (Herald)* 2:17–19
- Bungard RA, Ruban AV, Hibberd JM et al (1999) Unusual carotenoid composition and a new type of xanthophyll cycle in plants. *Proc Natl Acad Sci U S A* 97:1135–1139
- Cantor ChR, Schimmel PR (1980) *Biophysical chemistry. Part II: Techniques for the study of biological structure and function*. Freeman, San Francisco
- Chauhan VS, Singh V, Singh S, Bisen PS (2001) Regulation of sodium influx in the NaCl-resistant (NaCl(r)) mutant strain of the cyanobacterium *Anabaena variabilis*. *Curr Microbiol* 42:100–105
- Chen R, Edelhock F (eds) (1976) *Biochemical fluorescence concepts*. Dekker, New York
- Danilova IG, Shevelev IV, Isaev-Ivanov VV et al (2005) Molecular bases of regulation of the enzymatic activity of bovine pancreatic deoxyribonuclease I as determined by laser correlation and fluorescence spectroscopy. *Biophysics (Biofizika translated into English from Russian)* 50(1):43–55
- Demming-Adams B (1990) Carotenoids and photoprotection of plants: a role for xanthophylls zeaxanthin. *Biochim Biophys Acta* 1020:1–24
- Demming-Adams B, Adams WW III (1990) The carotenoid zeaxanthin and “high-energy state quenching” of chlorophyll fluorescence. *Photosynth Res* 25:187–197
- Demming-Adams B, Adams WW (1992) Photoprotection and other responses of plants to high light stress. *Annu Rev Plant Physiol Plant Mol Biol* 43:599–626
- Demming-Adams B, Adams WW (1996) The role of xanthophylls cycle carotenoids in the protection of photosynthesis. *Trends Plant Sci* 1:21–26
- Demming-Adams B, Adams WW III, Heber U et al (1990) Inhibition of zeaxanthin formation and of rapid changes in radiationless energy dissipation by dithiothreitol in spinach leaves and chloroplasts. *Plant Physiol* 92:293–301
- Demming-Adams B, Winter K, Czygan FC et al (1989) Photosynthetic characteristics and the ratios of chlorophyll,  $\beta$ -carotene, and the components of xanthophylls cycle upon a sudden increase in growth light regime in several plant species. *Bot Acta* 102:319–325
- Demming-Adams B, Winter K, Krüger A, Czygan FC (1987) Photoinhibition and zeaxanthin formation in intact leaves. *Plant Physiol* 84:218–244
- Dietz KJ, Schreiber U, Heber U (1985) The relationship between the redox state of  $Q_A$  and photosynthesis in leaves at various carbon-dioxide, oxygen and light regimes. *Planta* 166:219–226
- Diner B (1974) Cooperativity between photosystem II centers at the level of primary electron transfer. *Biochim Biophys Acta* 368(3):371–385
- Dobretsov GE (1987) The study of interaction of biologically active compounds with membranes by the method of fluorescent probes. In: Sviderskii VL, Leont'ev VG, Saakov VS (eds) *Spectroscopic methods of research in physiology and biochemistry. Collection of research papers*. Nauka, Leningrad, pp 3–12 (in Russian)
- Doskoch JaE, Parkhomenko, Tarusov BN (1971) Spontaneous and induced chemiluminescence of spores of thermophilic microorganisms in relation to their thermal stability. *Mikrobiologia* 40:849–857

- Dzhanumov DA, Veselovskii VA, Tarusov BN, Marenkov VS, Pogosyan SJ (1970) Temperature resistance of plants studied by methods of spontaneous and photoinduced chemiluminescence. *Sov Physiol Rastanii* 18:588–593
- Egorova EA, Bukhov NG, Krendeleva TE, Rubin AB, Wiese K, Heber U (2001) Ways of the electron transfer from the photosystem 1 to the photosystem 2 in intact leaves. *Vestnik Bashkir Univ* 2:35–37
- Fork DC, Hiyama T (1973) The photochemical reactions of photosynthesis in an alga exposed to extreme conditions. *Carnegie Inst Wash YBK* 72:384–388
- Fork DC, Mohaty P, Hoshina S (1985) The detection of early events in heat disruption of thylakoid membranes by delayed light emission. *Physiol Veget* 23:511–521
- Foyer CH, Dujardin M, Lemoine EY (1990b) Turnover of the xanthophylls cycle during photoinhibition and recovery. In: Baltscheffsky M (ed) *Current research in photosynthesis*, vol 2. Kluwer, Dordrecht, pp 491–494
- Foyer CH, Furbank R, Harbinson J, Horton P (1990a) The mechanisms contributing to photosynthetic control of electron transport by carbon assimilation in leaves. *Photosynth Res* 25:83–100
- Genty B, Briantais JM, Baker NR (1989) The relationship between the quantum yield of photosynthetic electron transport and quenching of chlorophyll fluorescence. *Biochim Biophys Acta* 990:87–92
- Goncharova NV, Sheverdov VV (1993) III S'ezd Vseros. Ob–va fiziolog. Rastanii (III Congress of the All-Russia 128 Saakov V.S Society of Plant Physiologists), vol 8, St. Petersburg, p 788
- Gonzalez FJ, Moreno MO (1983) Report of Junta de energia nuclear. Madrid, 30p
- Gounaris K, Brain APR, Quinn PJ, Williams WP (1983) Structural and functional changes associated with heat-induced phase-separations of non-bilayer lipids in chloroplast thylakoid membranes. *FEBS Lett* 153:47–52
- Green BR, Durnford DG (1996) The chlorophyll-carotenoid proteins of oxygenic photosynthesis. *Annu Rev Plant Physiol Plant Mol Biol* 47:685–714
- Guex N, Peitsch MC (1997) Swiss-Model and the Swiss-PdbViewer: an environment for comparative protein modeling. *Electrophoresis* 18:2714–2723, <http://www.expasy.org/spdbv/>
- Havaux M (1988) Effects of temperature on the transitions between state-1 and state-2 intact maize leaves. *Plant Physiol Biochem* 26:245–251
- Havaux M, Devaud A (1994) Photoinhibition of photosynthesis in chilled potato leaves is not correlated with a loss of photosystem II activity – preferential inactivation of photosystem I. *Photosynth Res* 40:75–92
- Heber U, Bukhov NG, Shuvalov VA, Kobayashi Y, Lange OL (2001) Protection of the photosynthetic apparatus against damage by excessive illumination in homoiohydric leaves and poikilohydric mosses and lichens. *J Exp Bot* 52(363):1999–2006
- Heber U, Santarius KA (1973) Cell death by cold and heat and resistance to extreme temperatures. Mechanisms of hardening and dehardening. In: Precht H, Christophersen J, Hensel H, Larcher W (eds) *Temperature and life*. Springer, Berlin, pp 232–263
- Henckel PA (1954) Sur la résistance des plantes à la sécheresse et les moyens de la diagnostiquer et de l'augmenter. In: *Essais de botanique*. V 2. Editions de l'Académie des sci. de L'URSS, Moscow-Leningrad, pp 436–453
- Hoshida H, Tanaka Y, Hibino T et al (2000) *Plant Mol Biol* 43(1):103–111
- Ignacimuthu S, Babu CR (1989) Improving productivity promoting traits in wild and cultivated urd and mung beans. *J Nucl Agr Biol* 18:6–12
- Isaev-Ivanov VV, Kozlov MG, Baitin DM et al (2000) Fluorescence and excitation *Escherichia coli* RecA protein spectra analyzed separately for tyrosine and tryptophan residues. *Arch Biochem Biophys* 376:124–140
- Ivanova SV, Kirpichenok LN (2008) Application of fluorescence methods in medicine. *Med News* 12:56–61 (in Russian)
- Jajoo A, Bharti S, Govindjee (1998) Inorganic anions induce state changes in spinach thylakoid membranes. *FEBS Lett* 434:193–196
- James WO (1953) *Plant respiration*. Clarendon, Oxford, 439p.

- Junowicz E, Spencer JH (1973) Studies on bovine pancreatic deoxyribonuclease A. II The effect of different bivalent metals on the specificity of degradation of DNA. *Biochim Biophys Acta* 312:72–84
- Klimov VV, Krasnovskii AA (1981) Pheophytin as a primary electron acceptor in photosystem II reaction center. *Photosynthetica* 15:592–609
- Klimov VA, Krasnovsky AA (1977) Reduction of pheophytin in the primary light reaction of photosystem II. *FEBS Lett* 82:183–186
- Kochetov YuB, Tarusov BN (1975) The effect of heavy metal salts on the ultraweak chemiluminescence of aquatic plants leaves. *Biophysics (Biofizika)* 20:537–539
- Kochetov Yu, Tarusov BN (1977) Chemiluminescence of plant tissue preserved in aldehydes and exposed to the salt of heavy metals. *Biophysics (Biofizika)* 22:872–875
- Krause GH (1988) Photoinhibition of photosynthesis. An evaluation of damaging and protective mechanisms. *Physiol Plant* 74:566–574
- Krause GH, Somersalo S (1989) Fluorescence as a tool in photosynthesis research: application in studies of photoinhibition? Cold acclimation and freezing stress. *Philos Trans R Soc Lond B* 323:281–293
- Krause GH, Weis E (1984) Chlorophyll fluorescence as a tool in plant physiology. II Interpretation of fluorescence signals. *Photosynth Res* 5:139–157
- Krause GH, Weis E (1991) Chlorophyll fluorescence and photosynthesis: the basics. *Annu Rev Plant Physiol Plant Mol Biol* 43:313–349
- Kreps EM (1976) About the morpho-physiological and biochemical evolutions. *Zh Evol Biokhim Fiziol* 12(6):493–502
- Lahm A, Suck D (1991) DNase I-induced DNA conformation. 2 A structure of a DNase I-octamer complex. *J Mol Biol* 222:645–667
- Lakowicz JR (ed) (1983) *Principles of fluorescence spectroscopy*. Springer, London
- Lang M (1994) Blue, green and red fluorescence signatures and images of tobacco leaves. *Bot Acta* 107:230–236
- Lichtenthaler HK (ed) (1988a) *Application of chlorophyll fluorescence*. Kluwer, Dordrecht, 356 p
- Lichtenthaler HK (1988b) In vivo chlorophyll fluorescence. In: Lichtenthaler HK (ed) *Application of chlorophyll fluorescence*. Kluwer, Dordrecht, P. 129–142
- Lichtenthaler HK (ed) (1996a) *Vegetation stress*. Fischer, Stuttgart, 656p
- Lichtenthaler HK (1996b) Vegetation stress: an introduction to the stress concept in plant. *J Plant Physiol* 148:4–14
- Lichtenthaler HK (2000) *Discoveries in plant biology*, vol 3. World Scientific, Singapore, pp 141–161
- Lichtenthaler HK, Rinderle UR (1988) The role of chlorophyll fluorescence in the detection of stress conditions in plants. *CRC Crit Rev Anal Chem* 19(Suppl 1):S29–S85
- Malkin S, Siederer Y (1977) Delayed luminescence. In: Barber J (ed) *Primary process of photosynthesis*. Elsevier, Amsterdam, pp 349–432
- McSwain BD, Tsujimoto HY, Arnon DI (1976) Effects of magnesium and chloride ions on light-induced electron transport in membrane fragments from a blue-green alga. *Biochim Biophys Acta* 423(2):313–322
- Mohammed GH, Binder WD, Gilles SL (1996) Chlorophyll fluorescence: a review of its practical forestry applications and instrumentation. *Scand J Forest Res* 10:383–410
- Monson RK, Stihm MA, Williams GJ et al (1982) Temperature dependence of photosynthesis in *Agropyron-smithii* Rydb 1 Factors affecting net CO<sub>2</sub> uptake in intact leaves and contribution from ribulose-1,5-bisphosphate carboxylase measured in vivo and in vitro. *Plant Physiol* 69:921–928
- Nytek Instruments (2004) *Fluorofory u fluorestsentnye zondy (Fluorophores and fluorescent probes)*. <http://www.nytek.ru> (In Russian)
- Oefner C, Suck D (1986) Crystallographic refinement and structure of DNase I at 2 Å resolution. *J Mol Biol* 192:605–632

- Oshima RG, Price PAJ (1974) Effect of sulfate on the activity and the kinetics of deoxyribonucleic acid degradation by porcine spleen deoxyribonuclease. *Biol Chem* 249:4435–4438
- Perelygin VV, Tarusov BN (1966) Flash ultra weak radiation during damage of living tissue. *Biophysika* 11:539–541
- Peterman EJ, Cradinaru CC, Calkoen F et al (1997) Xanthophylls in light-harvesting complex II of higher plants: light harvesting and triplet quenching. *Biochemistry* 36:12208–12215
- Popov GA, Tarusov BN (1964) Kinetics of chemi-luminescence during decomposition of hydrogen peroxide with water-salt animal liver extracts. *Biofizika* 9:528–529
- Richter M, Gross R, Böthn B, Wild A (1994) Zeaxanthin dependent and zeaxanthin independent changes in nonphotochemical energy dissipation. *J Plant Physiol* 143:495–499
- Rinderle U, Haitz M, Lichtenthaler HK, Kähny DH, Shi Z, Wiesbeck W (1988) Correlation of radar reflectivity and chlorophyll fluorescence of forest trees. In: Remote sensing: moving towards the 21st century: 1988 International geoscience and remote sensing symposium: IGARSS'88, vol 3, 12–16 September, Edinburgh, pp 1343–1346. doi:[10.1109/IGARSS.1988.569462](https://doi.org/10.1109/IGARSS.1988.569462)
- Rozengart EV, Saakov VS (2002) The chelating ability of the anti-coccidial drug 1,3-bis (p-chlorbensilidenoamino)guanidine: the Complexes with Ca<sup>2+</sup> and La<sup>3+</sup>. *Dokl Biochem Biophys* 385:219–223, Translated from Russian *Dokl RAN* 385:699–703
- Rubin AB (1987) *Biophysika*. Volume 1: Theoretical biophysics, 319p; Volume 2: Biophysics of cellular processes, 302p. Publishing House Higher School, Moscow
- Rubin AB (1997) Primary processes of photosynthesis. *Soros Educ Mag* 10:79–84
- Rubin AB (2000a) Biophysical methods in ecological monitoring. *Soros Educ Mag* 6:1–9
- Rubin AB (2000b) *Biophysics*, 2nd edn. Volume 1: Theoretical biophysics, 448p (1999–2000), volume 2: Biophysics of cellular processes, 467p (2000). Publishing House of Moscow University, Moscow
- Rubin AB (2004) *Biophysics*, 3rd edn. Volume 1: Theoretical biophysics, 462p (2004), volume 2: Biophysics of cellular processes, 469p (2004). Publishing House of Moscow University, Moscow
- Saakov VS (1959) The comparative characteristic of gasometric and radiometric methods of estimation of photosynthesis intensity. *Vestn Leningrad Univ Ser 4* 21(4):42–50
- Saakov VS (1960) Some questions of the methodology of manometric determination of photosynthesis of terrestrial plants leaves (in Russian). *Vest Leningrad Univ Ser 4* 4(21):33–41
- Saakov VS (1961) Einige methodische Probleme der manometrischen Bestimmung der Photosynthese an Blättern von Landpflanzen. *Sowjetwiss Naturwissenschaftl Beitrage* 9:53–962, Translated from Russian into German from *Vestn Len Univ, Ser Biol*, 1960, (21): 33–41
- Saakov VS (1963) To mechanism of the light reaction of xanthophylls in chloroplasts suspension (in Russian). *Bot Zhurn* 48:888–891
- Saakov VS (1965) On the possible role of xanthophylls in oxygen transfer during photosynthesis. *Sov Plant Physiol* 12:377–385
- Saakov N (1971) Reactions of pigment system of *Euglena* under conditions of artificially created heterotrophism. *Dokl Akad Nauk USSR* 204:744–747
- Saakov VS (1971a) Relation between xanthophylls deepoxidation reaction and electron transport chain of photosynthesis (in Russian). *Dokl Akad Nauk SSSR* 201:1257–1260
- Saakov VS (1971b) Correlation between light-induced xanthophyll conversions and electron transport chain of photosynthesis (in Russian). *Sov Physiol Rastenii* 18:1088–1097
- Saakov VS (1972) [Reactions of the pigment system of *Euglena* under conditions of artificially created heterotrophism]. *Dokl Akad Nauk SSSR* 204:744–747
- Saakov VS (1973) Die durch Hemmstoffe induzierten Umwandlungen der Karotinoidpigmente in Pflanzenzellen Der Einfluss einiger Inhibitoren auf den Chlorophyllgehalt in grünen Zellen. *Biochem Physiol Pflanzen* 164:199–227
- Saakov VS (1976) Research of damaging influences localization centers in chloroplast membranes with methods of molecular spectroscopy (in Russian). *Trudy Prikl Bot Genet Selektsii L VIR* 57:17–34

- Saakov VS (1987) Spectrophotometrical methods in study of reactions of plant plastid apparatus under extremal influences (in Russian). In: Svidersky VL, Saakov VS (eds) Spectrophotometrical research methods in physiology and biochemistry. Nauka, Leningrad, pp 115–126
- Saakov VS (1990) Die Anwendung der Lumineszenz, der Ableitungen der Spektrophotometrie und der photoakustischen Spektroskopie zur Charakterisierung von Schaden in Chlorophyll-Protein Komplex der Chloroplasten. Colloq Pflanzenphysiol d Humboldt-Universitaet zu Berlin 14:163–170
- Saakov VS (1992) Die Anwendung der Lumineszenz, der Ableitungen der Spektrophotometrie und der photoakustischen Spektroskopie zur Charakterisierung von Schaden in Chlorophyll-Protein-Komplex der Chloroplasten. Colloq Pflanzenphysiol der Humboldt Universitaet (HU) zu Berlin 14:163–170
- Saakov VS (1993a) The effect of gamma-radiation on the stability of energetics and pigment system of the photosynthetic apparatus. (in Russian). Dokl Akad Nauk 328:520–523
- Saakov VS (1993b) The inhibition of kinetics of light deepoxidation of violaxanthin and the activity of xanthophyll cycle under the influence of gamma-radiation (in Russian). Dokl Akad Nauk 329:96–99
- Saakov VS (1993c) The alteration of phenylalanine optical-spectra under its radiational chemical conversions (in Russian). Dokl Akad Nauk 333:661–665
- Saakov VS (1993d) The influence of gamma-radiation on the kinetic of changes in violaxanthin content and on the xanthophyll cycle. Photosynthetica 28:439–445
- Saakov VS (1994) Peculiarities of the optical-spectra changes of tyrosine under its radiolysis. (in Russian). Dokl Akad Nauk 334:517–521
- Saakov VS (1996) Application of the PAM-method for estimating the damage of photosynthetic apparatus of chloroplasts during gamma-irradiation. In: Abstracts of international conference on spectroscopy and optical techniques in animal and plant biology, Münster Universität, BRD, Sept 30–Okt 3, p 96
- Saakov VS (1998a) Some mechanisms of adaptation to stress in plant and animal cells. Doklady Biol Sci 361:371–375, Translated from Doklady Akad Nauk 361:568–572
- Saakov VS (1998b) Specific changes of modulated fluorescence F<sub>0</sub> and F<sub>m</sub> under dithiothreitol influence on zeaxanthin content (in Russian). Dokl Akad Nauk 361:830–833
- Saakov VS (2000a) Characteristics of structural stability of the photosystem II light-harvesting complex exposed to gamma-radiation. Dokl Biochem Biophys 373:123–128, Translated from Doklady Akad Nauk 373:112–116
- Saakov VS (2000b) Changes of gamma-globulin optical spectra and possible mechanisms of its physiological action in organism under gamma-irradiation (in Russian). Dokl Akad Nauk 370:562–567
- Saakov VS (2000c) Energetics of green cell stress resistance: a concept. Dokl Biol Sci 375:613–620, Translated from Doklady Akademii Nauk 375:278–285
- Saakov VS (2000d) A coupling between albumin high orders derivative spectra changes and the precision of detection of albumin globulin coefficient under gamma-irradiation shock (in Russian). Dokl Akad Nauk 371:548–552
- Saakov VS (2000e) To evolution of hypothesis on location of damage influences of environmental factors in green leaf: the after-effect of gamma-irradiation on energetic of chloroplasts (in Russian). Dokl Akad Nauk 371:280–285
- Saakov VS (2001a) New aspects of the concept of energy mechanisms determining stability of prokaryotic and eukaryotic green cells Effects of negative temperature on kinetic parameters of modulated pulse fluorescence (F<sub>0</sub>, F<sub>max</sub>, and F<sub>v</sub>). Dokl Biochem Biophys 381:378–383, Translated from Doklady Akad Nauk 381:126–131
- Saakov VS (2001b) Materials to justification of energetic bases of the theory of tolerance of the photosynthetic apparatus of Prokaryota and Eucaryota cells (in Russian). Vestn Bashkir Univ PH Bashkir Univ Ufa specific issue 2(v1):73–76
- Saakov VS (2002a) High-temperature stress-related changes in the harmonics F<sub>0</sub>, F<sub>m</sub>, and F<sub>v</sub> of pulse-amplitude modulated fluorescence signals: locating thermal damage in reaction centers

- of photosystem II. Dokl Biochem Biophys 382:4–9, Translated from Doklady Akad Nauk 382:118–123
- Saakov VS (2002b) Effect of  $\text{Na}^+$ ,  $\text{Cl}^-$ , and  $\text{SO}_4^{2-}$  ions on changes in the kinetic parameters of modulated pulse fluorescence: the characteristics of the phototrophic function tolerance of photosystem 2 under the conditions of salinization. Dokl Biochim Biophys 385:228–234, Translated from Dokl Akad Nauk 2002, 385:823–829
- Saakov VS (2002c) Specific effects of gamma-radiation on the fine structure of the photosynthetic apparatus: evaluation of the character of disturbances in vivo using high-order derivative spectrophotometry. Dokl Biochem Biophys 387:313–319, Translated from Doklady Akad Nauk 387:265–271
- Saakov VS (2003a) Specific effects induced by gamma-radiation on the fine structure of the photosynthetic apparatus: evaluation of the pattern of changes in the high-order derivative spectra of a green leaf in vivo in the red spectral region. Dokl Biochem Biophys 388:22–28, Translated from Doklady. Akad. Nauk. 388:265–271
- Saakov VS (2003b) Association of the mechanisms of green cell resistance with changes in the parameters of modulated pulse fluorescence under the exposure to atmospheric drought: localization of damage in the link P680QA. Dokl Biochem Biophys 388:8–14, Translated from Doklady Akad. Nauk. 388:123–130
- Saakov VS (2004) The coupling of disturbance of an electron transport in link of a primary electron acceptor under the influence of low temperature. In: Materials of international symposium of plant physiologists “Problems of phytophysiology of a north”, Petrozavodsk, 23–29 Sept 2004, pp 157–158
- Saakov VS, Baranov AA (1987) Spektroskopicheskie metody issledovaniya v fiziologii i biokhimii (Spectroscopic methods in physiology and biochemistry) (in Russian). Nauka, Leningrad, pp 97–126
- Saakov VS, Baranov AA, Hoffmann P (1978) Pigmentphysiologischen Untersuchungen mit Hilfe der Derivat-Spektrophotometrie. Studia Biophys 70:129–142
- Saakov VS, Barashkova EA (1999) To development of a hypothesis about localization of extreme factors damaging influences of an environmental affairs in chloroplast. In: Materials of 4th congress of All Union Society of Plant Physiologists, Moscow, 4–9 Oct 1999
- Saakov VS, Barashkova EA, Kozhushko NN et al (1975) The centres of localization of harmful influences of extreme factors in chloroplasts. In: Abstr of XII Intern Botan Congr Leningrad II, p 477
- Saakov VS, Barashkova EA, Rutman GI, Boyarshinova GA et al (1976) The centers of localization of damaging influences in plants chloroplasts. In: Materials of All Union meeting “Biochemical aspects of plants resistance to adverse factors of an environmental affairs”, Irkutsk, 20–26 Sept 1976, pp 93–95
- Saakov VS, Drapkin VZ, Krivchenko AI, Rozengart EV, Bogachev TV, Knyazev MN (2013) Derivative spectrophotometry and electron-spin resonance spectroscopy for ecological and biological questions. Springer, Heidelberg, 357p
- Saakov VS, Hoffmann P (1974) Zur Bedeutung der Karotinoide fuer die Photosynthese unter besonderer Beruecksichtigung der Photophosphorylierung. Wiss Zt d Humboldt-Universitaet Zu Berlin Math-Nat Reihe Bd XXIII 6:577–580
- Saakov VS, Lang M, Schindler C, Lichtenthaler HK (1993) Changes in chlorophyll fluorescence and photosynthetic activity of French bean leaves induced by gamma radiation. Photosynthetica 27:369–383
- Saakov VS, Leontjev VG (1988) Untersuchungen ueber die molekularspektro-photometrische Reaktion des pflanzliche Photosynthese-apparates auf Stressbedingungen. Colloq Pflanzenphysiol d Humboldt-Univer zu Berlin 12:143–156
- Saakov VS, Nazarova GD (1972) Reactions of the pigment system of Euglena under conditions of artificially created heterotrophism. Dokl Akad Nauk 204:744–747
- Saakov VS, Nazarova GD, Myl'nikova EV, Alekseeva NR (1971a) Influence of inhibitors of photosynthesis on a pigment system (in Russian). Biochem Biophys Photosynthesa Irkutsk SIFIBR SO AN SSSR 28–36



- Saakov VS, Nasarova GD, Myl'nikova EV, Alekseeva NR (1971b) Reactions of xanthophylls metabolism in plants (in Russian). *Biochem Biophys Photosynthesa Irkutsk SIFIBR SO AN SSSR* 43:51
- Saakov VS, Shiryayev AV (2000) To evolution of hypothesis on location of damage influences of environmental factors in green leaf: the after-effect of gamma-irradiation on energetic of chloroplasts (in Russian). *Dokl Akad Nauk* 371:280–285
- Sakamoto A, Murata A, Murata N (1998) Metabolic engineering of rice leading to biosynthesis of glycinebetaine and tolerance to salt and cold. *Plant Mol Biol* 38:1011–1019
- Sakamoto A, Murata A, Murata N (1999) Metabolic engineering of rice leading to biosynthesis of glycinebetaine and tolerance to salt and cold (corrections to vol 38, pp 1011, 1998). *Plant Mol Biol* 40:195–198
- Schindler C, Lichtenthaler HK (1990) In: Alscher RG, Cumming JR (eds) *Stress responses in plants: adaptation and acclimation mechanisms*, vol 5. Wiley-Liss, Dordrecht, pp 4253–4258
- Schindler C, Lichtenthaler HK (1996) Photosynthetic CO<sub>2</sub>-assimilation, chlorophyll fluorescence and zeaxanthin accumulation in field grown maple trees in the course of a sunny and a cloudy day. *J Plant Physiol* 148:399–412
- Schreiber U (1983) Chlorophyll fluorescence yield changes as a tool in plant physiology. I. The measuring system. *Photosynth Res* 4:361–373
- Schreiber U (1986) Detection of rapid induction kinetics with a new type of high frequency modulated chlorophyll fluorometer. *Photosynth Res* 9:261–272
- Schreiber U (1998) Chlorophyll fluorescence: new instruments for special applications. In: Garab G (ed) *Photosynthesis: mechanisms and effects*, vol 5. Kluwer, Dordrecht, pp 4253–4258
- Schreiber U, Bery JA (1977) Heat-induced changes of chlorophyll fluorescence in intact leaves correlated with damage of the photosynthetic apparatus. *Planta* 136:233–238
- Schreiber U, Bilger W (1987) Rapid assessment of stress effects on plant leaves by chlorophyll fluorescence measurements. In: Tenhungen JD, Catarino FM, Lange OL, Oeschel WC (eds) *Plant responses to stress: functional analysis in Mediterranean ecosystems*, vol 15, NATO ASI subseries G: Ecological sciences. Springer, New York, pp 27–53
- Schreiber U, Bilger W (1993) Progress in chlorophyll fluorescence research: major developments during the past years in retrospect. *Prog Bot* 54:151–173
- Schreiber U, Bilger W, Hormann H, Neubauer C (1997) Chlorophyll fluorescence as a diagnostic tool: basics and some aspects of physiological relevance. In: Raghavendra AS (ed) *Photosynthesis: a comprehensive treatise*. Cambridge University Press, Cambridge, pp 320–336
- Schreiber U, Bilger W, Neubauer C (1994) Chlorophyll fluorescence as a nonintrusive indicator for rapid assessment of in vivo photosynthesis. In: Schulze ED, Caldwell MM (eds) *Ecophysiology of photosynthesis*, vol 100, Ecological studies. Springer, Heidelberg, pp 49–70
- Schreiber U, Neubauer C (1987) The polyphasic rise of chlorophyll fluorescence upon onset of strong continuous illumination. II. Partial control by the photosystem II donor side and possible ways of interpretation. *Zt Naturforsch* 42c:1255–1264
- Schreiber U, Neubauer C (1990) O<sub>2</sub>-dependent electron flow, membrane energization and mechanisms of nonphotochemical quenching of chlorophyll fluorescence. *Photosynth Res* 25:279–293
- Semikhatova OA, Saakov VS (1962) The study of high temperature after- effect on the photosynthesis intensity of *Polygonum sachalinense* (in Russian). *Tr Bot Inst Akad Nauk SSSR Ser IV Eksp Bot* 15:25–42
- Snel JFH, van Kooten O (eds) (1990) The use of chlorophyll fluorescence and other noninvasive spectroscopic techniques in plant stress physiology. *Photosynth Res (Special Issue)* 25 (3):146–332
- Strehler BL, Arnold WA (1951) Light production by green plants. *J Gen Physiol* 34:809–811
- Tarusov BN (1966) On the 70th anniversary of laureate of the Nobel prize of academician NN Semenov. The influence of NN Semenov and his school on the development of radiation biophysics. *Radiobiologia* 6:161–165

- Tarusov BN, Polivoda AI, Zhuravlev AI (1962) Ultraweak spontaneous luminescence in animal tissue. *Tsitologiya* 4:696–699
- Timofeev-Ressovsky NV, Savich AV, Shalnov MI (1981) Introduction in molecular radiobiology. Medicine, Moscow
- Tuba Z, Lichtenthaler HK, Czintalan Z et al (1994) Reconstitution of chlorophylls and photosynthetic CO<sub>2</sub> assimilation in the desiccated poikilochlorophyllous plant *Xerophyta scabrida* upon rehydration. *Planta* 192:414–420
- Udovenko GV (ed) (1976) Methods of assessment of plant resistance to unfavorable environmental conditions. Publishing House “Kolos”, Leningrad, 340p
- Udovenko GV, Saakov VS (1976) Resistenz der getreidepflanzen gegen unguenstige Bedingungen des Milieus: physiologische und genetische Aspekte. *Wissenschaftl Zeit der Humboldt Univer zu Berlin Math Naturwiss Reihe* 25:776–786
- van Kooten O, Snel JFH (1990a) The use of chlorophyll fluorescence nomenclature in plant stress physiology. *Photosynth Res* 25:147–150
- van Kooten O, Snel JFH (eds) (1990b) *Photosynth Res* 25(Spl Iss):147–150
- Veselovskii VA (1987) Хемилюминесцентный метод анализа в биологии. In: Svidersky VL, Saakov VS (eds) *Spectrophotometrical research methods in physiology and biochemistry*. Nauka, Leningrad, pp 34–38
- Veselovskii VA, Leshinskaya LV, Tarusov BN et al (1976) Effect of illumination of cotton leaves on heat resistance of the photosynthetic apparatus. *Sov Fiziol Rast* 23:399–403
- Weis E (1981a) Reversible effects of high, sublethal temperatures on light induced light-scattering changes and electrochromic pigment absorption shift in spinach leaves. *Zt Pflanzenphysiologie* 101:169–178
- Weis E (1981b) Reversible effects of high, sublethal temperatures on light induced light-scattering changes and electrochromic pigment absorption shift in spinach leaves. *Z Pflanzenphysiol* 101:169–178
- Weston SA, Lahm A, Suck D (1992) X-ray structure of the DNase I-d(GGTATACC)<sub>2</sub> complex at 2.3 Å resolution. *J Mol Biol* 226:1237–1256
- Wydrzynski T, Gross EL, Govindjee (1975) Effects of sodium and magnesium cations on the “dark-” and light-induced chlorophyll *a* fluorescence yields in sucrose-washed spinach chloroplasts. *Biochim Biophys Acta* 376:151–161
- Yamamoto HY (1995) Xanthophyll cycle. *Methods Enzymol* 110:303–312
- Yamamoto HY, Nakayama TOM, Chichester CO (1962) Studies on the light and dark interconversions of leaf xanthophylls. *Arch Biochem Biophys* 97:168–173
- Zakarian AE, Tarusov BN (1966) Inhibition of chemiluminescence of the blood plasma in malignant growth. *Biofizika* 11:919–921
- Zhukovskii YuG, Saakov VS (2002) Re-evaluation of the heterogeneity and specificity of promising antitumoral properties by means of high order derivative spectroscopy (in Russian). *Dokl Akad Nauk* 386(6):839–844

Derivative Spectrophotometry and PAM-Fluorescence in  
Comparative Biochemistry

Saakov, V.S.; Krivchenko, A.I.; Rozengart, E.V.; Danilova,  
I.G.

2015, XIII, 611 p. 293 illus., 1 illus. in color., Hardcover

ISBN: 978-3-319-11595-5